Investigation of the molecular basis of PAMP-induced resistance

A thesis submitted to the University of East Anglia for the degree of Doctor of Philosophy

Laura Masini

The Sainsbury Laboratory

Norwich, UK

September 2014

Abstract

The recognition of conserved microbial features termed pathogen-associated molecular patterns (PAMPs) by surface-localized pattern-recognition receptors (PRRs) constitutes the first layer of plant innate immunity. Although details of early immune signaling events are starting to be unveiled, the molecular mechanisms leading to restriction of pathogen growth are still poorly understood. To gain more insight into this process, two different approaches were employed. I used reverse genetics to study the involvement of three different secondary metabolites, namely camalexin, glucosinolates and callose, in PAMP-triggered immunity (PTI) against the phytopathogenic bacterium *Pseudomonas syringae* pv. *tomato* (*Pto*) DC3000. These are well known active defences Arabidopsis employs to restrict fungi and oomycetes invasion. Results showed that these compounds are dispensable for antibacterial resistance triggered by the bacterial PAMP flagellin (flg22). In addition, as an unbiased approach, I performed a novel genetic screen aimed at identifying molecular components required for induced resistance to *Pto* DC3000. For this, I developed a high-throughput assay for bacterial infection in Arabidopsis seedlings that enabled to select mutants impaired in flg22-induced resistance to *Pto* DC3000. The *pir* (<u>P</u>AMP-<u>i</u>nduced <u>r</u>esistance) screen identified four loci whose mutation leads to a reproducible reduction of flg22-induced resistance. These genes have not been previously characterized for their role in immunity, and therefore can be considered as novel components of PTI. By employing a combination of reverse genetics, metabolomics and chemistry approaches, I obtained preliminary data suggesting that flavonoids act as cellular buffers and/or are employed as active defenses against bacteria. In addition, interference with the mevalonic acid biosynthetic pathway impairs antibacterial defenses, suggesting a role in immunity. Additional tests are underway to better assess the contribution of these *PIR* genes to PTI. Therefore, through the *pir* screen, I have identified several novel loci required for plant immunity that will increase our knowledge of the plant immune system.

Table of contents

List of figures

List of tables

Acknowledgments

With this PhD thesis a four-year journey comes to an end. And this is also the time to say thanks.

Thanks to Cyril who offered me the opportunity to join his group and work on this project. It was not always easy, but I learned a lot.

Thanks to the great colleagues I had. To those that officially and unofficially mentored me, but also to everyone that helped, listened or discussed with me. Or that were just there to support. I'll miss you.

And last, but not least, thanks to my family, my boyfriend and all my friends. All of them never really understood much of what I have been doing, but nonetheless they stood by me and supported me. They really had a very important part during this time.

Abbreviations

AACT	acetoacetyl-CoA thiolase
ABA	abscissic acid
ABC	ATP-binding cassette
ACA	Arabidopsis Ca^{2+}-ATPase
ACC	aminocyclopropane-1-carboxylic acid
ACS	1-AMINOCYCLOPROPANE-1-CARBOXYLIC ACID SYNTHASE
AGB1	Arabidopsis G protein β-subunit 1
AGG	ARABIDOPSIS G PROTEIN γ-SUBUNIT
AHA	ARABIDOPSIS H^+-ATPASES
ANR	ANTHOCYANIDIN REDUCTASE
ANS	ANTHOCYANIDIN SYNTHASE
AO	ASPARTATE OXIDASE
ARF	ADP ribosylation factor
At	Arabidopsis thaliana
AtMIN7	Arabidopsis thaliana HopM1 interactor 7
ATP	Adenosine 5′-triphosphate
AtPep	*Arabidopsis thaliana* PEPTIDE 1
Ave1	Avirulence on Ve1
BAK1	BRI1-ASSOCIATED RECEPTOR KINASE 1
BAN	BANYULS
BEE2	BRASSINOSTEROID ENHANCED EXPRESSION 2
BIK1	BOTRYTIS-INDUCED KINASE1
BIR2	BAK1-INTERACTING RECEPTOR-LIKE KINASE 2
BR	brassinosteroid
BRI1	BR RECEPTOR BRASSINOSTEROID INSENSITIVE 1
BSK1	BR-SIGNALLING KINASE1
Bti9	AVRPTOB TOMATO-INTERACTING 9
BZR1	BRASSINAZOLE-RESISTANT 1
CaM	calmodulin
CBL	calcineurin B-like protein
CDPK	calcium-dependent protein kinase
CEBiP	CHITIN ELICITOR BINDING PROTEIN
CERK1	CHITIN ELICITOR RECEPTOR KINASE 1
CFU	colony forming units
CHI	CHALCONE ISOMERASE
CHS	CHALCONE SYNTHASE
CHX	cation/H^+ exchanger
CIB1	CRYPTOCHROME-INTERACTING BASIC HELIX-LOOPHELIX

COR	coronatine
CPA	CATION PROTON ANTIPORTER
DAMP	damage-associated molecular pattern
DFR	dihydroflavonol reductase
DMAPP	dimethylallyl diphosphate
DMSO	dimethyl sulfoxide
DORN1	DOES NOT RESPOND TO NUCLEOTIDES 1
DRMs	detergent-resistant membranes
DTT	dithiothreitol
EFR	EF-TU RECEPTOR
EF-Tu	ELONGATION FACTOR Tu
EGF	epidermal-growth factor
EGL3	ENHANCER OF GL3
EIL3	EIN3-LIKE
EIN2	ETHYLENE INSENSITIVE 2
EIN3	ETHYLENE INSENSITIVE 3
EIX	Ethylene-inducing xylanase
elfin	*elf18 insensitive*
ERF104	ETHYLENE RESPONSE FACTOR 104
ER-QC	endoplasmic reticulum-quality control
ESCRT	endosomal sorting complex required for transport
ET	ethylene
ETI	effector-triggered immunity
ETS	effector-triggered susceptibility
F3H	FLAVANONE 3-HYDROXYLASE
F3'H	FLAVANOID 3'-HYDROXYLASE
FER	FERONIA
fin	*flagellin insensitive*
FLIM	fluorescence lifetime imaging microscopy
FLS1	FLAVONOL SYNTHASE 1
FLS2	FLAGELLIN-SENSING 2
FRET	Förster resonance energy transfer
FRK1	FLG22-INDUCED RECEPTOR-LIKE KINASE 1
GA	gibberellin
GEF	guanine nucleotide exchange factor
GID1	GIBBERELLIN INSENSITIVE DWARF 1
GL3	GLABRA3
Glc	glucose
GlcNAc	*N*-acetylglucosamine
Gm	*Glycine max*
GPA1	G protein α-subunit 1
GPCR	G protein-coupled receptor

GPI	glycosylphosphatidylinositol
GRP	glycine-rich RNA-binding protein
GST	glutathione-S-transferases
H$_2$O$_2$	hydrogen peroxide
HBI1	HOMOLOG OF BRASSINOSTEROID ENHANCED EXPRESSION 2 INTERACTING WITH IBH1
HID	2-HYDROXYISOFLAVANONE DEHYDRATASE
HMG-CoA	3-hydroxy-3-methylglutaryl-CoA
HMGR	HMG-CoA reductase
HMGS	HMG-CoA synthase
Hpa	*Hyaloperonospora arabidopsidis*
HR	hypersensitive response
hrc	hypersensitive response and conserved
IAA	indolic acetic acid
IAA	indole-3-acetic acid
IOS1	IMPAIRED OOMYCETE SUSCEPTIBILITY 1
IPP	isopentenyl diphosphate
JA	jasmonic acid
KAPP	kinase-associated protein phosphatase
LDOX	LEUCOANTHOCYANIDIN DIOXYGENASE
LE	Late endosome
LecRK	L-type lectin RLK
LIK1	LYSM RLK1-INTERACTING KINASE 1
LRR	leucine-rich repeat
LYK	LYSM CONTAINING RECEPTOR-LIKE KINASE
LYM	LYSM DOMAIN CONTAINING GPI-ANCHORED PROTEIN
LYP	LYSM-CONTAINING PROTEIN
LysM	lysine motif
MAMP	microbe-associated molecular pattern
MAPK	mitogen-activated protein kinase
MAPKK/MKK	MAP kinase kinase
MAPKKK/MEKK	MAP kinase kinase kinase
MATE	multidrug and toxic compound extrusion
MEP	methylerythritol
MES	2-(N-morpholino)-ethanesulfonic acid
MK	mevalonate kinase
MKS1	MAP KINASE 4 SUBSTRATE 1
mob	*modifier of bak1-5*
MPK	MAP kinase
MurNAc	*N*-acetylmuramic acid

MVB	multivesicular compartment
MVD	MEVALONATE DIPHOSPHATE DECARBOXYLASE
NAA	1-naphthaleneacetic acid
NAD	nicotinamide adenine dinucleotide
NaT-DC	Na^+-transporting carboxylic acid decarboxylase
NLR	nucleotide-binding leucine-rich repeat
O^{2-}	superoxide
OD	optical density
OG	oligogalacturonide
OMT1	*O*-methyltransferase
Os	Oryza sativa
PAD3	PHYTOALEXIN DEFICIENT 3
PAL	phenylalanine ammonia lyase
PAMP	pathogen-associated molecular pattern
PANK	plant-specific ankyrin-repeat
PAP	PRODUCTION OF ANTHOCYANIN PIGMENT
PBL	PBS1-like
PBS1	AVRPPHB SUSCEPTIBLE 1
PEPR	AtPep receptor
PFG	PRODUCTION OF FLAVONOL GLYCOSIDES
PGIP	polygalacturonase-inhibiting protein
PGN	peptidoglycan
PIF4	phytochrome-interacting factor 4
PIN1	PIN-FORMED1
PIP	PAMP-induced secreted peptide
PIR	PAMP-induced resistance
PMK	PHOSPHOMEVALONATE KINASE
PMR4	POWDERY MILDEW RESISTANT 4
PP2A	Protein phosphatase 2A
PP2C	the protein phosphatase 2C
PPO	POLYPHENOL OXIDASE
PRR	pattern–recognition receptor
PSKR1	PSK RECEPTOR 1
PSK-α	Phytosulfokine-α
psl	*priority to sweet life*
PSY1	PLANT PEPTIDE CONTAINING SULFATED TYROSINE 1
PSY1R	PSY1 RECEPTOR
PTI	PAMP-triggered immunity
Pto	*Pseudomonas syringae* pv. *tomato* DC3000
PUB	plant U-box
RALF	rapid alkalinization inducing factor

RBOH   RESPIRATORY BURST OXIDASE HOMOLOGUE
Rha   rhamnose
RLCK   receptor-like cytoplasmic kinase
RLK   receptor-like kinase
RLP   receptor-like protein
RLU   relative light units
ROS   reactive oxygen species
RRS1   RESISTANCE TO R. SOLANACEARUM 1
SA   salicylic acid
SDF2   STROMAL-DERIVED FACTOR 2
SDS   sodium dodecyl sulphate
SERK   SOMATIC EMBRYOGENESIS RECEPTOR-LIKE KINASE
SGI   seedling growth inhibition
Sl   *Solanum lycopersicum*
SOBIR   SUPPRESSOR OF *BIR1-1*
SUD1   SUPPRESSOR OF DRY2 DEFECTS 1
T3SS   type-III secretion system
TMD   transmembrane domain
TPC   two-pore channel
TT   TRANSPARENT TESTA
TTG   TRANSPARENT TESTA GLABRA
UGT   UDP-GLUCOSYL TRANSFERASE
UMP   uridine 5′-monophosphate
VPS37-1   vacuolar protein sorting 37-1
WAK   wall-associated kinase
XB25   XA21-BINDING PROTEIN 25
Xcc   *Xanthomonas campestris* pv. *campestris*
Xoo   *Xanthomonas oryzae* pv. *oryzae*

Chapter 1. General introduction

1.1 Plant immunity: an overview

Although plants are constantly exposed to a wide array of beneficial and pathogenic microorganisms, diseases are the exception, not the rule. Yet, diseases cause massive losses to agriculture and pose a threat to food security (Strange and Scott, 2005). Therefore, understanding the mechanisms plants employ to resist infections is of high importance in the view of engineering crops for durable resistance against pathogens.

To cause disease, pathogens need to overcome both passive, pre-formed defences, and induced immune responses that are activated in response to their perception (Nürnberger et al., 2004). Unlike animals, plants do not possess adaptive immunity and mobile immune cells (Dodds and Rathjen, 2010), and therefore rely solely on their innate immune system to fight against pathogens. As every plant cell has the potential to detect pathogens and trigger local and systemic defences, the plant immune system can be considered cell-autonomous. Although not conserved, the innate immune systems of plants and animals share many similarities (Nürnberger et al., 2004; Dodds and Rathjen, 2010).

The local establishment of plant innate immunity depends on two different levels of pathogens recognition: first at the cell surface and then intracellularly. Surface immunity recognizes features that are common among different classes of microbes and pathogens commonly referred to as pathogen- or microbe-associated molecular patterns (PAMPs or MAMPs, referred to herein as PAMPs for simplicity), and is known as pattern-triggered immunity (PTI) (Dodds and Rathjen, 2010). Examples of PAMPs include bacterial flagellin and ELONGATION FACTOR Tu (EF-Tu) and fungal chitin (Zipfel, 2014). In addition to PAMPs, plants can also perceive endogenous damage-associated molecular patterns (DAMPs), which are released either due to pathogen-caused damage or wounding and are thought to amplify PTI (Albert, 2013; Zipfel, 2014).

PAMP recognition is mediated by pattern–recognition receptors (PRRs) at the plasma membrane (Figure 1.1) (Zipfel, 2014). Establishment of PTI is of high importance in the context of immunity, as loss of PAMP recognition enables enhanced pathogen growth (Zipfel et al., 2004). Furthermore, PTI confers broad spectrum disease resistance (Lacombe et al., 2010). PTI is a localized response at the site of pathogen attack, whose mechanism is still unknown. However, research to understand why non-pathogenic mutant bacteria grow poorly and are unable to cause disease in plants could give some hints on this defence response (Collmer et al., 2000; Hauck et al., 2003; Kim et al., 2005; Soylu et al., 2005; Mitchell et al., 2014). Papillae containing cellulose and callose have been found to accumulate between the plasma membrane and the cell wall next to bacterial colonies (Soylu et al., 2005; Mitchell et al., 2014). Moreover, these deposits are characterized by cross-linking of phenolics and indolic derivatives (Forcat et al., 2010). At the same sites, local accumulation of reactive oxygen species (ROS) has been also observed (Soylu et al., 2005; Mitchell et al., 2014). Taken together, it has been proposed that ROS-dependent cross-linking of secreted glycoproteins and polysaccharides causes agglutination of these non-pathogenic bacteria, impairing their growth (Mitchell et al., 2014).

Successful pathogens can, however, overcome PTI by translocating effectors inside the plant cell or in the apoplast, triggering what is generally called effector-triggered susceptibility (ETS) (Figure 1.1) (Jones and Dangl, 2006; Win et al., 2012). Effectors are proteins that target host molecules in order to suppress or evade the immune response triggered by pathogen perception, and thereby promote pathogen growth (Lindeberg et al., 2012).

Nonetheless, in resistant plants, effectors are specifically recognized leading to what is known as effector-triggered immunity (ETI), which constitutes the second layer of plant immunity (Figure 1.1) (Jones and Dangl, 2006). ETI relies on nucleotide-binding leucine-rich repeat (NLR) proteins, which are activated upon perception of pathogen effectors (Takken and Goverse, 2012). In the context of ETI, effectors can be recognized by the host directly

or indirectly. Direct recognition is a very uncommon form of effector recognition, as it has been described in only few cases, as, for example, in the recognition of *Ralstonia solanacearum* PopP2 by RESISTANCE TO R. SOLANACEARUM 1 (RRS1) in Arabidopsis (Deslandes et al., 2003). More commonly, effectors are recognized by the plant cell in an indirect way, which relies on detecting the activity of the effector on a host molecule.

Indirect recognition was initially postulated as the "guard hypothesis", where NLRs "guard" the effector target. NLRs can detect alterations of the target and consequently mount a defence response (van der Biezen and Jones, 1998; Dangl and Jones, 2001). However, the "guard hypothesis" was later expanded into the "decoy" model, when it became clear that effectors can have several targets, and these targets do not necessarily have a role in immunity (Hoorn and Kamoun, 2008). According to this model, a decoy is a non-functional target which mimics the susceptibility target. The decoy has the only function of luring the effector into a non-functional target, which is monitored by a NLR that can induce a defence response when the decoy is altered (Hoorn and Kamoun, 2008). A more recent expansion on this model is the "integrated decoy", which is based on the finding that several NLRs work as pairs, with one of the partner exhibiting domains which are not usually found in NLRs (Cesari et al., 2014). According to this model, the effector target is fused to a receptor NLR, which senses the activity of the effector and triggers a defence response via a paired signalling NLR (Cesari et al., 2014; Wu et al., 2015)

ETI generally induces the same cascade of events as PTI, but in a faster manner and with bigger amplitude, and it is race- or strain-specific (Dodds and Rathjen, 2010). ETI is also commonly linked to development of a hypersensitive response (HR), a form of programmed cell death in the infected tissue (Dodds and Rathjen, 2010). It is still matter of debate whether the HR directly restricts pathogen growth or not (Coll et al., 2011). HR is preceded by ROS production, which is required for its establishment (Torres

et al., 2006; Mur et al., 2008). HR can also be induced during PTI, although it is not very common (Taguchi et al., 2003; Naito et al., 2008).

Because effectors are under constant host surveillance, and individual effectors are dispensable for pathogens viability, effectors are under constant positive selection to evade recognition (Jones and Dangl, 2006). These effectors can be modified or lost to avoid recognition, or new effectors can be acquired to suppress ETI and further trigger ETS. Nonetheless, natural selection will then promote new ways to detect effectors and trigger again ETI. Therefore ETI and ETS are under constant coevolution in the context of plant-pathogen arms race.

PAMP-triggered immunity (PTI)
= no disease

Effector-triggered Susceptibility (ETS)
= disease

Effector-triggered Immunity (ETI)
= no disease
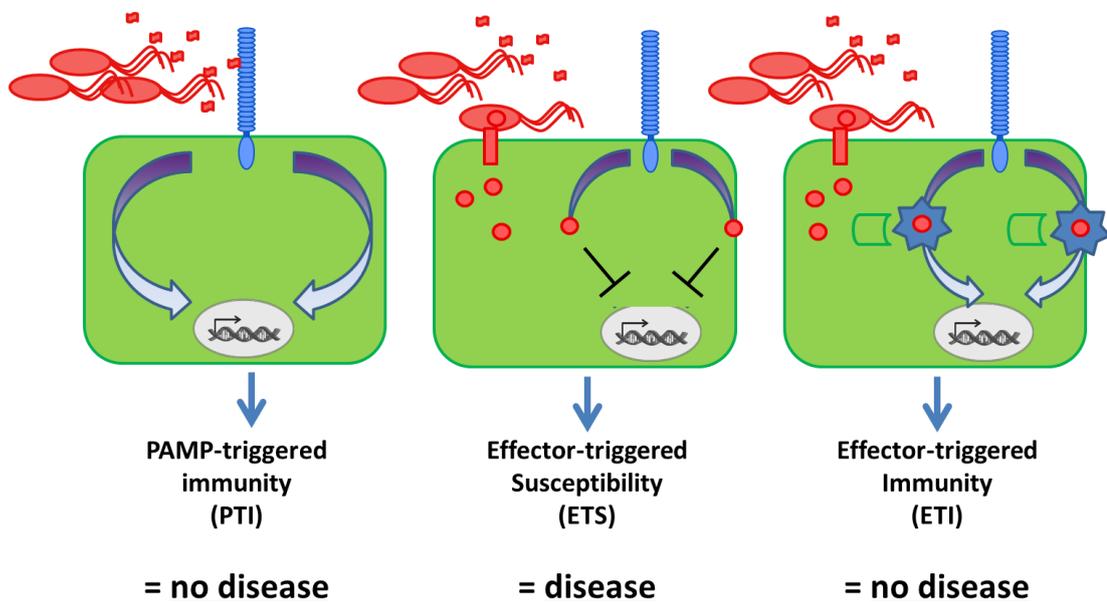
Figure 1.1. Overview of the immune system in plants.

Different pathogens can be recognized at the cell surface via recognition of their PAMPs by PRR receptors (left). This recognition leads to PTI. However, successful pathogens can deliver effectors inside the plant cell (middle). Effectors bind to and manipulate their target proteins to suppress PAMP recognition/PTI and promote disease. This leads to ETS (middle). Effectors can be additionally recognized by intracellular NLRs directly or indirectly, through perception of the effector activity on a host protein(right). Intracellular perception of effectors activates NLRs and induces ETI.

In the following sections, a detailed overview of the PAMP flagellin, its recognition in Arabidopsis, and the flagellin-dependent signalling pathway is given. This will be used as a model to describe other PAMPs and their recognition in Arabidopsis and in other plant species. The chapter will be concluded with a summary of the known mechanisms through which bacterial effectors can suppress PTI, and an overview of this thesis.

1.2 PAMP-triggered immunity (PTI)

PTI is the first layer of molecular immunity, which relies on the recognition of PAMPs at the plasma membrane. PAMPs are conserved features of microorganisms and are often indispensable for microbial survival (Pel and Pieterse, 2012). PAMPs contain highly conserved minimal epitopes that can retain full elicitor activity at subnanomolar concentrations (Boller and Felix, 2009). PAMPs are recognized by plant PRRs (Macho and Zipfel, 2014). PRRs are receptor-like kinases (RLKs) or receptor-like proteins (RLPs). Both classes are characterized by an extracellular domain, involved in PAMP perception, and a single-pass transmembrane domain (TMD). In addition, RLKs possess an intracellular kinase domain, which is missing in RLPs (Zipfel, 2014). The extracellular ligand-binding domains of characterized PRRs contain either leucine-rich repeats (LRRs), lysine motifs (LysMs) or epidermal-growth factor (EGF)-like domains. In general, LRRs bind proteins or peptides, like flagellin or EF-Tu, while LysM domains bind sugars, like peptidoglycan (PGN) and chitin, and EGF-like domains bind oligogalacturonides (OGs) (Macho and Zipfel, 2014).

In general, PAMP perception leads to a cascade of events that can be temporally grouped (Boller and Felix, 2009; Nicaise et al., 2009). Very early responses, happening within minutes, include ion fluxes and extracellular alkalinisation, a burst of ROS, activation of mitogen-activated and calcium-

dependent protein kinases (MAPKs and CDPKs) and changes in protein phosphorylation status. Other early responses occurring between 5 and 30 minutes include ethylene (ET) biosynthesis, receptor endocytosis, and changes in gene expression. Later responses include callose deposition and seedling growth inhibition (SGI). The final output of PTI is the restriction of pathogen growth (Zipfel et al., 2004). Some of these measurable outputs are often used to determine whether an elicitor possesses PAMP properties.

1.2.1 PTI in *Arabidopsis thaliana*

1.2.1.1 Flagellin and FLS2

Flagellin is the molecular scaffold of bacterial flagella. Its N- and C-terminus are fundamental for the correct export and the assembly of the flagellum (Felix et al., 1999). In particular, the N-terminus contains a conserved epitope of 22 amino acids (flg22) that alone is recognized by the cognate receptor and elicits defence responses (Felix et al., 1999). Although flagellin is a feature that is vital for bacteria and unlikely to be altered, mutations within *fliC*, which encodes the major component of flagellin, were found in *Pseudomonas syringae* pv. *tomato* (*Pto*) DC3000 and *Xanthomonas campestris* pv. *campestris* (*Xcc*), leading to evasion of recognition (Sun et al., 2006; Cai et al., 2011). Similarly, *Agrobacterium tumefaciens*, *Rhizobium meliloti and Ralstonia solanacearum* carry a key mutation in the active epitope of flagellin which allow them to evade recognition (Felix et al., 1999; Pfund et al., 2004). Altogether, these examples indicate that although PAMPs are highly conserved, selective pressure can actually lead to modifications, with the result of reducing or evading recognition of bacteria.

In Arabidopsis, flagellin or flg22 is recognized at the cell surface by the PRR FLAGELLIN-SENSING 2 (FLS2) and its co-receptor BRI1-ASSOCIATED RECEPTOR KINASE 1/SOMATIC EMBRYOGENESIS RECEPTOR-LIKE

KINASE 3 (BAK1/SERK3) (Gómez-Gómez and Boller, 2000; Chinchilla et al., 2006, 2007; Heese et al., 2007; Sun et al., 2013a). FLS2 is a LRR-RLK with 28 LRRs in its ectodomain, a transmembrane domain and a cytoplasmic serine/threonine protein kinase domain and belongs to the subfamily XII of LRR-RLKs (Gómez-Gómez and Boller, 2000; Shiu and Bleecker, 2001). Arabidopsis plants carrying loss-of-function mutations in *FLS2* are more susceptible to *Pto* DC3000, and pre-treatment with flg22 provides resistance to a wide spectrum of pathogens (Zipfel et al., 2004; Ferrari et al., 2007; Fabro et al., 2011), confirming the importance of PAMP perception and PTI in plant immunity. In the following sections a detailed overview of our current knowledge regarding the FLS2 pathway is given (Figure 1.2).
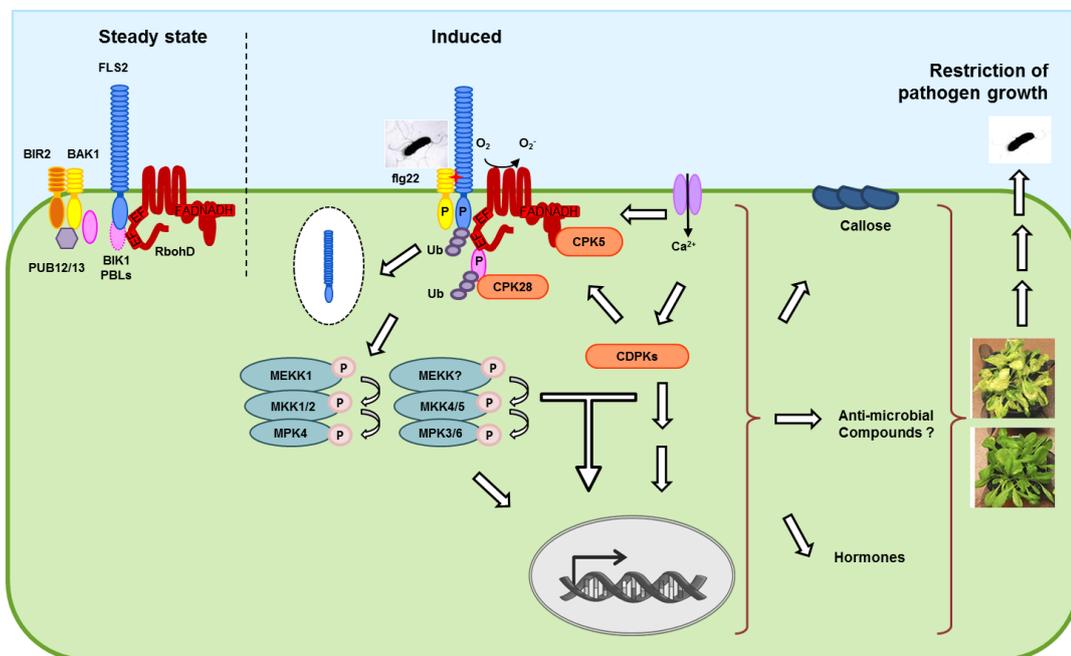
Figure 1.2. Scheme of the FLS2-dependent pathway in Arabidopsis.

In the resting state, BIR2 prevents association of FLS2-BAK1. BIK1 and related PBLs associate with both BAK1 and FLS2, which also interacts with RBOHD. BAK1 also associates with PUB12/13. Upon flg22 perception, FLS2 associate with co-receptor BAK1 and auto- and trans-phosphorylation events take place. BIK1 is released from the complex and phoshphorylates and activates RBOHD for ROS production. Flg22 also induces Ca^{2+} influx, which activates CDPKs that, in turn, also activate RBOHD. FLS2 is endocytosed and, in addition, PUB12/13 ubiquitinates FLS2, inducing FLS2 degradation. CPK28 contributes to BIK1 protein turnover through a currently unknown mechanism. Activation of the receptor complex induces downstream signalling via MAPKs and CDPKs, which can function independently or synergistically to promote transcriptional reprogramming. PTI ultimately leads to restriction of pathogen growth.

1.2.1.1.1 Receptor complex formation and regulation

1.2.1.1.1.1 PRR complex formation

Upon ligand-binding, FLS2 forms a heterocomplex with BAK1 almost instantaneously, which is required to initiate and transduce the signal downstream to mount a defence response (Chinchilla et al., 2007; Heese et al., 2007; Schulze et al., 2010; Roux et al., 2011). Mutation of *BAK1* leads to compromised downstream responses and resistance to bacteria, supporting the biological relevance of this interaction (Chinchilla et al., 2007; Heese et al., 2007). Recent structural work showed that flg22 binds to FLS2 between the LRRs 3 and 16 of its ectodomain, and to the N-terminal of BAK1 via the 18th glycine, which acts as a 'molecular glue' between the two receptors (Sun et al., 2013a). BAK1 is also co-receptor of the BRASSINOSTEROID (BR) RECEPTOR BRASSINOSTEROID INSENSITIVE 1 (BRI1) (Santiago et al., 2013; Sun et al., 2013b), although its role in PTI is independent of its role in BR signalling pathway (Li et al., 2002; Chinchilla et al., 2007). BAK1 has additional roles in cell death and senescence (He et al., 2007; Kemmerling et al., 2007; Jeong et al., 2010).

In addition to BAK1, other RLKs have been shown to be part of the receptor complex (Macho and Zipfel, 2014). These proteins do not have an active role in flg22 perception but rather modulate the activity/inactivity of the receptor complex and/or contribute to flg22-dependent signalling. For example, IMPAIRED OOMYCETE SUSCEPTIBILITY 1 (IOS1) constitutively interacts with FLS2 and BAK1, positively regulating their association, and BAK1-INTERACTING RECEPTOR-LIKE KINASE 2 (BIR2) constitutively interacts with BAK1 (Chen et al., 2014a; Halter et al., 2014). Although it is unclear how IOS1 contributes to immunity through its interaction with FLS2 and BAK1, BIR2 was shown to prevent activation of downstream signalling and defence by interfering with FLS2-BAK1 association in the absence of flg22 (Halter et al., 2014). In fact, only following flg22 perception, BAK1-BIR2 interaction is

disrupted, allowing BAK1 to be released for the activation of the receptor complex (Halter et al., 2014).

Lectin-receptor kinases may also have a role as components of the receptor complex and/or regulators of PTI. L-TYPE LECTIN RLK I.9 (LecRK-I.9)/ DOES NOT RESPOND TO NUCLEOTIDES 1 (DORN1) is localized at the plasma membrane and its mutation affects flg22-dependent callose deposition (Bouwmeester et al., 2011). LecRK-VI.2 is a positive regulator of FLS2-dependent signalling (Singh et al., 2012). Its mutation leads to reduced PTI signalling and enhanced susceptibility to virulent and avirulent strains of *Pto* (Singh et al., 2012). Because LecRK-1.9/DORN1 perceives ATP and *lecrk-VI.2* mutation does not affect FLS2-BAK1 association, it is possible that these two receptors could have an indirect contribution to PTI via amplification of immune responses through perception of ATP and a as yet unknown endogenous DAMPs (Zipfel, 2013; Choi et al., 2014).

1.2.1.1.1.2 Phosphorylation events controlling PRR complex activation

Although heteromerization of FLS2 with BAK1 does not depend on the functionality of their kinase domains, the kinase domains are indispensable for the downstream signalling and defence responses (Chinchilla et al., 2007; Schulze et al., 2010; Schwessinger et al., 2011). The importance of receptor phosphorylation for its functionality is supported by the finding that mutation of several phosphorylation sites in the cytoplasmic domain of FLS2 can abolish FLS2-dependent ROS production (Robatzek et al., 2006; Cao et al., 2013). Because these mutations do not affect FLS2-flg22 binding, phosphorylation of FLS2 clearly has a role in specifying and transducing the signal, which is affected when these phosphorylation sites are mutated (Robatzek et al., 2006; Cao et al., 2013). Moreover, kinase-dead versions of FLS2 and BAK1 cannot activate downstream responses in response to flg22,

further supporting the importance of receptor phosphorylation for flg22-dependent responses (Asai et al., 2002; Lu et al., 2010).

1.2.1.1.1.3 Receptor-like cytoplasmic kinases (RLCKs) as PRR complex substrates

Downstream of the receptor complex, RLCKs have emerged as substrates of PRR complexes and key regulators of downstream responses (Lu et al., 2010; Zhang et al., 2010; Shi et al., 2013). In fact, a number of RLCKs constitutively or dynamically interact with FLS2 and BAK1, including BOTRYTIS-INDUCED KINASE1 (BIK1) and closely related AVRPPHB SUSCEPTIBLE 1 (PBS1)-LIKE (PBL) proteins PBL1 and PBL2, and BR-SIGNALING KINASE 1 (BSK1) (Lu et al., 2010; Zhang et al., 2010; Shi et al., 2013; Lin et al., 2014). Mutation of both *BIK1* and *BSK1* leads to a number of reduced flg22-dependent responses, which does not include MAPK activation, and immunity to bacteria (Lu et al., 2010; Zhang et al., 2010; Feng et al., 2012; Shi et al., 2013). Therefore RLCKs appear to be a signalling link between the receptors and the downstream defence responses, although via a route that does not involve MAPKs.

1.2.1.1.1.4 Negative regulation of PRR complexes

Constant activation of defence responses leads to detrimental effects on plant fitness. One clear examples is the reduced growth in seedlings constantly exposed to PAMPs (Gómez-Gómez et al., 1999; Zipfel et al., 2006). Therefore, it is clear that PTI must be under tight negative control to keep the signalling pathway in an 'off' state in the absence of ligand, and also to attenuate the signalling once it has completed its function.

Many PRRs are protein kinases, which are activated by phosphorylation and subsequently initiate downstream signalling. Therefore it is likely that de-

phosphorylation of protein kinases by protein phosphatases is a major mechanism for down-regulating protein kinase-dependent signalling (Schweighofer et al., 2004). In fact, the addition of phosphatase inhibitors leads to defence-like outputs and, similarly, chemical inhibition of kinase activity impairs defence responses (Felix et al., 1994; MacKintosh et al., 1994; Chandra and Low, 1995).

Currently, both FLS2 and BAK1 have been shown to be negatively regulated by protein phosphatases. The kinase domain of FLS2 binds to the kinase interaction domain of KINASE-ASSOCIATED PROTEIN PHOSPHATASE (KAPP) *in vitro*, and the PROTEIN PHOSPHATASE (PP) 2A subunits A1, C4, and B'η/ζ interact with BAK1 constitutively *in vivo* (Gómez-Gómez et al., 2001; Segonzac et al., 2014).

Both KAPP and PP2A seem to act by modulating the phosphorylation status of FLS2 and BAK1, respectively, and therefore their activity (Gómez-Gómez et al., 2001; Segonzac et al., 2014). Accordingly, overexpression of *KAPP* abolishes flg22-dependent ROS production and SGI, and mutation of individual PP2A components enhances flg22-dependent responses, including ROS and resistance to *Pto* DC3000 (Gómez-Gómez et al., 2001; Segonzac et al., 2014). Therefore this supports the role of protein phosphatases as modulator of defence signalling responses by controlling the phosphorylation, and therefore the activation, status of the flg22 receptor.

In addition to protein phosphatases, signalling can also be attenuated by protein degradation through ubiquitination. A number of PLANT U-BOX (PUB) E3 ubiquitin ligases have been shown to negatively regulate PTI responses, as their mutation results in enhanced resistance to bacteria and enhanced PAMP-dependent responses (Trujillo et al., 2008; Lu et al., 2011). However, different PUBs act via different mechanisms. For example, PUB22 interact with and degrade the exocyst subunit Exo70B2, a positive regulator of PTI, in a flg22-dependent manner (Stegmann et al., 2012). Because exocytosis is believed to contribute to plant immunity through transport and

secretion of antimicrobials, and mutation of *Exo70B2* leads to reduced PTI responses and enhanced susceptibility, it is possible that PUB22 deregulates immunity through degradation of Exo70B2 (Bednarek et al., 2010; Stegmann et al., 2012). Additionally, PUB12 and PUB13 were shown to contribute to attenuation of defence responses via polyubiquitination and degradation of FLS2 in response to flg22 (Lu et al., 2011).

Interestingly, CPK28 was recently found to be a negative regulator of PTI, by by controlling BIK1 levels through protein degradation, thereby maintaining optimal levels of immune signalling (Monaghan et al., 2014). This may suggest that CPK28 works together with as yet unknown PUB protein.

1.2.1.1.2 Ion fluxes

In plant cells, H^+-ATPases pump protons from the cytoplasm to the apoplast, maintaining a negative potential at the plasma membrane and a differential pH between the two compartments (Elmore and Coaker, 2011). This difference in membrane potential is used to move solutes and ions across the membrane, and for the growth of the cell wall (Elmore and Coaker, 2011; Wu et al., 2014).

Flg22 perception very quickly induces an alteration of ion fluxes across the plasma membrane, leading to alkalinisation of the apoplast and membrane depolarization, although the physiological relevance of these changes is still unclear (Felix et al., 1999; Jeworutzki et al., 2010). The ARABIDOPSIS H^+-ATPASES AHA1 and AHA2 were found to be dephosphorylated, and therefore downregulated, in response to flg22 treatment, which would suggest that they are involved in extracellular alkalinisation (Benschop et al., 2007; Nühse et al., 2007). However, pre-activation of H^+-ATPases does not stop flg22-dependent membrane depolarization, and therefore H^+-ATPases may not be the major player in this physiological responses (Jeworutzki et al., 2010).

Ca^{2+} influx is also a common hallmark of PTI (Blume et al., 2000; Lecourieux et al., 2002). Using the reporter protein aequorin, flg22 was found to increase the amount of cytosolic Ca^{2+}, peaking within a minute from PAMP application (Jeworutzki et al., 2010; Ranf et al., 2011). Flg22-dependent Ca^{2+} influx is responsible for the subsequent efflux of nitrates and chlorides, which contribute to membrane depolarization and extracellular alkalinization (Jeworutzki et al., 2010; Ranf et al., 2011). However, to date, the identity of PAMP-dependent Ca^{2+} channel is still unknown. The plasma membrane-localized CA^{2+}-ATPASE ACA8 was found to interact with FLS2 and, along with its close homolog ACA10, positively regulate the flg22-dependent Ca^{2+} burst (Frey et al., 2012). However, ACAs pump Ca^{2+} outwards, into the apoplast or into the vacuole and therefore may have a role in Ca^{2+} homeostasis after the PAMP-dependent Ca^{2+} burst (Bonza et al., 2004; Conn et al., 2011).

Ca^{2+} is a widespread second messenger in plants, through which signals are transduced and decoded into downstream responses via Ca^{2+} binding proteins (Kudla et al., 2010). Most Ca^{2+}-sensor proteins are characterized by the presence of EF-hand motifs that bind to Ca^{2+} (Gifford et al., 2007). Ca^{2+}-binding induces conformational changes, which are necessary for activation and/or target association (Gifford et al., 2007). Plants have three major calcium sensors: calmodulin (CaM), calcineurin B-like proteins (CBLs) and CDPKs (DeFalco et al., 2010). In Arabidopsis, CPK4, 5, 6 and 11 are positive regulators of flg22-dependent signalling, since triple and quadruple mutant plants show a reduced flg22-dependent ROS burst, reduced flg22-dependent gene activation and slightly enhanced disease susceptibility when inoculated with *Pto* DC3000 (Boudsocq et al., 2010; Gao et al., 2013). Interestingly mutation in one or multiple CDPK genes does not impair flg22-dependent MAPK activation, indicating that the two cascades act independently (Boudsocq et al., 2010).

1.2.1.1.3 Oxidative burst

Production of apoplastic reactive oxygen species (ROS) happens within minutes after PAMP perception and in Arabidopsis is mainly dependent on the plasma membrane-localized NADPH oxidase encoded by the *RESPIRATORY BURST OXIDASE HOMOLOGUE D* (*RBOHD*) gene (Torres et al., 2002; Nühse et al., 2007; Zhang et al., 2007). Additional sources of apoplastic ROS are cell wall-localized peroxidases (Daudi et al., 2012). RBOHs contain two EF-hand motifs in their N-terminus and are regulated by Ca^{2+}. They catalyse the production of superoxide (O^{2-}) which is the substrate of peroxidases that convert O^{2-} to hydrogen peroxide (H_2O_2) (Torres et al., 2002; Marino et al., 2012).

Production of ROS in plant immunity has been suggested to exert antimicrobial activity against pathogens, contribute to strengthen the plant cell wall, and mediate activation of defence genes (Torres, 2010; Mott et al., 2014). RBOHD is also required for PAMP-induced stomatal closure, which probably limits the colonization of Arabidopsis leaves (Mersmann et al., 2010; Macho et al., 2012). Furthermore, ROS generated during PTI can spread and transduce the signal systemically (Dubiella et al., 2013; Baxter et al., 2014).

Several CDPKs have been shown to regulate ROS production upon PAMP perception by phosphorylating RBOHD (Dubiella et al., 2013; Gao et al., 2013; Kadota et al., 2014). This would indicate that, upon flg22 perception, Ca^{2+} regulates RBOHD-dependent ROS via CDPKs. However, it was recently shown that, in response to PAMPs, RBOHD is also regulated in a Ca^{2+}-independent manner by BIK1 (Kadota et al., 2014; Li et al., 2014b). BIK1-dependent phosphorylation of RBOHD was found important for PAMP-dependent stomatal closure and immunity towards weakly virulent bacteria (Kadota et al., 2014; Li et al., 2014b). This dual regulation of RBOHD has been integrated into a model where, upon PAMP perception, BIK1-dependent RBOHD phosphorylation happens first, and further "primes" Ca^{2+}-dependent RBOHD regulation (Kadota et al., 2014; Li et al., 2014b).

1.2.1.1.4 MAPK activation

Protein phosphorylation is a widespread post-translational modification that controls protein activity, and, as described earlier, has a fundamental role in plant immunity (Benschop et al., 2007; Nühse et al., 2007; Rayapuram et al., 2014). Similar to other proteins involved in plant immunity (*i.e.* FLS2 and BAK1), MAPKs are activated by sequential and hierarchical phosphorylation and contribute to signal transduction following PAMP perception (Meng and Zhang, 2013). Activation of MAPK involves three different types of proteins: MAP KINASE KINASE KINASE (MAPKKK/MEKK), MAP KINASE KINASE (MAPKK/MKK) and MAP KINASE (MPK) (Meng and Zhang, 2013). Two different MAPK cascades are activated following PAMP perception. One cascade comprises MKK4 and MKK5, and MPK3 and MPK6 (Asai et al., 2002; Ren et al., 2002), whereas the second cascade includes MEKK1, MKK1 and MKK2, and MPK4 and MPK11 (Ichimura et al., 2006; Nakagami et al., 2006; Suarez-Rodriguez et al., 2007; Qiu et al., 2008a; Bethke et al., 2011; Eschen-Lippold et al., 2012; Kong et al., 2012).

Although no evidence has been documented so far on how activation of the ligand-induced receptor complex formation and the MAPK cascades are linked, the role of MAPKs in signal transduction and immunity after PAMP perception is believed to contribute to the transcriptional reprogramming happening during PTI (Meng and Zhang, 2013; Bigeard et al., 2015). For example, ETHYLENE RESPONSE FACTOR 104 (ERF104) interacts with MPK6 and their interaction is disrupted upon flg22 perception, allowing ERF104-mediated gene expression (Bethke et al., 2009). As flg22 induces ET biosynthesis (Felix et al., 1999), it could be possible that this happens via ERF104. Similarly, the transcription factor WRKY33 was found in a complex MPK4 and MAP KINASE SUBSTRATE 1 (MKS1) (Qiu et al., 2008b). Upon flg22 perception, MPK4 phosphorylates MKS1, which is released with WRKY33 from the complex, which then induces the expression of *PHYTOALEXIN DEFICIENT 3 PAD3*, a camalexin biosynthetic gene (Andreasson et al., 2005; Qiu et al., 2008b).

1.2.1.1.5 Transcriptional reprogramming

Upon flg22 treatment, about 1,000 genes are up-regulated, and 202 down-regulated (Navarro et al. 2004; Zipfel et al. 2004). Up-regulated genes can be categorized as genes involved in signal perception, signal transduction and transcription factors. In addition, a small set of genes are potentially involved in synthesis of antimicrobials (Navarro et al. 2004; Zipfel et al. 2004). WRKY transcription factors are a class of transcription factors that are rapidly up-regulated upon PAMPs/pathogen perception (Dong et al., 2003). They bind to the W-box motif in target promoters and they are either positive or negative modulators of gene expression. The W-box motif is over-represented in flg22-induced genes, suggesting that flg22-dependent induction of transcription factors from the WRKY family is required to amplify the signal and mount plant defences (Dong et al., 2003; Navarro et al. 2004; Zipfel et al., 2004; Ishihama and Yoshioka, 2012). For example, in Arabidopsis, *WRKY22* and *WRKY29* are induced by flg22 and are positive regulators of immunity downstream of MPK3 and MPK6 (Asai et al., 2002). Moreover, *WRKY18*, *WRKY40* and *WRKY60* are induced by *Pto* DC3000 infection and they act redundantly as negative regulators of immunity (Chen and Chen, 2002; Xu et al., 2006b).

1.2.1.1.6 Stomatal closure

Stomata are natural openings on the plant surface that are used for transpiration and entry of carbon dioxide for photosynthesis. Stomata are defined by a pair of guard cells that can actively open and close in response to different exogenous stimuli (Arnaud and Hwang, 2015). In addition, stomata provide a perfect entry point for bacteria to reach the apoplastc compartment (Melotto et al., 2008). However, stomata are not just passive entry points on the leaf surface for potential pathogens. In fact, stomata have been shown to close in response to pathogens or flg22, and to actively

contribute to immunity (Melotto et al., 2008). In support of the active role of stomata in antibacterial immunity, it was demonstrated that *Pto* DC3000 can induce re-opening of stomata by secreting the toxin coronatine (COR) (Melotto et al., 2006). Accordingly, the *Pto* DC3000 COR-deficient strain is weakly virulent on Arabidopsis after surface-inoculation (Zeng and He, 2010). Furthermore, *Pto* DC3000 COR$^-$ becomes fully virulent in *fls2* mutants, suggesting that FLS2 has a major role in stomata-mediated defence responses and that stomata contribute to immunity against bacteria (Zeng and He, 2010). What is less clear is the mechanism through which flg22 perception leads to stomatal closure.

PAMP-triggered stomatal closure shares many components with the well-characterized abscisic acid (ABA)-dependent stomatal closure, which controls stomata in response to abiotic stresses like drought, although the two pathways function independently (Joshi-Saha et al., 2011; Montillet et al., 2013). In ABA-dependent stomatal closure, ABA inhibits H$^+$ efflux and promotes anion efflux, leading to membrane depolarization and consequent activation of K$^+$ channels for extrusion of K$^+$ (McLachlan et al., 2014). Stomatal opening is triggered by the opposite mechanism and induces K$^+$ uptake (McLachlan et al., 2014). Perception of flg22 in guard cells has been shown to regulate these K$^+$ fluxes, thereby inducing stomatal movement (Zhang et al., 2008). H$^+$ fluxes are controlled by H$^+$-ATPases, and it was demonstrated that constitutive expression of AHA1 affects flg22-induced stomatal closure (Merlot et al., 2007; Liu et al., 2009). Although the mechanism through which PAMP perception leads to stomatal closure is not clear yet, flg22 can affect K$^+$ fluxes and H$^+$-ATPase activity. This would indicate that, similarly to ABA, flg22 could control stomatal closure by modulation of ion fluxes.

1.2.1.1.7 Receptor endocytosis

Protein endocytosis is a very well-known mechanism used in eukaryotic cells to regulate the abundance of plasma-membrane localized proteins upon external stimuli (Murphy et al., 2005). In Arabidopsis, FLS2 is internalized and degraded after flg22 perception (Robatzek et al., 2006; Lu et al., 2011; Smith et al., 2014). Flg22-dependent endocytosis decreases levels of FLS2 within 40 minutes from PAMP perception (Beck et al., 2012a; Smith et al., 2014) and if the plant tissue is re-elicited after this time, it is incapable of inducing ROS burst or MAPK activation (Smith et al., 2014). This would suggest that endocytosis of FLS2 leads to its degradation and desensitization to additional flg22 stimulus.

One long-lasting question is whether FLS2 endocytosis contributes to intracellular signalling. Treatment with Wortmannin and Tyrphostin A23, two inhibitors of vesicular trafficking, reduces flg22-dependent FLS2 endocytosis and affects the flg22-dependent ROS burst, but not MAPK activation (Robatzek et al., 2006; Beck et al., 2012; Smith et al., 2014). However, Tyrphostin A23 is also a tyrosine kinase inhibitor (Levitzki and Mishani, 2006) and its effect on flg22-dependent responses was shown to be dependent on the inhibition of tyrosine phosphorylation (Smith et al., 2014).

Ubiquitination of plasma membrane localized protein has been shown to lead to endocytosis and vacuolar degradation (Scheuring et al., 2012). FLS2 contains a PEST motif, which is usually involved in ubiquitin-triggered receptor endocytosis (Haglund et al., 2003). Accordingly, mutation of the PEST motif in FLS2 affects flg22-dependent FLS2 endocytosis (Robatzek et al., 2006). Treatment with MG132, a proteasome inhibitor, also compromises FLS2 internalization, and FLS2 was shown to be degraded via PUB12/13-mediated polyubiquitination (Robatzek et al., 2006; Lu et al., 2011). However, mutation of the PEST motif does not affect PUB12/13-mediated FLS2 ubiquitination *in vitro*, suggesting that PUB12/13-mediated FLS2 degradation is not involved in FLS2 endocytosis (Li et al., 2014a).

Once proteins are marked for endocytosis with ubiquitin, the ENDOSOMAL SORTING COMPLEX REQUIRED FOR TRANSPORT (ESCRT) is responsible for sorting to late endosome (LE)/multivesicular compartment (MVB) (Reyes et al., 2011). Endocytosed FLS2 was shown to co-localize and co-purify with VACUOLAR PROTEIN SORTING 37-1 (VPS37-1), one of the subunits of the ESCRT complex (Choi et al., 2013; Spallek et al., 2013). Mutation of *VPS37-1* affects flg22-dependent FLS2 endocytosis and stomatal closure, and leads to enhanced susceptibility to *Pto* DC3000 (Spallek et al., 2013). This showed for the first time the role of FLS2 endosomal sorting in flg22-dependent stomatal closure.

1.2.1.1.8 Callose deposition

Callose is a β-1,3-glucan polymer deposited between the plasma membrane and the cell wall in response to different stresses, which has been proposed to create a physical barrier against invading bacteria (Boller and Felix, 2009; Nicaise et al., 2009). POWDERY MILDEW RESISTANT 4 (*PMR4*) encodes a callose synthase responsible for flg22-dependent callose deposition, which is one of the measurable outputs for PTI (Jacobs et al., 2003; Nishimura et al., 2003; Kim et al., 2005). Mutation of *PMR4* abolishes flg22-dependent callose deposition, but, surprisingly, leads to increased resistance to *Pto* DC3000 (Nishimura et al., 2003; Flors et al., 2008). However, the Arabidopsis *pmr4* mutant has high SA due to constitutive up-regulation of genes involved in SA biosynthesis and signalling, which could explain the enhanced resistance towards *Pto* DC3000 (Nishimura et al., 2003). Intriguingly, *pmr4* was found to be more susceptible to *Pto* DC3000 *hrcC*⁻, a non-pathogenic strain of *Pto* DC3000 that cannot deliver effectors inside the plant cell, suggesting a role for callose in PTI (Kim et al., 2005). However, recent work showed that *pmr4* is more resistant to *hrpA*⁻, another non-pathogenic strain of *Pto* DC3000 (Forcat et al., 2010). This enhanced resistance of *pmr4* to bacteria was shown to correlate with increased levels of indole carboxylic acid and *p*

hydroxybenzaldehyde at the cell wall, which could contribute to strengthen the cell wall in response to bacteria (Forcat et al., 2010).

1.2.1.1.9 PAMP-induced resistance

Pre-treatment with flg22 induces resistance to *Pto* DC3000 (Zipfel et al., 2004). This resistance is broad spectrum, as pre-treatment with bacterial flg22 can protect from *Botrytis cinerea* and *Hyaloperonospora arabidopsidis* (*Hpa*) infection (Ferrari et al., 2007; Fabro et al., 2011), and flg22 can reduce *A. tumefaciens*-dependent T-DNA transformation (Zipfel et al., 2006).

Although the mechanism whereby flg22 induces resistance to subsequent bacterial challenge is still unknown, some molecular components required for this response have been described. *FLS2* expression is controlled by the ET-responsive transcription factors ETHYLENE-INSENSITIVE 3 (EIN3) and EIN3-LIKE (EIL3) (Boutrot et al., 2010). ETHYLENE-INSENSITIVE 2 (EIN2) is a key component of ET signalling (Alonso et al., 1999) and its mutation, which affects EIN3 and EIL3 accumulation, also affects flg22-induced resistance *to Pto DC3000* (Boutrot et al., 2010; Mersmann et al., 2010). Therefore, precise transcriptional regulation of *FLS2* expression is necessary for its accumulation at the plasma membrane and its functionality.

In addition to PAMP receptors, components of the receptor complex are also important for PAMP-induced resistance. In fact, alterations in the co-receptor BAK1 or in the regulatory kinase BIK1 affect flg22-induced resistance to *Pto* DC3000 (Shan et al., 2008; Lu et al., 2010; Zhang et al., 2010). This indicates that correct assembly of the receptor complex is necessary for full downstream signalling and flg22-induced resistance. Nonetheless, the functionality of member of the receptor complex is required for flg22-induced resistance. In fact, mutations in phosphorylation sites important for PAMP-dependent BIK1 function affect flg22-induced resistance to *Pto* DC3000 (Lin et al., 2014). Consistently, enhanced BAK1 phosphorylation caused by

mutation of the PP2A subunits A1, B'η, and C4, which negatively regulate BAK1, leads to enhanced flg22-induced resistance to bacteria when compared to wild-type plants (Segonzac et al., 2014).

Although the correct formation and activation of the PAMP receptor complex at the plasma membrane is of paramount importance for PAMP-induced resistance, signalling components are also required for the full establishment of induced immunity. The double mutant *cpk5 cpk6* is affected in flg22-induced resistance to *Pto* DC3000, which is even more compromised in the triple mutant *cpk5 cpk6 cpk11* (Boudsocq et al., 2010). This indicates that impairment in CDPK-dependent downstream signalling affects PAMP-induced resistance. However, the downstream signalling also depends on MAPK activation and ROS. Therefore impairment of one branch only partially compromises PAMP-induced resistance, as the signalling can still be transduced via alternative pathways.

Another component of PAMP-induced resistance is SUPPRESSOR OF BIR1-1 2 (*SOBIR2*), which encodes the *ARABIDOPSIS G PROTEIN B-SUBUNIT 1* (*AGB1*) (Liu et al., 2013a). In animals, G proteins comprise α-, β-, and γ-subunits and perceive external signals via a seven-pass transmembrane G PROTEIN-COUPLED RECEPTOR (GPCR) (Urano and Jones, 2014). Upon ligand-binding, GPCR activates the G protein, inducing separation of the α-subunit from the βγ dimer, which then independently interact with downstream components for signalling (Urano and Jones, 2014). In Arabidopsis, there is one α subunit (GPA1), one β subunit (AGB1) and three γ subunits (ARABIDOPSIS G PROTEIN γ-SUBUNIT1 [AGG1], AGG2, and AGG3), but no canonical GPCRs (Urano and Jones, 2014). Mutation of *SOBIR2*/*AGB1* affects flg22-induced resistance to *Pto* DC3000 (Liu et al., 2013a). Interestingly, in the double mutant *agg1 agg2* is also compromised in induced resistance to *Pto* DC3000 triggered by flg22 (Liu et al., 2013a). However, mutation in the α subunit *GPA1*, which is required for flg22-induced K^+ influx and efflux during stomatal closure/opening, does not affect PAMP-induced resistance (Liu et al., 2013a; Zhang et al., 2008). This

suggests that the Gβ and two Gγ subunits contribute to integrate the signal leading to PAMP-induced resistance downstream of FLS2 (Liu et al., 2013a). Yet, no interaction has been found between these components. *agb1* and *agg1 agg2* mutants are also compromised in PAMP-dependent ROS and MPK4, but not MPK3 and MPK6, activation (Liu et al., 2013a). However, when PAMP-dependent MPK4 activation is compromised, PAMP-dependent ROS production is unaffected. Therefore, it is likely that plant G protein subunits β and γ contribute to PAMP-induced resistance dependent on different signalling cascades (Zhang et al., 2012).

Hormones also contribute to full activation of PAMP-induced resistance. Flg22 induces ET production (Felix et al., 1999). In addition, flg22 activates MPK6 (Nühse et al., 2000; Asai et al., 2002), which phosphorylates and activates the ET biosynthetic enzymes 1-AMINOCYCLOPROPANE-1-CARBOXYLIC ACID SYNTHASE 2 (ACS2) and ACS6, and EIN3 (Liu and Zhang, 2004; Yoo et al., 2008). Because EIN3 regulates *FLS2* expression levels (Boutrot et al., 2010), flg22-triggered ET production plays a role in maintaining optimal levels of FLS2, and therefore optimal signalling and PAMP-induced resistance. In addition, ET acts synergistically with SA and JA for full flg22-induced resistance to *Pto* DC3000 (Tsuda et al., 2009). In fact, a quadruple mutant which is blocked in JA-, ET- and SA- dependent pathways (*dde2 ein2 sid2 pad4*) is strongly affected in this response (Tsuda et al., 2009).

1.2.1.1.10 Trade-offs between immunity and growth, and cross-talk between hormone and PTI signalling

Among all the physiological responses triggered by PAMP perception, constant exposure of Arabidopsis seedlings to PAMPs often leads to SGI (Gómez-Gómez et al., 1999; Zipfel et al., 2006). Although the mechanism underlying SGI is still not known, trade-off between growth and immunity

allows the plant to properly allocate its resources according to the external stimuli (Pieterse et al., 2012). The opposite effect is exerted by BRs that negatively affect PTI (Albrecht et al., 2012; Belkhadir et al., 2012). BRs are perceived at the plasma membrane by BRI1 and its co-receptor BAK1 (Li et al., 2002; Nam and Li, 2002). As BAK1 is also a co-receptor of FLS2 and possibly many more PRRs, it was hypothesized to be a limiting factor between BR- and PAMP-dependent responses (Chinchilla et al., 2007; Heese et al., 2007; Sun et al., 2013a). Although Belkhadir et al. (2012) suggested a partial BAK1-dependent inhibition of PTI responses upon BR perception, further work indicated that the inhibition was not dependent on BAK1 (Albrecht et al., 2012; Lozano-Durán et al., 2013; Malinovsky et al., 2014a). In addition, FLS2 associates with the cytoplasmic kinase BSK1 (Shi et al., 2013). BSK1 was initially characterized as a substrate of BRI1 and has a role in BR-downstream signalling (Tang et al., 2008). BSK1 is a positive regulator of flg22-triggered PTI, although its role in the cross-talk between the two pathways has not been elucidated (Shi et al., 2013). Comparatively, BRI1 associates with BIK1, which has a role as negative regulator of BR-dependent signalling (Lin et al., 2013). Association and dissociation of BIK1 from BRI1 does not require BAK1, suggesting it may exert different functions in the two pathways (Lin et al., 2013).

BRASSINAZOLE-RESISTANT 1 (BZR1) is a transcription factor which mediates BR-dependent transcriptional responses (He et al., 2002; Wang et al., 2002). Constitutive activation of BZR1 leads to inhibition of a subset of PAMP-dependent responses, which do not include MAPK activation (Lozano-Durán et al., 2013). In addition, BZR1 interacts with WRKY40. Arabidopsis *wrky40* mutants show enhanced resistance to *Pto* DC3000 and impairment in the BR-mediated suppression of PAMP-triggered ROS, suggesting that the association of BZR1 and WRKY40 leads to activation of a set of transcription factors to suppress PTI (Lozano-Durán et al., 2013). Repression of PTI at the level of transcription is also mediated by the transcription factor HOMOLOG OF BRASSINOSTEROID ENHANCED EXPRESSION 2 INTERACTING

WITH IBH1 (HBI1), which is also a target of BZR1 (Sun et al., 2010; Fan et al., 2014; Malinovsky et al., 2014a). HBI1 transcription and protein accumulation is induced by BR treatment and HBI1 is a positive regulator of BR-dependent responses (Fan et al., 2014; Malinovsky et al., 2014a). Accordingly, *HBI1* expression is down-regulated following PAMP perception, as well as the expression of its close homologs *BRASSINOSTEROID ENHANCED EXPRESSION 2* (*BEE2*) and *CRYPTOCHROME-INTERACTING BASIC HELIX-LOOP-HELIX* (*CIB1*) (Fan et al., 2014; Malinovsky et al., 2014a). When over-expressed, *HBI1* reduces the PAMP-dependent ROS burst, SGI, induction of marker genes, and leads to enhanced susceptibility to virulent and hypo-virulent strains of *Pto* DC3000 (Fan et al., 2014; Malinovsky et al., 2014a). Therefore BR-dependent induction of HBI1 accumulation mediates inhibition of PAMP-dependent responses. This indicates that HBI1, together with BRZ1, plays a role in the cross-talk between growth and immunity.

The BR-biosynthetic pathway works together with the gibberellin (GA)-dependent pathway to control plant growth. When seedlings germinate in the dark, hypocotyl elongation is induced. This phenomenon, called etiolation, depends on the interaction between BZR1 and the PHYTOCHROME-INTERACTING FACTOR 4 (PIF4), which accumulates in the dark (Bai et al., 2012; Oh et al., 2012). BZR1 and PIF4 together regulate a large set of genes, including genes for cell elongation (Oh et al., 2012). GA-dependent growth is negatively controlled by DELLA proteins (Peng et al., 1997; Silverstone et al., 1998). When GA is perceived by its receptor GIBBERELLIN INSENSITIVE DWARF 1 (GID1), DELLAs are degraded (Silverstone et al., 2001). DELLAs bind to and inhibit BZR1 and PIF4; perception of GA relieves this inhibition and cell elongation is induced (Bai et al., 2012; Gallego-Bartolomé et al., 2012; Li et al., 2012; Oh et al., 2012). Consistently, PAMP-dependent SGI is inhibited when seedlings are grown in the dark in a BR-dependent manner. Co-treatment with brassinolide and GA enhances the suppression of SGI (Lozano-Durán et al., 2013). In addition,

flg22 reduces DELLA degradation and DELLA stabilization reduces flg22-triggered SGI (Navarro et al., 2008).

Cross-talk between immunity and auxins has been also described. Several pathogens, including many *Pseudomonas* species, can synthesize auxins or manipulate the auxin-dependent pathway to promote disease (Fett et al., 1987; Glickmann et al., 1998). In addition, *Pto* DC3000 induces promotion of auxin biosynthetic genes and indolic acetic acid (IAA) levels increase during *Pto* DC3000 infection; accordingly, exogenous application of 1-naphthaleneacetic acid (NAA) enhances Arabidopsis susceptibility to *Pto* DC3000 (Navarro et al., 2006; Thilmony et al., 2006; Chen et al., 2007). Conversely, flg22 treatment inhibits the auxin biosynthetic pathway, at least via microRNA-mediated down-regulation of auxin receptors, although other mechanisms probably also play a role (Navarro et al., 2006).

1.2.1.2 EF-Tu and EFR

EF-Tu is another bacterial elicitor of plant defence responses (Kunze et al., 2004). EF-Tu is highly abundant in bacteria, where it has an important role in binding many aminoacyl-tRNAs and catalysing their incorporation into the forming peptide chain (Kunze et al., 2004). As flagellin, the N-terminus of EF-Tu is recognized in Arabidopsis, with the first 18 amino acids (elf18) being the minimal epitope possessing the same activity as the full length protein (Kunze et al., 2004). Although EF-Tu is a cytoplasmic protein, it has been detected in the secretome of different bacteria, suggesting that it may be released outside the cell by an as yet unknown mechanism (Zipfel et al., 2006).

In Arabidopsis, EF-Tu is recognized by EF-TU RECEPTOR (EFR), a LRR-RLK belonging to the same subfamily of LRR-RLKs as FLS2 (Shiu and Bleecker, 2001; Zipfel et al., 2006). Recognition of EF-Tu is restricted to the

Brassicaceae family and, accordingly, EFR is not found in other plant families, indicative of recent evolution (Kunze et al., 2004; Zipfel et al., 2006; Boller and Felix, 2009). EFR has an extracellular LRR domain composed of 24 LRRs, a transmembrane domain and a C-terminal cytosolic kinase domain (Zipfel et al., 2006). While EFR is classified as a serine/threonine kinase, it was recently shown to be phosphorylated on tyrosine residues, suggesting that it has a dual-specificity kinase (Macho et al., 2014). The tyrosine residue Y836 in the EFR kinase domain was found to be critical for EFR activity and EFR-dependent immunity, as its mutation leads to impairment of elf18-induced resistance to *Pto* DC3000 (Macho et al., 2014).

Proper receptor accumulation at the plasma membrane is important for the correct establishment of PAMP-induced resistance. STROMAL-DERIVED FACTOR 2 (SDF2) is part of the endoplasmic reticulum involved in protein quality control (ER-QC) and is required for proper protein folding during EFR biogenesis (Nekrasov et al., 2009). Mutation of *SDF2* affects EFR accumulation, and reduces elf18-induced resistance to *Pto* DC3000 (Nekrasov et al., 2009). Therefore reduced levels of plasma membrane-localized EFR compromise PAMP-induced resistance to *Pto* DC3000, suggesting the existence of an optimal receptor threshold for full establishment of PTI. Glycosylation of EFR is also important for proper protein folding and localization (Häweker et al., 2010). Nonetheless, under-glycosylated EFR is unable to perceive its ligand elf18, suggesting that glycosylation could have a role in correct conformation of the ectodomain or in ligand-binding affinity (Häweker et al., 2010).

Treatment with elf18 induces a set of responses similar to those induced by flg22, yet co-treatment with the two peptides together does not induce enhanced responses (Kunze et al., 2004). However, a double *fls2 efr* mutant plant is more susceptible to *Pto* DC3000 compared to *fls2* and *efr* single mutants (Nekrasov et al., 2009). This indicates that the same pathogen can be perceived by different PRRs, which work additively in restricting pathogen growth.

1.2.1.3 The role of LysM receptors in chitin and peptidoglycan (PGN) perception

Chitin is the main component of fungal cell walls. Plant chitinases degrade fungal chitin into oligosaccharide fragments (*N*-acetylglucosamine (GlcNAc)), which can induce defence responses in monocot and dicot plants (Shibuya and Minami, 2001).

Arabidopsis can recognize GlcNAc-containing glycans via LysM-containing receptors (Gust et al., 2012). LysM domains were first discovered in bacterial enzymes with roles in the synthesis, modification, and degradation of the bacterial cell wall, which mediate the contact with the carbohydrate-based substrate (Buist et al., 2008). In Arabidopsis, CHITIN ELICITOR RECEPTOR KINASE 1 (CERK1)/ LYSM-CONTAINING RECEPTOR-LIKE KINASE1 (LYK1) and LYK5 are the receptors for chitin (Miya et al., 2007; Wan et al., 2008; Cao et al., 2014a). Mutation of *CERK1* or *LYK5* results in plants with enhanced susceptibility to fungal pathogens and impaired chitin-induced resistance to *Alternaria brassicicola* (Miya et al., 2007; Wan et al., 2008). As for flg22 and elf18, pre-treatment with chitin induces resistance *A. brassicicola*, which is lost in *cerk1* and *lyk5*, but can also restrict *Pto* DC3000 growth (Tanabe et al., 2006; Wan et al., 2008; Cao et al., 2014a).

Chitin octamers bind to both LYK5 and CERK1, although they have higher affinity for LYK5, suggesting that LYK5 is the main chitin receptor (Iizasa et al., 2010; Petutschnig et al., 2010; Liu et al., 2012b; Cao et al., 2014a). The current model proposes that LYK5 exists in the form of homodimers already prior to chitin perception (Cao et al., 2014a). Upon perception of chitin, CERK1 associates with LYK5 that is additionally required for CERK1 dimerization and phosphorylation (Cao et al., 2014a). Although LYK5 does not possess any kinase activity, it is required for CERK1 phosphorylation, which is a requisite for the activation of downstream signalling (Petutschnig et al., 2010; Cao et al., 2014a). This would suggest that LYK5 kinase domain

has major role in mediating the interaction with CERK1, which would be the receptor partner responsible for signal transduction.

In addition to LYK5 and CERK1, other members of the receptor complex have been identified, with a possible role as regulators rather than active receptors. LYK4 is another LysM RLK which constitutively interacts with CERK1 (Wan et al., 2012). Interestingly, LYK4 is also able to bind chitin *in vitro* (Petutschnig et al., 2010; Wan et al., 2012). However, its mutation does not lead to severe impairment in chitin-dependent signalling, as observed with *cerk1* and *lyk5* (Wan et al., 2012; Cao et al., 2014a). This would indicate that LYK4 may not have a primary role in chitin-binding, but rather contribute to chitin-dependent immunity as a member of the receptor complex (Wan et al., 2012). In addition, the LRR-RLK LYSM RLK1-INTERACTING KINASE 1 (LIK1) interacts with CERK1, from which it dissociates after chitin perception (Le et al., 2014). Because mutation of *LIK1* leads to enhanced chitin-triggered responses, including ROS and MAPKs activation, LIK1 may act as a negative regulator of CERK1 in chitin-dependent immunity (Le et al., 2014).

In contrast to FLS2 and EFR, BAK1 is not required for chitin-binding and chitin-dependent responses, suggesting that LysM receptors have evolved a different strategy for ligand binding and initiation of defence signalling (Shan et al., 2008; Gimenez-Ibanez et al., 2009a). However, co-immunoprecipitation experiments in Arabidopsis protoplasts indicate that BIK1, similarly to FLS2 and EFR, also interacts with CERK1, supporting its role as a substrate of multiple PRRs (Lu et al., 2010; Zhang et al., 2010).

LYSM DOMAIN CONTAINING GPI-ANCHORED PROTEIN 2 (LYM2) is required for chitin-dependent closure of plasmodesmata and resistance to *Botrytis cinerea* (Faulkner et al., 2013). Although LYM2 does not have a kinase domain, it does not require CERK1 for its function. Accordingly, chitin defence responses are not affected in the *lym2* mutant, suggesting that Arabidopsis has two chitin-dependent pathways that can act independently

from each other can follow two LYM2-dependent signalling differs from the chitin one (Shinya et al., 2012; Wan et al., 2012; Faulkner et al., 2013).

Comparison of transcriptomic data sets showed that there is a large overlap of genes upregulated by chitin octamers, flg22 and elf18, suggesting that different PAMP-dependent signalling convene to a common set of genes (Wan et al., 2008). However, genes down-regulated by bacterial PAMPs hardly overlap with those down-regulated by chitin, suggesting the existence of PAMP-specific downstream responses (Wan et al., 2008).

Interestingly, fungal chitin shares structural similarities with bacterial PGN. PGN is a component of the bacterial outer membrane, with the function of providing rigidity and structure (McDonald et al., 2005). PGN consists of chains of *N*-acetylmuramic acid (MurNAc) and GlcNAc, cross-linked by short peptides (McDonald et al., 2005). The sugar chain is the active epitope of Gram-positive bacteria PGN which is recognized in Arabidopsis (Gust et al., 2007). In contrast, the active epitope of Gram-negative bacteria PGN are muropeptides (Erbs et al., 2008). Arabidopsis can perceive Gram-positive and Gram-negative bacteria PGN and trigger typical PAMP-dependent responses, including extracellular alkalinisation, Ca^{2+} influx, and activation of MAPKs, indicating that PGN is a *bona fide* PAMP (Gust et al., 2007; Erbs et al., 2008).

In Arabidopsis LysM domain proteins LYM1 and LYM3 bind to both Gram-negative and Gram-positive bacterial PGNs (Willmann et al., 2011; Liu et al., 2012a). CERK1 was found to be co-receptor of LYM1 and LYM3 and is required for PGN-dependent defences (Willmann et al., 2011). Because LYM1 and LYM3 do not possess a cytoplasmic kinase, CERK1 could be their kinase partner to transduce the signalling, although direct interaction between the three receptors has not yet been shown (Willmann et al., 2011). Because mutation of *CERK1* and *LYK4* was shown to cause enhanced susceptibility to *Pto* DC3000 without affecting flg22- and elf26-dependent gene expression, it would suggest that CERK1 and LYK4 could contribute to

PGN-dependent immunity (Gimenez-Ibanez et al., 2009a, 2009b; Wan et al., 2012). Similarly, *LIK1* mutation leads to enhanced resistance to *Pto* DC3000 and enhanced ROS production in response to flg22 and elf26, other than chitin, suggesting a role of LIK1 as negative regulator of multiple PAMPs (Le et al., 2014).

Transcriptomic data indicates that the changes in gene expression in response to *Staphylococcus aureus* PGN and flg22 strongly overlap, suggesting that the two PAMP-dependent signaling pathways converge to a common transcriptional reprogramming (Gust et al., 2007). Altogether, this demonstrates that perception of the structurally related PAMPs chitin and PGN depends on common LysM-containing receptors, indicating that plants have evolved a common strategy to bind to and recognize related elicitors from different organisms. However, chitin- and PGN-triggered medium alkalinisation and gene expression follows different induction patterns (Gust et al., 2007). This would suggest that, despite being structurally similar and relying on common receptors, chitin and PGN act via different mechanisms and/or different kinetics.

1.2.1.4 DAMPs

1.2.1.4.1 AtPeps

In addition to pathogen-derived elicitors, plants also perceive endogenous signals derived from damage or wounding caused by the pathogen (Zipfel, 2014). One example includes AtPeps, which are presumably cleaved from precursor PROPEPs (Huffaker et al., 2006; Yamaguchi et al., 2006). In Arabidopsis there are seven AtPep paralogs (Huffaker et al., 2006). AtPeps are perceived by the LRR-RLK receptors PEP RECEPTOR 1 (PEPR1) and PEPR2 (Yamaguchi et al., 2006; Krol et al., 2010; Yamaguchi et al., 2010). PEPR1 binds AtPeps1 to 6, whereas PEPR2 specifically bind AtPep1 and

AtPep2 (Yamaguchi et al., 2006; Krol et al., 2010; Yamaguchi et al., 2010). Expression of *PROPEP*s and *PEPR* receptors is induced by both flg22 and elf18 (Huffaker et al., 2006). Like FLS2 and EFR, PEPR1 and PEPR2 also interact with BAK1, which is phosphorylated in response to AtPep1 (Postel et al., 2010; Schulze et al., 2010). BIK1 also interacts with and is phosphorylated by PEPR1 (Liu et al., 2013). Furthermore, perception of AtPep1 triggers plant responses which closely resemble canonical PTI responses, including generation of ROS, defence gene expression, and induced resistance to *Pto* DC3000, which is PEPR1/PEPR2-dependent (Krol et al., 2010; Yamaguchi et al., 2010). Taken together, this evidence supports a role of AtPeps in plant immunity.

Recent work has shed the light on how AtPeps contribute to PTI. The working model indicates that ET biosynthesis, which is induced upon PAMP perception, could promote AtPeps production and AtPeps-dependent signalling to amplify immunity via BIK1 (Zipfel, 2013). This model is supported by several evidences. Firstly, expression *PROPEP1* and *PROPEP2* is induced by ET (Tintor et al., 2013). In addition, the triple mutant is severely affected in elf18-induced resistance to *Pto* COR- (Tintor et al., 2013). However, *EFR* transcript levels in *ein2-1* are comparable to WT, indicating that the susceptibility phenotype of *ein2-1 pepr1 pepr2* is not due to reduced *EFR* expression (Tintor et al., 2013). Therefore this would rather indicate that ET has a role in EFR-dependent immunity via PEPR1/2. Because ET also induces BIK1 phosphorylation (Laluk et al., 2011), and BIK1 interacts with PEPR1 and contributes to ET-dependent defence responses (Liu et al., 2013b), BIK1 could be the link between ET, PEPR1/2 and EFR. In fact, *bik1* mutants are affected in AtPep-induced defence responses, including induced resistance to *B. cinerea* (Liu et al., 2013b), and ET- and AtPep-dependent BIK1 phosphorylation is abolished in *pepr1 pepr2* (Liu et al., 2013b). Therefore induction of However PEPR1/2 and ET also contribute to EFR-dependent immunity independent of each other (Zipfel, 2013).

1.2.1.4.2 Oligogalacturonides (OGs)

OGs are released by the activity of plant extracellular polygalacturonase-inhibiting proteins (PGIPs) (Ferrari et al., 2013). PGIPs recognize and limit the activity of fungal polygalacturonases on the plant cell wall (Cervone et al., 1989). OGs can induce canonical defence responses, including a ROS burst, defence gene induction and resistance to *B. cinerea* (Ferrari et al., 2007). Their elicitor activity depends on their length (degree of polymerization), and the level of methyl-esterification (Ferrari et al., 2007; Denoux et al., 2008; Galletti et al., 2008; Hématy et al., 2009). In Arabidopsis, OGs are perceived by the EGF-containing receptor WALL-ASSOCIATED KINASE 1 (WAK1) (Decreux et al., 2006; Brutus et al., 2010).

Transcriptomic analysis comparing OGs- and flg22-dependent gene expression showed that both elicitors induce a high number of common genes at one hour post-treatment, whereas the response to the two elicitors diverged at three hours (Denoux et al., 2008). The major difference was in the number of induced genes, which was higher upon flg22 treatment, and in the amplitude of the induction, which was greater upon flg22 treatment (Denoux et al., 2008). Moreover, OGs-dependent gene expression returned to basal levels within three hours post-treatment, whereas flg22-dependent gene expression was sustained and only returned to basal levels after 24 hours (Denoux et al., 2008). This finding would support the hypothesis that different elicitors trigger similar defence responses. However, the differences observed would suggest that they also diverge in the kinetics and/or in the threshold required for the induction of defence responses, which could be due to binding different receptors.

1.2.1.4.3 PAMP-induced secreted peptide 1 (PIP1)

PIP1 is cleaved from its precursor prePIP and can trigger PTI-like responses, including MAPK activation, defence gene expression and immunity to *Pto*

DC3000 (Hou et al., 2014). PIP1 binds to the LRR-RLK receptor RLK7 in Arabidopsis, which is required for PIP1- and PIP2-dependent responses. Moreover, PIP1 activity is partially dependent on BAK1 (Hou et al., 2014). Arabidopsis contains 11 prePIP homologs, and orthologs are present in different monocot and dicot plant species (Hou et al., 2014). Because of the similarities between PIP1 and AtPeps it was suggested that PIP1 could function to sustain or amplify FLS2-dependent responses (Hou et al., 2014). This hypothesis was based on the evidence that PIP precursors and *RLK7*, as *AtPeps*, are PAMP-inducible, and that flg22-induced resistance is impaired in *rlk7* mutant plants. However, PIP1-dependent responses do not depend on BIK1 (Hou et al., 2014). This would indicate that, although possibly contributing to the amplification of PTI, PIPs act via a distinct route compared to AtPeps.

1.2.1.4.4 Phytosulfokine-α

Additional endogenous peptides have been described to have a role in plant immunity. Phytosulfokine-α (PSK-α) is a growth-promoting plant-derived peptide which is perceived by the LRR-RLK PSK RECEPTOR 1 (PSKR1) to control cell proliferation and differentiation (Matsubayashi and Sakagami, 1996; Matsubayashi et al., 2002, 2006). PSK-α derives from precursor peptides via tyrosine sulfation and proteolytic cleavage (Yang et al., 1999; Srivastava et al., 2008; Komori et al., 2009). Six Arabidopsis genes encode precursors of PSK-α (Yang et al., 2001; Matsubayashi and Sakagami, 2006). Interestingly, PSKR1-dependent signalling negatively regulates PTI responses (Igarashi et al., 2012). For example, mutation of PSKR1 leads to enhanced elf18-triggered immunity to *Pto* DC3000 and elf18-dependent gene expression (Igarashi et al., 2012). This would suggest that growth-promoting hormones may have a role in keeping the balance between the plant growth and the defence system.

1.2.1.4.5 Adenosine 5′-triphosphate (ATP)

Adenosine 5′-triphosphate (ATP) is the source of energy in the cell. Mechanical damage can induce release of extracellular ATP (eATP) into the apoplast where, in animal cells, it is recognized by purinoreceptors (Cao et al., 2014b). Recently, the Arabidopsis receptor for ATP, DORN1/LecRK-I.9, was isolated (Choi et al., 2014). DORN1 binds to ATP with high affinity. It is required for ATP-dependent responses, including gene expression and MAPK activation (Choi et al., 2014). ATP was found to be released in the apoplast in response to damage and to induce defence-like responses (Choi et al., 2014). This would suggest that ATP could act as a DAMP when plant cells are damaged by mechanical injuries.

1.2.1.4.6 RAPID ALKALINIZATION INDUCING FACTOR (RALF)

The rapid alkalinization inducing factor (RALF) is a short peptide first isolated in tobacco (Pearce et al., 2001a). RALF induces extracellular alkalinisation and activation of MAPKs in tobacco and tomato cells (Pearce et al., 2001a, 2001b). It is widely present in different plant families and can inhibit root growth and development when applied exogenously to tomato and Arabidopsis seedlings (Pearce et al., 2001b). Recently, RALF was found to bind to FERONIA (FER), a *Catharanthus roseus*-like RLK (Haruta et al., 2014). Interestingly, flg22 induces FER phosphorylation, and FER is enriched in FLS2-containing detergent-resistant membranes (DRMs) (Benschop et al., 2007; Keinath et al., 2010). Although no direct evidence has been found so far, this would suggest that RALF could act as DAMP via FER.

1.2.2 PTI in other plant species

1.2.2.1 *Solanaceae*

1.2.2.1.1 Perception of bacteria

Flagellin and flg22 can be perceived in plants belonging to the *Solanaceae* family. Both tomato and *Nicotiana benthamiana* plants contain a FLS2 receptor, which shares high degree of homology with Arabidopsis FLS2 (Hann and Rathjen, 2007; Robatzek et al., 2007). However, tomato and other *Solanum* species can perceive a different flagellin epitope, flgII-28, which is recognized in a FLS2-independent manner (Clarke et al., 2013). This is another example of arms race between adapted pathogens successfully evolving their PAMPs to evade PTI, and the corresponding evolution of plants to detect a novel PAMP feature.

EFR is restricted to the *Brassicaceae* family (Zipfel et al., 2006). Nonetheless, transgenic expression of *EFR* in *N. benthamiana* and tomato leads to EF-Tu recognition, indicating that the downstream signalling after ligand perception is conserved in this plant species (Zipfel et al., 2006). This observation also led to the successful transfer of EFR from Arabidopsis to tomato and *N. benthamiana*, creating plants which gained resistance to several adapted pathogens (Lacombe et al., 2010).

1.2.2.1.2 Perception of fungi

1.2.2.1.2.1 EIX - LeEIX1/2

ETHYLENE-INDUCING XYLANASE (EIX) is a fungal β-1-4-endoxylanase isolated from cultures of the fungus *Thrichoderma viride* (Dean et al., 1989). Application of EIX to tobacco or tomato induces a wide array of responses characteristic of plant defences (Bailey et al., 1990; Avni et al., 1994). Receptors for EIX, *SlEIX1* and *SlEIX2*, were cloned in tomato (Ron and Avni,

2004). Both genes encode RLPs and can independently bind EIX (Ron and Avni, 2004). SlEIX1 and SlEIX2 form heterodimers upon EIX perception (Ron and Avni, 2004). SlEIX2 is endocytosed after ligand perception and inhibitor studies showed that blocking endocytosis blocked EIX-dependent signalling (Sharfman et al., 2011). SlEIX1 interacts with SlBAK1, which has a role in attenuating the response following elicitor perception (Bar et al., 2010).

1.2.2.1.2.2 Ave1 - Ve1

In tomato the RLP Ve1 confers resistance to *Verticillium dahliae* and *V. albo-atrium* race 1 and silencing of *BAK1* compromises Ve1-dependent resistance (Kawchuk et al., 2001; Fradin et al., 2009). A bioinformatics approach identified Avirulence on Ve1 (Ave1) as the putative ligand in tomato (Jonge et al., 2012).

RLPs lack an intracellular kinase domain, indicating that they require additional components to transduce the signalling downstream of PAMP perception. It is becoming apparent that the LRR-RLK SOBIR1 is fulfilling this function (Gust and Felix, 2014). In fact, SOBIR1 and SOBIR-like from tomato interact with several RLPs, including Cf-4, Ve1, and EIX2, and not, for example, with FLS2 or BAK1 (Liebrand et al., 2013). To further support the role of SOBIR1 and SOBIR1-like in RLP-dependent immunity, both were shown to be required for Cf-4 and Ve1-mediated resistance to *Cladosporium fulvum* and *V. dahliae*, respectively, (Liebrand et al., 2013).

1.2.2.2 Rice

1.2.2.2.1 Perception of bacteria

XA21 was the first PRR identified (Song et al., 1995). The protein confers resistance to *Xanthomonas oryzae* pv. *oryzae* race 6 (*Xoo*) in transgenic rice expressing the gene (Song et al., 1995). XA21 falls in the subclass XII of LRR-RLKs alongside FLS2 and EFR, and contains 23 LRRs in its extracellular domain (Shiu et al., 2004; Dardick and Ronald, 2006). The XA21 ligand is currently unknown.

Null mutations of the Arabidopsis *FLS2* receptor can be complemented by transgenic expression of *OsFLS2*, suggesting that flg22-FLS2-dependent signalling is conserved between dicots and monocots (Takai et al., 2008). This also indicates that recognition of flagellin is an ancient adaptation plants evolved as antibacterial strategy.

Rice does not recognize elf18, but it can recognize a different epitope in the central region of *Acidovorax avenae* EF-Tu (Furukawa et al., 2013). This would suggest that rice evolved independently a recognition system for this PAMP. However, transgenic expression of *EFR* in rice leads to gain of elf18 perception, which can activate elf18-dependent signalling and enhanced resistance to weakly virulent *Xoo* (Schwessinger et al., 2015). Similarly, transgenic expression of an EFR:XA21 chimera in Arabidopsis was also found to be functional in inducing elf18-dependent signalling and antibacterial immunity (Holton et al., 2015). Taken together, this would indicate that, despite relying on different and evolutionary distant receptors, monocots and dicots share common signalling pathway to mount immune responses against bacteria

Similar to Arabidopsis, one member of the OsSERK family, OsSERK2, contributes to immunity to bacteria in rice (Chen et al., 2014b). In fact, silencing of *OsSERK2* in transgenic XA21 rice disrupts resistance to *Xoo*.

Interestingly, in transgenic EFR rice, OsSERK2 was found to interact with EFR and contribute to elf18-triggered responses (Schwessinger et al., 2015). Moreover, silencing of *OsSERK2* impairs flg22-dependent, but not chitin-dependent, gene expression, which correlates with the dispensability of AtBAK1 for chitin-dependent responses in Arabidopsis (Chen et al., 2014b). This would support a role of OsSERK2 as key component of rice antibacterial immunity similar to AtBAK1 in Arabidopsis. However, differences between rice and Arabidopsis do exist. The interaction between OsSERK2 and XA21 or OsFLS2 is constitutive, and it requires a functional kinase of both partners (Chen et al., 2014b). This would indicate that a direct and non-ligand-dependent interaction between the two receptors is required for immunity, and that the kinase domains are pivotal for their function. To further support this hypothesis, it was shown that mutation of three phosphorylation sites in XA21 affects XA21 stability, reducing its accumulation and resistance to *Xoo* (Xu et al., 2006a).

Several proteins have been shown to interact with XA21, suggesting the existence of a receptor complex where partners appear to contribute to XA21 stability and accumulation. XA21-BINDING PROTEIN 25 (XB25) is part of the plant-specific ankyrin-repeat (PANK) family and interacts with the transmembrane domain of XA21 (Jiang et al., 2013). XB25 is weakly trans-phosphorylated by XA21 and *Xoo* challenge induces its accumulation. Reduction in *Xb25* expression leads to reduction in XA21 protein levels, suggesting a major role for XB25 in stabilizing XA21 after *Xoo* perception (Jiang et al., 2013).

The ATPase XB24 interacts with XA21 and is a negative regulator of XA21-mediated resistance, as it silencing causes enhanced resistance to *Xoo* in transgenic XA21 plants (Chen et al., 2010). The protein phosphatase 2C (PP2C) XB15 also interacts with and dephosphorylates XA21 (Park et al., 2008). XB15 mutation leads to spontaneous cell death and enhanced resistance to *Xoo* (Park et al., 2008). It is thought that both XB24 and XB15 control XA21 functionality by controlling its phosphorylation status.

Interestingly, in Arabidopsis, the orthologues of OsXB15 and OsXB24 can associate with EFR, and contribute to elf18-dependent signalling and resistance to bacteria (Holton et al., 2015). Furthermore, in transgenic rice expressing EFR, EFR and XB24 were found to interact (Schwessinger et al., 2015). This further supports the existence of conserved signalling pathway downstream of PRRs in monocots and dicots.

Another negative regulator of XA21 is the E3 ubiquitin ligase XB3, which interacts with the kinase domain of XA21 (Wang et al., 2006). Reduced expression of *XB3* leads to reduced accumulation of XA21 and compromised resistance to *Xoo* (Wang et al., 2006). Interestingly, OsWRKY62 is also a negative regulator of XA21-mediated resistance, which was shown to directly interact with XA21 (Peng et al., 2008). Although surprisingly, it was found that the XA21 intracellular domain is cleaved and translocated to the nucleus after infection, supporting the significance of the interaction (Park and Ronald, 2012).

1.2.2.2.2 LysM receptors involved in chitin and PGN perception in rice

In rice, chitin is perceived by CHITIN ELICITOR BINDING PROTEIN (OsCEBiP), a LysM-RLP (Ito et al., 1997; Kaku et al., 2006). OsCEBiP has an ectodomain characterized by two LysM domains and a short cytoplasmic tail, which lacks a kinase domain (Kaku et al., 2006). OsCEBiP requires OsCERK1 to activate downstream signalling, although OsCERK1 does not bind chitin (Shimizu et al., 2010). OsCEBiP binds to chitin octamers and upon chitin perception it forms homodimers (Shimizu et al., 2010; Hayafune et al., 2014). The two OsCEBiP receptors can simultaneously bind one chitin octamer, and the first LysM domain is essential for the binding (Hayafune et al., 2014). Upon ligand-binding, OsCERK1 dimers are recruited to form a heterotetramer with OsCEBiPs (Shimizu et al., 2010; Hayafune et al., 2014). Because silencing of CEBiP still retains residual chitin-dependent signalling,

it was postulated that rice should contain additional chitin receptors (Kaku et al., 2006). In fact, it was later found that LYSM-CONTAINING PROTEIN 4 (OsLYP4) and OsLYP6 bind chitin and together contribute to chitin-dependent responses (Liu et al., 2012a).

OsLYP4 and OsLYP6 are closely related to Arabidopsis LYM1 and LYM3, which bind PGN (Willmann et al., 2011; Liu et al., 2012a). Similarly, OsLYP4 and OsLYP6 have been shown to bind PGN (Liu et al., 2012a). OsLYP4 and OsLYP6 and are localized at the plasma membrane via glycosylphosphatidylinositol (GPI) anchor, suggesting the requirement of a partner kinase for transducing downstream signalling (Liu et al., 2012a). This partner kinase was found to be OsCERK1 (Liu et al., 2012a; Ao et al., 2014; Kouzai et al., 2014).

Altogether, this demonstrates that perception of structurally related chitin and PGN in rice and Arabidopsis depends on LysM-containing receptors. Although different receptors (CEBiP in rice and LYK5 in Arabidopsis) perceive chitin in different plant species, they both seem to require the same partner CERK1 (Cao et al., 2014a; Hayafune et al., 2014). Because CERK1 is also required for PGN-dependent signalling in both species, CERK1 appears to be the universal adaptor for transducing defence signalling upon perception of GlcNAc-containing PAMPs.

Similar to the role of the RLCK BIK1 in Arabidopsis, RLCKs appear critical regulators of PTI downstream of PRRs across plant species. In rice, OsRLCK185 and OsRLCK176 are substrate of OsCERK1 and mediate chitin-dependent defence responses (Yamaguchi et al., 2013a; Ao et al., 2014). However, differently from Arabidopsis, OsRLCK185 and OsRLCK176 seem to transduce signalling downstream of the receptor via MAPKs (Yamaguchi et al., 2013a; Ao et al., 2014).

1.3 Targeting of PTI by pathogenic effectors

Effector triggered-susceptibility is established when successful pathogens deploy effectors to counteract PTI and cause disease. *Pto* DC3000 uses the type-III secretion system (T3SS), a needle-like structure, to deliver effectors directly into the host cell (Roine et al., 1997; Kubori et al., 1998; Dou and Zhou, 2012). Bacterial strains defective in the T3SS are unable to multiply and cause disease on their host plants, confirming the significance of the effectors for bacterial pathogenicity (Yuan and He, 1996; Roine et al., 1997). In *Pto* DC3000 the effector repertoire includes 28 effectors (Collmer et al., 2009). These effectors can be individually deleted without penalty for the pathogen viability and its virulence (Collmer et al., 2009; Xin and He, 2013). In fact, deletion studies of *Pto* DC3000 effectors revealed the presence of two redundant effector groups which contribute synergistically to bacterial virulence (Kvitko et al., 2009). Moreover, a minimal set of effectors was found to be sufficient to support bacterial growth and disease with hierarchical roles in promoting virulence (Cunnac et al., 2011). Collectively this suggests that individual effectors are not sufficient for bacterial virulence, but they rather function in a cooperative and redundant way (Li et al., 2005; Oh and Collmer, 2005; Lindeberg et al., 2012).What follows is an overview of knowmechanisms of ETS triggered by bacterial T3SS effectors (Figure 1.3).
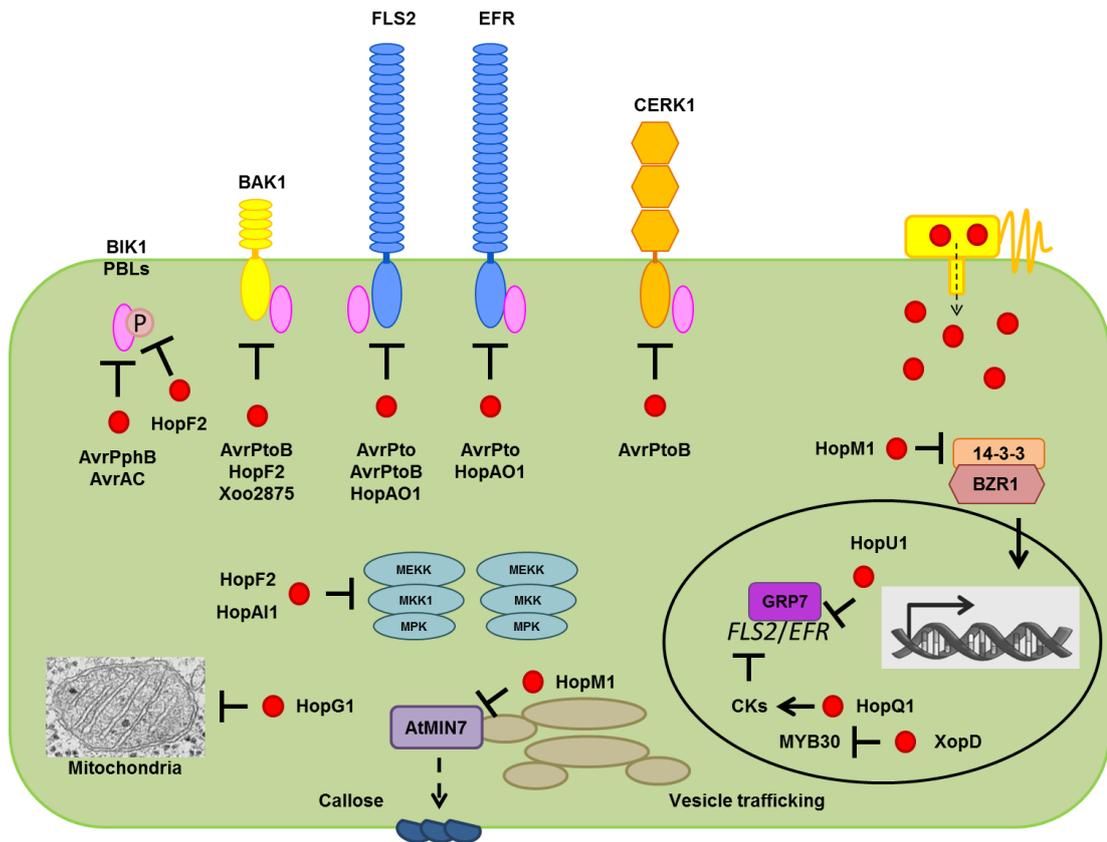
Figure 1.3. Overview of bacterial effector and their cellular targets during ETS.

Bacteria secrete their effectors inside the plant cell via the T3SS. Effectors target several key components of PTI, therefore disrupting immunity and promoting disease. Several effectors (Avrpto, AvrPtoB, HopAO1, HopF2, AvrPphB, AvrAC) target members of the receptor complex (FLS2, EFR, CERK1, BAK1, BIK1), while others promote disease by disrupting downstream signalling components (HopF2, HopAI1, HopM1) or by affecting transcription (HopM1, HopU1, HopQ1, XopD). The mitochondria picture was found in http://web.mit.edu/esgbio/www/.

The *Pto* DC3000 effector AvrPto interacts with FLS2 and EFR, and this interaction leads to inhibition of their kinase activities (Shan et al., 2008; Xiang et al., 2008; Zong et al., 2008; Xiang et al., 2010). Expression of *AvrPto* impairs FLS2-BAK1 association and affects flg22-dependent signalling (He et al., 2006; Shan et al., 2008; Xiang et al., 2008). Deletion of *AvrPto* from *Pto* DC3000 (Δa*vrPto*) reduces bacterial virulence in wild-type, but not in *fls2* plants, indicating that FLS2 is a main target of AvrPto (Xiang et al., 2008; Zong et al., 2008). AvrPto also interferes with FLS2-dependent

BIK1 phosphorylation (Xiang et al., 2011). Because AvrPto does not interact with BIK1, this effect is most likely caused by its inhibitory effect on FLS2 kinase activity (Xiang et al., 2011; Zhang et al., 2010).

Another *Pto* DC3000 effector that targets FLS2 is AvrPtoB (Göhre et al., 2008; Shan et al., 2008). The N-terminal region of AvrPtoB (aa 1-387) interacts with the kinase domain of FLS2, and, in addition, with BAK1 (Göhre et al., 2008; Shan et al., 2008). Structural data identified the AvrPtoB domain (aa 250-359) as specifically required for the interaction with BAK1 *in vitro* (Cheng et al., 2011). This domain interacts with the P+1 loop of BAK1, important for substrate binding and adjacent to the activation loop, whose phosphorylation activates BAK1 kinase activity (Cheng et al., 2011). Consistently, interaction of AvrPtoB with BAK1 inhibits BAK1 autophosphorylation *in vitro* (Cheng et al., 2011). However, it is unclear whether AvrPtoB possess catalytic activity to interfere with BAK1 phosphorylation (Cheng et al., 2011). Nonetheless, by binding a domain which is critical for BAK1 phosphorylation and functionality, AvrPtoB could simply hinder this domain and prevent binding of the actual substrate.

As in the case of AvrPto, deletion of AvrPtoB (Δa*vrPtoB*) reduces bacterial virulence, which can be restored to WT levels when bacteria are inoculated on *fls2* mutant plants (He et al., 2006; De Torres et al., 2006; Göhre et al., 2008). In agreement with this, AvrPtoB can suppress several flg22-dependent responses (He et al., 2006; De Torres et al., 2006; Gimenez-Ibanez et al., 2009a).

AvrPtoB has additional ubiquitin ligase activity *in vitro*, which is unrelated to its ability to block BAK1 phosphorylation (Abramovitch et al., 2006; Janjusevic et al., 2006; Shan et al., 2008). Mutation of the residues required for ubiquitin ligase activity reduces *Pto* DC3000 virulence in tomato (Janjusevic et al., 2006). Later, AvrPtoB was shown to mediate FLS2 degradation via ubiquitination (Göhre et al., 2008). Interestingly, AvrPtoB can additionally ubiquitinate EFR and BAK1, although BAK1 accumulation is not

altered (Göhre et al., 2008). Unlike AvrPto, AvrPtoB does not affect FLS2 and EFR kinase activity (Göhre et al., 2008). Remarkably, AvrPtoB also suppresses chitin-dependent responses through ubiquitination and degradation of CERK1 (Gimenez-Ibanez et al., 2009a). CERK1 is also involved in PGN perception (Gimenez-Ibanez et al., 2009a). Therefore AvrPtoB-dependent suppression of chitin responses is the consequence of the inhibitory activity of AvrPtoB on CERK1. A shorter version of AvrPtoB (aa 1-307) interacts with CERK1 and reduces its accumulation through proteasomal degradation (Gimenez-Ibanez et al., 2009a). In addition, AvrPtoB interacts with AVRPTOB TOMATO-INTERACTING 9 (Bti9), a tomato LysM-LRK, suggesting that AvrPtoB can target a broad spectrum of PRRs (Gimenez-Ibanez et al., 2009a; Zeng et al., 2012).

HopAO1 from *Pto* DC3000 possesses tyrosine phosphatase activity *in vitro* and contributes to bacterial virulence (Bretz et al., 2003; Espinosa et al., 2003). Arabidopsis plants expressing HopAO1 show reduced flg22-dependent responses, which do not include MAPK activation. This effect depends on its phosphatase activity (Underwood et al., 2007). It was recently shown that HopAO1 targets both EFR and FLS2, and inhibits elf18-dependent responses through reduction of EFR tyrosine phosphorylation (Macho et al., 2014).

HopU1 from *Pto* DC3000 has mono-ADP-ribosyltransferase activity and can suppress flg22-dependent callose deposition (Fu et al., 2007). Its substrates are glycine-rich RNA-binding proteins (GRPs), including GRP7 (Fu et al., 2007). GRP7 is part of the feedback regulation system of the circadian clock and can auto-regulate its abundance through binding and regulation of its own messenger RNA (Heintzen et al., 1997; Staiger et al., 2003). Mutation of GRP7 affects PAMP-dependent callose deposition and ROS production, and leads to enhanced susceptibility to *Pto* DC3000 (Fu et al., 2007; Jeong et al., 2011). A similar effect is caused by over-expression of *HopU1*, which also reduces FLS2 accumulation (Nicaise et al., 2013). GRP7 constitutively binds

FLS2 and *EFR* mRNAs. HopU1, through ADP-ribosylation of GRP7, disrupts this binding and thus affecting FLS2 protein levels (Nicaise et al., 2013).

Another *Pto* DC3000 effector with ADP-ribosyltransferase activity is HopF2 (Wang et al., 2010). HopF2 localizes at the plasma membrane via myristoylation, which is important for its activity (Robert-Seilaniantz et al., 2006; Wu et al., 2011). HopF2 has the ability to suppress a wide array of PAMP-dependent responses, including activation of MPK3, MPK6 and MPK4 (Li et al., 2005; Guo et al., 2009; Wang et al., 2010; Wu et al., 2011). HopF2 has been shown to target several MKKs, including MKK5, and mutation of the key residues for its ADP-ribosylation activity affects its ability to inhibit MAPKs activation and promote virulence (Singer et al., 2004; Wang et al., 2010; Wu et al., 2011). Although HopF2 inhibits BIK1, PBS1 and PBL1 phosphorylation, it does not interact with BIK1, indicating that HopF2 has an additional target upstream of BIK1 (Wu et al., 2011; Zhou et al., 2014). Interestingly, recent data showed that HopF2 interacts with BAK1. This interaction requires the transmembrane and the kinase domain of BAK1 and is independent of FLS2 (Zhou et al., 2014). The effector Xoo2875 from *Xoo* also interacts with OsBAK1, and its ectopic expression in rice leads to reduced resistance to *Xoo* infection (Yamaguchi et al., 2013b).

HopQ1 is a *Pto* DC3000 effector that was recently shown to affect *FLS2* expression (Hann et al., 2014). Arabidopsis plants expressing HopQ1 are impaired in flg22-dependent ROS production and MAPK activation and this effect is dependent on its nucleoside hydrolase domain (Hann et al., 2014). In addition, HopQ1 induces accumulation of cytokinins and expression of cytokinin-responsive genes. Exogenous application of cytokinins reduces *FLS2* expression and flg22-triggered ROS production and MAPK activation, suggesting that HopQ1 suppresses PTI responses by down-regulating *FLS2* expression through induction of cytokinin signalling (Hann et al., 2014). HopQ1 also interacts with multiple 14-3-3 proteins, which phosphorylate and stabilize HopQ1 (Giska et al., 2013; Li et al., 2013). Transgenic expression of

HopQ1 in tomato enhances susceptibility to virulent and avirulent strains of *Pto* DC3000 and reduces expression of *GRAS2* marker gene (Li et al., 2013).

Transgenic Arabidopsis plants expressing AvrPphB from *P. syringae* pv. *phaseolicola* are impaired in several PAMP-dependent responses. AvrPphB is a cysteine protease and was found to cleave several members of the family VII of RLCKs, including BIK1 (Shao et al., 2003; Zhang et al., 2010). AvrAC from *Xcc* also targets BIK1 (Feng et al., 2012). It was demonstrated that AvrAC interacts with and inhibits phosphorylation of BIK1. AvrAC is a uridine 5′-monophosphate (UMP) transferase that uridylylates BIK1 in conserved sites required for its phosphorylation and functionality. Uridylylation of BIK1 prevents its activation (Feng et al., 2012). PBL1 was also found to be uridylylated, suggesting that AvrAC also targets BIK1 homologues (Feng et al., 2012).

In addition to HopF2, HopAI1, a *Pto* DC3000 effector with phosphothreonine lyase activity, also targets MAPKs (Zhang et al., 2007). HopAI1 can suppress flg22-induced gene expression and callose deposition and contributes to *Pto* DC3000 virulence (Li et al., 2005; Zhang et al., 2007). HopAI1 directly binds to and dephosphorylates MPK3 and MPK6. Mutation of the residue required for HopAI1 enzymatic activity impairs HopAI1-dependent MAPK inactivation. Follow-up work showed that HopAI1 additionally interacts with MPK4 and inactivates flg22-dependent MPK4 activation (Zhang et al., 2012). Therefore, HopAI1 interferes with PTI by broadly impairing PAMP-dependent MAPKs activation. Interestingly, MPK4 is also target of AvrB, which induces, directly or indirectly, MPK4 phosphorylation, possibly to promote susceptibility through induction of JA (Cui et al., 2010).

HopG1 is a *Pto* DC3000 effector that is targeted to the mitochondria (Block et al., 2010). Constitutive expression of *HopG1* in Arabidopsis affects PTI responses and supports higher growth of the hypovirulent strain *hrcC-* of *Pto* DC3000. In addition, this effector impairs mitochondria respiration and

enhances the cellular accumulation of ROS, although the exact target of HopG1 is not known (Block et al., 2010).

HopM1 is a *Pto* DC3000 effector that is conserved among *P. syringae* pathovars and is a major determinant of bacteria virulence (Alfano et al., 2000; DebRoy et al., 2004; Badel et al., 2006). Among other plant proteins, HopM1 binds to *Arabidopsis thaliana* HopM1 interactor 7 (AtMIN7), an ADP ribosylation factor (ARF) guanine nucleotide exchange factor (GEF) protein that regulates vesicle trafficking and is required for flg22-dependent callose deposition, and targets it for proteasomal degradation (Nomura et al., 2006, 2011). Flg22 treatment increases AtMIN7 accumulation and mutation of AtMIN7 impairs the induced resistance to *Pto* DC3000 following flg22-pre-treatment, suggesting that HopM1-dependent degradation of AtMIN7 affects PTI (Nomura et al., 2006, 2011). Transgenic expression of *HopM1* in Arabidopsis reduces PAMP-dependent ROS and stomatal closure and allows higher growth of the hypovirulent COR⁻ strain of *Pto* DC3000 (Lozano-Durán et al., 2014). In addition, treatment with the proteasome inhibitor MG132 reduces the effect of HopM1 on these PTI responses, indicating that the ability of HopM1 to promote proteasomal degradation of plant targets underlies this effect. However, *atmin7* plants are not affected in PAMP-triggered ROS production or stomatal closure, supporting the idea that AtMIN7 is not the only target of HopM1, as previously indicated by interaction data (Lozano-Durán et al., 2014; Nomura et al., 2006). An additional target of HopM1 is AtMIN10, a 14-3-3 protein that can bind to the transcription factor BZR1 and sequester it to the cytoplasm, interfering with its transcriptional activity (Nomura et al., 2006; Gampala et al., 2007; Ryu et al., 2007). Transient expression of HopM1 in *N. benthamiana* induces BZR1 accumulation in the nucleus, which can be reverted by application of MG132, suggesting that HopM1-dependent degradation of 14-3-3 proteins promotes nuclear accumulation of BZR1. Accordingly, chemical disruption of 14-3-3 activity phenocopies transgenic expression of HopM1. It impairs PAMP-dependent ROS production, stomatal closure and nuclear accumulation of

BZR1. In addition, silencing of the AtMIN10 ortholog in tomato and *N. benthamiana* reduces PAMP-dependent ROS (Lozano-Durán et al., 2014).

1.4 Overview of the thesis

Establishment of PAMP-triggered immunity (PTI) confers broad spectrum disease resistance. Although the molecular events through which PTI develops upon recognition of PAMPs at the plasma membrane are beginning to be uncovered, the exact mechanism that eventually restricts pathogens growth is still largely unknown. Chapter 3 describes two different approaches that were employed to gain insight into the flg22-induced anti-bacterial resistance mechanism. A biased approach used reverse genetics to study the involvement of camalexin, glucosinolates and callose in flg22-induced resistance against bacteria, as they are three well known active defences Arabidopsis employs to restrict invasion by fungi and oomycetes. In addition, a novel genetic screen was set-up and carried-out as an unbiased approach to identify novel PTI components and/or "executors" of the induced resistance. The screen used flg22-induced resistance as read-out and aimed at identifying mutants impaired in this response among a collection of uni-mutant T-DNA insertion lines. In fact, with flg22-induced resistance being the latest measurable PTI output, it should be possible to uncover mutants with a role in the resistance mechanism, other than in the signalling pathway. The *pir* screen identified four loci whose mutation leads to a reproducible reduction of flg22-induced resistance. These genes have not been described for their role in immunity yet, and therefore can be considered as novel components of this pathway.

Chapter 4 describes the work done towards understanding the role of flavonoids in PTI. In fact, one of the *pir*s encodes *UGT78D1*, a glycosyltranferase involved in flavonol glycosylation. The T-DNA insertion

caused overexpression of the gene, but the phenotype was found unstable. Several approaches were employed to confirm that overexpression of *UGT78D1* leads to reduced flg22-induced resistance. In addition, through the use of reverse genetics, it was assessed whether lack of flavonols can impair immunity to bacteria. Furthermore, metabolomic analysis of leaves extracts was employed to determine whether elicitor application could lead to differences in the pool of flavonoids. As a complementary strategy, exogenous application of quercetin, a flavonol aglycon, was used to assess the role of these compounds/flavonoids in flg22-dependent PTI.

Chapter 5 describes the preliminary characterization of three additional *pir*s. The study included work to determine the effect of the mutations on basal immunity and flg22-dependent ROS production and SGI. For one of these *pir*s, an additional pharmacological approach was employed.

Chapter 2. Material and methods

2.1 Plant material and growth conditions

2.1.1 Arabidopsis plants and seedlings

Arabidopsis thaliana Col-0 ecotype was used as wild-type control, unless otherwise stated. Arabidopsis plants were grown in individual pots of P24 cell trays at 20ºC with 65% humidity in controlled environment rooms. Arabidopsis plants for phenotypic assays were grown in short-day conditions (10-hours photoperiod). Plants for genotyping and seed production were grown in long-day conditions (16-hours photoperiod).

Arabidopsis seedlings for *in vitro* bioassays (SGI, MAPKs, PAMP-induced gene expression, flg22-induced resistance, see 2.7-2.8) were germinated on solid Murashige and Skoog (MS) 1% (Duchefa; see 2.3.2) for five days and subsequently pricked-out individually in liquid MS 1% in transparent multi-well plates (Greiner Bio-one). Arabidopsis seedlings were grown at 22 ºC with a 16-hours photoperiod.

The SALK uni-mutant T-DNA insertion collection (Alonso et al., 2003) and additional mutant lines used in this study were purchased from the Nottingham Arabidopsis Stock Centre (NASC). A comprehensive list of the mutant and transgenic lines used is in Appendix 1.

2.1.2 Sterilization of Arabidopsis seeds

Seeds were gas-sterilized in a dessicator with 50 mL sodium hypochlorite solution and 2 mL 37% HCl. Seeds were sterilized for 3-4 h and dried for an additional hour in a sterile flow cabinet prior sowing.

2.1.3 Generation of transgenic Arabidopsis lines

Arabidopsis WT plants were transformed via floral-dip inoculation method with *A. tumefaciens* (Clough and Bent, 1998) by the TSL tissue culture support team. Selection of transformants was carried out on MS 1%-agar plates supplemented with kanamycin or gentamycin. Transgene expression was confirmed either by qRT-PCR (see section 2.5) or by western blot (see 2.6).

2.1.4 Generation of crosses between Arabidopsis mutants

Individual flowers of mature Arabidopsis plants were emasculated with tweezers. Fresh pollen from donor plant was gently tapped onto individual stigmas. Individual mature siliques were harvested when ripe, and individual F1 seeds were germinated in soil. Plants were genotyped to confirm the success of the cross and left to self-pollinate. Double homozygous mutant plants were isolated in the F2 generation by genotyping.

2.2 Bacterial strains and growth conditions

2.2.1 Preparation of bacterial inoculum

Bacteria were streaked-out from the respective glycerol stocks on fresh L-agar plates, supplemented with the appropriate antibiotics. Plates were incubated at 28ºC for two days. Bacteria were then gently scraped off with a spreader and 10 mM $MgCl_2$, and a 100 µL aliquot was spotted and evenly spread on a fresh L-agar plate and incubated O/N at 28ºC. Bacteria were scraped off with a spreader and 10 mM $MgCl_2$, and spun down at 3000 rpm

for 10 min. Bacteria were re-suspended in 10 mM MgCl$_2$ to the desired OD$_{600}$ prior use.

Table 2.1. *Pto* DC3000 strains used in this study.

Strain	Description	Selection	Reference
Pto DC3000	WT	Rif	(Whalen et al., 1991)
Pto DC3000-*LuxCDABE*	strain constitutively expressing LuxCDABE operon from *Photorhabdus luminescens*	Rif Kan	(Fan et al., 2008)

2.2.2 Transformation of chemically competent *E. coli* cells

E.coli cells (strain DH5α) were thawed on ice and mixed with the appropriate plasmid to be transformed. After 2 min incubation on ice, cells were heat shocked at 42ºC for 45 sec and then placed on ice for 2 min. 500 µL of L media was added to each tube and cells were incubated at 37ºC for 1h under constant shaking. Cells were plated on L-agar plates with kanamycin and incubated overnight at 37ºC.

2.2.3 Transformation of electro-competent *A. tumefaciens*

A. tumefaciens cells (strain GV3101) were thawed on ice, diluted 1:1 with 60% glycerol, mixed with the appropriate plasmid (1-2 µL), and transferred to a pre-chilled electroporation cuvette (Bio-Rad). Cells were transformed with an electroporator (Bio-Rad) with the following settings: 1800V, 25µF capacity, 200 Ω resistance. Cells were supplemented with 500 µL L-media and incubated at 28ºC for at least one hour. Cells were plated on L-agar plates (Gent, Rif, plus plasmid selection) and incubated at 28ºC for two days.

2.3 Chemicals, media, buffers and antibiotics

2.3.1 Chemicals

Flg22 and elf18 were purchased from Peptron (Daejeon, South-Korea). The stock peptides were dissolved in sterile water at a concentration of 10mM and stored at -20ºC until use. Dilutions were made in water. Quercetin (≥95%), naringenin (98%) and atorvastatin calcium salt trihydrate (≥98%) were purchased from Sigma-Aldrich. Quercetin and naringenin stocks (100 mM/10 mM) were made fresh prior use. Quercetin and naringenin were dissolved in pure dimethyl sulfoxide (DMSO) (Sigma-Aldrich) and diluted in water (100X) to a final 1% DMSO concentration. Atorvastatin was diluted in pure DMSO to a 10 mM stock and stored at -20ºC. Dilutions were made in water to a final 1% DMSO concentration.

2.3.2 Media

All the recipes are for 1L.

MS 1%: 4.41 g MS salts (including vitamins), 10 g sucrose, pH 5.8. For solid MS 1%-agar, 8 g agar was added. Variations on this media included the addition of 0.5 g/l 2-(N-morpholino)-ethanesulfonic acid (MES) (MS 1%+MES), or removal of sucrose (MS).

L media (Luria Broth Base): 10 g tryptone, 5 g yeast extract, 0.5 g NaCl, pH 7. For solid media, 10 g Agar are added.

Tryptic Soy Agar (TSA): casein peptone 15 g, soya peptone 5 g, NaCl 5 g, Agar 10 g, pH 7.3.

2.3.3 Antibiotics (working concentrations)

Kanamycin: 50 µg/mL

Hygromycin: 100 µg/mL

Rifampicin: 50 µg/mL

Gentamicin: 25 µg/mL

2.3.4 Buffers

FTA 1X: 10 mM Tris pH 8, 2 mM ethylenediaminetetraacetic acid (EDTA), 0.1% Tween-20.

TE-1: 10 mM Tris pH 8, 100 µM EDTA.

Orange G loading dye: 100 mg Orange G, 15 mL glycerol, water up to 50 mL.

TBE (Tris-borate-EDTA) buffer 10X: 89 mM Tris, 89 mM boric acid, 2 mM EDTA, pH of 10X TBE 8.3

Lacus buffer: 50 mM TRIS-HCl pH 7.5, 10 mM $MgCl_2$, 15mM ethylene glycol tetraacetic acid (EGTA), 100 mM NaCl, 1 mM sodium fluoride, 1 mM sodium molybdate, 0.5 mM activated sodium ortho-vanadate, 30 mM β-glycero-phosphate, 0.1% NP-40, water up to 200 mL. Before use, add 0.5 mM phenylmethanesulfonyl fluoride (PMSF), 1% protease inhibitors P9599, 100 nM calyculin A and 2 mM dithiothreitol (DTT). To activate sodium ortho-vanadate, pH should be adjusted to 10, which gives a yellow solution. Then boil the solution until it turns colourless and re-adjust pH to 10. Repeat the procedure until the solution stays colourless at pH 10.

6x SDS loading dye (with DTT): 300 mM Tris pH 6.8, 60% glycerol, 6% sodium dodecyl sulphate (SDS), 0.05% bromophenol blue. Add dithiothreitol (DTT) to 50 mM before use.

Transfer buffer: 1x Tris-Glycine, 20% methanol and 0.08% SDS (electrophoresis grade).

1x TBST: 1x TBS, 0.1% Tween-20.

Blocking buffer: 1x TBST, 5% dried milk.

Coomassie stain solution: 0.5% Coomassie brilliant blue R-250, 50% MeOH, 7.5% glacial acetic acid.

De-stain solution: 20% MeOH, 5% acetic acid.

2.4 DNA work

2.4.1 Plant genotyping

2.4.1.1 DNA extraction

DNA for plant genotyping was obtained using FTA card (Whatman). A sample of Arabidopsis leaves were collected, pressed onto FTA cards and left to dry. Micro disks (1.2 mm) were punched from the card and placed in non-skirted PCR plates. DNA was extracted with 50 μL of 1X FTA (see 2.3.4) for 5 minutes. DNA was then washed twice with 200 μL TE-1 (see 2.3.4) for 5 minutes. Disks were left to air-dry for an additional 10 minutes prior addition of PCR mix.

2.4.1.2 PCR

The PCR mix for one reaction contained:

2.5 μL Qiagen CoralLoad PCR Buffer 10X

0.5 µL dNTPs

0.5 µL primer 1

0.5 µL primer 2

0.05 µL Qiagen Taq

Water up to 25 µL

Primers were purchased from Sigma-Aldrich and dissolved in water to a 10 µM stock concentration. dNTPs (Invitrogen) were dissolved to a 2 mM stock. A complete list of the primers used is in Appendix 2. The PCR was conducted with a termocycler PCR machine with the following program:

Initial denaturation	95ºC 5 mins
40 cycles:	95ºC 1 min (denaturation)
	51ºC 1.5 mins (annealing)
	72 ºC 2 mins (extension)
Final extension	72 ºC 10 mins

2.4.1.3 Gel electrophoresis

PCR products were analysed by gel electrophoresis. Agarose gel was prepared with 1% agarose in 1X TBE (see 2.3.4) and 1 µg/mL ethidium bromide (Sigma-Aldrich). Gels were run at 100V until optimal separation. PCR product size was evaluated using a short wavelength UV transilluminator (GelDoc1000, BioRad).

2.4.1.4 Genotyping with CAPS

When genotyping with CAPS (cleaved amplified polymorphic sequence) markers, the PCR product was cleaned by elution through a sepharose column. The PCR product was digested with the appropriate enzyme at 37ºC for 1 hour prior to loading on an agarose gel. The digestion mix contained: 4

µL PCR product, 2 µL 10X buffer, 0.5 µL restriction enzyme, and water up to 20 µL.

2.4.2 Gateway® Gene Cloning

2.4.2.1 Gene amplification (cloning)

cDNA was obtained as in 2.5.1-2.5.4. PCR forward primers contained a CACC extension at the 5' end for integration with the pENTR-D-TOPO vector (Invitrogen, see below). Amplification of the desired gene was obtained by PCR as follows:

2.5 µL High Fidelity Buffer 10X
0.5 µL dNTPs
0.5 µL primer 1
0.5 µL primer 2
1 µL cDNA template
0.2 µL Phusion High Fidelity DNA polymerase
Water up to 25 µL

The PCR program was:

Initial denaturation   98ºC 30 s
30 cycles: 98ºC 10 s (denaturation)
                       55ºC 30 s (annealing)
                       72 ºC 2 mins (extension)
Final extension   72 ºC 10 mins

2.4.2.2 Gel-purification

The PCR product was loaded on to an agarose gel and DNA was visualized with a long wavelength UV transilluminator (TM40, UVP). The DNA fragment

was excised with a razor blade and placed in an Eppendorf tube. DNA was eluted with Macherey-Nagel NucleoSpin Gel and PCR Clean-up according to the manufacturer's protocol. DNA was eluted in 15 µL of water.

2.4.2.3 pENTR-D-TOPO® reaction

The pENTR-D-TOPO® reaction allows directional cloning of a PCR product into a Gateway® vector without the need of ligase. The pENTR-D-TOPO vector (Invitrogen) contains *att*L sites, which are required for site-specific recombination into a Gateway®-compatible destination vector.

PCR product was ligated into the pENTR-D-TOPO vector with the following mix: 0.5 µL PCR product, 1 µL salt solution (1.2 M NaCl, 0.06 M MgCl$_2$), 4.25 µL sterile water, and 0.25 µL pENTR-D-TOPO vector. The mix was incubated at room temperature for at least 1 h. The reaction was transformed into *Escherichia coli* DH5α chemically competent cells (see 2.2.2).

2.4.2.4 Confirmation of the insert

Five individual colonies were tested for the presence of the insert by colony PCR. A little swab from individual colonies was mixed with the PCR mix. PCR mix, PCR program and analysis of the PCR products were as described in 2.4.1.2-2.4.1.3. Colonies positive for the presence of the insert were inoculated in 5 mL L media with kanamycin and incubated O/N at 37ºC. Plasmids were extracted with Macherey-Nagel NucleoSpin Plasmid kit following the manufacturer's instructions. Plasmids were sequenced to confirm the correct insert sequence. Sequencing mix contained 7 µL water, 1µL primer 1 (or primer 2), 2 µL plasmid. Samples were submitted for sequencing to GATC Biotech AG, Germany. Sequencing results were analysed with CLC Main Workbench.

2.4.2.5 LR reaction

LR reaction allows the recombination between and entry clone and a destination vector. The entry clone contains the gene of interest flanked by *att*L sites, which specifically recombine with the *att*R sites on the destination vector through Gateway® LR Clonase® II (Invitrogen).

The insert was transferred from pENTR-D-TOPO to a compatible destination vector via the LR recombination reaction. Destination vectors were selected from the pGWB series (Nakagawa et al., 2007). LR reaction mix included: 0.5 µL destination vector, 0.5 µL entry vector, 1 µL water, and 0.5 µL LR clonase II. The mix was incubated at room temperature for 1-5 hours. The reaction was transformed into chemically competent cells *E. coli* DH5α cells (see 2.2.2). Cells were plated on L-agar plates with appropriate selection and incubated overnight at 37ºC. Presence of the correct fragment was evaluated by colony PCR (see 2.4.2.4). For Arabidopsis transformation, plasmids were transformed into *A. tumefaciens* (see 2.2.3).

Table 2.2. Vector backbones and plasmids used in this study.

Vector	Source	Use	Selection
pENTR-D-TOPO	Invitrogen	Cloning	Kan
pGWB2	Nakagawa et al., 2007	Arabidopsis transformation	Kan Hyg
Plasmid	**Backbone**	**Insert**	
pENTR-UGT78D1	pENTR-D-TOPO	UGT78D1 (At1g30530)	Kan
pENTR-UGT78D2	pENTR-D-TOPO	UGT78D2 (At5g17050)	Kan
35S:UGT78D1	pGWB2	UGT78D1 (At1g30530)	Kan Hyg
35S:UGT78D2	pGWB2	UGT78D2 (At5g17050)	Kan Hyg
35s:At1g30530-TAP (J. Monaghan-ABRC)	pLIC-C-TAP	UGT78D1 (At1g30530)	Spec

2.5 RNA work

2.5.1 RNA extraction

RNA was extracted from whole 14-day-old seedlings grown in sterile conditions or from adult Arabidopsis plants (see 2.1.1). When RNA was extracted from adult plants, six leaf disks (cork borer nr. 3, Ø 0.36 cm) from six leaves of the same plant were collected. Tissue was immediately frozen in liquid N_2 and stored at -80ºC until processed. Plant tissue was ground in liquid N_2 and RNA was extracted with TRI reagent (Sigma) following manufacturer's protocol. RNA was re-suspended in 30-50 µL DNAse-free water by incubation at 53ºC for 5 minutes. If not directly processed, RNA was stored at -80ºC.

2.5.2 DNase treatment

RNA samples were treated with Turbo DNA-free kit (Ambion) following manufacturer's instructions. RNA was mixed with 0.1 volume 10X TURBO DNase Buffer and 1 µL TURBO DNase, and incubated at 37ºC for 30 min. The reaction was then stopped by adding 0.1 volume DNase inactivation reagent and briefly vortexing. After 5 min incubation at room temperature, the samples were spun down at 10,000 × g for 90 sec and the RNA was then transferred to a fresh tube.

2.5.3 RNA quantification

RNA samples were quantified with a Nanodrop spectrophotometer (Thermo Scientific). In addition, the RNA quality was evaluated by gel electrophoresis (see 2.4.1.3). 1 µL from each sample was mixed with 1 µL OrangeG loading dye (see 2.3.4) and loaded onto a 2% gel.

2.5.4 cDNA synthesis

First-strand cDNA was synthesized from 1-3 µg RNA with SuperScript III reverse transcriptase (Invitrogen) and oligodT18 primers following manufacturer's protocol. When cDNA was synthesized from 2-3 µg RNA, it was diluted with sterile water 1:1 or 1:2, respectively. When the starting RNA was 1 µg, cDNA was used undiluted.

2.5.5 Quantitative real-time PCR (qRT-PCR)

The synthesized cDNA was amplified in duplicate or triplicate by qPCR using SYBR Green JumpStart Taq ReadyMix (Sigma-Aldrich) and CFX96 Real Time System Thermal Cycler (BioRad). The qPCR mix included 1 µL cDNA, 7 µL water, 1 µL primer Fw, 1 µL primer Re, 10 µL SYBR green. The qPCR program used was as follows:

Initial denaturation   95ºC 4 mins
40 cycles: 95ºC 10 s (denaturation)
                       62ºC 15 s (annealing)
                       72 ºC 30 s (extension)

Plates were read after each cycle. Additionally, the melting curve was calculated from 65ºC to 95ºC, with a read every 0.5ºC, hold 5 seconds.

Expression was normalized to the *UBOX* (At5g15400) expression. Unless otherwise specified, values were then expressed as relative to WT. Primers used in this study can be found in Appendix 2.

2.6 Protein work

2.6.1 Sample preparation

To evaluate gene overexpression in transgenic plants, six leaf disks (cork borer nr. 3) from each individual plant were collected and were ground in liquid N_2. Proteins were extracted with 50 µL 2x SDS loading dye (see 2.3.4) by boiling at 95ºC for 5 minutes. Samples were spun down and 30 µL were loaded on a polyacrylamide gel.

For MAPK activation assay, seedling samples were ground in liquid N_2 and extracted with 100 µL Lacus buffer (see 2.3.4) for 10-20 min in ice. After centrifugation at full speed for 5 min, 15 µL of supernatant were mixed with 15 µL 2X loading dye (see 2.3.4) and loaded on polyacrylamide gel.

Since each sample derived from equal amounts of plant material, the protein levels were not measured before loading them on polyacrylamide gel, assuming equal amounts. Equal loading was subsequently determined by Coomassie staining (see 2.6.6).

2.6.2 Protein separation on one-dimensional polyacrylamide gel electrophoresis

Samples were loaded on a 10% SDS PAGE gel (Laemmli, 1970). Polyacrylamide gels were run using a Mini-PROTEAN Tetra cell vertical electrophoresis system (Bio-Rad) with 10% SDS running buffer at 120V until optimal sample separation was reached. Pre-stained protein marker (NEB) was added.

2.6.3 Tank (Wet) electrotransfer

Gels were washed in transfer buffer (see 2.3.4) for 5-10 min prior to transfer. PVDF membrane (Bio-Rad) was activated by incubation in MeOH and equilibrated in transfer buffer. The "sandwich" transfer was assembled in transfer buffer with one sponge, two Whatman filter papers, the activated membrane, the acrylamide gel and two Whatman filter papers and one sponge. Proteins were transferred for 1 h at 100V at 4⁰C using Mini Trans-Blot cell (Bio-Rad). Membranes were then washed with TBS-T and blocked with blocking buffer O/N (see 2.3.4).

2.6.4 Immuno-detection

The membrane was quickly washed in TBS-T for removal of the blocking buffer. Membranes were incubated with the primary antibody for at least 1 h and then washed 3x with TBS-T. Anti-rabbit-HRP (Sigma) (1:10,000) was used as secondary antibody and was incubated with the membrane for at least one hour. The membrane was then washed 3x with TBS-T and 1x with TBS. Proteins were detected through enhanced chemiluminescent (ECL) substrate Pico/Femto (Thermo Scientific), which reacts with the HRP-secondary antibody conjugate. 25 µL of Femto luminol/enhancer were mixed with 225 µL of pico luminol/enhancer and 500 µL of stable peroxide buffer. Membranes were exposed on Fuji medical X-Ray film (Fuji) for 1-5 minutes.

2.6.5 Coomassie staining

Membrane were stained with Coomassie stain solution (see 2.3.4) for five minutes and de-stained 2x 5 minutes with the de-stain solution (see 2.3.4).

2.7 Microbiological work

2.7.1 Pathogenicity assays

Bacteria were prepared as described in 2.2.1, unless otherwise stated.

2.7.1.1 *In vitro* flg22-induced resistance

For the screen set-up, Arabidopsis seeds were sterilized and sown directly in liquid media or on solid medium in transparent multi-well plates (Greiner Bio-One) (see 2.1.1, 2.1.2 and 2.3.2). Depending on the well size, four to eight replicates were used per treatment per genotype. Plates were sealed with Micropore Tape (3M) and stratified for 2-3 days and then moved to long day conditions in a growth chamber. After six days seedlings germinated in liquid media were elicited by replacing the medium with fresh MS 1% containing elf18/flg22 at different concentrations (100 nM, 500 nM or 1 µM). Seeds germinated on solid medium were submerged with MS 1% containing flg22 1 µM. Seedlings were elicited for 24 hours prior to bacterial infection. *Pto* DC3000-*LuxCDABE* was added to each well to a final OD_{600}=0.02 or 0.002. Bacterial growth was evaluated at 1 and 2 days post-infection (DPI) by serial dilutions and quantification of bacterial luminescence (see 2.7.2.1 and 2.7.2.2).

For screening purposes, sterile Arabidopsis seeds were sown directly into transparent 24-well plates (Greiner Bio-One) containing 1 mL MS 1%. Five seeds were sown in each well. WT was sown in six wells, whereas *fls2* and each mutant line were sown in triplicate. Plates were sealed with Micropore Tape (3M) and stratified for 2-3 days. Plates were then moved to long day conditions in a growth chamber. Plates were placed on a rotatory shaker at 100 rpm constant speed. After six days, the media was removed from each plate by suction using a 25 mL pipette fitted with a 1 mL sterile tip. Fresh MS 1% media containing 1 µM flg22 was added to each well and seedlings were

elicited for 24 hours prior to infection. *Pto* DC3000-*LuxCDABE* was added to each well to a final OD_{600}=0.02. Bacterial growth was evaluated at 1 DPI by a CCD camera (Photek) (see 2.7.2.2).

For the secondary screen, Arabidopsis seeds were sterilized and sown on MS 1% agar plates (see 2.1.1, 2.1.2 and 2.3.2). Plates were stratified for 2-3 days and then moved to long day conditions in a growth chamber. After five days individual seedlings were pricked-out into transparent 96-well plates (Greiner Bio-One), containing 100 µL liquid MS 1%. Eight seedlings per treatment per genotype were used. One day later, seedlings were elicited with flg22 1 µM (final concentration) for 24 hours prior bacterial infection. *Pto* DC3000-*LuxCDABE* was added to each well to a final OD_{600}=0.02. Bacterial growth was evaluated at 2 DPI by quantification of bacterial luminescence (see 2.7.2.2).

2.7.1.2 *In planta* flg22-induced resistance

Five-week-old Arabidopsis plants were elicited by syringe-infiltration with water or flg22 1 µM for 24 hours prior bacterial infection. Three leaves per plant and four to eight plants per treatment were used. *Pto* DC3000 was infiltrated at a final OD_{600}=0.0002. Bacterial growth was evaluated at 2 DPI by plating serial dilutions (see 2.7.2.1).

2.7.1.3 Bacterial spray-infection

Five-week-old Arabidopsis plants were spray-inoculated with *Pto* DC3000 at a final OD_{600}=0.2. Silwet L-77 0.02% was mixed with bacteria immediately prior spraying. Four to six plants per treatment were used and two-three leaves per plant were pre-marked to avoid bias in the sampling. Bacterial growth was evaluated at 3 DPI by plating serial dilutions (see 2.7.2.1).

2.7.1.4 Atorvastatin treatment

Five-week-old Arabidopsis plants were syringe-infiltrated with DMSO 1% or atorvastatin 100 µM (in water, DMSO 1%) for 24 hours. The following day each set of plants (DMSO or Atorvastatin pre-treated) was elicited with water or flg22 100 nM. Additional plants were co-infiltrated with ± atorvastatin (100 µM) ± flg22 100 nM. Three leaves per plant, five plants per treatment were used. One day later, *Pto* DC3000 was infiltrated at a final $OD_{600}=0.0002$. Bacterial growth was evaluated at 2 DPI by plating serial dilutions (see 2.7.2.1).

2.7.1.5 Quercetin-induced resistance

Five-week-old Arabidopsis plants were sprayed with quercetin 1mM, 100 µM or DMSO 1%. Quercetin was diluted in water to the desired concentration to a final DMSO concentration of 1%. Silwet L-77 0.01% was added to each solution. Four to six plants per treatment were used and two-three leaves per plant were pre-marked to avoid bias in the sampling. After three days, plants were spray-inoculated with *Pto* DC3000 at a final $OD_{600}=0.2$. Silwet L-77 0.02% was mixed with bacteria immediately prior to spraying. Bacterial growth was evaluated at 3 DPI by plating serial dilutions (see 2.7.2.1).

Alternatively, five-week-old Arabidopsis plants were syringe-infiltrated with the different chemicals as above. Flg22 100 nM was used as positive control. Three leaves per plant and four to six plants per treatment were used. After 24 hours, *Pto* DC3000 was infiltrated at a final $OD_{600}=0.0002$. Bacterial growth was evaluated at 2 DPI by plating serial dilutions (see 2.7.2.1).

2.7.2 Evaluation of bacterial growth

2.7.2.1 Serial dilutions

For *in vitro* experiments, each seedling was surface sterilized by dipping into ethanol 70%, quickly rinsed in water and gently blotted dry. Weight was recorded with an electronic precision balance (Sartorius). Each seedling was ground in 100 µL $MgCl_2$ and 10-fold serial dilutions were made. Twenty microliters of each dilution were plated on TSA (see 2.3.2) and let dry. Plates were incubated at 28ºC for two days and colony forming units (CFU) were then counted. Results were expressed as CFU/cm^2.

For adult plant experiments, two leaf disks (cork borer nr. 3) from two leaves of the same plant were pooled together in a 1.5 mL Eppendorf tube. Samples were ground in 100 µL $MgCl_2$ and 10-fold serial dilutions were made. Twenty microliters of each dilution were plated on TSA (see 2.3.2) and let dry. Plates were incubated at 28ºC for two days and colony forming units (CFU) were then counted. Results were expressed as CFU/cm^2.

2.7.2.2 Bacterial luminescence

Plates were placed inside a High-Resolution Photon Counting System (Photek) coupled to an aspherical wide lens (Sigma). Photon count was measured for two minutes and data extracted from each well every 15 seconds to estimate a sample average. Samples of each treatment were then averaged together to allow comparisons between treatments and genotypes. Results were expressed as average of photon counts or relative light units (RLU). For the *pir* screen, bacterial growth was evaluated visually, by comparing each mutant line with the positive and the negative controls. A mutant line was considered positive for loss of flg22-induced resistance when in at least two out of three wells the bacterial luminescence was greater than the highest bacterial luminescence observed among WT seedlings.

2.7.2.3 *In vitro* bacterial growth

One single *Pto* DC3000 colony was inoculated into 50 mL L-Rif media and incubated O/N in the shaker at 28ºC. Cells were spun down and re-suspended in L-Rif media to a final $OD_{600}=0.1$ in 50 mL L-Rif. Quercetin was then added to a final concentration of 1 mM, 100 µM or 10 µM (DMSO 1%). DMSO 1% was used as control. Flasks were incubated in the shaker at 28ºC and 1 mL samples taken every two hours. Bacterial numbers were estimated by measuring the absorbance at 600nm. For each treatment, a blank was made without bacterial inoculum and kept at 28ºC with the bacterial cultures.

2.7.3 Antibiosis assay

Bacteria were diluted in 10 mM $MgCl_2$ to a final $OD_{600}=0.2$, 0.02 or 0.002. Two hundred fifty microliters of each dilution were plated onto L-Rif agar plates and let dry. Sterile, 5 mm filter paper disks were soaked with 25 µL of each chemical. Quercetin was tested at 1 mM and 100 µM concentration, both in pure DMSO or in water (to a final DMSO 1% concentration). Pure DMSO and DMSO 1% were used as negative controls. Kanamycin 500 µg/mL was used as positive control. Plates were incubated up-right at 28ºC O/N. Pictures were taken the following day.

2.8 Bioassays

2.8.1 Measurement of reactive oxygen species

Eight leaf disks (cork borer nr 1) from eight five-week-old Arabidopsis plants were collected and placed into individual wells of a white 96-well plate (Greiner Bio-One) with 150 µL of water. The following day, water was

replaced with 100 µL of water containing flg22 100 nM, luminol 100µM (Sigma-Aldrich), and horseradish peroxidase 10 µg/mL(Sigma-Aldrich). Luminescence was measured over 45 minutes using a Photek camera. Data was extracted every minute and averages were made per sample per treatment.

For quercetin experiments, 12 leaf disks from 12 five-week-old Arabidopsis WT plants were used for each treatment. Quercetin was tested at 1 mM and 100 µM concentration, diluted in water to a final DMSO 1% concentration. DMSO 1% was used as control. Luminescence was measured O/N (approximately 15-16 hours). Data was extracted every five minutes and averages were made per treatment.

2.8.2 Seedling growth inhibition

Arabidopsis seeds were sterilized and sown on MS 1% agar plates (see 2.1.1, 2.1.2 and 2.3.2). Plates were stratified for 2-3 days and then moved to long day conditions in a growth chamber. After five days individual seedlings were pricked-out into transparent 48-well plates (Greiner Bio-One) containing either: 1 mL liquid MS 1%, MS 1% with flg22 100 nM or 10 nM, MS 1% with elf18 100 nM or 10 nM. Plates were placed back into the growth chamber for an additional seven days. Seedlings were blotted dry and weighed on an electronic precision balance (Sartorius) to record individual weights.

For quercetin/naringenin treatment, five day-old seedlings were transferred to 48-well plates containing MS 1% supplemented with quercetin 1 mM or 100 µM or naringenin 100 µM to a final DMSO concentration of 1%. DMSO 1%, flg22 (or elf18) 100 nM were used as controls. In addition, seedlings were also co-treated with: flg22 (or elf18) 100nM and quercetin (1 mM or 100 µM), flg22 (or elf18) 100 nM and naringenin 100 µM, or flg22 (or elf18) 100nM and DMSO 1%.

2.8.3 Activation of mitogen active protein kinases

Six two-week-old Arabidopsis seedlings were elicited with flg22 1 µM, quercetin 100 µM, DMSO 1% or co-elicited with flg22 1 µM and quercetin 100 µM or flg22 1 µM and DMSO 1%. Samples were taken at 10 min, 30 min, 1 h, 3 h, 6 h, and 24 h post treatment and immediately frozen in liquid N_2. Samples were prepared as in 2.6.1. MAPK activation was detected by western blot (see 2.6.2-2.6.5) using Phospho-p44/42 MAPK (Erk1/2; Thr-202/Tyr-204) rabbit monoclonal antibodies (Cell Signaling) (1:2,000 dilution). Membranes were stained with Coomassie Brilliant Blue to verify equal loading (see 2.6.6).

2.8.4 PAMP-induced gene expression

Four two-week-old Arabidopsis seedlings were elicited with flg22 1 µM, quercetin 100 µM, DMSO 1% or co-elicited with flg22 1 µM and quercetin 100µM or flg22 1 µM and DMSO 1%. Samples were taken at 30 min, 1 h, 3 h, 6 h, and 24 h post treatment and immediately frozen in liquid N_2. Samples were ground in liquid nitrogen. RNA extraction, cDNA synthesis and qRT-PCR procedure are described in section 2.5. Expression was normalized to *UBOX* expression. Results were expressed as expression relative to DMSO treatment.

2.9 Metabolomic analysis of Arabidopsis leaf extracts

2.9.1 Extraction of flavonols

Five week-old Arabidopsis WT plants were syringe-infiltrated with water or flg22 1 µM. Three to four leaves per plant and six plants per treatment were

used. Leaves were excised with scissors at 0, 5, 10, and 24 hours post-infiltration and immediately frozen in liquid N_2. Samples were ground in liquid N_2 and aliquots were subject to methanolic extraction (5 μL 80% MeOH/mg of sample). Samples were incubated at room temperature for 15 min, followed by centrifugation at 15000g for 15 min (room temperature). The supernatant was used directly for LC-MS. The protocol was adapted from (Hagemeier et al., 2001; Yonekura-Sakakibara et al., 2008)

2.9.2 Liquid chromatography-tandem mass spectrometry (LC-MS)

LC-MS analysis was performed by Dr. Lionel Hill, at the JIC Metabolite Service (Norwich, UK). Samples were diluted 1:1 with water, centrifuged, and 60 μL were transferred to a new glass tube.

The samples were run on a Shimadzu IT-ToF mass spectrometer attached to a Nexera/Prominence LC system (Shimadzu). Separation was on a 100×2.1mm 2.7μ Kinetex XB-C18 column (Phenomenex) using the following gradient of acetonitrile (ACN) versus 0.1% formic acid in water, run at 500μL.min^{-1} and 40°C:

Time (minutes)	% ACN
0	2
0.5	2
3.0	10
13	30
18	90
18.8	90
19	2
23.1	2

Detection was by UV/visible absorbance and positive electrospray MS. Absorbance data were collected at 12.5Hz from 200-600nm, with a 0.24s time constant. MS data were collected from m/z 200-1700, using automatic sensitivity control (10ms maximum ion accumulation time, 10×10^6 total ion target). In addition, the instrument was set up to collect data-dependent MS2 with an isolation width of m/z 3.0, 50% collision energy, and 50% collision gas, using 20ms maximum ion accumulation time and a target ion count of 70% of the base peak chromatogram intensity. Dynamic exclusion was used such that after a single repeat, the precursor ion would be ignored for 1 s. This maximised the number of ions for which MS2 data were collected, while ensuring that replicate spectra were available across the chromatographic peak. Spray chamber conditions were 250°C curved desorbation line temperature, 1.5 L.min^{-1} nebulizer gas, 300°C heat block, and drying gas "On". The instrument was calibrated immediately before running the samples, following the manufacturer's instructions, using sodium TFA. In some runs during the sequence, the instrument was also set up to infiltrate standard solution instead of part of the run, so that intermediate mass calibrations could be carried out. For best mass accuracy, in some cases background phthalate contaminations were used to apply a mass compensation within each run.

A standard mix (shown below) was prepared and diluted serially by addition of 173.1µL to 200µL 20% MeOH to provide calibration curves.

Compound	Volume (µL)	final concentration (µM)
Chlorogenic acid 3mM	20	150
Kaempferol rutinoside 1mM	40	100
Naringenin 1mM	40	100
Naringin 1mM	40	100
Rutin 2mM	50	250
Quercetin 1mM	40	100
50% MeOH	170	
Total:	400µL	

2.9.2 Quantification

The calibration curves for the estimation of absolute concentration of target compounds were based on UV detection. UV peak areas were plotted versus MS peak areas for all the samples.

2.10 Statistical analysis

Statistical significance was based on Student's t test and one-way ANOVA, using Prism 6 software (GraphPad Software).

Chapter 3. Approaches to identify the molecular mechanisms underlying PAMP-triggered immunity in Arabidopsis.

3.1 Introduction

PAMP recognition at the plasma membrane is the key event that triggers PTI. PAMP perception is mediated by plasma membrane-localized receptors and extracellular recognition is followed by propagation of the signal, eventually providing immunity against pathogens, as described in more detail in the general introduction (Chapter 1). To date, several molecular components underlying PTI signalling have been uncovered, but the mechanisms that actually lead to plant immunity are still poorly understood (reviewed in Macho and Zipfel, 2014).

To date, a number of genetic screens have been carried out in the plant model *Arabidopsis thaliana* with the goal of uncovering novel molecular components of PTI. The *elf18 insensitive* (*elfin*) screen, using seedling growth inhibition, and the *priority to sweet life* (*psl*) screen, using repression of anthocyanin biosynthesis following eff18 perception, both isolated mutants that were insensitive to elf18 treatment. They independently identified mutants in several endoplasmic-reticulum quality control and N-glycosylation components, showing that the correct biogenesis of EFR is required for its translocation to the plasma membrane (Li et al., 2009; Lu et al., 2009; Nekrasov et al., 2009; Saijo et al., 2009; Farid et al., 2013). The *elfin* screen also discovered *bak1-5*, a novel allele of *bak1* that is specifically impaired in PTI, but not in BR responses or cell death control (Schwessinger et al., 2011).The *flagellin insensitive* (*fin*) mutant screen used forward genetics to isolate mutants with reduced flg22-dependent ROS (Boutrot et al., 2010). In addition to new *fls2* and *bak1* alleles, this screen identified the key ethylene signaling component EIN2 as being involved in *FLS2* transcriptional regulation via activation of the transcription factors EIN3/EIL3 that directly bind to the *FLS2* promoter (Boutrot et al., 2010; Mersmann et al., 2010). The *fin* mutant screen also identified ASPARTATE OXIDASE (AO), responsible for *de novo* biosynthesis of nicotinamide adenine dinucleotide (NAD). AO is required for the RBOHD-dependent ROS burst and stomatal closure (Macho et al., 2012). The isolation of *bak1-5* led to the development of a novel

suppressor screen (*mob* screen for *modifier of bak1-5*) to identify mutants that re-gain responsiveness to flg22 using production of ROS as a read-out (Monaghan et al., 2014). The *mob* mutant screen revealed CPK28 as negative regulator of PTI via regulation of BIK1 turnover.

Although successful in discovering novel molecular regulators of early PTI responses and regulators of receptors biosynthesis or function, previous screens failed to identify components of downstream signalling and, more importantly, "executors" of the resistance induced by PAMPs. When looking into different pathosystems, camalexin, glucosinolates and callose have been described to play active roles in resistance against fungi (Glazebrook et al., 1997; Thomma et al., 1999; Vogel and Somerville, 2000; Ferrari et al., 2003; Nishimura et al., 2003; Kliebenstein et al., 2005; Flors et al., 2008; Bednarek et al., 2009; Sanchez-Vallet et al., 2010; Iven et al., 2012).

The phytoalexin camalexin is a low molecular weight sulphur-containing antimicrobial compound released by Arabidopsis in response to pathogen aggression (reviewed in Ahuja et al., 2012) and abiotic stresses (Zhao et al., 1998), first isolated from *Camelina sativa* (Lois M. Browne, 1991; Rogers, 1996). The two final steps of camalexin biosynthesis are catalysed by the cytochrome P450 CYP71B15/PAD3 (Schuhegger et al., 2006; Böttcher et al., 2009). Camalexin biosynthesis is regulated via activation of MAPK cascade (Ren et al., 2008; Xu et al., 2008) through the WRKY transcription factor WRKY33 (Qiu et al., 2008b; Mao et al., 2011). Camalexin appears to play a major role in resistance against different fungi (Glazebrook et al., 1997; Thomma et al., 1999; Ferrari et al., 2003; Kliebenstein et al., 2005; Nafisi et al., 2007; Sanchez-Vallet et al., 2010; Stotz et al., 2011; Iven et al., 2012), *Phytophtora brassicae* (Schlaeppi et al., 2010) and the green peach aphid *Myzus persicae* (Prince et al., 2014). Although camalexin is produced in response to *Pseudomonas syringae* pv *syringae* (*Pss*) (Tsuji et al., 1992) and exogenous application of camalexin is toxic towards *P. syringae* pv *maculicola* (*Psm*) ES4326 and other microorganisms (Rogers, 1996),

mutations that cause defects in camalexin biosynthesis do not lead to enhanced susceptibility to bacteria (Glazebrook and Ausubel, 1994).

Glucosinolates are nitrogen- and sulphur-containing secondary metabolites. They can be divided in three groups depending on the amino acid they derive from: aliphatic (mainly methionine), benzenic (phenylalanine or tyrosine) and indolic glucosinolates (tryptophan) (Sønderby et al., 2010). CYP79B2 and CYP79B3 are key enzymes in the indolic glucosinolate branch and the double-mutant *cyp79b2 cyp79b3* has no detectable levels of indolic glucosinolates (Hull et al., 2000; Mikkelsen et al., 2000; Zhao et al., 2002). The aliphatic glucosinolate branch is controlled by the two transcription factors MYB28 and MYB29. The double mutant *myb28 myb29*, like *cyp79b2 cyp79b3*, also has no detectable aliphatic glucosinolates (Hirai et al., 2007; Sønderby et al., 2007). Glucosinolates are non-toxic compounds, but when the plant tissue is damaged, they come in contact with myrosinases that degrade glucosinolates into more toxic compounds, like isothiocianates (ITCs) and nitriles (Bones and Rossiter, 1996). Glucosinolates and their degradation products are well known to have a role in defence against generalist insects and human pathogens (Fahey et al., 2001), other than protect against different fungi and *Phytophtora brassicae* (Tierens et al., 2001; Bednarek et al., 2009; Sanchez-Vallet et al., 2010; Schlaeppi et al., 2010; Stotz et al., 2011; Buxdorf et al., 2013). Regarding the role of glucosinolates in resistance to bacteria, it was found that sulphoraphan displays toxicity towards *Pto* DC3000 *in vitro* (Tierens et al., 2001), and contributes to non-host resistance against *P. syringae* in Arabidopsis (Fan et al., 2011). In fact, virulent *Pseudomonas* species carry a *saxCAB/F/D/G* operon for detoxification of glucosinolate derivatives (Fan et al., 2011). In addition, overexpression of *CYP79A2* leads to enhanced resistance to *Pto* DC3000 (Wittstock and Halkier, 2000; Brader et al., 2006), suggesting that different glucosinolates could play different roles in disease resistance. Double mutant *cyp79b2 cyp79b3* is impaired in flg22-dependent callose deposition during PTI, as well as well as *pen2* and *pen3* (Clay et al., 2009).

PEN2 encodes a myrosinase and PEN3 an ATP-binding cassette-type (ABC) transporter involved in non-host resistance (Lipka et al., 2005; Stein et al., 2006). It was suggested that PEN2 would start the breakdown of indolic glucosinolates that are then transported by PEN3 (Clay et al., 2009).

Callose is deposited between the plasma membrane and the cell wall in response to different stresses. The role of callose deposition in plant immunity has been described in section 1.2.2.9.

With the aim of elucidating the molecular mechanism that leads to PTI, two different approaches, one targeted and one unbiased, were employed. In the targeted approach, reverse genetics was employed to test the ability of selected Arabidopsis mutants to mount effective PAMP-induced resistance. The genes selected have key roles in biosynthetic pathways that lead to the production of chemical defences described to be effective in protection against fungi (camalexin, glucosinolates and callose). In parallel, a novel genetic screen was designed and carried out, with the aim of identifying novel components of the late PTI signalling pathway in an unbiased manner. In contrast to previous screens, flg22-induced bacterial resistance was recorded in this study. Since the screen was based on the growth of bacteria, the mutants identified would not be restricted to early signalling events and therefore should identify novel PTI components required for resistance against bacteria.

3.2 Results

3.2.1 Assessing the potential role of camalexin, glucosinolates, SA and callose in flg22-induced resistance to *Pto* DC3000

Camalexin is a phytoalexin that is involved in resistance against a wide array of pathogens (reviewed in Ahuja et al., 2012). In addition, camalexin is produced in response to bacteria and displays antimicrobial properties *in vitro* (Tsuji et al., 1992; Rogers, 1996), indicating that it could be a candidate for the restriction of bacteria following PAMP perception. Therefore *pad3* was tested for loss of flg22-induced resistance to *Pto* DC3000. Results indicated that the reduction of bacterial growth triggered by flg22 pre-treatment in *pad3* was comparable to WT Col-0 (Figure 3.1). This suggests that camalexin is not required for mounting effective flg22-induced resistance against this bacterium.
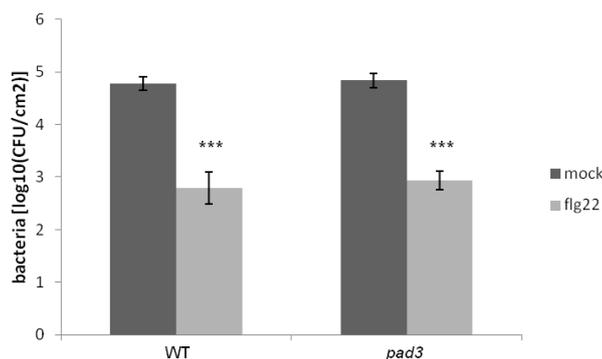
Figure 3.1. Camalexin is not required for flg22-induced resistance to *Pto* DC3000.

Five-week-old wild-type (Col-0) or *pad3* Arabidopsis plants were elicited with 1 µM flg22 for 24 hours and then inoculated with *Pto* DC3000 (OD_{600}=0.0002). Bacterial growth was measured at 2 DPI by plating serial dilutions of homogenized leaf disks. Bars are means ± SE, n=6. Asterisks indicate a statistically significant difference between mock and flg22 treatment (***p<0.001) using two-tailed unpaired t-test. The experiment was repeated three times with similar results.

Glucosinolates are known to play a role in resistance to different pathogens, mainly insects and fungi (reviewed in Bednarek, 2012). Although *Pto* DC3000

is able to detoxify aliphatic glucosinolates, and indolic glucosinolates are required for flg22-dependent callose deposition (Clay et al., 2009; Fan et al., 2011), it is currently unknown whether they are involved in providing resistance to bacterial pathogens during PTI. To assess this, the double mutants *myb28/29* and *cyp79b2/b3*, and the quadruple mutant *cyp79b2/b3 myb28/29* were tested for their ability to mount flg22-induced resistance. Double and quadruple mutants displayed a similar inhibition of bacterial growth triggered by flg22 as WT (Figure 3.2), indicating that glucosinolates are dispensable for flg22-induced resistance.
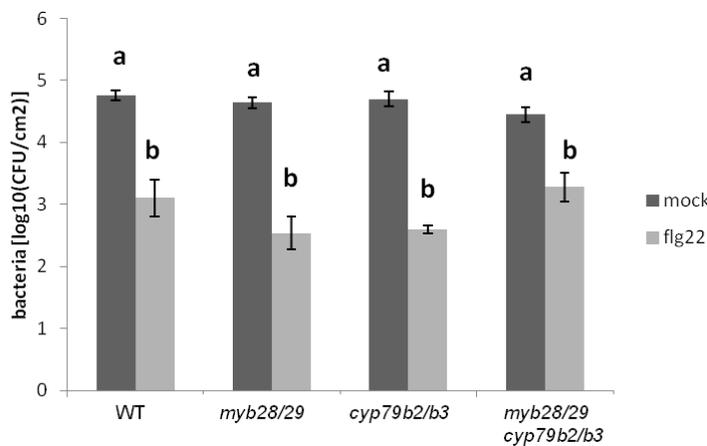
Figure 3.2. Glucosinolates are not required for flg22-induced resistance to *Pto* DC3000.

Five-week-old wild-type (Col-0) or *myb28/29*, *cyp79b2/b3* and *myb28/29 cyp79b2/b3* Arabidopsis plants were elicited with 1 µM flg22 for 24 hours and then inoculated with *Pto* DC3000 (OD_{600} 0.0002). Bacterial growth was measured at 2 DPI by plating serial dilutions of homogenized leaf disks. Bars are means ± SE, n=6. Significantly different groups ($p < 0.0001$) are indicated with lower-case letters based on one-way ANOVA analysis and Tukey's multiple comparisons post-test. The experiment was repeated three times with similar results.

Callose is deposited between the plasma membrane and the plant cell wall in response to pathogens, as well as following flg22 perception (Bestwick et al., 1995; Kim et al., 2005). In addition, it was demonstrated that callose deposition has an active role in resistance against fungi (Ellinger et al., 2013). The callose synthase mutant *pmr4* was tested for flg22-induced

resistance. In addition, *pmr4 sid2-1* and *sid2-1* were used as controls, since *pmr4* has constitutive high levels of SA (Nishimura et al., 2003) and SA induction deficient 2 (SID2) is required for SA biosynthesis (Nawrath and Métraux, 1999; Wildermuth et al., 2001). Results indicated that, when mock-pre-treated, *pmr4* was more resistant to bacterial infection. However, plants pre-treated with flg22 showed impaired flg22-induced resistance, which was restored to WT levels by removing the high levels of SA by crossing *pmr4* with *sid2-1* (Figure 3.3). This indicates that the resistant phenotype of *pmr4* is caused by the constitutive up-regulation of SA-dependent genes, and suggests that callose deposition is not required for flg22-induced resistance to *Pto* DC3000.
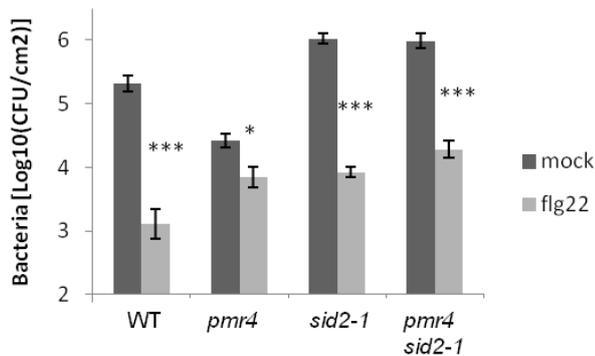
Figure 3.3. Callose is not required for flg22-induced resistance to *Pto* DC3000.

Five-week-old wild-type (Col-0) or *pmr4*, *sid2-1* and *pmr4 sid2-1* Arabidopsis plants were elicited with 1 µM flg22 for 24 hours and then inoculated with *Pto* DC3000 (OD$_{600}$ 0.0002). Bacterial growth was measured at 2 DPI by plating serial dilutions of homogenized leaf disks. Bars are means ± SE, n=6. Asterisks indicate a statistically significant difference between mock and flg22 treatment (***p<0.001) using two-tailed unpaired t-test. The experiment was repeated three times with similar results.

3.2.2 The *PAMP-induced resistance* (*pir*) screen

To identify novel molecular components required for induced-immunity following perception of flg22 by FLS2, the *PAMP-induced resistance* (*pir*) screen was designed. The screen used flg22-induced resistance to *Pto* DC3000 (Zipfel et al., 2004) as an output to identify mutants impaired in this response.

3.2.2.1 Screen set-up

The flg22-induced resistance is normally performed with soil-grown plants and syringe-infiltration of flg22 in Arabidopsis leaves prior to infiltration of *Pto* DC3000 (Zipfel et al., 2004). This, however, is challenging for a screen, due to the considerable amount of growth space required and the time needed for experimental handling. To overcome this, an assay to measure bacterial growth in Arabidopsis seedlings in sterile conditions was developed. At the time the screen was set-up, a few publications described methods to assess bacterial growth in seedlings *in vitro* (Schreiber et al., 2008; Anderson et al., 2011; Danna et al., 2011; Ishiga et al., 2011). Of these, only Schreiber and co-workers used the *in vitro* set-up for a chemical screen, whereas others were used for pathogenicity assays. The protocols differed in the media, size of the multiwell plates, age of the seedlings, the way seedlings were grown and in the bacterial inoculum. Two protocols made use of derivative strains of *P. syringae* that carry the *LuxCDABE* operon from *Photorhabdus luminescence*; their luminescence correlates with bacterial numbers and can be detected with a CCD camera (Fan et al., 2008; Anderson et al., 2011; Danna et al., 2011). It was reasoned that the use of *Pto-Lux* would be ideal for the *pir* screen, as it could simplify the evaluation of bacterial numbers in Arabidopsis seedlings by measuring bacterial luminescence rather than bacterial numbers as determined by colony-forming units.

In order to determine which conditions ensured a clearer determination of flg22-induced resistance in seedlings *in vitro*, the assays were carried out by evaluating bacterial growth after flg22 treatment in WT, using *fls2* as a control. One important aspect to evaluate was the type of media for the Arabidopsis seedlings. Addition of sucrose was found important, as it allowed seedlings to grow more vigorously and quicker if compared to media without sucrose (data not shown). The presence of MES in the media led to smaller flg22-induced resistance at 1 DPI, but did not make a difference at 2 DPI (Figure 3.4).
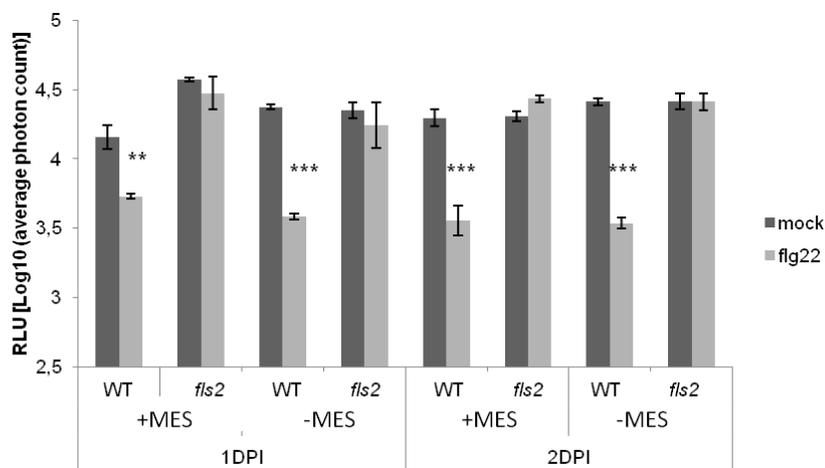
Figure 3.4. Seedlings germinated in liquid MS with 1% sucrose are able to induce resistance to bacteria following flg22 pre-treatment, similarly to adult plants.

Six-day-old wild-type (Col-0) and *fls2* seedlings (approximately five seedlings per well) were grown in MS +1% sucrose media, with or without MES (0.5 g/l) and were elicited with either water or 1 µM flg22 for 24 hours and then inoculated with *Pto-Lux* to a final OD_{600} 0.02. Bacterial growth was measured at 1 and 2 DPI by quantification of average photons emission. Bars are means ± SE, n=6. Asterisks represents statistical difference between mock and flg22 treatment (***p<0.001).The experiment was repeated three times with similar results. RLU, relative light units.

It was also noticed that flg22-induced resistance was already clear at 1 DPI, as published in adult plants (Zipfel et al., 2004). It was therefore decided to carry out the evaluation of the reduction of flg22-induced resistance in the

mutant population already at 1 DPI, to allow a higher number of mutants to be tested every week.

Another critical aspect to be determined was the most effective way to germinate seedlings directly in liquid medium in the wells of the plates in order to avoid the time-consuming transplanting step. This was evaluated by comparing the amplitude of flg22-induced resistance in seedlings germinated on solid media to seedlings germinated in liquid media. One seedling per well was germinated in 96-well plates, three to five seedlings were germinated in 24-well plates. When seedlings were germinated on solid media, they were elicited by submersion with liquid media with flg22; for seedlings germinated in liquid media, the media was replaced one day prior to infection with fresh medium containing flg22. Results indicated that seedlings germinated on solid media did not respond to the treatment and did not show any induced resistance to bacteria both in 96- (Figure 3.5A) and 24-well plates (Figure 3.5B).
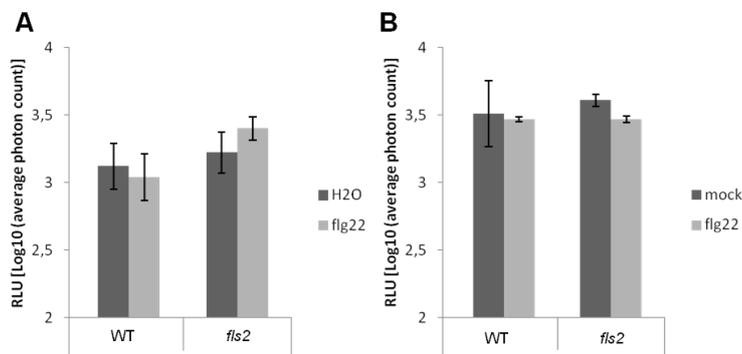
Figure 3.5. Seedlings germinated on solid agar media are not able to induce resistance to bacteria following flg22 pre-treatment.

Six-day-old wild-type (Col-0) and *fls2* seedlings were elicited with either water or 1 µM flg22 for 24 hours and then inoculated with *Pto-Lux* to a final OD_{600} 0.02. Bacterial growth was measured at 2 DPI by quantification of average photons emission. (A) Seedlings individually grown in 96-well plates; (B) approximately five seedlings grown in each well of a 24-well plate; two different media were compared. Bars are means ± SE, n=4. The experiment was repeated three times with similar results. RLU, relative light units.

However, seedlings germinated in liquid media in a 24-well plate gave a significant and reproducible responses (Figure 3.6); no response was observed among seedlings grown in 96-well plates. Therefore it was concluded that the best reduction in bacterial growth following flg22 treatment could be achieved by eliciting 5 seedlings germinated in liquid media in each well of a 24-well plate.
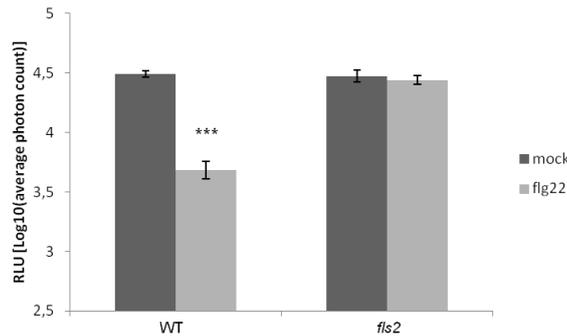
Figure 3.6. Seedlings germinated in liquid media in a 24-well plate are able to induce resistance to bacteria following flg22 pre-treatment, similarly to adult plants.

Six-day-old wild-type (Col-0) and *fls2* seedlings (approximately five seedlings per well) were elicited with either water or 1 µM flg22 for 24 hours and then inoculated with *Pto-Lux* to a final OD_{600} of 0.02. Bacterial growth was measured at 2 DPI by quantification of average photon emission. Bars are means ± SE, n=4. Asterisks represents statistical difference between mock and flg22 treatment using two-tailed unpaired t-test (***p<0.001).The experiment was repeated three times with similar results. RLU, relative light units.

The appropriate age of the seedlings was also investigated by comparing flg22-induced resistance using 7-, 10- and 14-days-old seedlings. Although 10- and 14-day-old seedlings were used successfully in previous publications (Lu et al., 2010; Anderson et al., 2011; Danna et al., 2011), it was observed that seedlings of these ages occupied most of the space in the wells. This led me to question whether the elicitor treatment and the bacterial inoculum could be applied to every seedling homogenously. Seven-day old seedlings seemed to have an appropriate size for a 24-well plate and therefore appeared to be homogenously in contact with both the elicitor and bacteria.

Regarding the bacteria, one aspect to consider was the density of the bacterial inoculum. When carrying-out flg22-induced resistance in adult plants, the density of the inoculum is $OD_{600}=0.0002$ (10^5 CFU/mL) (Zipfel et al., 2004), but bacteria are infiltrated in the leaves. At this density, however, bacterial luminescence cannot be quantified, as it is below the detection limit of the Photek camera used in our laboratory. In Schreiber et al. (2008), *Pto-Lux* was used at $OD_{600}=0.02$, that is more similar to what is used in spray-infection in adult plants (Zipfel et al., 2004). This density seemed quite high to be used on very young seedlings and therefore was compared to $OD_{600}=0.002$ to evaluate the response of the seedlings following flg22 treatment. Results demonstrated that, although equally effective, differences in flg22-induced resistance in WT were clearer when a higher inoculum was used (Figure 3.7). $OD_{600}=0.02$ was therefore chosen as bacterial density for the screen.
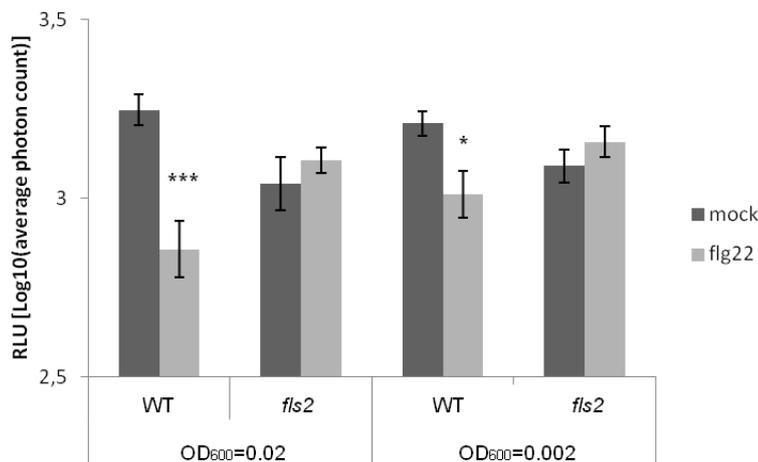
Figure 3.7. Arabidopsis seedlings elicited with flg22 and inoculated with *Pto-Lux* to a final OD_{600=}0.02 display the best induced resistance.

Six-day-old wild-type (Col-0) and *fls2* seedlings were elicited with either water or 1 μM flg22 for 24 hours and then inoculated with *Pto-Lux* to a final $OD_{600}=0.02$ or 0.002. Bacterial growth was measured at 2 DPI by quantification of average photons emission. Bars are means ± SE, n=6. Asterisks represents statistical difference between mock and flg22 treatment and mutant genotypes using two-tailed unpaired t-test (***$p<0.001$, *$p<0.05$). The experiment was repeated twice with similar results. RLU, relative light units.

Previous forward-genetics screens for mutants affected in flg22 or elf18 responses identified a number of receptor alleles, or mutants affected in the transcriptional or post-translational regulation of PRR biogenesis (Li et al., 2009; Nekrasov et al., 2009; Boutrot et al., 2010). To avoid isolation of receptor mutants, flg22 and elf18 were tested alone or in combination to evaluate their ability to induce resistance to *Pto-Lux*. In addition, different peptide concentrations (100 nM, 500 nM and 1 µM) were compared, in order to determine which was the optimal. The peptides were tested on WT that is responsive to both, *fls2*, only responsive to elf18, *efr*, only responsive to flg22, and *fls2 efr* double mutant that does not perceive either, as control. When the two peptides were tested individually, flg22 induced resistance in WT and *efr* in a dose-dependent manner. No resistance was observed in *fls2* or *fls2 efr* (Figure 3.8A), as expected. In the case of elf18, hardly any resistance was observed in WT and *fls2*, even at higher concentrations (Figure 3.8B). The combination of flg22 and elf18 showed induced-resistance in a dose-dependent manner, although it could be accounted for by only flg22, as no resistance was observed in *fls2* (Figure 3.8C). In addition, 1 µM flg22 was found to be the most effective concentration in inducing resistance (Figure 3.8A and C). Taken together, these results show that elf18 was not effective in eliciting resistance under these conditions, even at high concentrations. Therefore, it was decided that the screen would have to be performed with flg22 alone.
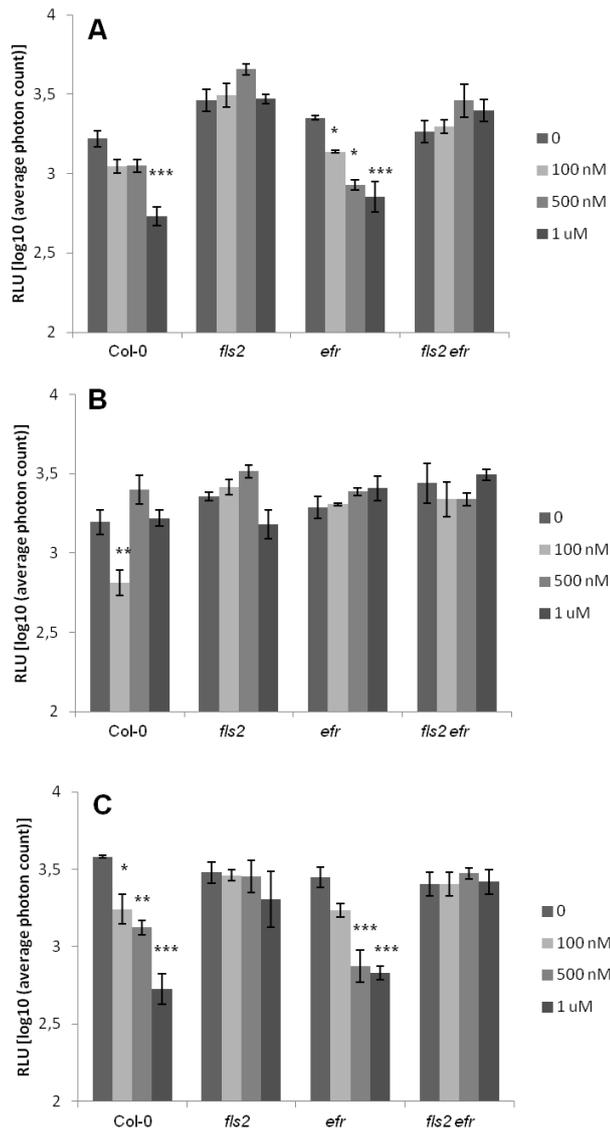
Figure 3.8. flg22 is more effective than elf18 in inducing resistance in tissue culture conditions and their combination is not synergistic.

Col-0, *fls2*, *efr* and *fls2 efr* seedlings were elicited with water or 1 µM, 500 nM or 100 nM of flg22 or flg22+elf18 for 24 hours and then inoculated with *Pto* DC3000-*Lux*. Bacterial growth was quantified at 2 days post inoculation (DPI) as $\log_{10}$ of relative light units (RLU). (A) flg22 pre-treatment (B) elf18 pre-treatment (C) flg22+elf18 pre-treatment. Bars are means ± SE, n=4. Asterisks represents statistical difference between Col-0 and mutant genotypes (***p<0.001, **p<0.01, *p<0.05) using one way ANOVA and Tukey's multiple comparisons post-test.

To summarize, the most appropriate conditions to replicate flg22-induced resistance in Arabidopsis seedlings grown *in vitro* were: germinate seedlings in liquid 1xMS with 1% sucrose in 24-well plates (approximately 5 seedlings/well); after six days, replace the medium with fresh medium containing flg22 1 μM and treat seedlings for 24 hours prior to bacterial infection with *Pto* DC3000-*Lux* at OD_{600} 0.02; bacterial levels would then be determined through evaluation of bacterial luminescence at 1 DPI. Using this experimental set-up, bacterial luminescence in WT seedlings pre-treated with flg22 was barely detectable, in contrast to *fls2* seedlings or mock-treated seedlings (Figure 3.9).
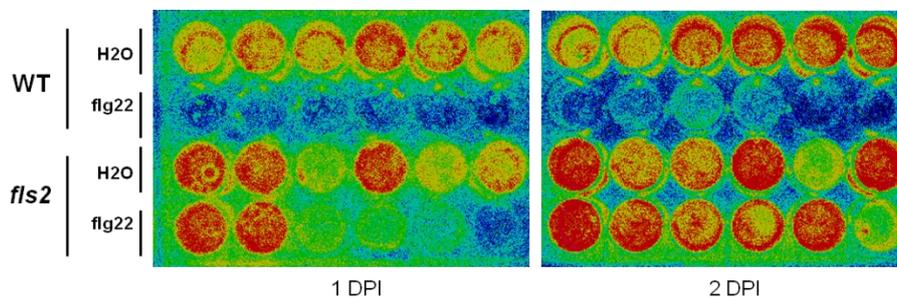
Figure 3.9. Seven day-old seedlings previously germinated in liquid media in 24-well plates show the greater flg22-induced resistance to *Pto* DC3000.

Six-day-old wild-type (Col-0) and *fls2* seedlings were elicited with either water or 1 μM flg22 for 24 hours and then inoculated with *Pto-Lux*. Heat map image of bacterial luminescence in Col-0 and *fls2* seedlings. Images were taken with Photek camera at 1 and 2 DPI.

Overall, this indicated that WT seedlings can mount effective immunity toward bacteria when grown *in vitro*, similar to what happens in adult plants. It is worth noting that enhanced disease susceptibility in *fls2* is not always clear under these conditions, in contrast to what happens in adult plants (Zipfel et al., 2004; Zeng and He, 2010).

In order to demonstrate that measuring bacterial luminescence to evaluate bacterial growth in the seedlings reflects the actual bacterial numbers, bacteria were quantified both in the seedlings and in the surrounding media.

Seedlings were surface-sterilized in ethanol, rinsed in water and blot-dried. The weight of individual seedlings was recorded with a precision scale. Individual seedlings were homogenized in 10 mM MgCl$_2$ and placed under the Photek camera to take luminescence measurements prior to serial dilutions. Bacterial growth in WT seedlings pre-treated with flg22 was significantly reduced compared to mock treatment and *fls2* seedlings (Figure 3.10A). This was reflected by the decrease in luminescence detected in homogenized seedlings (Figure 3.10B). Furthermore, bacterial numbers in the media surrounding the seedlings were also reduced when WT was elicited with flg22, but not when mock-treated or with *fls2* (Figure 3.10C).
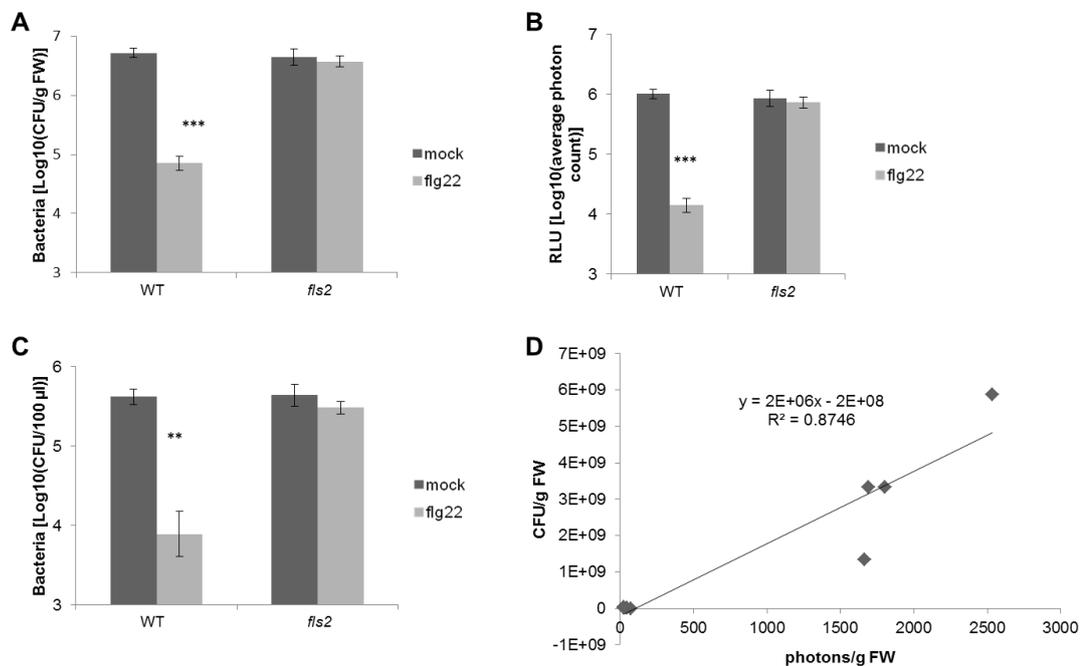
Figure 3.10. Pre-treatment with flg22 in Col-0 reduces growth of *Pto-Lux* in the seedlings and in the surrounding media and it correlates with bacterial luminescence.

Six-day-old wild-type (Col-0) and *fls2* seedlings were elicited with either water or 1 µM flg22 for 24 hours and then inoculated with *Pto-Lux*. Bacterial growth was measured at 2 DPI by plating serial dilutions (A) or by quantification of average photons emission (C) of homogenized seedlings previously surface-sterilized with ethanol and rinsed in sterile water. Bacterial growth in the surrounding media was quantified at 2 DPI by plating serial dilutions (B). Bars are means ± SE, n=4. Asterisks represents statistical difference between water and flg22 pre-treatment (**p<0.01; ***p<0.001) using two-tailed unpaired t-test. (D) Correlation between bacterial growth, as in (A) and bacterial luminescence, as in (C). The experiment was repeated twice with similar results. RLU, relative light units.

Moreover, when the amount of bacteria, expressed as CFU/g FW, was plot against the amount of photons emitted by the same samples, expressed as photons/g FW, a correlation of 0.87 was found (Figure 3.10D). Taken together, these results indicate that bacterial luminescence reflects actual bacterial numbers in the newly developed system. Furthermore, reduction in bacterial growth triggered by flg22 happens both inside the seedlings and in the surrounding media, with no need of further manipulations. Therefore bacterial luminescence could be used as a measure of bacterial growth.

In addition, the luminescence emitted by the *Pto-Lux* bacterial strain was quantified over time to confirm the stability of the luminescence produced. Results showed that over a five minutes time-frame luminescence levels were steady (Figure 3.11), suggesting that the chlorophyll auto-luminescence had negligible effects on the overall luminescence counts.
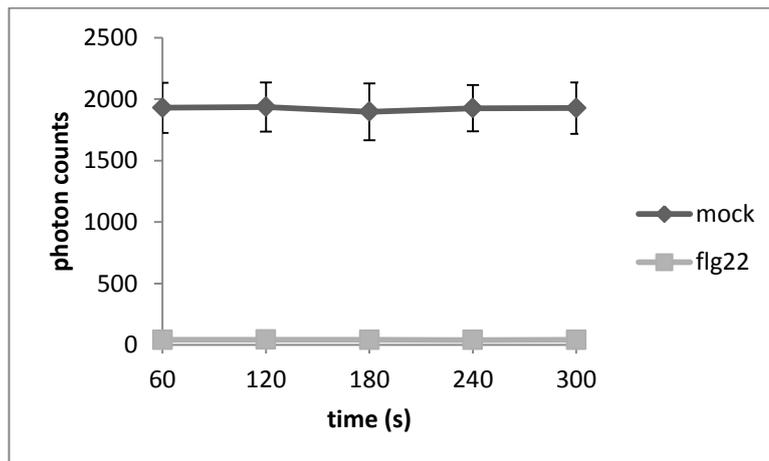
Figure 3.11. Bacterial luminescence of *Pto-Lux* strain is stable.

Six-day-old wild-type (Col-0) seedlings were inoculated with *Pto-Lux* to a final $OD_{600}=0.02$. Bacterial growth was measured at 2 DPI by quantification of average photons emission. Lines represent average measurement of bacterial luminescence in individual seedlings taken at 60 seconds intervals. The experiment was repeated twice with similar results.

3.2.2.2 Proof of concept

The *pir* mutant screen aims at isolating novel PTI components. To test whether the settings described in the previous section were effective to this end, known components of FLS2-mediated PTI were tested. *bak1-4* (Chinchilla et al., 2007; Heese et al., 2007) and *bik1 pbl1* (Zhang et al., 2010) were chosen due to their impairment in inducing immunity to bacteria after flg22 pre-treatment and were compared to WT and *fls2*. In addition, because it is difficult to evaluate enhanced disease susceptibility or resistance to bacteria with the *in vitro* infection assay, as shown previously, it was decided to carry out the *pir* screen without mock treatment. Consequently, this test also aimed at assessing whether differences in flg22-induced resistance between mutants and WT were still consistent. Results showed the known defect of *bak1-4* and *bik1 pbl1* in flg22-induced resistance with the settings designed for the *pir* screen, making the *in vitro* pathogenicity assay effective for the purpose of the screen (Figure 3.12A). Moreover, differences were visually detectable, indicating that mutants could be isolated by visual inspection of the luminescence read-out (Figure 3.12B) and that the screening conditions were sufficient to identify known PTI mutants.
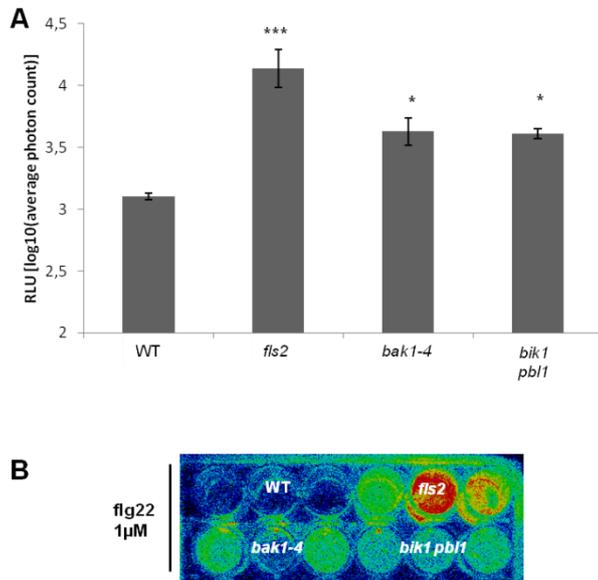
Figure 3.12. Arabidopsis *bak1-4*, *bik1 pbl1* and *fls2* mutant seedlings are impaired in flg22-induced resistance to *Pto* DC3000-*LuxCDABE*.

Six-day-old wild-type (Col-0), *fls2*, *bak1-4* and *bik1 pbl1* seedlings were elicited with 1 µM flg22 for 24 hours and then inoculated with *Pto* DC3000 *LuxCDABE*. Bacterial growth was quantified at 1 DPI as relative light units (RLU), corresponding to the $\log_{10}$ of the average photon count. (A) Heat map image of bacterial luminescence detected with a CCD camera (B) Bacterial growth expressed as RLU. Bars are means ± SE, n=3. Asterisks represents statistical difference between Col-0 and mutant genotypes (***p<0.001, *p<0.05) using using one way ANOVA and Tukey's multiple comparison post-test. The experiment was repeated three times with similar results.

3.2.2.3 The *pir* primary screen

The SALK homozygous uni-mutant collection includes 14144 individual mutant lines, covering approximately 50% of the Arabidopsis genome (Alonso et al., 2003; O'Malley and Ecker, 2010). The *pir* primary screen was solely qualitative. Each individual SALK line was sown in triplicate in a 24-well plate. Every second plate, the maximum that can fit a Photek camera, six WT and three *fls2* seedlings were used as negative and positive control, respectively.

Lines positive for reduced flg22-induced resistance were evaluated visually. A positive line was considered when the bacterial luminescence in at least

two out of three wells was greater than the highest bacterial luminescence observed among WT seedlings. Wells containing too many seedlings (> 5) or containing seedlings that showed signs of stress (eg. purple anthocyanins production) were excluded, as they may be false positives. A schematic representation of the different steps is shown in Figure 3.13.
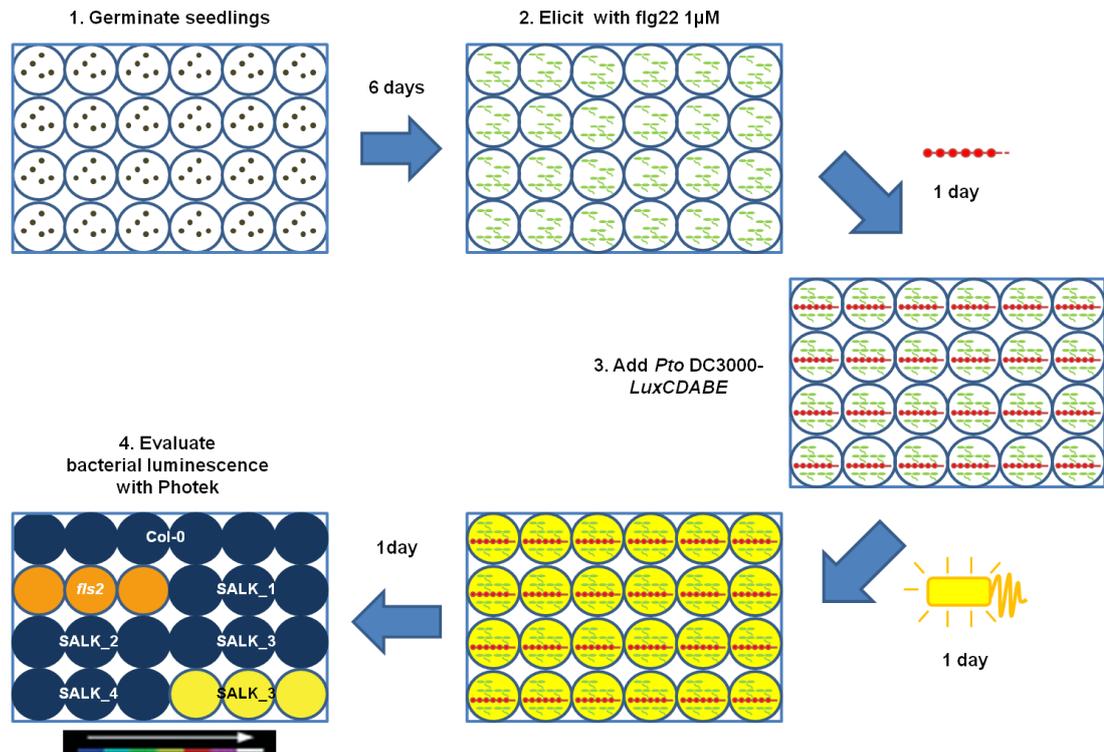
Figure 3.13. Schematic representation of the evaluation of positive candidates during the primary screen.

Arabidopsis WT (Col-0), *fls2* and each SALK line were sown in liquid MS 1% in 24-well plates. Each line was sown in triplicate, except WT that was sown in six wells. After 6 days, seedlings were pre-treated by removing the media and add fresh media containing 1 μM flg22. After 24 hours, *Pto-Lux* was added to each well to a final $OD_{600}=0.02$. Evaluation of reduction of flg22-induced resistance was carried out visually, evaluating the bacterial luminescence. A positive line was considered when the luminescence emitted from at least two out of three wells was greater than the highest observed among WT.

Of the 14,144 uni-mutant lines, 12,828 were screened for reduction of flg22-induced resistance. About 10% of the lines could not be screened due to very poor germination rate. Of the lines used in the primary screen, 1,029 tested

positive for reduced flg22-induced resistance. Figure 3.14 shows an example of the primary screen. When the SALK uni-mutant collection was received, it was divided in 4 buckets and 141 bags. To keep track of each SALK line during the primary screen, each tube was labelled according to the bucket and the bag where they were from (*ie.* D129) and assigned a tube number (*ie.*14). SALK numbers were then retrieved at the end of the primary screen.
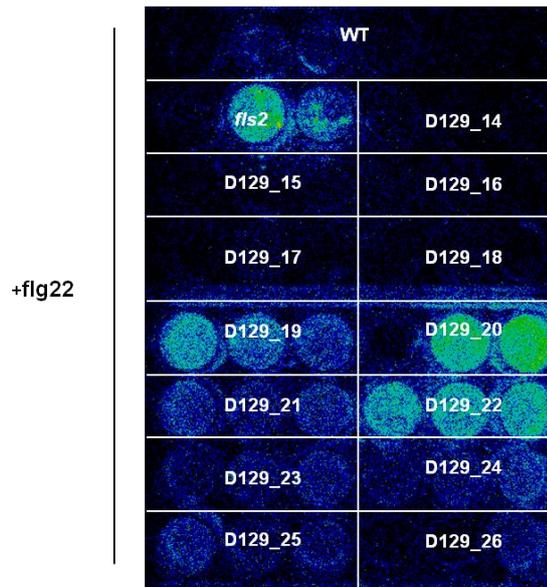
Figure 3.14. SALK lines D129_19, D129_20 and D129_22 are positive candidates for reduction of flg22-induced resistance.

Heat map image of bacterial luminescence detected with a CCD camera (Photek). Six-day-old wild-type (Col-0), *fls2*, and individual SALK lines were elicited with 1 µM flg22 for 24 hours and then inoculated with *Pto-Lux*. Bacterial growth was evaluated by the luminescence emitted from individual wells at 1DPI. The SALK collection is divided in 141 bags. Lines are labelled according to bag (D129) and the tube number (14-26).

To test whether the reduced induced-resistance observed in seedlings could be confirmed in adult plants, the first 35 positive lines isolated were re-tested for impairment of flg22-induced resistance at the adult stage. To reduce the number of samples to handle and reproduce the experimental set-up of the primary screen, the test was carried out without a mock treatment. WT and *fls2* were used as controls. Of the 35 lines tested, four showed bacterial

levels significantly higher than WT after flg22 treatment. An example is given in Figure 3.15. The rest of the lines showed bacterial levels comparable to WT and were discarded, as false positives. Although this result confirmed the validity of the primary screen, it should be noted that it did not give any information on the basal resistance of the different mutants. Therefore, confirmed candidates would need further tests to confirm the phenotype.
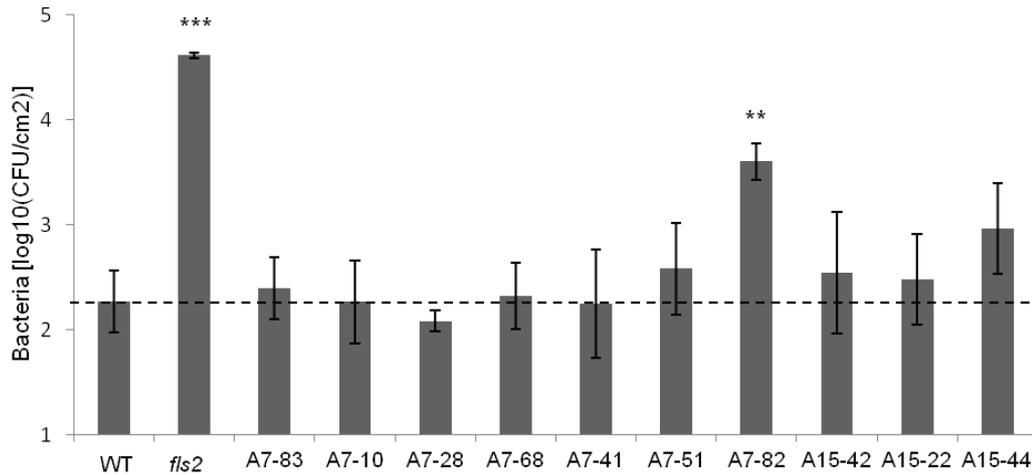
Figure 3.15. A7-82 is affected in the flg22-induced resistance at the adult stage.

Five-week-old plants were elicited with 1 µM flg22 for 24 hours and then inoculated with *Pto* DC3000 (OD$_{600}$=0.0002). Bacterial growth was measured at 2 DPI by plating serial dilutions of homogenized leaf disks. Bars are means ± SE, n=4. Asterisks represents statistical difference between Col-0 and mutant genotypes (***p<0.001, **p<0.01) using using one way ANOVA and Dunnet's Multiple comparison test.

3.2.2.4 The *pir* secondary screen

Although the confirmation of the *pir* phenotype in adult plants for a small number of selected candidate mutants was successful, this was found to be labour-intensive and not feasible to confirm all the 1,029 mutants initially identified during the primary screen. In addition, only 4 out of 36 mutants could be confirmed within this initial set, indicating a large number of false positives. Instead, an *in vitro*-based assay similar to the one developed for the primary screen was used. A mock treatment was introduced to allow

quantitative comparison with flg22 treatment. Seeds were germinated on solid media in Petri dishes and seedlings were individually pricked-out in 96-well plates in liquid media. Mutants were tested in groups of ten, each with Col-0 and *fls2* as controls. Out of the 1,029 candidate mutants identified in the primary screen, the secondary screen confirmed 108 *pir* mutants with reduced flg22-induced resistance. This included lines with induced resistance (IR) ≤ 65% of WT, calculated as the difference between mock and flg22 treatment, normalized against WT (*ie*. WT=100%, *fls2*=0%). In the event that, due to an experimental error, WT did not show any flg22-induced resistance, but at least six out of ten mutant lines did, the % of IR was calculated on the average of the induced resistance of these lines. In other cases, the lines were re-tested. Notably, one of *pir* mutants confirmed during the secondary screen was a novel allele of *fls2*, which served as an additional proof of the validity of the approach. The 108 *pir* mutants are listed in Table 1 and an example is given in Figure 3.16 A and B.
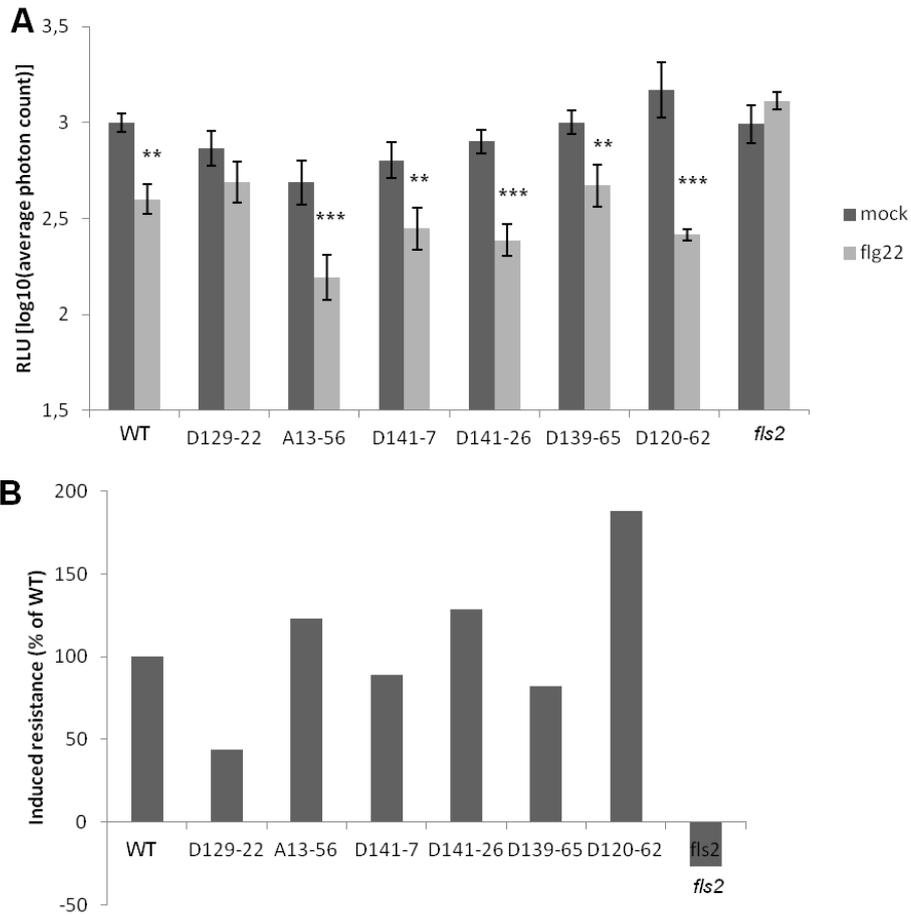
Figure 3.16. Reduced flg22-induced resistance is confirmed in D129-22 (*pir60*).

WT (Col-0), *fls2* and individual candidates from the primary screen were elicited with either water or 1 µM flg22 for 24 hours and then inoculated with *Pto-Lux*. (A) Bacterial growth was quantified at 2 DPI as relative light units (RLU), corresponding to the $\log_{10}$ of the average photon count. Bars are means ± SE, n=8. Asterisks represents statistical difference between mock and flg22 treatment (***p<0.001, **p<0.01) using two-tailed unpaired t-test. (B) Induced resistance, calculated as the difference between the average of mock and flg22 treatment, normalized against WT (Col-0 =100%).

119

Table 3.1. List of *pir* mutants selected after the secondary screen.

The 108 *pir* mutants confirmed for reduction of flg22-induced resistance are listed below. SALK number, predicted targeted locus, predicted location of the T-DNA insertion and annotated function are indicated (when known). In case one SALK line was annotated to have two or more T-DNA insertions, each insertion is labeled with a different letter. Induced resistance (IR) was calculated as the difference between the average of mock and flg22 treatment of each mutant line, normalized against WT (*ie*. IR in WT =100%). [a] indicates that the IR was normalized against the average of the induced resistance of other mutant lines, when WT was found unresponsive but at least six lines showed flg22-induced resistance. For *pir*s with multiple insertions, the IR is indicated for #a only. *pir* 1 to 4 were confirmed in adult plants (see section 3.2.2.3). *pir*s highlighted in grey were tested as top45 (see next paragraph).

	SALK#	AGI	insertion	Locus	IR (%)
pir1	SALK_070074C	At4g13965	promotor	Putative F-box/LRR-repeat protein	
pir2	SALK_033267C	At5g20050	promotor	RLCK	
pir3	SALK_029789C	At3g56730	5'UTR	Putative endonuclease or glycosyl hydrolase	
pir4	SALK_103071C	At1g02610	intron	RING/FYVE/PHD zinc finger superfamily protein	
pir6	SALK_128309C	At5g65970	promotor	MILDEW RESISTANCE LOCUS O 10	51.16
pir8	SALK_107900C	At1g69560	exon	ATMYB105, LATERAL ORGAN FUSION 2	55.43
pir10	SALK_086181C	At3g45755	exon	transposable element gene	36.65
pir12	SALK_037779C	At3g18650	exon	AGAMOUS-LIKE 103	55.18
pir14a	SALK_061729C	At1g31140	intron	AGAMOUS-LIKE 63	46.92
pir14b		At1g31150	promotor	sequence-specific DNA binding transcription factor activity	
pir15	SALK_063824C	At3g21230	intron	4-COUMARATE:COA LIGASE 5	60,73[a]
pir16	SALK_009815C	At1g16980	exon	TREHALOSE -6-PHOSPHATASE SYNTHASE S2	47.64
pir17	SALK_027635C	At1g06020	exon	pfkB-like carbohydrate kinase family protein	-7.82
pir18a	SALK_039347C	At1g06925	5' UTR	unknown	44.19
pir18b		At3g61690	5' UTR	nucleotidyltransferases	
pir19	SALK_099012C	At5g62560	exon	RING/U-box superfamily protein with ARM repeat domain	-8.42
pir20	SALK_125815C	At3g47770	intron	ABC2 HOMOLOG 5	14.58
pir21a	SALK_046567C	At3g25730	promotor	ETHYLENE RESPONSE DNA BINDING FACTOR 3	-26.19
pir21b		At1g78860	3'UTR	curculin-like (mannose-binding) lectin family protein	
pir21c		At1g78850	promotor	curculin-like (mannose-binding) lectin family protein	
pir22a	SALK_131086C	At5g34860	promotor	transposable element gene	13.12
pir22b		At5g34870	promotor	zinc knuckle (CCHC-type) family protein	
pir23a	SALK_015817C	At5g25470	promotor	AP2/B3-like transcriptional factor family protein	-19.13
pir23b		At5g25475	exon	AP2/B3-like transcriptional factor family protein	
pir24a	SALK_049092C	At3g01760	exon	Transmembrane amino acid transporter family protein	18.39
pir24b		At1g62090	exon	peudogene	
pir25	SALK_089110C	At3g05545	intron	RING/U-box superfamily protein	-29.95
pir26a	SALK_124232C	At1g11790	exon	AROGENATE DEHYDRATASE 1,	61.00
pir26b		At1g11785	promotor	unknown	
pir27a	SALK_062847C	At4g11100	promotor	unknown	63.23
pir27b		At3g30802	exon	transposable element gene	
pir28	SALK_140348C	At1g73450	3'UTR	Protein kinase superfamily protein	42,61[a]
pir29	SALK_053005C	At2g03410	5'UTR	Mo25 family protein	14.81
pir30	SALK_109179C	At4g10720	promotor	Ankyrin repeat family protein	-14.62

(continues on next page)

pir31	SALK_104865C	At1g18950	exon	DDT domain superfamily	56.09
pir32	SALK_018535C	At1g08135	exon	cation/H+ exchanger 6B (CHX6B)	32.57
pir33	SALK_106920C	At1g49860	promotor	GLUTATHIONE S-TRANSFERASE (CLASS PHI) 14	46.50
pir34	SALK_142024C	At2g16250	5' UTR	Leucine-rich repeat protein kinase family protein	-35.78
pir35	SALK_110320C	At2g28290	exon	CHROMATIN REMODELING COMPLEX SUBUNIT R 3	-24.71
pir36	SALK_138650C	At2g36480	exon	ENTH/VHS family protein	45.85
pir38	SALK_048972C	At1g30530	5'UTR	UDP-GLUCOSYL TRANSFERASE 78D1	11.67
pir39	SALK_056086C	At5g16650	intron	Chaperone DnaJ-domain	33.84
pir40	SALK_133460C	At5g67420	5'UTR	LOB-domain protein	52.05
pir42	SALK_137516C	At1g10810	intron	NAD(P)-linked oxidoreductase superfamily protein	13.20
pir43a	SALK_125391C	At1g71080	promotor	RNA polymerase II transcription elongation factor	40.41
pir43b		At1g71090	promotor	Auxin efflux carrier family protein	
pir44	SALK_139843C	At3g42790	intron	Alfin1-like family of nuclear-localized PHD (plant homeodomain)	49.03
pir45	SALK_090688C	At1g72410	intron	COP1-interacting protein-related	62.69
pir46	SALK_087652C	At1g55930	5'UTR	CBS domain/transporter associated domain-containing protein	-39.16
pir47	SALK_074806C	At1g05830	intron	homolog of trithorax, a histone-lysine N-methyltransferase	45,61[a]
pir49	SALK_093949C	At5g56250	exon	HAPLESS 8 (HAP8)	48,04[a]
pir50	SALK_054063C	At4g16490	5'UTR	ARM repeat superfamily protein	49.04
pir51	SALK_098044C	At4g18490	intron	unknown	53.20
pir52	SALK_113810C	At3g55960	exon	Haloacid dehalogenase-like hydrolase (HAD) superfamily protein	55.59
pir53	SALK_061320C	At5g58100	exon	unknown	36.95
pir54a	SALK_072862C	At2g27080		Late embryogenesis abundant (LEA) family	4.58
pir54b		chr3 2094515			
pir55a	SALK_114593C	At3g56020	5'UTR	Ribosomal protein L41 family	50.18
pir55b		At3g56030	exon	Tetratricopeptide repeat (TPR)-like superfamily protein	
pir57	SALK_030145C	At2g16700	intron	Encodes actin depolymerizing factor 5 (ADF5)	45.87
pir58	SALK_026801C	At5g46330	exon	FLS2	-5.57
pir59a	SALK_094830C	At3g18140	promotor	LETHAL WITH SEC THIRTEEN 8-1	56.71
pir59b			exon	pseudogene	
pir60	SALK_013999C	At2g38700	5'UTR	MEVALONATE DIPHOSPHATE DECARBOXYLASE 1	50.93
pir61	SALK_108656C	At3g09360	exon	Cyclin/Brf1-like TBP-binding protein	-16.18
pir62	SALK_009646C	At3g62390	exon	TRICHOME BIREFRINGENCE-LIKE 6	60.87
pir63	SALK_071004C	At2g41140	intron	CDPK-RELATED KINASE 1	54,81[a]
pir64	SALK_134892C	At1g47310	5'UTR	unknown	-4.90
pir65a	SALK_110864C	At3g46630	promotor	unknown	22.50
pir65b		At3g46640	promotor	LUX, LUX ARRHYTHMO, PCL1, PHYTOCLOCK 1	
pir66	SALK_055351C	At5g01890	exon	Leucine-rich receptor-like protein kinase family protein	22.22
pir67	SALK_012496C	At1g50720	promotor	Stigma-specific Stig1 family protein	39.47
pir68	SALK_052748C	At2g41700	exon	ARABIDOPSIS THALIANA ATP-BINDING CASSETTE A1	59.48
pir69	SALK_089787C	At3g16230	5'UTR/intron	Predicted eukaryotic LigT	56.61
pir71	SALK_046603C	At3g56600	exon	Protein kinase superfamily protein	52,80[a]
pir72a	SALK_035970C	At1g71850	5'UTR	Ubiquitin carboxyl-terminal hydrolase family protein;	40.96
pir72b		At1g71860	promotor	PROTEIN TYROSINE PHOSPHATASE 1	
pir73	SALK_143098C	At1g04510	exon	MAC3A, MOS4-ASSOCIATED COMPLEX 3A	33.84
pir74a	SALK_138456C	At1g19930	5'UTR	Galactose oxidase/kelch repeat superfamily protein	-1.28
pir74b		At1g19920	promotor	ATP SULFURYLASE ARABIDOPSIS 1	
pir75	SALK_055489C	At5g59150	intron	ARABIDOPSIS RAB GTPASE HOMOLOG A2D	53.95
pir80	SALK_026829C	At2g30220	intron	GDSL-like Lipase/Acylhydrolase family protein	39.56

(continues on next page)

pir82	SALK_063557C	At4g04880	5'UTR	adenosine/AMP deaminase family protein	56.33
pir83	SALK_115133C	At1g59720	exon	CHLORORESPIRATORY REDUCTION28	38.19
pir84	SALK_140384C	At5g49630	intron	AMINO ACID PERMEASE 6	17.88
pir86	SALK_026036C	At5g03540	intron	ATEXO70A1	56.68
pir87a	SALK_060611C	At1g05135	5'UTR	pseudogene	54.41
pir87b		At1g05136	exon	unknown	
pir88	SALK_035543C	At4g13110	5'UTR	BSD domain-containing protein	32.52
pir91	SALK_009133C	At1g55290	exon	similar to oxidoreductase, 2OG-Fe(II) oxygenase	62.13
pir92a	SALK_005663C	At1g15080	5'UTR	phosphatidic acid phosphatase	42.84
pir92b		At1g15060	promotor	conserved protein UCP031088, alpha/beta hydrolase	
pir93	SALK_040073C	At3g33193		transposable element	46.71
pir94	SALK_037715C	At5g18230	intron	transcription regulator NOT2/NOT3/NOT5 family protein	50,31[a]
pir95a	SALK_043816C	At5g06210	exon	RNA binding (RRM/RBD/RNP motifs) family protein	36.96
pir95b		At5g06200		CASPARIAN STRIP MEMBRANE DOMAIN PROTEIN 4	
pir96	SALK_030374C	At2g18380	5'UTR	GATA TRANSCRIPTION FACTOR 20	20.56
pir97	SALK_012944C	At3g47980	promotor	Integral membrane HPP family protein	59.91
pir99	SALK_027726C	At5g64610	exon	HISTONE ACETYLTRANSFERASE OF THE MYST FAMILY 1	39,25[a]
pir100	SALK_116446C	At4g12570	intron	UBIQUITIN PROTEIN LIGASE 5	53,80[a]
pir102	SALK_116115C	At4g26640	3'UTR	ATWRKY20	60.52
pir103	SALK_064346C	At4g39410	exon	ATWRKY13	50.05
pir104	SALK_053802C	At1g53450	promotor	unknown	59.57
pir105	SALK_023283C	At4g31870	exon	GLUTATHIONE PEROXIDASE 7	48.35
pir106	SALK_062717C	At4g21323	exon	Subtilase family protein	50.68
pir107	SALK_104120C	At5g07720	5'UTR	Galactosyl transferase GMA12/MNN10 family protein	60.60
pir108	SALK_117852C	At2g30800	intron	HELICASE IN VASCULAR TISSUE AND TAPETUM	-22.59
pir109	SALK_119194C	At3g45580	exon	RING/U-box protein with C6HC-type zinc finger	32.20
pir110	SALK_014602C	At5g08600	exon	U3 ribonucleoprotein (Utp) family protein	44,32[a]
pir111	SALK_025511C	At2g10980	exon	transposable element	45.87
pir112	SALK_027830C	At4g07516	exon	transposable element	41.55
pir113	SALK_131099C	At5g28635	exon	transposable element	45.69
pir114	SALK_062231C	At3g23550	exon	MATE efflux family protein	37.28
pir115	SALK_032680C	At5g64950	exon	Mitochondrial transcription termination factor family protein	59.11
pir116	SALK_045570C	At3g02660	exon	EMBRYO DEFECTIVE 2768	60,42[a]
pir117	SALK_062938C	At5g29028	promotor	transposable element	57,43[a]
pir118a	SALK_057621C	At4g03390	exon	STRUBBELIG-receptor family 3 (SRF3)	40.81
pir118b		At2g03040	promotor		
pir118c		At5g61520	promotor		
pir119	SALK_032655C	At3g18230	exon	Octicosapeptide/Phox/Bem1p family protein	19.02
pir122	SALK_151254C	At3g19670	intron	PRE-MRNA-PROCESSING PROTEIN 40B	34.37
pir123	SALK_106028C	At5g56075	exon	aminoacyl-tRNA ligase activity	43.40
pir124	SALK_136210C	At3g53270	promotor	Small nuclear RNA activating complex (SNAP43)	50.10
pir125	SALK_066562C	At4g24050	exon	NAD(P)-binding Rossmann-fold superfamily protein	-15.91
pir126a	SALK_140285C	At3g06970	exon	RNA-binding (RRM/RBD/RNP motifs) family protein	23.65
pir126b		At3g06980	promotor	DEA(D/H)-box RNA helicase family protein	
pir126c		chr3 2094490			
pir127a	SALK_106269C	At4g14805	5'UTR	protease inhibitor/seed storage/lipid transfer protein (LTP)-related	29.74
pir127b		At4g14810	promotor	unknown	
pir128	SALK_037019C	At2g45570	exon	CYP76C2	39,67[a]
pir129	SALK_092066C	At5g28310	exon	oxidoreductase-related	32,74[a]

To further eliminate false positives, a list of the 45 *pir* mutants with greater reduction of flg22-induced resistance was compiled. This was determined by ranking the *pir* mutants according to the %IR (see Table 1). The 45 *pir* mutants with the lowest %IR were re-tested at the seedling stage at least three times to confirm the phenotype. Four *pir* mutants showed a reproducible reduction of flg22-induced resistance, *pir32*, *pir54*, *pir65* and *pir66* (Figure 3.17). The remaining 46 either showed WT induced resistance or results were inconclusive and were therefore discarded.
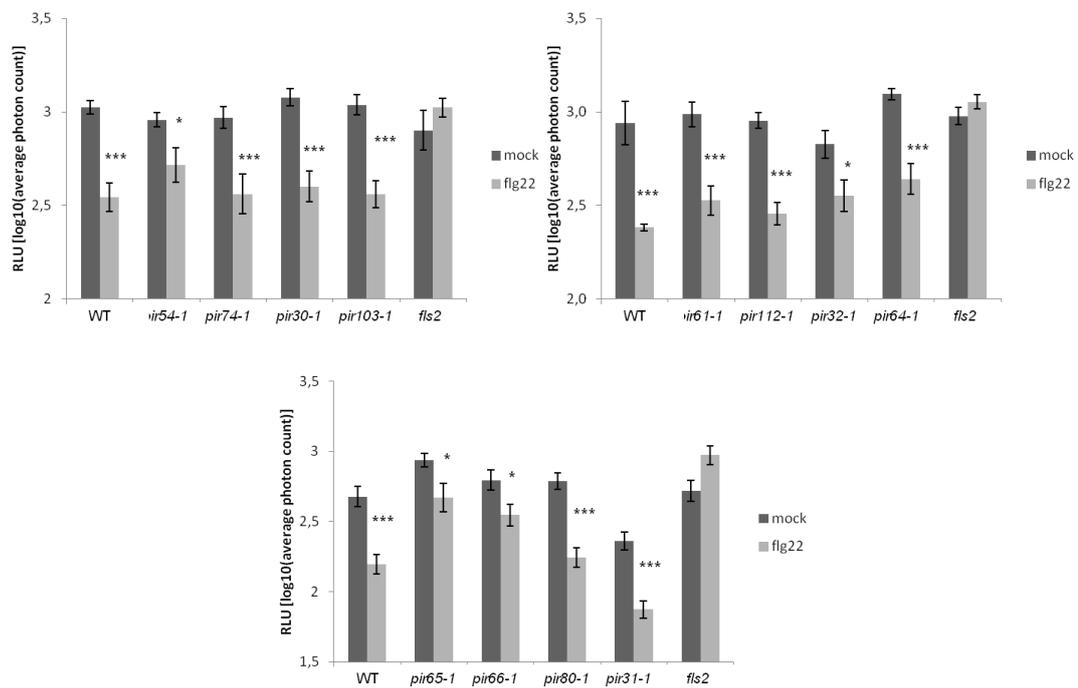
Figure 3.17. *pir54*, *pir32*, *pir65* and *pir66* are impaired in flg22-induced resistance at the seedling stage.

WT (Col-0), *fls2* and individual *pir* mutants were elicited with either water or 1 µM flg22 for 24 hours and then inoculated with *Pto-Lux*. Bacterial growth was quantified at 2 DPI as relative light units (RLU), corresponding to the $\log_{10}$ of the average photon count. Bars are means ± SE, n=8. Asterisks represents statistical difference between mock and flg22 treatment (***$p < 0.001$, *$p < 0.05$) using two-tailed unpaired t-test. The experiment was repeated three times with similar results.

3.2.2.5 The *pir* tertiary screen

The candidate *pir* mutants confirmed after the secondary screen were taken forward to the tertiary and final round of screen. A schematic summary of the three round of screen is in Figure 3.18.
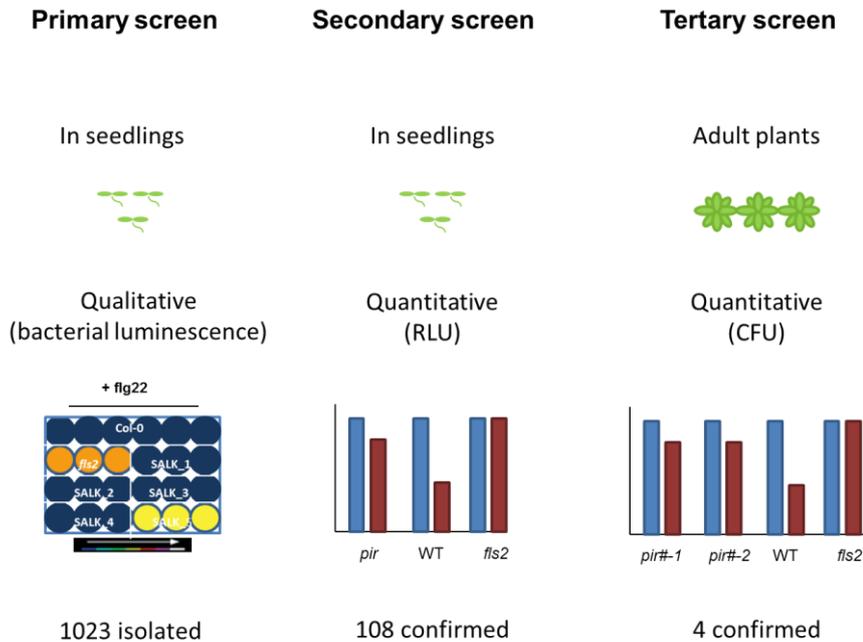
Figure 3.18. Schematic summary of the *pir* screen.

The primary screen was carried out in seedlings and evaluation of the reduction in flg22-induced resistance in SALK mutant lines was carried out visually, using *Pto* DC3000 *LuxCDABE*. 1023 mutants were isolated and re-tested in a second round of screen. The secondary screen was also carried out in seedlings and compared mock and flg22 pre-treatment to confirm the impaired flg22-induced resistance. Bacterial levels were quantified through measurement of bacterial luminescence and expressed as relative light units (RLU). 108 *pir*s were confirmed. The tertiary screen compared, when possible, mutant alleles of the same locus, to confirm the link between impaired flg22-induced resistance and T-DNA insertion. Tests were carried out in adult plants and bacterial levels were evaluated by serial dilutions of homogenized leaves samples. Four *pir*s reproducibly showed impaired flg22-induced resistance to *Pto* DC3000.

For each individual SALK line data on the location of the insertion is available through the SALK institute website (http://signal.salk.edu/cgi-bin/tdnaexpress). To demonstrate that the locus responsible for the impairment of flg22-induced resistance was indeed the one annotated and

causative of the *pir* phenotype when mutated, two independent alleles were ordered, where available. In the case multiple insertions were annotated, alleles were ordered for each insertion. Each mutant allele was genotyped and tested with the corresponding original allele at the adult stage when possible.

The four re-confirmed *pir* mutants (*pir54*, *pir32*, *pir65* and *pir66*) were tested at the adult stage, although independent alleles were only available for *pir66*. In addition, 29 *pir* mutants from the list of 108 were hand selected for further tests. This was because their annotation was of special interest for the aim of the screen. These included transcription factors, molecular components of the secondary metabolism and transporters. Results indicated that *pir32* showed significant reduction of flg22-induced resistance in two out of three experiments (Figure 3.19A). In the third experiment, a reduction was also observed, but it was not statistically significant. *pir66* showed a significant reduction in two out of four experiments (Figure 3.19B and C). Because of this ambiguous phenotype, *pir66* was not tested further. *pir54* and *pir65* had a WT phenotype (Figure 3.19B) and were dismissed.
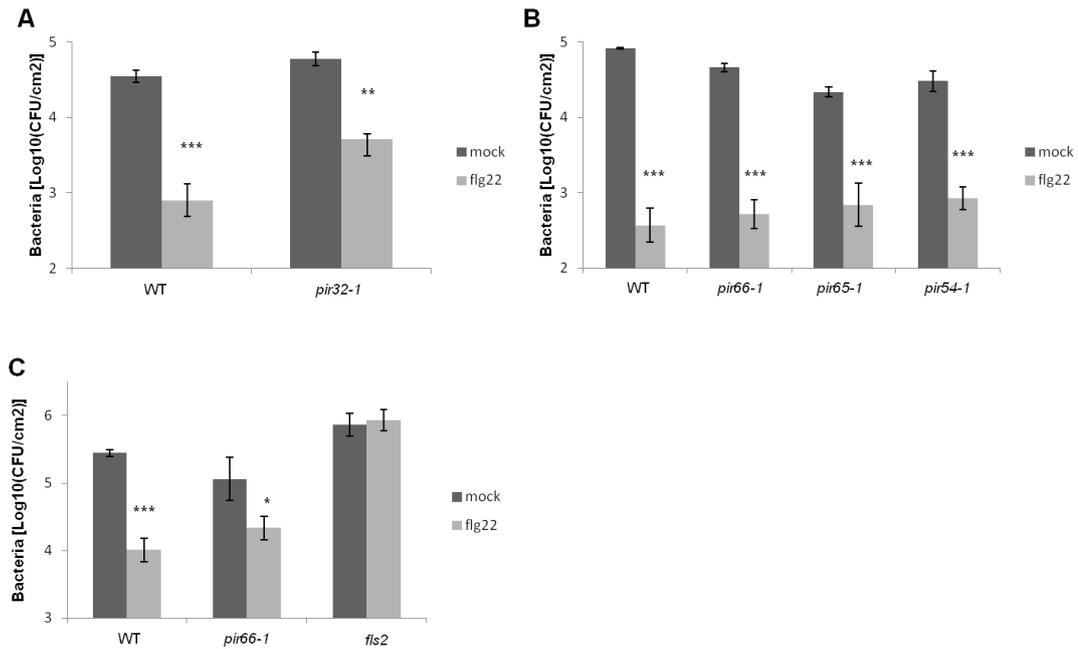
Figure 3.19. *pir32* is impaired in flg22-induced resistance at the adult stage.

Five-week-old plants were elicited with water or 1 µM flg22 for 24 hours and then inoculated with *Pto* DC3000 (OD_{600}=0.0002). Bacterial growth was measured at 2 DPI by plating serial dilutions of homogenized leaf disks. Bars are means ± SE, n=8. Asterisks indicate a statistically significant difference between mock and flg22 treatment (***p<0.001, **p<0.01) using two-tailed unpaired t-test. The experiment was repeated three times with similar results.

In addition, among the mutants that were hand selected based on their annotations, in at least two replicates, *pir20*, *pir38* and *pir60* showed reproducible reduction of flg22-induced resistance in adult plants. The remaining 26 showed a WT induced resistance or results were inconclusive and were therefore dismissed. Confirmed *pir*s are listed in Table 3.2 and a representative example is given below (Figure 3.20).

When considering the different replicates carried out, the overall penetration of the mutant phenotype could be estimated between 75% and 87.5%.
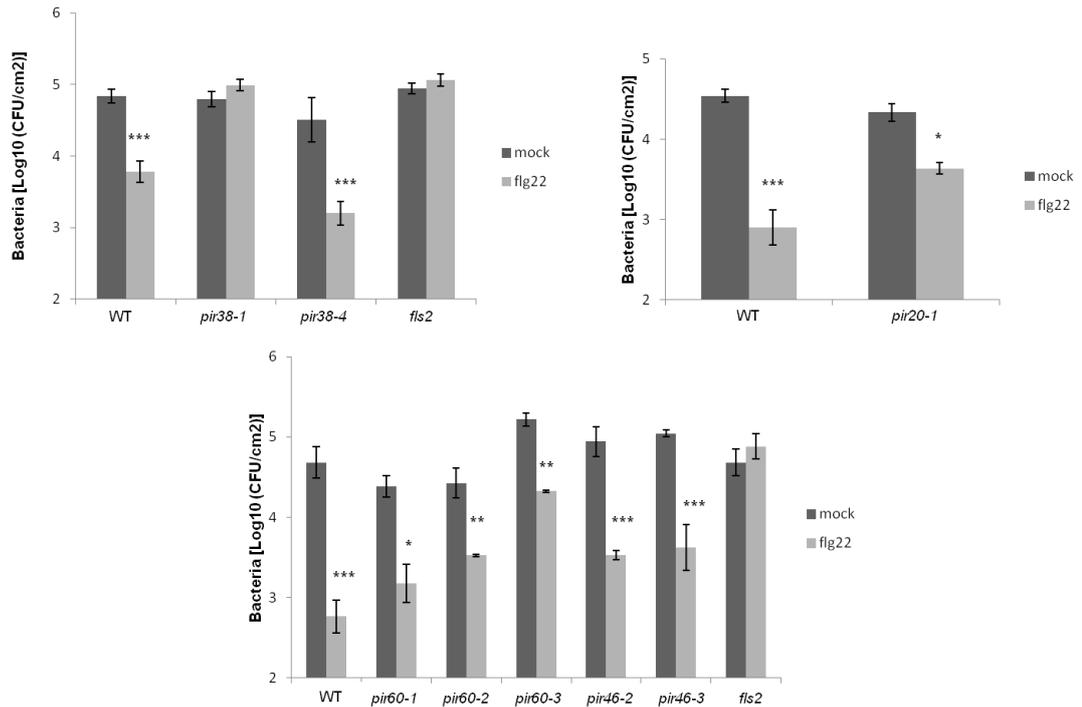
Figure 3.20. *pir38*, *pir20* and *pir60* alleles show impaired flg22-induced resistance.

Five-week-old plants were elicited with water or 1 µM flg22 for 24 hours and then inoculated with *Pto* DC3000 (OD_{600}=0.0002). Bacterial growth was measured at 2 DPI by plating serial dilutions of homogenized leaf disks. Bars are means ± SE, n=4. Asterisks indicate a statistically significant difference between mock and flg22 treatment (***p<0.001, **p<0.01, *p<0.05) using two-tailed unpaired t-test. The experiment was repeated three times with similar results.

Table 3.2. List of *pir* mutants confirmed after three round of screen.

pir #	SALK #	AGI	Locus
pir20	SALK_125815C	At3g47770	ABC2 HOMOLOG 5
pir32	SALK_018535C	At1g08135	cation/H$^+$ exchanger 6B (CHX6B)
pir38	SALK_048972C	At1g30530	UDP-GLUCOSYL TRANSFERASE 78D1
pir60	SALK_013999C	At2g38700	MEVALONATE DIPHOSPHATE DECARBOXYLASE 1

3.3 Summary and discussion

To gain more insights on how Arabidopsis restricts bacteria after flagellin perception, two different approaches were followed. Firstly, reverse-genetics was used to assess the role of camalexin, glucosinolates, SA and callose to PTI. These are known to provide chemical and physical defences against different pathogens, mostly fungi, and were tested to determine whether they also have a role in immunity against bacteria. Results showed that *pad3*, affected in camalexin biosynthesis, had WT induced-resistance following flg22 pre-treatment, suggesting that camalexin biosynthesis is not required for flg22-induced resistance to *Pto* DC3000. It is known that camalexin biosynthesis is induced by bacterial pathogens (Tsuji et al., 1992) and camalexin shows toxicity towards different bacteria in vitro (Rogers, 1996). In addition, *PAD3* expression is up-regulated by both flg22 and OGs (Denoux et al., 2008). However, *pad3* does not show enhanced susceptibility to bacteria (Glazebrook and Ausubel, 1994). Although this is in agreement with observation that *pad3* is not affected in flg22-induced resistance, it cannot be excluded that Arabidopsis produces a mixture of antimicrobials in response to bacteria, of which camalexin could be one. Therefore, the loss of camalexin alone would not be sufficient to observe a reduction of induced resistance. In addition, it cannot be excluded that camalexin could have a role in immunity against soil-borne pathogens, since it is synthesized in Arabidopsis roots via a different cytochrome P450 in response to flg22 (Millet et al., 2010).

When tested for defects in resistance against bacteria following flg22 perception, both indolic and aliphatic glucosinolates were found to be dispensable. Aliphatic glucosinolates can be detoxified by *Pto* DC3000 (Fan et al., 2011), and therefore the WT phenotype of *myb28 myb29* is in agreement with this. Indolic glucosinolates have been shown to have a role in flg22-dependent callose deposition (Clay et al., 2009). It has been proposed that PEN2-dependent degradation of indolic glucosinolates induces the transport of their breakdown products to the plasma membrane via PEN3

where callose is deposited (Clay et al., 2009). In addition *CYP79B2* and *CYP79B3* are also induced by flg22 and OGs (Denoux et al., 2008). However, *cyp79b2/b3* is not impaired in flg22-induced resistance. This is in contrast with Clay et al., (2009), which suggested that indolic glucosinolate-dependent callose deposition is involved in restriction of bacterial growth because of the enhanced susceptibility to *Pto* DC3000 of *cyp81f2* and *pen2*. However, CYP81F2 is placed downstream in the pathway and, if mutated, it could still accumulate intermediates upstream, opposite to *cyp79b2/b3* mutant plants, which are completely devoid of indolic glucosinolates. Moreover, Clay et al., (2009) failed to observe the enhanced resistance phenotype of *pmr4* to *Pto* DC3000, which would suggest that the experimental procedure they used may not reflect the actual biology. WT levels of induced resistance in cyp79b2/b3 also correlates with the finding that impairment in induced resistance of *pmr4,* a callose synthase mutant defective in flg22-dependent callose deposition, could be restored by crossing *pmr4* with *sid2-1* to reduce the endogenous SA level. Taken together, these results suggest that callose deposition is dispensable for resistance to bacteria following flg22 perception. In addition, the increased basal resistance of *pmr4* to bacteria is due to its constitutive upregulation of genes involved in SA biosynthesis and signaling (Nishimura et al., 2003; Kim et al., 2005). Interestingly, TTG1, a myrosinase that catalyzes glucosinolate degradation, was found overabundant in the guard cell proteome and *ttg1* is less responsive to ABA-dependent inhibition of stomata opening (Barth and Jander, 2006; Zhao et al., 2008). It would be interesting therefore to test whether glucosinolate mutants are affected in PAMP-dependent stomata responses.

A second unbiased approach involved the development of a novel genetic screen, which aimed at identifying mutants impaired in flg22-induced resistance to *Pto* DC3000 and was named <u>P</u>AMP-<u>i</u>nduced <u>r</u>esistance mutant screen (*pir*). This initially required the set-up of a novel *in vitro* screening procedure to allow the evaluation of bacterial growth in Arabidopsis seedlings

in a high-throughput manner. The set-up required extensive tests to determine the most suitable experimental condition for the screen, including the type of media and plates, the appropriate method to germinate seedlings directly in plates and the age of the seedlings to test, type and concentration of the peptide to elicit seedlings and the density of the bacterial inoculums. Although several publications now describe methods for pathogenicity assays *in vitro* (Schreiber et al., 2008; Anderson et al., 2011; Danna et al., 2011; Ishiga et al., 2011), not every condition used was found effective for the purpose of the *pir* screen. For example, 1x MS with 1% sucrose was found the best choice as growth media, and the addition of MES to stabilize the pH was not necessary. Surprisingly, when elf18 peptide was tested to determine whether a combination of peptides could give a better response and avoid the isolation of mutants that affect the stability or the regulation of the receptor, it was found ineffective. It is worth noting that elf18 is routinely used in our laboratory for different bioassays *in vitro* and *in vivo* (*ie*. Nekrasov et al., 2009; Kadota et al., 2014; Macho et al., 2014; Malinovsky et al., 2014), although in some cases (*ie*. elf18-induced resistance in adult plants) the amplitude of the response is smaller when compared to flg22. This and lower expression of *EFR* in young seedlings (http://bar.utoronto.ca/efp/cgi-bin/efpWeb.cgi) could explain the inability of elf18 of inducing resistance. Because of the availability of *Pto-Lux* strain (Fan et al., 2008), it was decided to use bacterial luminescence as proxy to evaluate bacterial levels during the *pir* screen. By quantifying bacterial levels by serial dilutions, it was demonstrated that, indeed, bacterial luminescence reflected the bacterial number in the seedlings and in the media. This also indicated that no manipulation of the plates were necessary to evaluate bacterial growth.

The primary screen was solely qualitative and designed to isolate mutants that showed impaired resistance to *Pto-lux* after flg22 pre-treatment. The primary screen identified 1029 candidates that were taken forward to the secondary screen to eliminate false positives. After the secondary screen the phenotype was confirmed for 108 *pir* mutants of which one was a novel allele

of *fls2*, supporting the biological significance of the screen. Although the secondary screen narrowed down the list of candidates, a survey of the 108 *pir* mutants by determination of the loci affected indicated a good number of transposable elements, likely to be false positive. Further tests were done *in vitro* and *in planta* to restrict the list to a manageable number of lines. Although not every *pir* has been tested so far, results confirmed four *pir* mutants (*pir20*, *pir32*, *pir38*, *pir60*) to be affected in flg22-induced resistance. In addition, *pir66*, carrying a T-DNA insertion in PXY/TDR-CORRELATED 2 (PXC2), showed a reduction in flg22-induced resistance in two out of four experiments, but it was not pursued further. However, it may be worth carrying out additional tests to determine whether loss of PXC2 could affect flg22-induced resistance. PXC2 is a LRR-RLK mainly expressed in vascular tissues (Wang et al., 2013). Although the mutant phenotype was not completely penetrant (observed between 75% and 87.5% of the individual), this could be ascribed to the variation that is intrinsic to pathogenicity assays, especially when carried out on a large number of mutants, as during a screen. However, the reproducibility of the results over different biological replicates would support the fact that these mutants are affected in flg22-induced resistance.

Briefly, *PIR20* encodes ABC2 HOMOLOG 5 (ABCA6), *PIR32* encodes cation/H+ exchanger 6B (CHX6B), *PIR38* encodes UDP-GLUCOSYL TRANSFERASE 78D1 (UGT78D1), a rhanmosyltransferase involved in glycosylation of flavonols (Jones et al., 2003), and *PIR60* encodes MEVALONATE DIPHOSPHATE DECARBOXYLASE 1 (MVD1), a biosynthetic enzyme of the mevalonate pathway (Cordier et al., 1999). To date, these genes have not been linked to immunity, thereby opening up the possibility of identifying novel components of PTI. Details of their functional characterization are given in the following chapters.

Chapter 4. Investigation on the role of flavonols in plant immunity

4.1 Introduction

4.1.1 General rules for characterisation of T-DNA mutants

Insertional mutagenesis is one of the methods commonly used for creating mutants in Arabidopsis. Mutation is achieved by integration of a foreign DNA sequence into the organism genome, disrupting genes. Insertional mutagenesis through transfer-DNA (T-DNA) is one the best established system (Krysan et al., 1999). In addition, this technique has been successfully used to create a mutant population in Arabidopsis, which can be used for genetic screens (Alonso et al., 2003; Alonso and Ecker, 2006; O'Malley and Ecker, 2010). In this population, each individual mutant line has been sequenced to determine the position of the T-DNA in the Arabidopsis genome (Alonso et al., 2003; Alonso and Ecker, 2006; O'Malley and Ecker, 2010). Although the position of the T-DNA is known and the affected loci have been annotated, several rules need to be followed for unequivocally linking a phenotype with the corresponding genotype. It has been estimated that a T-DNA insertion lines contain on average 1.5 T-DNA insertions, and ~50% of the lines contain multiple T-DNA insertions (Alonso and Ecker, 2006). Ideally, mutant lines should be backcrossed and re-tested to confirm whether the phenotype segregates with the T-DNA insertion (Krysan et al., 1999). However, co-segregation of the T-DNA with the phenotype would not prove that the T-DNA insertion is responsible for the phenotype. Although unlikely, a closely linked mutation could be causing the phenotype. For a definitive prove of the link between the T-DNA insertion and the phenotype, independent alleles should be collected and tested (Krysan et al., 1999; Østergaard and Yanofsky, 2004; O'Malley and Ecker, 2010). As alternative, generation and test of complementation lines could be carried out (Krysan et al., 1999).

Due to the size of T-DNA (5-25 Kb), insertions are mostly causing loss-of-function mutations (Krysan et al., 1999; Alonso et al., 2003; Wang, 2008). However, several T-DNA vectors used to generate T-DNA lines contain a

133

35S promoter (Ülker et al., 2008). Therefore, if they get inserted near the start codon, they have the potential of inducing overexpression of the gene (Ülker et al., 2008). In fact, knock-ups, where expression of the affected gene is up-regulated, have been reported (Krysan et al., 1999; Wang, 2008). Therefore it is important to test the effect of the T-DNA insertion on the gene expression. Nonetheless, when possible, testing the protein accumulation and functionality should be done, as the protein may accumulate but may not be functional (Wang, 2008). Moreover, in case of mutations in biosynthetic enzymes it is important to assess what is the effect of the mutation on the metabolite content, and if so, complement the mutation by exogenous chemical feedback (Shirley et al., 1995).

In the case of the *pir* screen, which was done on Arabidopsis seedlings, it was necessary to assess whether the differences observed were also relevant in adult plants. In fact, the phenotype observed could be strictly related to the specific stage of development.

4.1.2 Introduction to flavonoids

Secondary metabolites, also known as phytochemicals or specialized metabolites, are low abundant, low molecular weight molecules that are not essential for the basic physiology of plants but required for the interaction with the environment (Kroymann, 2011). It is estimated that within a plant species 5,000-25,000 secondary metabolites exist (Trethewey, 2004). Major classes of plant secondary metabolites include terpenoids, phenolic compounds and nitrogen-containing alkaloids (Yang et al., 2012).

Flavonoids are a large group of secondary metabolites characterized by the presence of two aromatic cycles (A-ring and B-ring) linked by a heterocycle (the C-ring) (Figure 4.1A) (Martens et al., 2010). They are divided into several classes, based on the level of oxidation of the C-ring: chalcones,

flavones, flavanones, flavonols, flavan-3-ols, flavandiols, anthocyanins, proanthocyanidins, aurones, 3-deoxyanthocyanins and isoflavonoids (Winkel-Shirley, 2001) (Figure 4.1B).
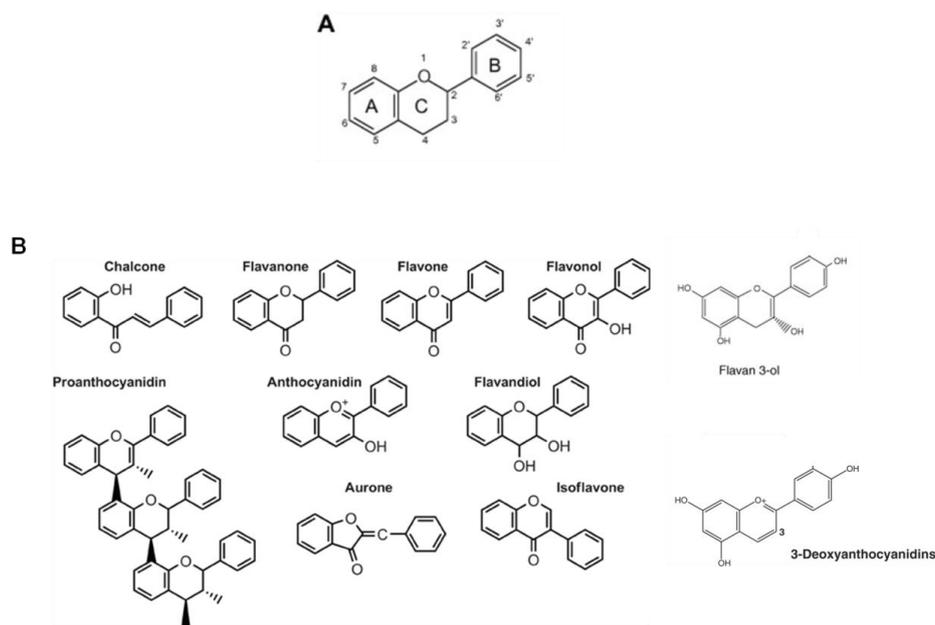
Figure 4.1. Structure of the main classes of flavonoids.

(A) Skeleton of flavonoids, showing the A-, B-, and C-ring. Numbers indicate the different carbons subject to modifications during flavonoids biosynthesis. (B) Structures of the different classes of flavonoids. Adapted from Liu et al., 2010; Martens et al., 2010; Falcone Ferreyra et al., 2012.

4.1.3 Flavonoids biosynthesis and transport in Arabidopsis

Flavonoid biosynthesis derives from the phenylpropanoid and the polyketide biosynthetic pathways. CHALCONE SYNTHASE (CHS) is the first committed enzyme of the flavonoid biosynthetic pathway and catalyses the condensation of 4-coumaroyl-coenzyme A (CoA) with three molecules of malonyl-CoA (Kreuzaler and Hahlbrock, 1972). The central biosynthetic pathway is conserved among plant species. Glycosylation, methylation and acylation further modify aglycones, leading to a large diversity in flavonoids (Saito et al., 2013). However, enzymes like isomerases and reductases

catalyse reactions that lead to the biosynthesis of specific flavonoids which are unique to a small group of plant species (Martens et al., 2010).
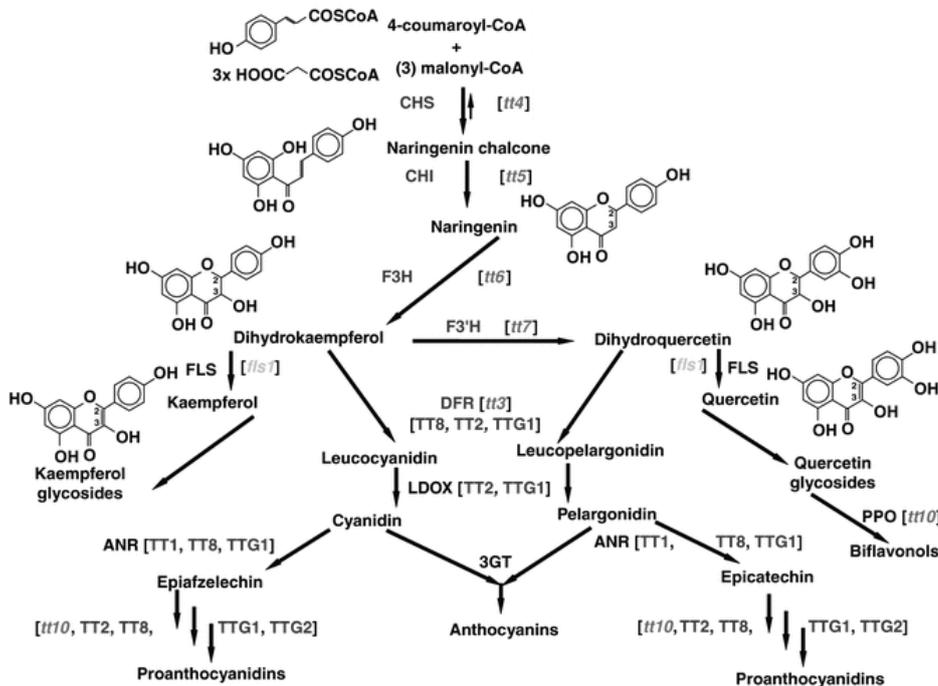
Figure 4.2. Schematic representation of the flavonoid biosynthetic pathway in Arabidopsis.

Known locations of Arabidopsis *transparent testa* (*tt*) mutations (in parentheses) are indicated on the phenylpropanoid pathway. The chemical structures of the aglycones produced during the early steps of the pathway are shown. The mutated structural genes and the affected products are TT3 (DFR: dihydroflavonol reductase); TT4 (CHS: chalcone synthase); TT5 (CHI: chalcone isomerase); TT6 (F3H: flavonol 3-hydroxylase); TT7 (F3′H: flavonol 3′-hydroxylase); and TT10 (PPO: polyphenol oxidase). Other genes involved in the pathway are 3GT (anthocyanidin 3-*O*-glycosyltransferase), ANR (anthocyanidin reductase), and LDOX (leucoanthocyanidin dioxygenase). Transparent testa 2 (TT2), transparent testa 8 (TT8), transparent testa glabra 1 (TTG1) and transparent testa glabra 2 (TTG2) are regulatory genes involved in controlling several points of the pathway (From Buer et al., 2010).

In Arabidopsis all the enzymes but one are encoded by a single gene, in contrast to other plant species (reviewed in Saito et al., 2013) (Figure 4.2). Following the synthesis of naringenin chalcone by CHS/TRANSPARENT TESTA 4 (TT4), subsequent steps involve CHALCONE ISOMERASE/TRANSPARENT TESTA 5 (CHI/TT5), leading to the production

136

of naringenin, FLAVANONE 3-HYDROXYLASE/TRANSPARENT TESTA 6 (F3H/TT6) responsible for the synthesis of dihydrokaempferol and FLAVANOID 3'-HYDROXYLASE/TRANSPARENT TESTA 7 (F3'H/TT7), which converts dihydrokaempferol in dihydroquercetin (Feinbaum and Ausubel, 1988; Shirley et al., 1992; Pelletier and Shirley, 1996; Schoenbohm et al., 2005; Owens et al., 2008a). Dihydroflavonols can then be channelled into two different branches, one leading to flavonol aglycones kaemferol and quercetin via FLAVONOL SYNTHASE 1 (FLS1), and another leading to anthocyanidins via DIHYDROFLAVONOL REDUCTASE/TRANSPARENT TESTA 3 (DFR/TT3), LEUCOANTHOCYANIDIN DIOXYGENASE/ANTHOCYANIDIN SYNTHASE (LDOX/ANS) (Shirley et al., 1992; Pelletier et al., 1997; Devic et al., 1999; Owens et al., 2008b). BANYULS/ANTHOCYANIDIN REDUCTASE (BAN/ANR) and POLYPHENOL OXIDASE/TRANSPARENT TESTA 10 (PPO/TT10) catalyse proanthocyanidin biosynthesis in the seed coat, with PPO/TT10 additionally involved in the production of quercetin rhamnoside dimers in Arabidopsis (Albert et al., 1997; Pourcel et al., 2005).

Once flavonoid aglycone backbones are formed, their structures are further modified by glycosylation, methylation and acylation (Bowles et al., 2005; D'Auria, 2006; Ferrer et al., 2008). Glycosylation, in particular, has the purpose of reducing the reactivity of flavonoid aglycones and increasing their solubility and stability (Vogt and Jones, 2000). In addition, glycosylated flavonoids are the storage form of flavonoids in the vacuole (Vogt and Jones, 2000).

Glycosylation occurs first in position C-3 of the aglycones, followed by additional glycosylation in position C-5 and/or C-7. Flavonoid glycosyltransferases (UGTs) belong to the family 1 of glycosyltransferases and use UDP-conjugated sugars as sugar donors (Li et al., 2001; Yonekura-Sakakibara and Hanada, 2011). There are three flavonol 3-O-glycosyltransferases known in Arabidopsis, UGT78D1, UGT78D2 and UGT78D3, which transfer rhamnose, glucose and arabinose, respectively

(Jones et al., 2003; Tohge et al., 2005; Yonekura-Sakakibara et al., 2008). UGT78D2 can also glucosylate anthocyanins (Tohge et al., 2005). Additional UGTs are anthocyanin 5-O-glucosyltransferase (UGT75C1), flavonol 7-O-glucosyltransferase (UGT73C6), flavonol 7-O-rhamnosyltransferase (UGT89C1) and anthocyanin 3-O-glucoside:2"-O-xylosyltransferase (Jones et al., 2003; Tohge et al., 2005; Yonekura-Sakakibara et al., 2008, 2012).

Flavonoid biosynthetic enzymes are organized in complexes that are loosely associated with the ER, although they have been also found in the cytoplasm, at the tonoplast, in the cell nucleus, and there are evidences of chloroplasts-localized flavonoid biosynthetic enzymes (Hrazdina and Wagner, 1985; Grandmaison and Ibrahim, 1995; Hutzler et al., 1998; Saslowsky and Winkel-Shirley, 2001; Feucht et al., 2004; Saslowsky et al., 2005; Agati et al., 2007; Kuhn et al., 2011). Protein-protein interactions have been described for the genes of the core biosynthetic pathway, including enzymes that do not catalyse consecutive reactions (Burbulis and Winkel-Shirley, 1999; Owens et al., 2008a, 2008b). More recently, Förster resonance energy transfer detected by fluorescence lifetime imaging microscopy (FRET-FLIM) has shown that FLS1 and DFR compete for CHS (Crosby et al., 2011). This supports the hypothesis that core flavonoid biosynthetic enzyme form a globular complex rather than a linear one; this could also indicate that different interaction between enzymes could direct the metabolic flux to different branches (Crosby et al., 2011).

Specific flavonoid staining coupled to HPLC analysis revealed that flavonoids mostly localize at the cotyledonary node, hypocotyl-root transition zone and elongation zone in roots in Arabidopsis seedlings (Peer et al., 2001; Saslowsky and Winkel-Shirley, 2001). Flavonol aglycones are predominant in the hypocotyl-root transition zone and at the root tip up to seven days post germination, after which glycosylated derivatives become predominant. Surprisingly, flavonoids were also localized in the stele, where the enzymes are not expressed, suggesting translocation (Peer et al., 2001; Saslowsky and Winkel-Shirley, 2001). Subsequent work confirmed that flavonoids are

translocated within the plant via the symplast when moving acropetally, whereas the basipetal movement is vascular (Buer et al., 2007, 2008). In adult plants, flavonoids can be found in maturing siliques, inflorescence stems, cauline and rosette leaves, floral primordia, stigmata, and pollen (Peer et al., 2001; Saslowsky and Winkel-Shirley, 2001; Buer et al., 2007).

Flavonoids can be found in different cell compartments, including the cytosol, vacuole, nucleus and the apoplast (Zhao and Dixon, 2010; Agati et al., 2012). Most glycosylated flavonoids are found in the vacuole, where they are stored (Vogt and Jones, 2000). In addition, the vacuole is the site for proanthocyanidin biosynthesis in the endothelium of the seed coat prior export in the apoplast (reviewed in Zhao and Dixon, 2010).

Two major transport mechanisms have been suggested for flavonoid translocation: vesicle-mediated transport and transporter-mediated transport (Zhao and Dixon, 2010). Regarding vesicle-mediated transport, one example are anthocyanoplasts, vesicle-like structures that accumulate in the cytoplasm and are imported in to the vacuole, likely by autophagy (Poustka et al., 2007; Pourcel et al., 2010). In addition, membrane trafficking was recently shown to have a role in accumulation of flavonoids in the vacuole (Ichino et al., 2014). Among membrane-localized transporters, multidrug and toxic compound extrusion (MATE) and ABC transporters are believed to have a role in transport of flavonoids, although not much is known to date. One example is TRANSPARENT TESTA 12 (TT12), responsible of the transport of proanthocyanidins to the vacuole of the seed coat endothelium, which shares similarity with MATE transporters (Debeaujon et al., 2001). Additional *in vitro* studies showed that TT12 is a cyanidin-3-*O*-glucoside/H^+-antiporter (Marinova et al., 2007). Inhibitor studies suggest that ABC transporters would mediate long-distance transport of flavonoids (Buer et al., 2007). Together with membrane-localized transporters, glutathione-S-transferases (GSTs) seem to have an active role in the transport of flavonoids. *TRANSPARENT TESTA 19* (*TT19*) encodes a GST that localizes in the cytoplasm and in the tonoplast, and can bind both glycosylated anthocyanins and aglycones (Sun

et al., 2011). Because TT19 does not conjugate anthocyanins with glutathione, it has been suggested that glutathione may serve as carrier for the transport to the vacuole, to prevent oxidation of flavonoids and oxidative damage to the cell (Mueller et al., 2000; Sun et al., 2011).

4.1.4 Regulation of flavonoid biosynthesis in Arabidopsis

In Arabidopsis, regulation of flavonoid biosynthesis is achieved by transcriptional regulation. TRANSPARENT TESTA 2 (TT2), TRANSPARENT TESTA 8 (TT8), and TRANSPARENT TESTA GLABRA 1 (TTG1) control proanthocyanidin biosynthesis in seeds (Baudry et al., 2004). TT8, TTG1, GLABRA3 (GL3), and ENHANCER OF GL3 (EGL3), together with PRODUCTION OF ANTHOCYANIN PIGMENT 1 and 2 (MYB75/PAP1 and MYB90/PAP2), MYB113, and MYB114 regulate anthocyanin biosynthesis in vegetative tissues (Borevitz et al., 2000; Zhang et al., 2003; Gonzalez et al., 2008). Regulation of flavonol biosynthesis in Arabidopsis is controlled by PRODUCTION OF FLAVONOL GLYCOSIDES 1, 2 and 3 (MYB12/PFG1, MYB11/PFG2 and MYB111/PFG3), which regulate the expression of *CHS*, *CHI*, *F3H*, *F3'H* and *FLS1*. MYB12 is prevalent in roots, whereas MYB111 prevails in cotyledons, with MYB11 plays only a marginal role (Mehrtens et al., 2005; Stracke et al., 2007). MYB11, MYB12 and MYB111 can also regulate the expression of different glycosyltransferases involved in flavonoid biosynthesis (Stracke et al., 2010). Furthermore, the TCP3 transcription factor (named after the three previously identified members of this transcription factors family, Teosinte Branched 1, Cycloidea, and Proliferating Cell Nuclear Antigen Factor) interacts with several flavonoid-specific transcription factors (TT2, PAP1, PAP2, MYB12, MYB111, MYB113 and MYB114) enhancing the production of flavonols, anthocyanins and proanthocyanidins (Li and Zachgo, 2013).

In addition to transcription factor-mediated regulation, feedback control through intermediates of the pathway has been described. For example, gene expression and biochemical studies showed that *chi*/*tt5* and *dfr*/*tt3* accumulate higher levels of other flavonoid biosynthetic enzymes, suggesting that intermediates of the pathway may act as inducers (Pelletier et al., 1999). In addition, expression of *DFR* and *LDOX* are enhanced in an *fls1* mutant (Stracke et al., 2009). This is further supported by the finding that myricetin and quercetin, products of FLS1, can bind to DFR and block its catalytic activity in grapevine (Trabelsi et al., 2008).

4.1.5 Biological functions of flavonoids

Flavonoids are phytochemicals with many beneficial roles in the physiology of the plant and in the interaction with the surrounding environment (Winkel-Shirley, 2001). They have antioxidant and antimicrobial properties and have been described, for example, to have a role in protection from UV-B stress, interaction with beneficial and pathogenic microbes, and attraction of pollinators (Taylor and Grotewold, 2005; Agati et al., 2013; Zhang et al., 2013b). They have also shown to interact with different hormones and be required for pollen viability (Taylor and Grotewold, 2005; Peer and Murphy, 2007). Additionally, they have many other beneficial properties in human health, like anti-inflammatory, anti-proliferative and estrogenic (Cushnie and Lamb, 2005; Ververidis et al., 2007).

Ultra-violet (UV) light, especially UV-B (280-320 nM), is not completely shielded by the ozone layer and can act as environmental regulator. UV-B induces damage in DNA, RNA, proteins and lipids (Ulm and Nagy, 2005). Plant responses to UV-B are both UV-B-specific and nonspecific. These include phenotypic responses, like inhibition of hypocotyl growth and curling of cotyledons, and induction of the genes of secondary metabolism (Chappell and Hahlbrock, 1984; Ballaré et al., 1991; Li et al., 1993; Wilson and

Greenberg, 1993; Kubasek et al., 1998). Low levels of UV-B and short exposure to high levels of UV-B both induce expression of genes involved in phenylpropanoid biosynthesis, including *PHENYLALANINE AMMONIA LYASE* (*PAL*), *CHS* and *FLS1* (Brosché et al., 2002; Ulm et al., 2004; Brown et al., 2005). High UV-B levels also increase the amount of quercetin flavonoids in leaves, and *chs*/*tt4*, *chi*/*tt5* and *f3h*/*tt6* are hypersensitive to high UV-B radiation (Li et al., 1993; Ryan et al., 2001), suggesting that flavonoids are required for protection against UV-B. In addition, a combination of transcriptomic and metabolomic analysis showed that *TT4*, *TT5*, *TT6* and *UGT78D2* were up-regulated after 24 hours of constant UV-B exposure, as well as accumulation of anthocyanins, kaempferol and quercetin derivatives, indicating that flavonoids are likely to have a role in adaptation to the UV-B stress (Kusano et al., 2011). All this evidence would point to the fact that flavonoids act as photoprotectants, possibly due to their antioxidant properties rather than their capability to act as sunscreens. *In vitro* studies showed that quercetin and cyanidin have stronger antioxidant potentials than Trolox, a vitamin E soluble analogue, and dihydroxy flavonoids can both inhibit the generation of and quench ROS (Rice-Evans et al., 1995; Agati et al., 2013). In addition, flavonols and their aglycones were shown to scavenge hydrogen peroxide (H_2O_2), with ascorbate involved in their recycling to the respective reduced forms (Bors et al., 1995; Yamasaki et al., 1997). Despite evidence on the antioxidant properties of flavonoids, their role *in planta* is still matter of debate. In fact, their wide diversity among plant species has made making generalizations challenging. In particular, a missing piece in the puzzle is the spatio-temporal correlation of flavonoid and oxidative stress (Hernández et al., 2009).

Interactions between flavonoids and plant hormones have been described. For example, they are non-essential negative regulators of auxin transport (Jacobs and Rubery, 1988; Brown et al., 2001). Polar auxin movement is controlled by auxin efflux and influx carriers (Palme and Gälweiler, 1999). In *tt4*/*chs* seedlings, auxin transport is increased, and it can be restored to a WT

level by addition of naringenin (Murphy et al., 2000; Brown et al., 2001). In addition, *tt4*/*chs* plants phenocopy auxin transport mutants (Murphy et al., 2000; Brown et al., 2001). Auxin transport is inhibited by flavonoids at the shoot apex and at the root tip, and this negative effect was suggested to be caused by modulation of vesicular cycling of PIN-FORMED1 (PIN1) (Peer et al., 2004). In addition, WRKY23 may control auxin-mediated root growth by modulating *TT7*/*F3'H* expression (Grunewald et al., 2012). Treatment with the ET precursor aminocyclopropane-1-carboxylic acid (ACC) inhibits root gravitropic responses by altering flavonoid biosynthesis (Buer et al., 2006). ET also induces flavonoid accumulation in guard cells that in turn modulates ABA-dependent stomatal closure through suppression of the ABA-dependent ROS burst (Watkins et al., 2014). Furthermore, both indole-3-acetic acid (IAA) and ACC induce expression of flavonoid biosynthetic genes, although the time of the response is different for the two hormones (Lewis et al., 2011). Naringenin also induces the expression of JA biosynthetic genes (Pourcel et al., 2013).

In certain species, flavonoids are important for male fertility, as shown by mutation of *CHS* in maize and petunia, but not in Arabidopsis (Coe et al., 1981; Taylor and Jorgensen, 1992; Burbulis et al., 1996). Exogenous application of kaempferol was shown to complement *chs* mutation and induce pollen germination in petunia (Mo et al., 1992).

Flavonoids have been described in playing an important role in the interaction with both pathogens and beneficial bacteria. Flavonoids are exuded from the roots to act as signals for nitrogen-fixing bacteria (Taylor and Grotewold, 2005). Several flavonoids induce expression of *nod* genes in bacteria, whose activation leads to the production of NOD factors, required for the formation of nitrogen-fixating nodules (Peters et al., 1986; Redmond et al., 1986; Djordjevic et al., 1987; Peters and Long, 1988). Silencing of key enzymes of the flavonoid biosynthetic pathway leads to reduction in nodulation (Subramanian et al., 2006; Wasson et al., 2006). However, there are also examples of flavonoids acting as repressors of *nod* gene expression

(Djordjevic et al., 1987; Savouré et al., 1997; Zuanazzi et al., 1998). This would suggest that the combination of both mechanisms could fine-tune plant responses to beneficial nitrogen-fixing bacteria in order to avoid that excessive stimulation could lead to elicitation of defence responses.

With regard to plant-pathogen interactions, different examples can be found in the literature. Constitutive overexpression of isoflavone *O*-methyltransferase leads to enhanced production of two isoflavonoids and resistance towards *Phoma medicaginis* in alfalfa (He and Dixon, 2000). In addition, *Colletotrichum trifolii* induces expression of genes of the flavonoid pathway and synthesis of phytoalexins (Saunders and O'Neill, 2004). In sorghum, 3-deoxyanthocyanidin is produced in response to fungal infection (Snyder and Nicholson, 1990). In tomato, rutin biosynthesis is induced following *Pto* DC3000 infection (López-Gresa et al., 2011) and exogenous application of quercetin induces reistance to *Pto* DC3000 in Arabidopsis (Jia et al., 2010). *2-HYDROXYISOFLAVANONE DEHYDRATASE* (*GmHID1*) is induced upon inoculation of *Pseudomonas syringae* pv. *glycinea* in soybean (Zhou et al., 2011). Elicitor-induced biosynthesis of isoflavones has also been shown in chickpea (Barz and Mackenbrock, 1994). However, early studies also showed that UV-induced flavonoid biosynthesis can be repressed by elicitor treatment (Chappell and Hahlbrock, 1984; Lozoya et al., 1991; Gläßgen et al., 1998). Interestingly, flavonoids possess antimicrobial properties (Cushnie and Lamb, 2005; Ververidis et al., 2007). *in vitro* studies suggest that the main mode of action could be due to one or a combination of three main mechanisms: damage of cytoplasmic membranes, inhibition of nucleic acid synthesis and/or inhibition of energy metabolism (reviewed in Cushnie and Lamb, 2011).

Flavonoids can also act as allelochemicals, which are molecules secreted by the plant in the interaction with neighbouring plants. For example, isoschaftoside, is exudated from roots of *Desmodium uncinatum* and inhibits radicle growth of the parasitic plants *Striga hermonthica* and *Striga asiatica* after their germination (Hooper et al., 2010; Khan et al., 2010).

4.1.6 Aim

One of the *pir* mutants with reduced resistance to bacteria following flg22 perception was found to affect *PIR38*/*UGT78D1*, encoding a flavonoid rhamnosyltransferase (see Chapter 3). To gain further insight into how UGT78D1 contributes to PTI, a combination of genetic, metabolomic and chemical approaches were employed.

4.2 Results

4.2.1 Confirmation of the phenotype in *pir38*

PIR38 carries a T-DNA insertion in *UGT78D1*, a rhamnosyltranserase of the flavonoid pathway (Jones et al., 2003) (Figure 4.3).
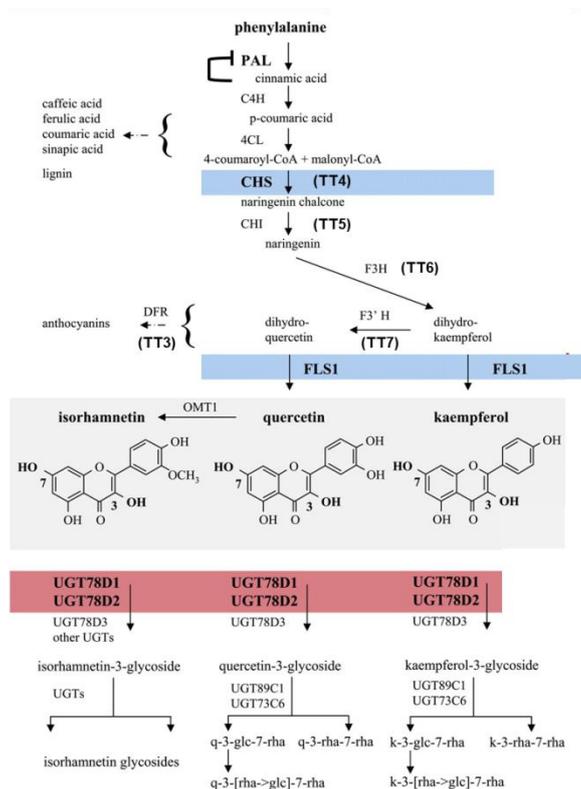
Figure 4.3. The flavonols biosynthetic pathway in Arabidopsis

The flavonol biosynthetic pathway derives from phenylalanine, and enzymes controlling the steps are, as indicated; phenylalanine ammonia-lyase (PAL), cinnamate 4-hydroxylase (C4H), 4-coumarate-CoA ligase (4CL), chalcone synthase (CHS/TT4), chalcone isomerase (CHI/TT5), flavanone 3-hydroxylase (F3H/TT6), flavonoid 3'-hydroxylase (F3'H/TT7), flavonol synthase (FLS1), *O*-methyltransferase (OMT1), dihydroflavonol 4-reductase (DFR/TT3), flavonol 3‑*O*-rhamnosyltransferase (UGT78D1), flavonoid 3‑*O*-glucosyltransferase (UGT78D2), flavonol 3‑*O*-arabinosyltransferase (UGT78D3), flavonol 7‑*O*-rhamnosyltransferase (UGT89C1), and flavonol 7‑*O*-glucosyltransferase (UGT73C6). Glycosylated flavonols are the following: k-3-glc-7-rha, kaempferol 3‑*O*-glucoside-7‑*O*-rhamnoside; k-3-[rha→glc]-7-rha, kaempferol-3‑*O*-[rhamnosyl (1→2 glucoside)]-7‑*O*-rhamnoside; k-3-rha-7-rha, kaempferol 3‑*O*-rhamnoside-7‑*O*-rhamnoside. The structurally equivalent quercetin (q) glycosides are abbreviated in an analogous way. Modified from Yin et al. 2012.

The T-DNA in *pir38* (hereafter referred to as *pir38-1*) is inserted 100bp upstream of the start codon, in the 5' UTR (Figure 4.4A). Gene expression analysis by RT- and qRT-PCR showed that the T-DNA insertion causes overexpression of the gene (Figure 4.4B and C). An additional allele of *pir38*, which was named *pir38-4* (SAIL_568 F08)*,* has an insertion in the second exon and is a null mutant (Jones et al., 2003). Insertions in *pir38-2* (SAIL_89 B04), located at the end of the second exon, and *pir38-3* (SALK_019478C), located in the 5' UTR, did not show any defect in *PIR38* expression and were therefore not used for further characterization.
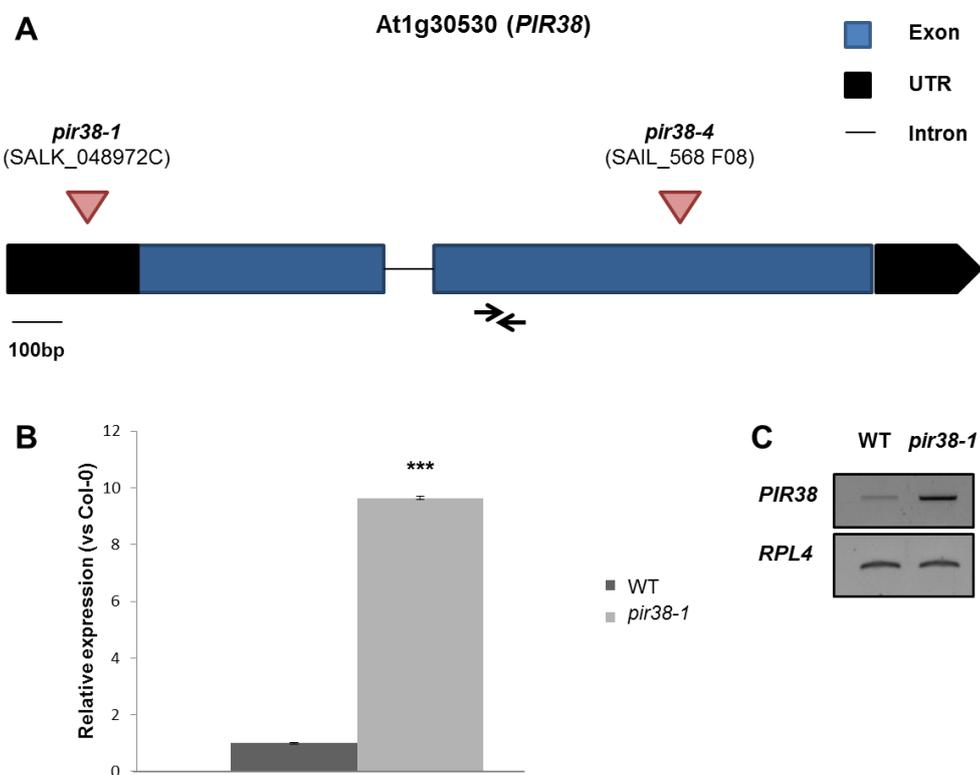
Figure 4.4. Localization and effect of *pir38* mutation.

(A) Structure of *UGT78D1* (At1g30530). The position of the T-DNA insertions in *pir38-1* and *pir38-4* are indicated. Arrows indicate the position of the primers for expression analysis. (B) and (C) Effect of the T-DNA insertion on the expression of *UGT78D1*. cDNA was generated from 14-days-old Arabidopsis seedlings. (B) Gene expression was determined by qRT-PCR using gene-specific primers (see in A). Expression values were normalized to the expression of the U-BOX and are shown as relative to wild-type (WT). Bars are means ± SE, n=3. Asterisks indicate a statistically significant difference between WT and *pir38-1* (***p<0.001) using two-tailed unpaired t-test. (C) Gene expression was determined by RT-PCR (25 cycles), using primers covering full-length *UGT78D1*. RPL4 was used as internal control. The experiment was repeated three times with similar results.

Initial tests to evaluate the effect of the T-DNA insertion in *pir38-1* towards the loss of flg22-induced resistance to *Pto* DC3000 indicated a significant reduction in resistance, when compared to WT (see Figure 3.18). In contrast, *pir38-4* showed WT induced resistance (see Figure 3.18). This different phenotype could be explained by the opposed effects of the insertions on the expression of *UGT78D1* in the two lines (Figure 4.4B) (Jones et al., 2003), suggesting that overexpression of *UGT78D1* could be linked to loss of flg22-induced resistance.

However, further tests showed that the loss of flg22-induced resistance in *pir38-1* was not consistent. *pir38-1* showed a significant reduction of flg22-induced resistance in five out of 10 experiments, in spite of all experiments being carried out in similar conditions. Seeds used for these experiments derived from two consecutive generations, but they were genotyped and gene expression analysis was carried out in all cases. Although unlikely, it cannot be excluded that the inconsistency of the phenotype over the different replicates could be caused by a temporary change in the growth conditions (*i.e.* light intensity, humidity) that cannot be traced back. One other possibility is the presence of an additional T-DNA elsewhere in the genome of *pir38-1*. One way to determine whether the T-DNA insertion caused the loss of flg22-induced resistance phenotype would have been to backcross this line. In fact, if the T-DNA was responsible for the phenotype, the segregation of the T-DNA should have followed the loss of flg22-induced resistance. However, this requires time to generate backcrossing lines and a high number of plants (>50) to test. In addition, performing flg22-induced resistance is quite time-consuming and laborious to carry-out in adult plants. Moreover, a stable transgenic Arabidopsis line overexpressing *UGT78D1* was already published at the time, and therefore I decided not to backcross.

To assess whether overexpression of *UGT78D1* caused a loss of flg22-induced resistance, it was decided to investigate the phenotype in published stable transgenic Arabidopsis lines (35S:*UGT78D1* and 35S:*UGT78D2*) (Yin et al., 2012). *UGT78D2* is a close homologue of *UGT78D1* and was used as

control, since metabolomic analysis of *ugt78d1* and *ugt78d2* mutants suggests distinct and non-overlapping functions for these enzymes (Jones et al., 2003; Yin et al., 2012). However, mutation of one seems to enhance the activity of the other (Jones et al., 2003; Tohge et al., 2005; Yin et al., 2012). Unfortunately, no seeds of *35S:UGT78D2* and only very few seeds of *35S:UGT78D1* germinated. In addition, overexpression of *UGT78D1* was not homogeneous between individuals and therefore the line was propagated to the next generation. However, uneven expression of the transgene could still be observed. This transgenic line was selected based on the overexpression of the transgene without considering multiple transgene integration within the genome. Therefore its use was found challenging.

At the same time, overexpression lines were also independently generated. Despite several overexpression lines being identified among T1 transformants of *35S:UGT78D2*, only one overexpressor (out of 35 transformants) was identified for *35S:UGT78D1*. In addition, overexpression of this line was only 3.8-fold compared to that of WT (Figure 4.5A), in contrast to *35S:UGT78D2* lines, where the overexpression of the transgene reached up to 151-fold that of WT (Figure 4.5B). Unfortunately, due to the difficulties in finding lines overexpressing *UGT78D1*, no tests were carried out on this material due to time limitations.
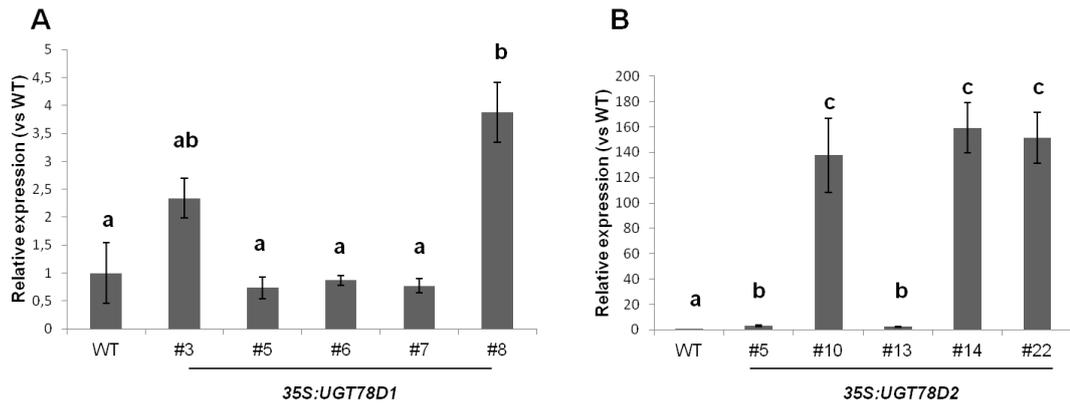
Figure 4.5. Expression analysis of *35S:UGT78D1* and *35S:UGT78D2* T1 transformants.

(A) *UGT78D1* expression in different *35S:UGT78D1* T1 lines. (B) *UGT78D2* expression in different *35S:UGT78D2* T1 lines. cDNA was generated from leaves of four-weeks-old Arabidopsis plants. Expression values were normalized to the expression of the U-BOX and are presented as relative to those of WT. Bars are means ± SE, n=3. Significantly different groups ($p < 0.0001$) are indicated with lower-case letters based on one-way ANOVA analysis and Tukey's multiple comparison post-test.

In an alternative approach, a different transgenic line was generated from a DKLAT clone of *UGT78D1* (Popescu et al., 2007). T1 transformants were analysed for *UGT78D1* over-expression by western blot using α-myc antibodies, and several transformants showing UGT78D1 protein over-accumulation were identified (Figure 4.6).
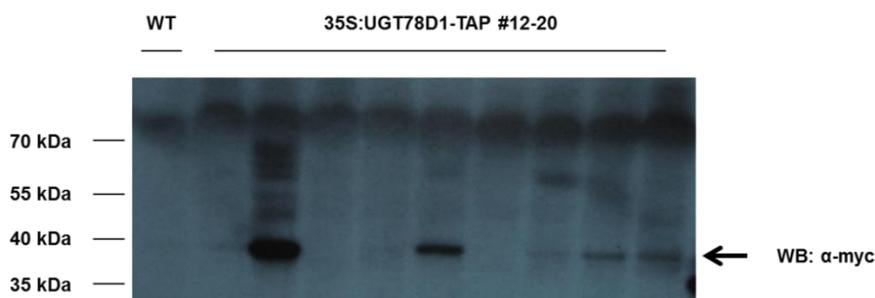
Figure 4.6. Expression analysis of 35S:UGT78D1-TAP transformants.

Crude protein extracts of Arabidopsis leaves from individual T1 35S:UGT78D1-TAP plants. WT leaves extracts were used as negative control. 35S:UGT78D1-TAP proteins were detected by immunoblot analysis using α-myc antibody.

However, when seeds were sown for selection of the T2s, seedlings did not show any susceptibility to the gentamycin selection. This was probably due to the weak effect of gentamycin as selectant. Hence, these lines were also unavailable for further tests.

Therefore, different attempts to determine whether overexpression of *UGT78D1* causes loss of flg22-induced resistance to bacteria have been unsuccessful so far, and additional approaches will be required to shed light on this matter.

4.2.2. Genetic analysis to assess the role of flavonoids in immunity to bacteria

Although it could not be confirmed that overexpression of *UGT78D1* leads to impairment of flg22-induced resistance to bacteria, there are many examples showing an active role of flavonoids in resistance against different pathogens (Dixon, 2001; Treutter, 2006). The flavonol biosynthetic pathway has been extensively characterized both at the molecular and metabolic level. In contrast to other species, in Arabidopsis, all the biosynthetic enzymes are encoded by a single gene, with the exception of *FLS1* (reviewed in Saito et al., 2013). Therefore, a reverse genetic approach was taken in order to address the question of whether flavonols have a role in resistance to bacteria and, if so, to identify the compound responsible for this function.

For this purpose, mutants of enzymes in different steps of the biosynthetic pathway were tested to assess their ability, or not, to mount resistance against bacteria following flg22 perception. The pathway was arbitrarily broken down in two at the level of flavonol aglycones for ease of handling the different mutant lines. Glycosylated flavonols are the form that plants use to store them in the vacuole and in some cases they have been shown to possess direct biological activities (Gachon et al., 2005; Zhang et al., 2013b).

Mutants of glycosyltrasferase enzymes downstream of flavonol aglycones should lack specific glycosylated flavonols and accumulate higher levels of products synthesized by enzymes at the same level in the pathway. To test whether alteration in glycosylated flavonols affected resistance to bacteria, *ugt78d1*, *ugt78d2-1*, *ugt78d2-2*, *ugt78d1 ugt78d2-1*, *ugt78d3*, *ugt89c1-2* and *ugt73c6* mutants were tested. These enzymes catalyse specific glycosylation of flavonols aglycones (Figure 4.3) (Jones et al., 2003; Tohge et al., 2005; Yonekura-Sakakibara et al., 2007, 2008; Yin et al., 2012). With the exception of *ugt78d2-2*, which is an unpublished allele, all the mutants have been previously published as knock-outs. Apart from that, *ugt78d3* was found to be a knock-down, but expression analysis was done on flower cDNA (Yonekura-Sakakibara et al., 2008). Additional analysis on *ugt78d3* with cDNA derived from two-week-old seedlings showed that the T-DNA insertion caused an overexpression of the gene in vegetative tissues (Figure 4.7B and C). The same analysis confirmed that both *ugt78d2-1* and *ugt78d2-2* are knock-outs (Figure 4.7A, C and D).
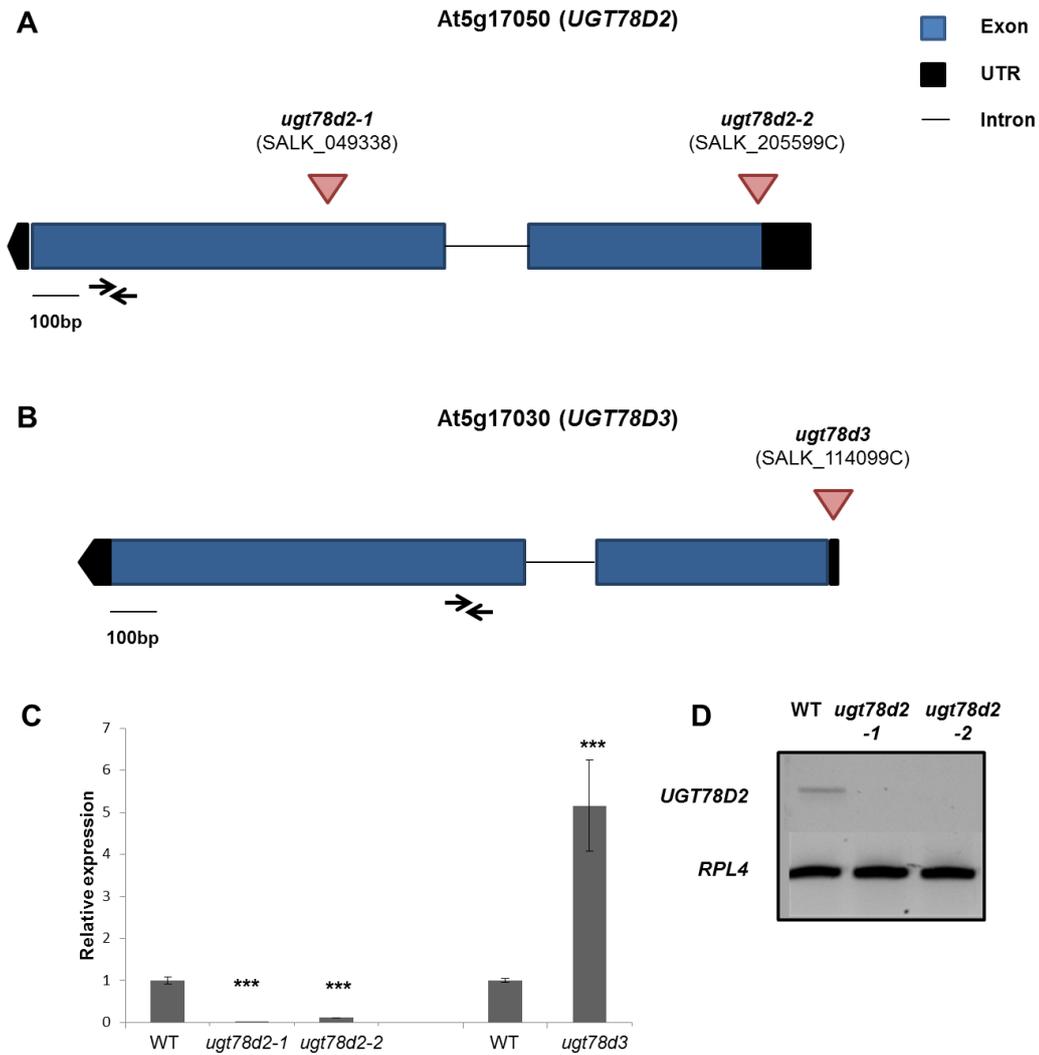
Figure 4.7. Localization and effect of *ugt78d2-1*, *ugt78d2-2* and *ugt78d3* mutations.

(A) Structure of *UGT78D2* (At5g17050). The position of the T-DNA insertions in *ugt78d2-1* and *ugt78d2-2* are indicated. Arrows indicate the position of the primers for expression analysis. (B) Structure of *UGT78D3* (At5g17030). The position of the T-DNA insertions in *ugt78d3* is indicated. Arrows indicate the position of the primers for expression analysis. (C) Effect of the T-DNA insertion on the expression of *UGT78D2* and *UGT78D3*. Gene expression was determined by qRT-PCR using gene-specific primers. cDNA was generated from 14-days-old Arabidopsis seedlings. Expression values were normalized to the expression of the U-BOX and relative expression was determined in comparison to WT. Bars are means ± SE, n=2. Asterisks indicate a statistically significant difference between WT and mutants (***p<0.001) using two-tailed unpaired t-test. (D) Gene expression was determined by RT-PCR (30 cycles), using primers covering full-length *UGT78D2*. RPL4 was used as internal control. The experiment was repeated twice with similar results.

It was then assessed whether any of these mutants had defects in flg22-induced resistance. Results showed that none of the mutants downstream of flavonol aglycones was affected, as the amplitude of the induced resistance was comparable to WT in all cases (Figure 4.8).
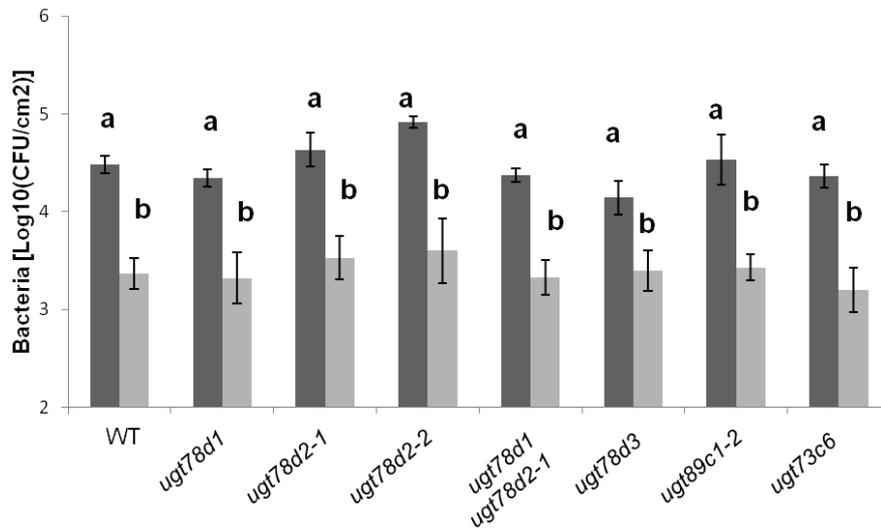
Figure 4.8. Arabidopsis mutants of enzymes downstream of quercetin production are not affected in flg22-induced resistance.

Five-weeks-old WT and mutant plants were elicited with 1 µM flg22 for 24 hours and then inoculated with *Pto* DC3000 (OD$_{600}$=0.0002). Bacterial growth was measured at 2 DPI by plating serial dilutions of homogenized leaf discs. Bars are means ± SE, n=6. Significantly different groups ($p < 0.0001$) are indicated with lower-case letters based on one-way ANOVA analysis and Tukey's multiple comparison post-test. The experiment was repeated three times with similar results.

Since none of the mutants of enzymes downstream of flavonol aglycones showed a defect in flg22-induced resistance, mutants in enzymes upstream of aglycones were tested. These included *chs/tt4-13*, *chi/tt5*, *dfr/tt3*, *f3h/tt6-3* and *f3h/tt6-5*, *f3'h/tt7-6*, *fls1-2*, and *omt1* (Buer et al., 2006; Owens et al., 2008a; Stracke et al., 2009; Tohge et al., 2009). *tt6-5* and *tt7-6* are unpublished alleles; *tt6-5* was confirmed to be a knock-out by qRT-PCR, similar to *tt6-3* (Figure 4.9A, B and C). Expression of *F3'H* in *tt7-6* showed

that the T-DNA insertion in this allele causes a weak overexpression of the gene, not statistically significant (Figure 4.9D and E).
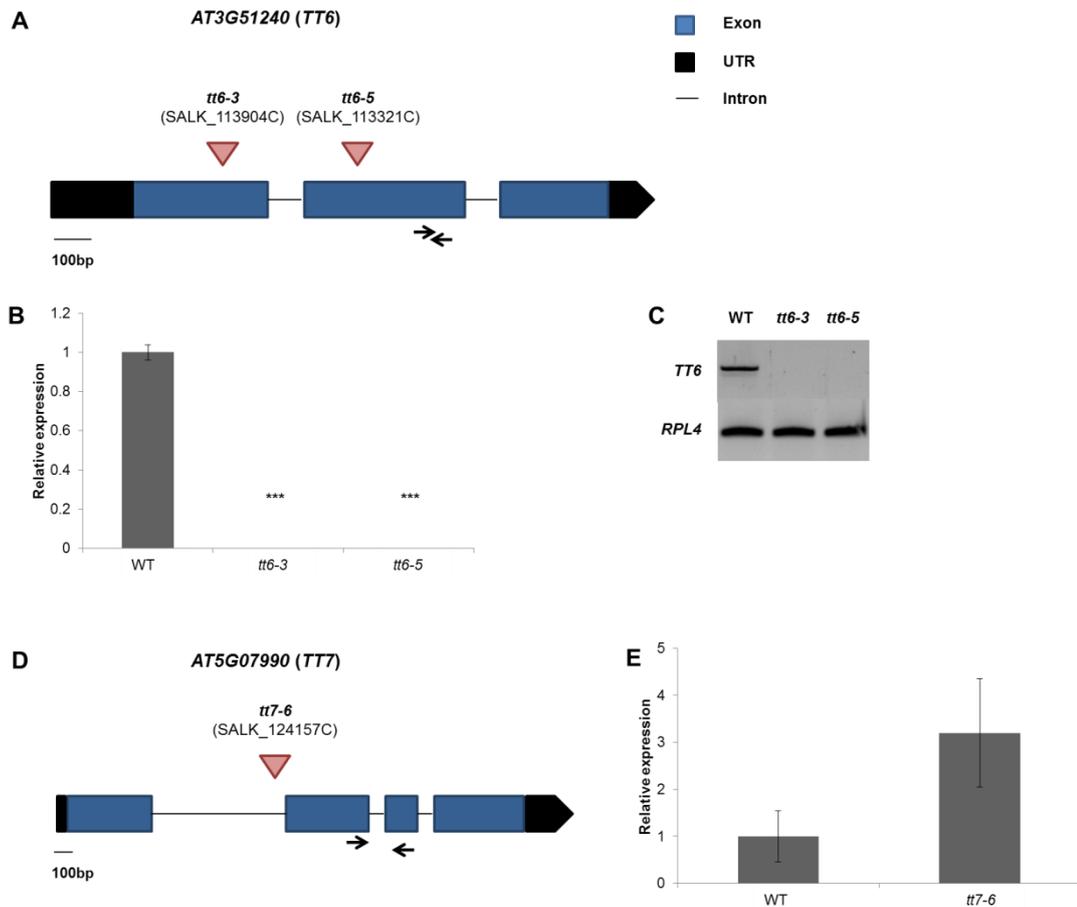
Figure 4.9. Localization and effect of *tt6-3*, *tt6-5* and *tt7-6* mutations.

(A) Structure of *TT6* (AT3G51240). The position of the T-DNA insertions in *tt6-3* and *tt6-5* are indicated. Arrows indicate the position of the primers for qRT-PCR. (B) and (C) Gene expression was determined by qRT-PCR and RT-PCR using gene-specific primers. cDNA was generated from 14-days-old Arabidopsis seedlings. (B) Expression values were normalized to the expression of the U-BOX and relative expression was determined in comparison to WT. (C) Gene expression was determined by RT-PCR (30 cycles), using primers covering full-length *TT6*. RPL4 was used as internal control. (D) Structure of *TT7* (AT5G07990). The position of the T-DNA insertions in *tt7-6* is indicated. Arrows indicate the position of the primers for qRT-PCR. (E) Gene expression was determined by qRT-PCR using gene-specific primers. cDNA was generated from 14-days-old Arabidopsis seedlings. Expression values were normalized to the expression of the U-BOX and relative expression was determined in comparison to WT. Bars are means ± SE, n=3. Asterisks indicate a statistically significant difference between WT and mutants (***$p < 0.001$) using two-tailed unpaired t-test. The experiment was repeated twice with similar results.

Arabidopsis *tt3* mutant has been chosen as DFR/TT3 controls the branching point from the flavonol pathway to the biosynthesis of anthocyanins, together with FLS1. Col-0, L*er* and No-0 were used as a control for mutants in the respective backgrounds. When tested for loss of flg22-induced resistance, none of the mutants upstream of flavonol aglycones showed any consistent impairment in the response (Figure 4.10).
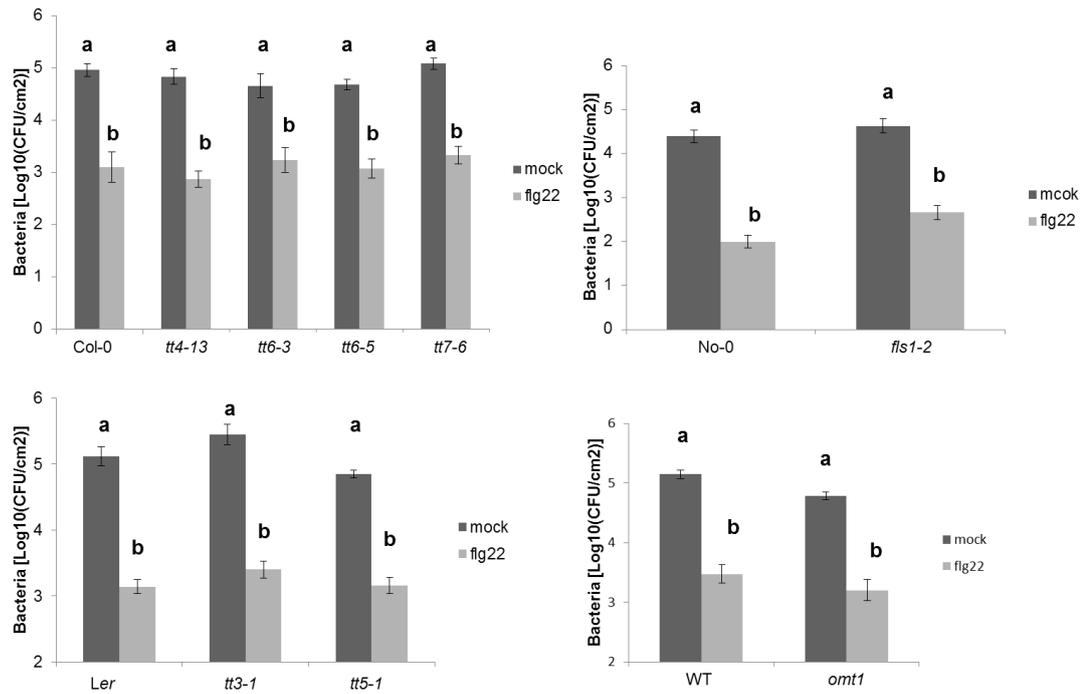
Figure 4.10. Arabidopsis mutants of enzymes upstream of quercetin are not affected in flg22-induced resistance.

Five-week-old WT and mutant plants were elicited with 1 µM flg22 for 24 hours and then inoculated with *Pto* DC3000 (OD_{600}=0.0002). Bacterial growth was measured at 2 DPI by plating serial dilutions of homogenized leaf discs. Bars are means ± SE, n=6. Significantly different groups ($p < 0.0001$) are indicated with lower-case letters based on one-way ANOVA analysis and Tukey's multiple comparison post-test. The experiment was repeated three times with similar results.

Flg22-induced resistance requires infiltration of bacteria in Arabidopsis leaves, allowing bacteria to bypass the natural barriers they would normally have to cross in order to invade the plant tissues. Since some of these barriers, such as the PAMP-triggered stomatal closure, are PTI responses,

bacterial infiltration may not be the best method to investigate the lack of resistance in the different mutants. Therefore, bacterial spray infection was used instead, as this assay mimics better the conditions of a natural bacterial infection (Zipfel et al., 2004). Again, mutants downstream of flavonol aglycones were tested to assess whether alterations in accumulation of glycosylated flavonols could lead to any impairment or increase in resistance to bacteria. Arabidopsis mutants were sprayed with *Pto* DC3000 and samples were taken three days post infection. Bacterial levels were estimated by plating serial dilution of homogenized samples. Results showed that only *ugt78d2-2* and *ugt78d3* were significantly more resistant to bacterial infection than WT (Figure 4.11). In addition, although with no statistical significance, *ugt78d1* and *ugt78d2-1* appeared to be slightly more resistant than WT to bacteria (Figure 4.11). However, the flavonol profiles of *ugt78d2-2* and *ugt78d3* have not been characterized. Assuming that *ugt78d2-2*, similarly to *ugt78d2-1*, has higher levels of 3-O-rhamnosylated flavonols and *ugt78d3* higher levels of 3-O-arabinoslated flavonols, these two pools may enhance the resistance to bacteria.
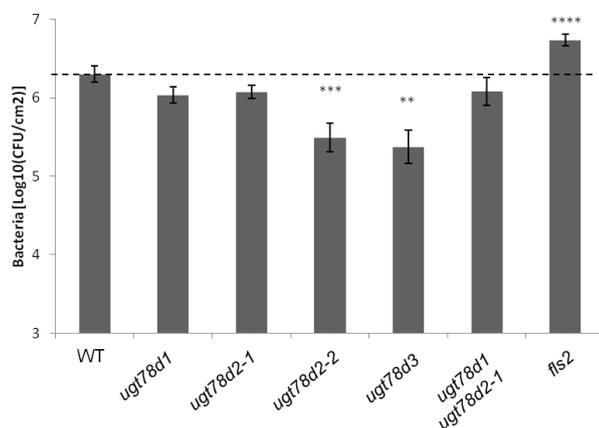
Figure 4.11. ***ugt78d2-2*** **and** ***ugt78d3*** **mutants show enhanced disease resistance to** ***Pto*** **DC3000.**

Five-weeks-old WT and mutant plants were sprayed with *Pto* DC3000 (OD_{600}=0.2). Bacterial growth was measured at 3 DPI by plating serial dilutions of homogenized leaf discs. Bars are means of pooled data from three independent experiments ± SE, n=12. Asterisks indicate a statistically significant difference between WT and mutants, using one-way ANOVA analysis and Tukey's multiple comparison post-test (****p<0.0001, ***p<0.001, **p<0.01) using two-tailed unpaired t-test.

157

If accumulation of glycosylated flavonols leads to enhanced resistance, mutants of enzymes upstream (*chs*/*tt4-13*, *chi*/*tt5*, *f3h*/*tt6-3* and *f3h*/*tt6-5*, *f3'h*/*tt7-6*, *fls1-2*, *omt1*) should show enhanced susceptibility to bacteria using the same spray-infection assay. However, none of the mutants was found to be more susceptible than the WT (Figure 4.12). It is worth noting that, although not supported by a statistically significant difference, when comparing the means, *chs*/*tt4-13*, *f3h*/*tt6-5* and *tt7* appeared to be more susceptible than WT, and *tt5* more resistant. The lack of statistical significance was likely due to the generalized high degree of variability between samples within the same genotype for most of the genotypes which is quite common with spray-inoculation assays (Figure 4.12).
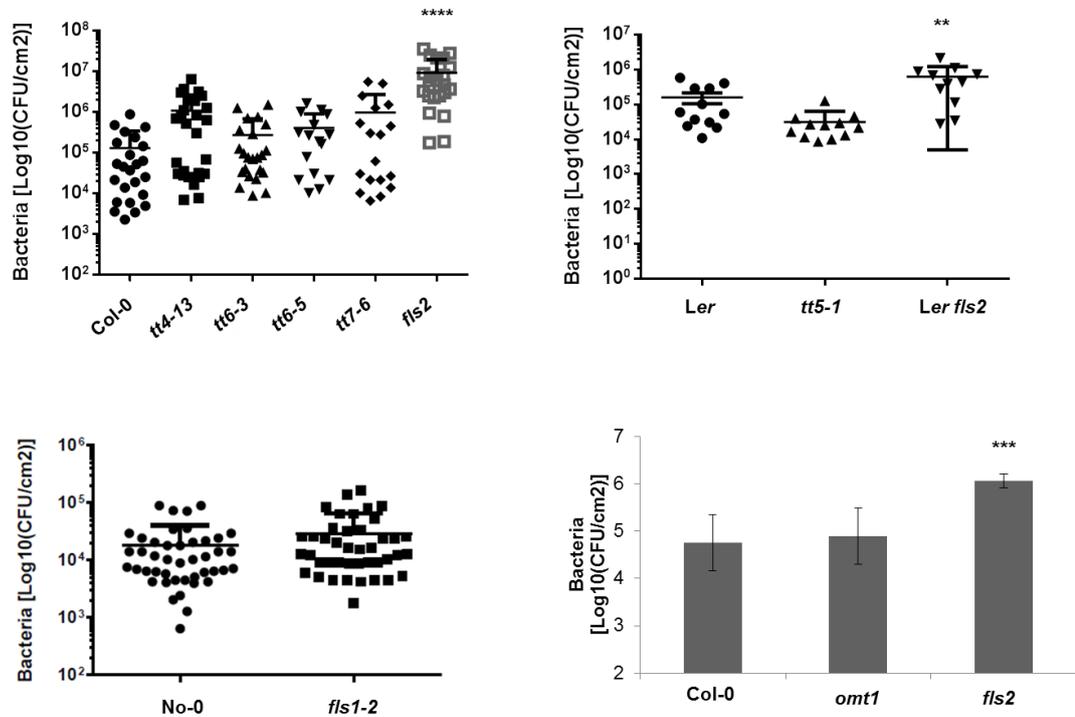
Figure 4.12. Evaluation of the basal level of resistance to bacteria of mutants of enzymes upstream upstream flavonol aglycones.

Five-weeks-old WT and mutant plants were sprayed with *Pto* DC3000 (OD_{600}=0.2). Bacterial growth was measured at 3 DPI by plating serial dilutions of homogenized leaf discs. Bars are means of pooled data from six independent experiments ± SE, n=24 (L*er*, *tt5-1* and L*er fls2* were tested three times, n=12; No-0 and *fls1-2* were tested five times, n=20; *omt1* was tested twice and a representative example is shown; n=6), Asterisks indicate significant difference (****$p < 0.0001$, ***$p < 0.001$, ** $p < 0.01$) based on one-way ANOVA analysis and Tukey's multiple comparison post-test.

Taken together, these results suggest that one or more compounds downstream of flavonol aglycones may be important for basal resistance to bacteria, although further research is needed to support this hypothesis.

4.2.3. Determination of flavonol contents following flg22 treatment

Note: The analysis of samples by LC-MS was performed by Dr. Lionel Hill (Head of JIC Metabolite Services).

It was reasoned that, if flavonols are involved in resistance to bacteria following PAMP perception, quantitative changes in flavonol contents should be detected, upon PAMP treatment. In order to determine whether this is the case, five week-old Arabidopsis plants were infiltrated with water or 1 µM flg22, and three leaves from six plants were collected at 0, 5, 10 and 24 hours post-infiltration and immediately frozen. Samples were ground in liquid nitrogen and approximately 100 mg were extracted with 80% methanol. After centrifugation, 50 µL were analysed using LC-MS. Major peaks were identified as Kaempferol-$(Rha)_2$, Kaempferol-$(Rha)_2$-Glc, Kaempferol-RhaGlc (Rha=rhamnose, Glc=glucose). Although not unequivocally identified by LC-MS, they are likely to correspond to kaempferol 3-*O*-rhamnoside-7-*O*-rhamnoside, kaempferol-3-*O*-[rhamnosyl (1→2 glucoside)]-7-*O*-rhamnoside and kaempferol 3-*O*-glucoside-7-*O*-rhamnoside, as these are the major flavonols in Arabidopsis leaves (Yin et al., 2012). Results showed a distinct decrease in the amount of these three flavonols in response to flg22 (Figure 4.13). The highest decrease was observed in KaeRha2 at 5 hours post treatment (Figure 4.13). The decrease was still detectable at 10 hours, but no differences between mock and flg22-treatment were observed at 24 hours (Figure 4.13). Unfortunately, this experiment was not repeated due to time constraints.
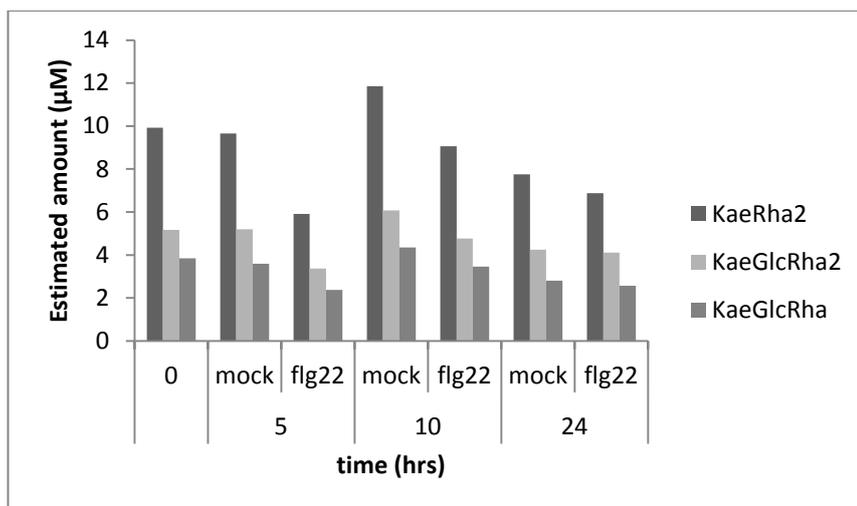
Figure 4.13. Flg22 treatment leads to decrease of three major flavonol glycosides in Arabidopsis leaves.

Amounts of the different flavonols were estimated based on the calibration curve for kaempferol rutinoside using UV.

In addition, sinapoyl malate, hydroxyferuloyl malate and sinapoyl-glucose were also identified, but changes in response to flg22 were minor (data not shown). These are common phenolic compounds present in Arabidopsis vegetative tissue and synthesized via the hydroxycinnamic acid pathway via cinnamic acid and *p*-coumaric acid (Lorenzen et al., 1996). No significant peaks corresponding to anthocyanins were found.

4.2.4. Analysis of PTI responses elicited by quercetin application

It was previously described that exogenous application of quercetin, a flavonol aglycon, can induce resistance to bacteria in a dose-dependent manner (Jia et al., 2010). This was of special interest because quercetin is one of the substrates of UGT78D1 (Figure 4.3). The work by Jia and co-workers showed that quercetin did not have a direct effect on bacteria, although contrasting results can be found in the literature. For example, it

was shown that quercetin inhibits *Pto* DC3000 growth using an antibiosis assay (Vargas et al., 2011). In addition, incubation of quercetin reduces the cell density of *Pseudomonas aeruginosa* PAO1 (Vandeputte et al., 2011).

In order to clarify whether quercetin can have a direct antimicrobial effect towards *Pto* DC3000, an antibiosis assay and a growth curve were set-up. Five millimetres sterile paper disks were soaked with quercetin (1 mM, 100 µM and 10 µM), using DMSO and kanamycin (500 µg/mL) as negative and positive controls, respectively. In addition, quercetin was diluted both in DMSO and in water (to a final concentration of DMSO of 1%). Overnight *Pto* DC3000 cultures were spun down and bacteria were re-suspended in $MgCl_2$ to a final OD_{600} of 0.2, 0.02 and 0.002; aliquots of each bacterial density were distributed on the top of L-agar medium in Petri dishes. Filter paper discs were soaked with the different chemicals, individually placed on the top of the bacteria-inoculated plates and incubated at 28ºC. Twenty-four hours later, plates were scored. As expected, kanamycin inhibited bacterial growth in the form of a clear halo around the paper disk, even at the highest bacterial density (Figure 4.14A, B and C). DMSO did not cause any inhibition, whether diluted in water or not (Figure 4.14A, B and C), in agreement with previous publications (Vargas et al., 2011). Only quercetin at 1 mM did show a weak inhibition of growth when in contact with low bacterial density (OD_{600}=0.002) (Figure 4.14D). No other concentration of quercetin, neither in DMSO nor in water, induced further inhibition of bacterial growth (Figure 4.14A, B and C).
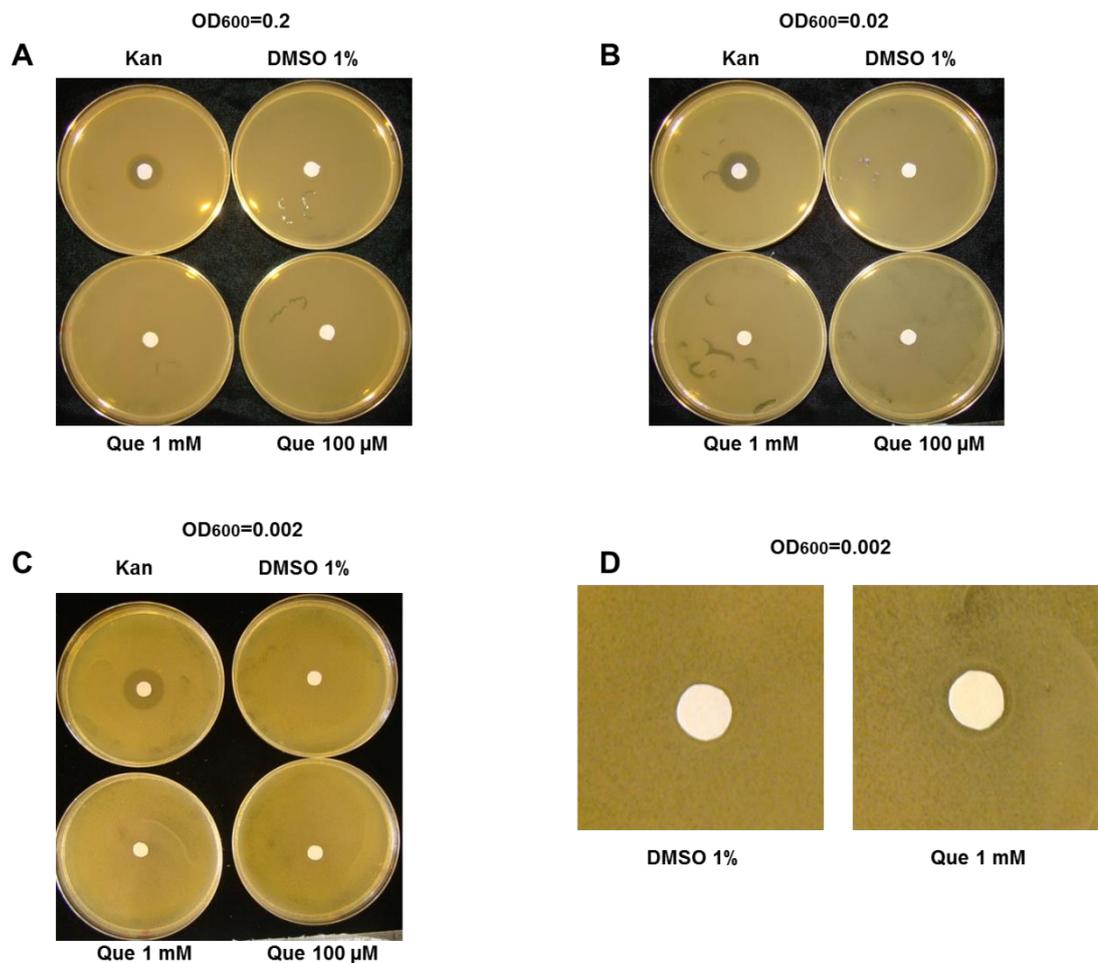
Figure 4.14. High concentration of quercetin shows weak inhibition of low density *Pto* DC3000.

Antibiosis assay was carried out with *Pto* DC3000 distributed on L-agar plates to a final density of $OD_{600}=0.2$ (A), 0.02 (B) or 0.002 (C) as a homogenous loan. Five mm sterile filter paper disks were soaked with kanamycin (Kan) (500 µg/mL), DMSO 1%, quercetin (Que) 1 mM or quercetin 100 µM and placed in the centre of the plate on the top of the bacteria. Plates were incubated at 28ºC. (D) Close-up of DMSO 0.1% and quercetin 1 mM in C. Pictures were taken after 24 hours.

In parallel, antimicrobial activity of quercetin was tested towards *Pto* DC3000 by monitoring the bacterial density of *in vitro*-grown liquid cultures. Bacterial cultures were set to a final $OD_{600}=0.1$ and quercetin was added to a final concentration of 1 mM, 100 µM and 10 µM. DMSO 1% and an un-treated bacterial culture were used as controls. Measurements were taken every two hours by quantifying the bacterial density at 600 nm. Results showed that the

different concentrations of quercetin delay bacterial growth at early time points, in a dose-dependent manner. However, bacterial densities were comparable to those of untreated or mock-treated cultures at eight hours (Figure 4.15).
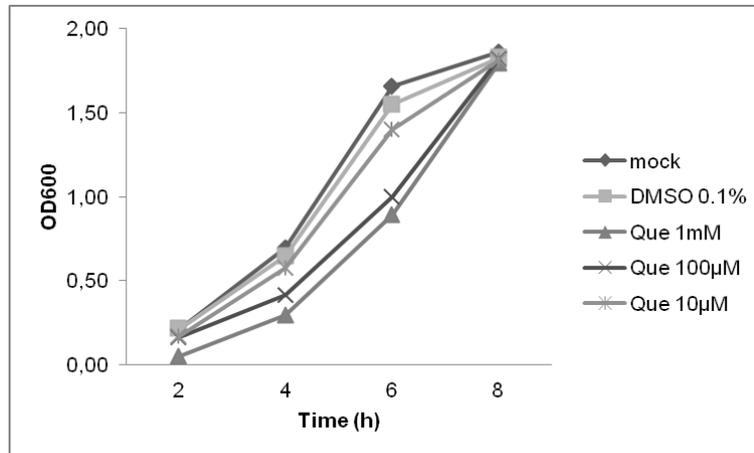
Figure 4.15. Application of quercetin delays *Pto* DC3000 growth *in vitro*.

Liquid *Pto* DC3000 cultures were set to an initial density of OD_{600}=0.1. Bacterial cultures were then treated with either DMSO 0.1% or quercetin (Que) 1 mM, 100 µM or 10 µM. A mock-inoculated culture was used as control. Time-course of *in vitro* growth of *Pto* DC3000 was monitored every two hours by measuring the bacterial density at 600 nm.

Taken together, these results would indicate that quercetin does not have a direct antimicrobial effect towards *Pto* DC3000, at least within the conditions tested, but it may be slightly bacteriostatic.

Subsequently, tests to reproduce the induction of resistance by application of quercetin on Arabidopsis were carried out. Five week-old Arabidopsis WT and triple receptor mutant *fls2 efr cerk1* were sprayed with quercetin diluted in water to a final concentration of 350 µg/mL (approximately 1.16 mM), which is the highest concentration tested in Jia et al. (2010). DMSO 0.1% was used as mock control. Three days post treatment, plants were sprayed with *Pto* DC3000 (OD_{600}=0.2); samples were taken three days post infection and bacterial growth was evaluated by plating serial dilution of homogenized

163

samples. Initial repeats confirmed the finding of Jia and co-workers (2010): mock-treated WT plants showed clear disease symptoms, including extended chlorosis and necrosis. In addition, disease symptoms were even more severe in *fls efr cerk1* when compared to WT. However, quercetin-sprayed plants of both genotypes showed hardly any symptoms with the exception of few chlorotic spots (Figure 4.16A). External symptoms correlated with bacterial levels quantified in leaf samples (Figure 4.16B); quercetin induced resistant to an amplitude similar to that induced by flg22.
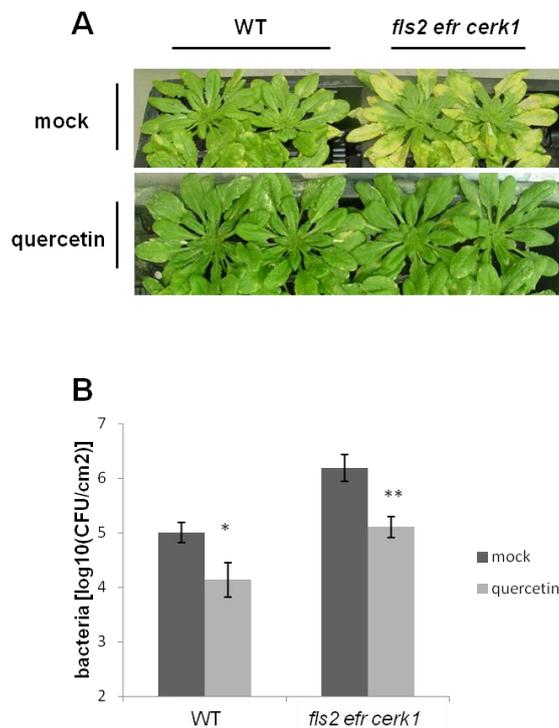
Figure 4.16. Exogenous application of quercetin protects Arabidopsis from bacterial infection.

Five-weeks-old WT and *fls2 efr cerk1* plants were sprayed with 0.1% DMSO (mock) or quercetin (Que) 350 µg/mL for three days prior spray-infection with *Pto* DC3000 (OD_{600}=0.2). (A) Disease symptoms at 3 DPI. (B) Bacterial growth was measured at 3 DPI by plating serial dilutions of homogenized leaf discs. Bars are means ± SE, n=4. Asterisks indicate a statistically significant difference between mock and quercetin treatment (***p<0.001, (**p<0.01) using two-tailed unpaired t-test. The experiment was repeated twice with similar results.

However, further tests did not support this initial observation. Additional experiments were carried out by pre-treating plants with quercetin 1 mM and 100 µM in 1% DMSO, instead of 0.1%, to increase the amount of quercetin in solution. Furthermore, quercetin 1 mM, 100 µM and 10 µM was infiltrated in Arabidopsis leaves side by side with flg22 for one day prior to bacterial inoculation. Two different batches of quercetin powder were also compared. None of the above could replicate the initial observation and it was not possible to confirm that exogenous application of quercetin could induce resistance against bacteria. However, because this result was previously published and initial results did confirm it, further tests were carried out to investigate whether exogenous application of quercetin could induce canonical PTI responses, such as production of ROS, MAPK activation, PAMP-induced genes (PIGs) expression, and SGI. These tests were perform with concentrations of 1 mM and 100 µM quercetin, as these concentrations were previously found to be effective to induce resistance to *Pto* DC3000 (Jia et al., 2010).

To test the effect of quercetin on ROS production, which is a very early measurable PTI output visible shortly after flg22 perception (Felix et al., 1999), Arabidopsis WT leaf disks were treated with quercetin (1 mM and 100 µM). DMSO 1% and flg22 100 nM were used as controls. Production of apoplastic ROS was detected with a luminol-based assay. Results showed that quercetin does not trigger a ROS burst like flg22 does (Figure 4.17A), but induces accumulation of ROS over an extended period of time (Figure 4.17B and C).
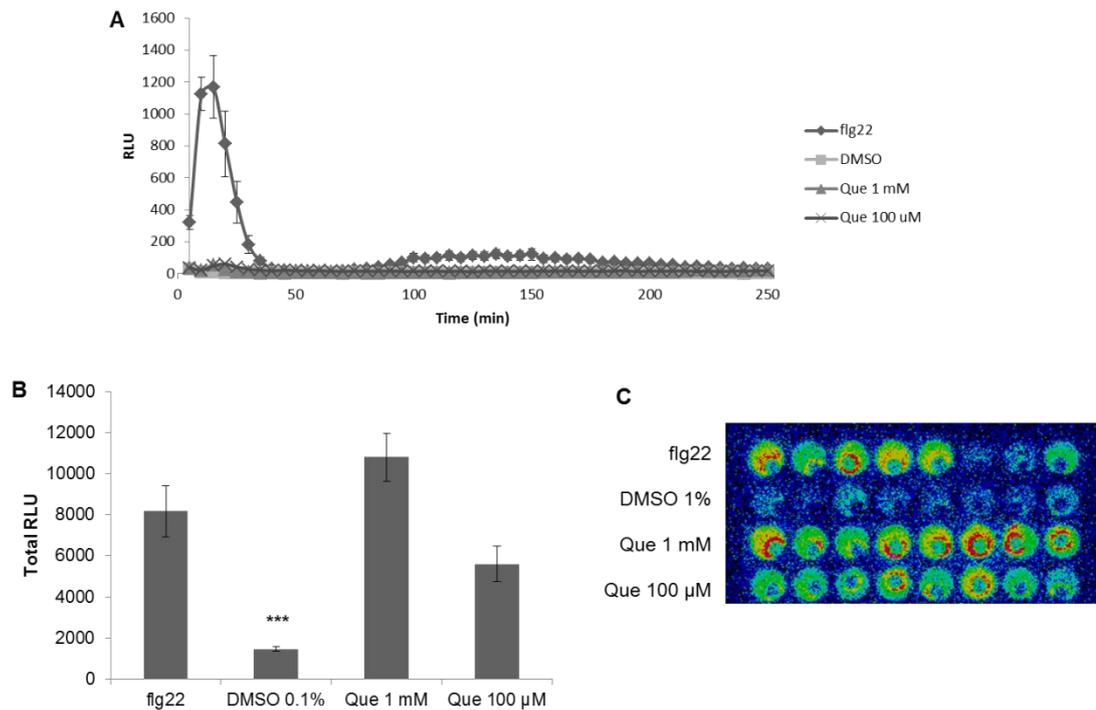
Figure 4.17. Application of quercetin induces accumulation of ROS.

Arabidopsis WT leaf discs were treated with flg22 100 nM, DMSO 0.1%, quercetin (Que) 1 mM or quercetin 100 µM and ROS production was quantified with a luminol-based assay and expressed as relative light units (RLU). Results are average ± SE, n=8. (A) Forty-five minutes time-course; (B) total RLU quantified after 15 hours; (C) Screenshot after 15 hours. The experiment was repeated three times with similar results. Asterisks indicate significant difference (***p < 0.001) based on one-way ANOVA analysis and Tukey's multiple comparison post-test.

It was then tested whether the quercetin-triggered ROS required a PAMP receptor and RBOHD, the NADPH oxidase responsible for the PAMP-dependent ROS burst (Nühse et al., 2007; Zhang et al., 2007). It was also evaluated whether the quercetin-dependent ROS could derive from a direct effect of quercetin on the peroxidase and/or luminol used to detect the production of ROS. Results showed that the accumulation of ROS in response to quercetin was independent of the PAMP receptors FLS2, EFR and CERK1 (Figure 4.18A), as accumulation of ROS in corresponding mutants was comparable to that in WT plants, but required RBOHD, as no ROS was detected in an *rbohd* mutant (Figure 4.18B). In addition, it could be

excluded that the effect of quercetin was caused by direct effect on the peroxidase and/or luminol, as no ROS could be detected in the absence of leaf disks (Figure 4.18B).
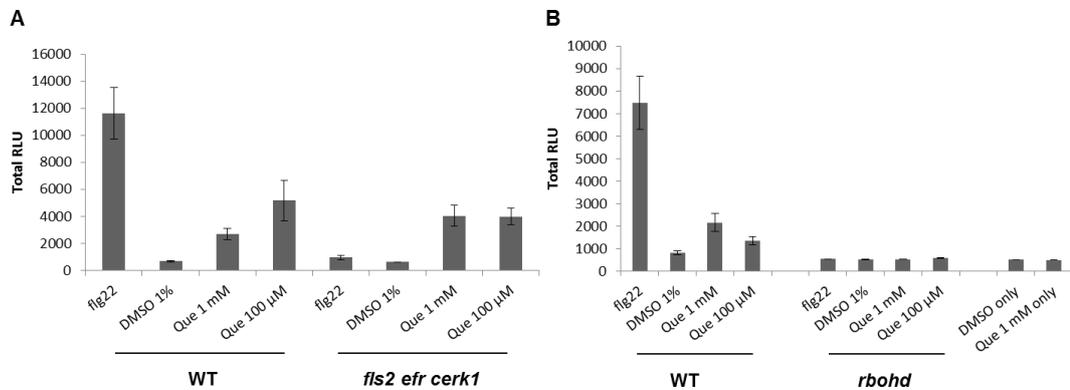
Figure 4.18. Quercetin-dependent ROS does not require the PAMP receptors FLS2, EFR, and CERK1, and RBOHD.

Arabidopsis WT leaf discs were treated with flg22 100 nM, DMSO 1%, quercetin (Que) 1 mM or quercetin 100μM and total ROS production was quantified with a luminol-based assay after 15 hours and expressed as relative light units (RLU). Results are average ± SE, n=12. (A) WT vs *fls2 efr cerk1*; (B) WT vs *rbohd* and quercetin and DMSO were tested in absence of leaf disks. The experiment was repeated twice with similar results.

Furthermore, the effect of co-treatment of Arabidopsis leaf disks with flg22 and quercetin on the flg22-triggered ROS burst was investigated, using flg22 with DMSO as control. Surprisingly, results showed that co-treatment with flg22 and quercetin led to a reduction of the flg22-dependent ROS burst in a dose-dependent manner (Figure 4.19).
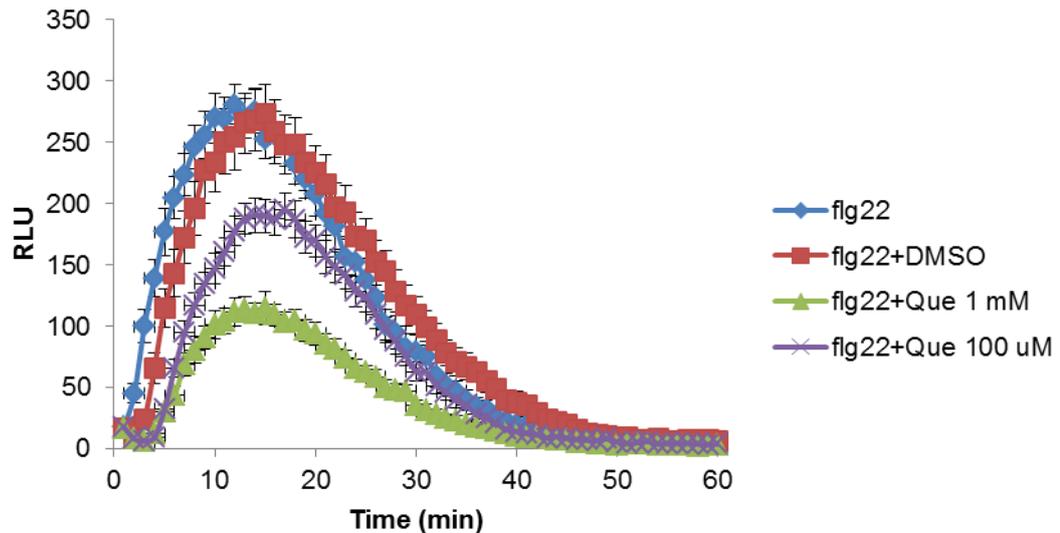
Figure 4.19. Simultaneous application of quercetin and flg22 reduces the flg22-dependent ROS burst in a dose-dependent manner.

Arabidopsis WT leaf disks were treated with flg22 100 nM or co-treated with flg22 100 nM and DMSO 1% or quercetin (Que) 1 mM or quercetin 100 μM and ROS production was quantified with a luminol-based assay and expressed as relative light units (RLU). Results are average ± SE, n=12. The experiment was repeated twice with similar results.

Taken together, these results indicate that quercetin can induce accumulation of ROS in Arabidopsis over time, in a RBOHD-dependent manner, whereas co-treatment with flg22 leads to quenching of the flg22-dependent ROS burst.

Another rather rapid plant response to perception of a PAMP is the activation of a MAPK cascade (Nühse et al., 2000; Tena et al., 2001; Asai et al., 2002). This activation can be detected as early as 5 minutes after treatment and generally decreases after 30 minutes. Quercetin was applied to WT seedlings and samples were taken at 10 and 30 minutes, as well as 1, 3, 6 and 24 hours after treatment, as quercetin may activate MAPKs with a different timing compared to a PAMP; flg22 and DMSO were used as positive and negative controls, respectively. In addition, co-treatment with flg22 and quercetin was tested to assess whether these treatments could have a

synergistic or antagonistic effect. A first test showed that quercetin did not induce any MAPK activation within 24 hours from the application, whereas flg22 did induce a strong activation at 10 minutes after treatment (Figure 4.20). It is worth noting that, although the activation of MAPKs triggered by flg22 decreased after 30 minutes, a second weak activation could be noticed after three hours (Figure 4.20), consistent with a second ROS burst induced by flg22 (Figure 4.17). It appeared that co-treatment with flg22 and quercetin could decrease flg22-dependent MAPK activation at 10 minutes, but could also prolong the activation up to 1 hour (Figure 4.20). However, a second test did not confirm this initial finding and further tests will be required in order to determine the exact role of quercetin in respect of PAMP-dependent MAPK activation.
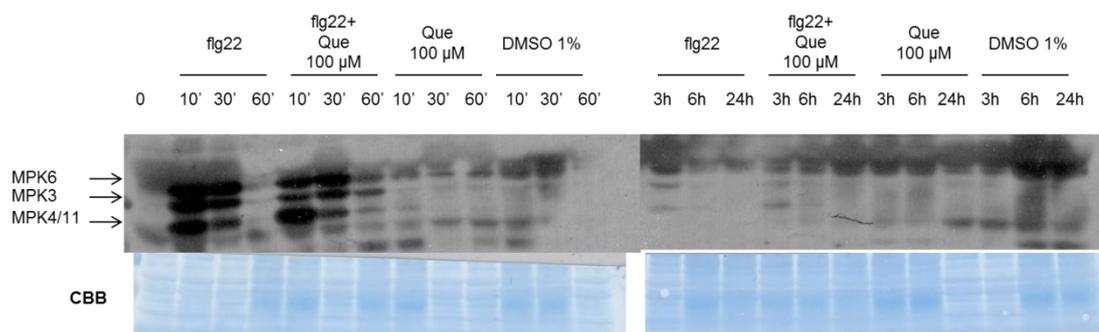
Figure 4.20. Effect of quercetin treatment on MAPK activation.

Two-week-old Arabidopsis seedlings were treated with flg22 100 nM, quercetin (Que) 100 µM, DMSO (1%) or co-treated with flg22 100 nM and quercetin 100 µM. Samples were taken at 10 and 30 minutes, 1, 3, 6 and 24 hours post treatment. Samples were ground in liquid N_2 and proteins extracted and subject to SDS-PAGE and western blot analysis, using α-p42/p44-erk antibody. Membranes were stained with CBB as a loading control.

Another typical output of the plant response to a PAMP is the induction of PIGs. In order to evaluate the effect of quercetin treatment on this response, two-weeks-old WT seedlings were treated with quercetin 1 mM or 100 µM and samples were taken at 30 minutes, 1, 3, 6 and 24 hours post treatment. DMSO and flg22 were used as controls. In addition, seedlings were co-treated with flg22 and quercetin 100 µM to determine the effect of a

169

simultaneous treatment. The marker genes used to evaluate the effect of quercetin were *PHI1*, *NHL10*, *PR1*, *CYP81F2*, *FRK1*, *At1g51890* (He et al., 2006; Boudsocq et al., 2010). Expression levels were quantified by qRT-PCR. Preliminary results indicated that quercetin did not generally induce PIGs, although some weak activation could be detected for *NHL10* (Figure 4.21A), *PR1* and *CYP81F2* at 6 hours after treatment (Figure 4.10C and D). When seedlings were co-treated, quercetin reduced *FRK1* expression at 3 and 6 hrs and increased *NHL10* expression at 1, 3 and 6 hrs (Figure 4.21A and B). Additional effects were not consistent between two replicates.
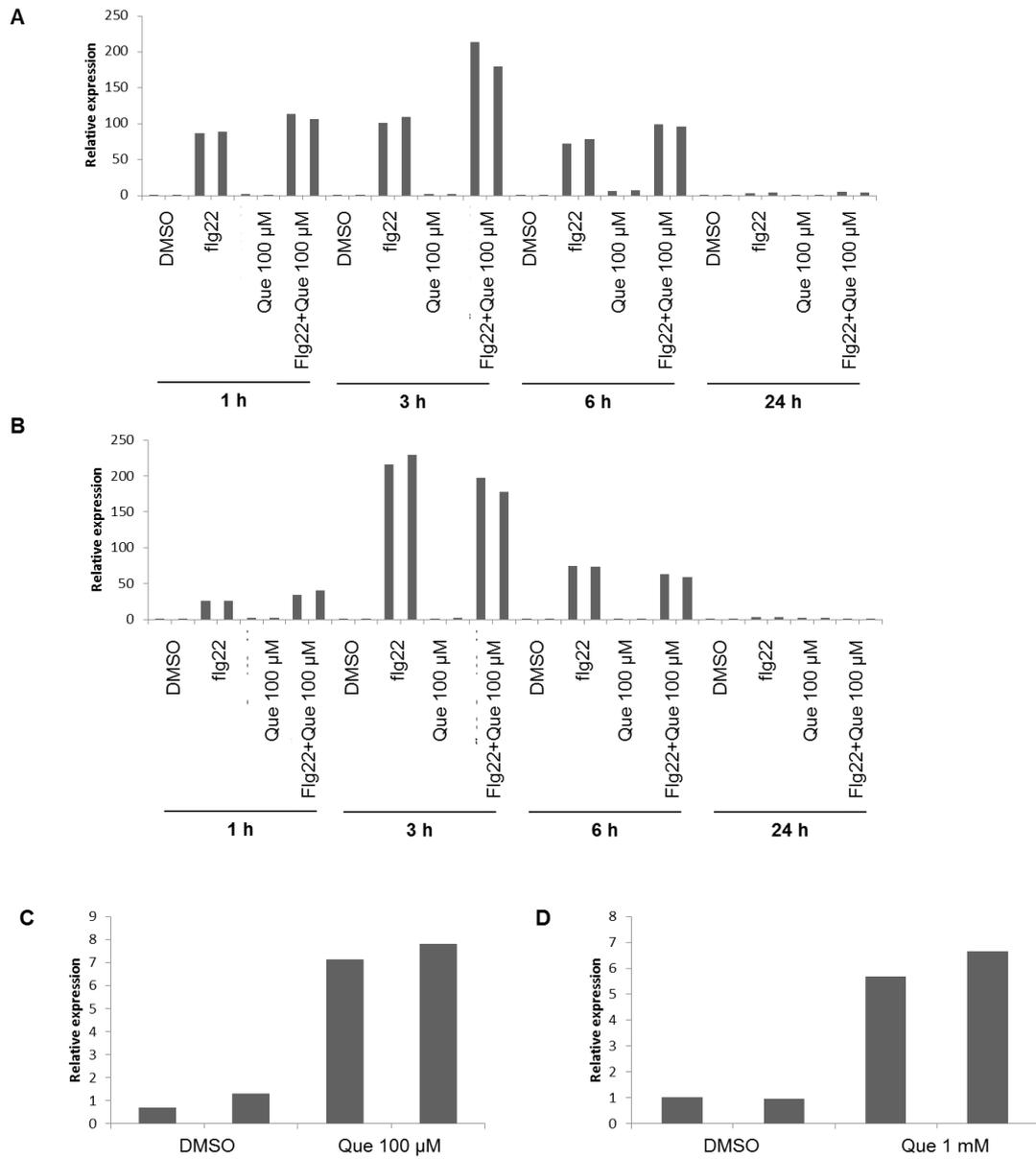
Figure 4.21. Effect of quercetin treatment on PIGs.

Two-weeks-old Arabidopsis seedlings were treated with flg22 100nM, quercetin (Que) 1 mM or 100 µM, DMSO (1%) or co-treated with flg22 100nM and quercetin 1 mM or 100 µM. Samples were taken at 1, 3, 6 and 24 hours post treatment. Gene expression was determined by qRT-PCR using gene-specific primers. Expression values were normalized to the expression of the *UBOX* and relative expression was determined in comparison to that of DMSO-treated seedlings. (A) *NHL10* gene expression; (B) *FRK1* gene expression; (C) *PR1* expression 6 hours post treatment; (D) *CYP81F2* expression 6 hours post-treatment. Bars represent technical replicates. The experiment was repeated twice with similar results.

171

A late measurable output of PTI is SGI (Gómez-Gómez et al., 1999; Zipfel et al., 2006). Five-day-old seedlings were transferred to 48-well plates in liquid media containing quercetin at 1 mM or 100 µM concentration. DMSO and flg22 or elf18 were used as controls. In addition, seedlings were also co-treated with flg22 (or elf18) and quercetin or DMSO. Results showed that seedlings exposed to quercetin grew smaller than those untreated, but the effect was caused by the presence of DMSO (Figure 4.22A). Interestingly, when seedlings were co-treated, the presence of quercetin partially relieved the growth inhibition caused by the PAMP (Figure 4.22A). This was a specific effect, as naringenin, a precursor of quercetin, did not have the same effect (Figure 4.22B). This was significant and reproducible with both flg22 and elf18, although the effect was stronger with elf18 (Figure 4.22A and C).
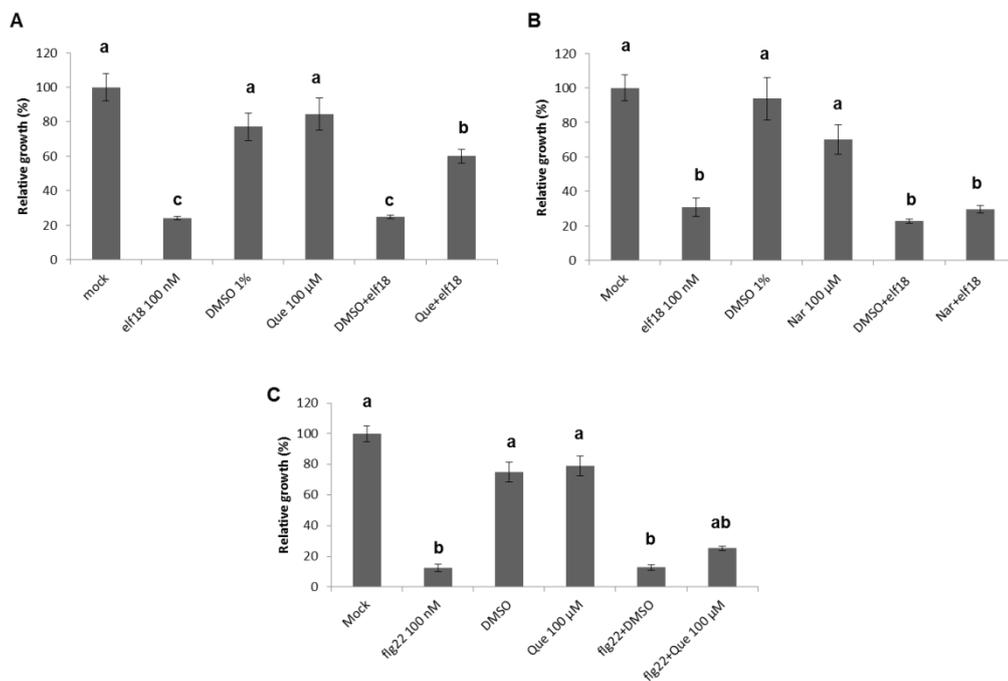
Figure 4.22. Quercetin reduces PAMP-induced SGI.

Five-days-old Arabidopsis WT seedlings were transferred to a liquid media containing flg22 or elf18 100 nM, quercetin (Que) 100 µM, DMSO (1%) or flg22/elf18 100 nM and quercetin 100 µM or DMSO. Weight of individual seedlings was recorded after 10 days. Results are represented as percentage of fresh weight compared to mock treatment. (A) elf18 100 nM and/or quercetin 100 µM; (B) elf18 100 nM and/or naringenin 100 µM; (C) flg22 100 nM and/or quercetin 100 µM. Bars are means ± SE, n=6. Significantly different groups are indicated with lower-case letters based on one-way ANOVA analysis and Tukey's multiple comparison post-test. The experiment was repeated twice with similar results.

Although seedling growth inhibition is a well-known effect of PAMP treatment, and it is known that trade-offs between growth and defence exists (Bruyne et al., 2014; Huot et al., 2014), the exact nature of the growth inhibition mechanism is currently unknown. One simple hypothesis could be that the constant presence of a PAMP continuously induces defences, including ROS production. Because quercetin can quench the flg22-dependent ROS, which requires RBOHD, *rbohd* was tested for SGI. Preliminary results showed that at lower PAMP concentration (10 nM), *rbohd* growth was less inhibited than WT, both with flg22 and elf18 (Figure 4.23). In addition, a similar enhanced growth was observed with high dose (100 nM) of elf18, but not flg22 (Figure 4.23). This would suggest that PAMP-triggered production of ROS partially contributes to PAMP-triggered SGI.
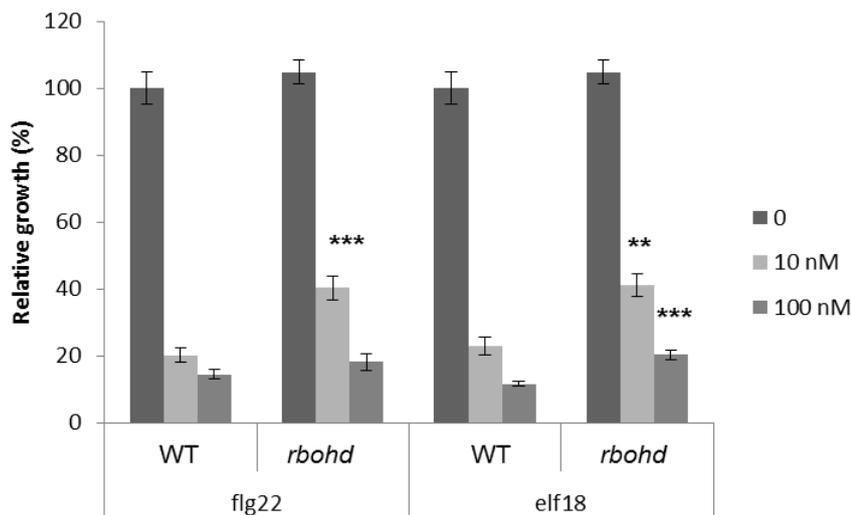
Figure 4.23. *rbohd* is less sensitive to PAMP-induced seedling growth inhibition

Five-days-old Arabidopsis WT seedlings were transferred to a liquid media containing flg22 or elf18 100 nM. Weight of individual seedlings was recorded after 10 days. Results are represented as percentage of fresh weight compared to mock treatment Bars are means ± SE, n=8. Asterisks indicate a statistically significant difference between WT and mutants at each treatment (***$p<0.001$, ***$p<0.01$) using two-tailed unpaired t-test. The experiment was repeated twice with similar results for elf18.

Taken together, these results would indicate that exogenous application of quercetin has a dual role toward immunity. On one hand, quercetin treatment

173

can induce the expression of certain defence-related genes (*NHL10*, *PR1* and *CYP81F2*). On the other hand, it seems to have a wider role in quenching other PAMP-dependent responses, such as the ROS burst, *FRK1* expression and SGI.

4.3 Summary and discussion

The *pir* screen identified several novel loci whose mutations led to impaired resistance to bacteria following flg22 perception. One of these was *PIR38*, carrying a T-DNA insertion in *UGT78D1*, a UDP-rhamnosyltransferase responsible for rhamnosylation of flavonol aglycones. Expression analysis in *pir38* revealed that the T-DNA insertion located in the 5'-UTR caused over-expression of *UGT78D1*. Although rare, this is not an uncommon effect of T-DNA mutagenesis (Kirik et al., 2002; Sorin et al., 2005). The over-expression could be caused either by a positive effect of the T-DNA on the promoter or to the *Cauliflower mosaic virus* 35S present on the vector, with the second being more likely (Alonso et al., 2003; Wang, 2008). Because this insertion line affected the expression of a biosynthetic gene of the flavonol pathway, it would have been informative to determine its flavonol profile. In fact, this could have given indications on which compound(s) may misaccumulate and therefore be possibly responsible for the loss of flg22-induced resistance to *Pto* DC3000. However, following initial confirmation, the phenotype was confirmed in five out of ten experiments. Therefore, this line was not found a reliable material for further tests and a different approach was sought

The flavonoid biosynthetic pathway is positively affected by many different environmental stimuli, like nutrient depletion, light and temperature (Chappell and Hahlbrock, 1984; Stewart et al., 2001; Lillo et al., 2008; Olsen et al., 2009). Although plants were grown in controlled environment rooms, variability in soil composition, light intensity and humidity can occur to some

extent. However it would seem unlikely that these variations could account for the inconsistency of the phenotype. An alternative explanation could be the presence of a second, segregating T-DNA insertion in this mutant line. Backcrossing the isolated *pir* mutant could help confirm or refute this hypothesis. However, whether the use of flg22-induced resistance as output would be strong enough is questionable. In fact, this assay is more prone to intrinsic variability than other assays, as observed during the *pir* screen. Taking these difficulties into account, the use of a stable transgenic Arabidopsis line over-expressing *UGT78D1* was chosen as an alternative approach. However, as later realized, over-expressing *UGT78D1* was not easily achievable. None of several constructs yielded an over-expression of *UGT78D1*, as opposed to the easy identification of *UGT78D2* over-expression lines, suggesting that *UGT78D1* expression may be tightly regulated. In summary, to date none of the attempts could confirm whether over-expression of *UGT78D1* can lead to impairment in induced resistance to bacteria.

Since the role of flavonoids in disease resistance has been demonstrated in different pathosystems (Dixon, 2001; Treutter, 2006), it was decided to use a genetic approach to address the broader question of whether flavonoids have a role in resistance to bacteria in Arabidopsis. In fact, the flavonoid biosynthetic pathway is very well characterized and, moreover, in Arabidopsis, all the enzymes, but *FLS*, are encoded by a single gene (Saito et al., 2013). Mutants in different key steps of the pathway were obtained and pathogenicity assays were carried out to determine whether loss of resistance to bacteria could be observed by blocking the pathway at different levels. None of the mutants tested showed a defect when tested for flg22-induced resistance. However, this assay is carried-out by infiltration of bacteria into the apoplast of Arabidopsis leaves, which would allow bacteria to bypass every natural physico-chemical barrier and could not be informative enough on the basal levels of resistance.

In order to evaluate the effect of mutations in the flavonoid biosynthetic pathway in bacterial penetration, spray-infection assays were performed. Results were affected by high variability within experiments and between biological replicates; the only statistically significant phenotype observed was enhanced disease resistance in *ugt78d2-2* and *ugt78d3*. Although with no statistical significance, *ugt78d1*, *ugt78d2-1* and *ugt78d1 ugt78d2* also showed weak enhanced resistance. These lines carry mutations in different UGTs responsible for glycosylation of flavonol aglycones. *ugt78d2-2* is a novel allele of *ugt78d2*, and, although expression analysis demonstrated that, like *ugt78d2-1*, this mutant was a knock-out, it is not known whether the two differ in flavonol composition. More surprisingly was the phenotype observed in *ugt78d3*. This mutant was initially published to be a knock-down, but the gene expression was tested on flower cDNA (Yonekura-Sakakibara et al., 2008). Further expression analysis on cDNA from whole two-week-old seedlings showed that the mutation was causing a weak overexpression. However, no data on the flavonol content was known for this line, as for *ugt78d2-2*, making it difficult to assess whether the phenotype could be ascribed to an enhancement or lack of a specific set of flavonoids and therefore draw any conclusion from it.

When mutants of enzymes upstream of flavonol aglycones were tested to evaluate any defect in basal resistance to bacteria, *tt4*/*chs*, *tt6*/*f3h* and *tt7*/*f3'h* seemed more susceptible than WT. This could suggest that loss of a compound between naringenin chalcone and flavonol aglycone could be responsible for resistance to bacteria. However, because *tt7*/*f3'h* was found to weakly over-express *TT7*, and *TT7* converts kaempferol to quercetin, kaempferol, or its glycosylated derivative, would seem the compound responsible for resistance to bacteria, as overexpression of *TT7* would deplete the substrate in favour of the product. This would also be in agreement with kaempferol derivatives being the most abundant flavonols in Arabidopsis leaves and quercetin derivatives most abundant in flowers (Yonekura-Sakakibara et al., 2008). However, no flavonoid profiles in *tt7*/*f3'h*

was determined and therefore no final conclusion could be drown. Surprisingly, *fls1* did not show any impairment in resistance. However, the insertion seemed to affect the viability of the seeds, as they stopped germinating shortly after bulking-up; a different mutant line needs to be tested. In addition, *LDOX* can have additional FLS activity*,* and a second functional *FLS* gene, *FLS3,* has also been found (Turnbull et al., 2000; Welford et al., 2001; Owens et al., 2008b; Stracke et al., 2009), suggesting functional redundancy. It would be interesting therefore to test double *fls1 ldox* and *fls1 fls3* mutants to make a better judgement on the phenotype of *fls1*.

Although with no statistical significance, *tt5*/*chi* seemed more resistant to bacteria than WT. Although not in line with the phenotype observed in *tt4*/*chs*, *tt6*/*f3h* and *tt7*/*f3'h*, expression analysis in *tt5* showed that *CHS*, *F3H, F3'H*, *DFR*, *FLS1* and *ANS* are enhanced both at the gene and at the protein level, suggesting a positive feedback induced by naringenin (Shirley et al., 1995; Pelletier et al., 1999; Pourcel et al., 2013). Therefore, the enhanced resistance of *tt5*/*chi* would be in agreement with the phenotype observed in *tt4*/*chs*, *tt6*/*f3h* and *tt7*/*f3'h*. Mutants in *OMT1* and *TT3*/*DFR* showed WT flg22-induced resistance to bacteria, indicating that isorhamnetin and anthocyanins do not have a role in resistance to bacteria.

Interestingly, publicly available microarray data indicate that 24 hours after pathogen infection the whole central pathway that leads to flavonols is downregulated. At earlier time points (2 and 6 hours post infection) the effect was much weaker if any (Naoumkina et al., 2010). This would be in contradiction with the susceptibility phenotype observed in some mutant enzymes of the pathway. However, one possible explanation could be that flavonoids are not readily synthesized but released from their storage sites in response to a pathogen attack. Therefore, the pathway could be down-regulated in order to re-allocate resources towards production of other components required for the immune response.

This hypothesis may also explain the results obtained by analysing the flavonoid profile of Arabidopsis leaves treated with flg22. The main peaks were identified as Kaempferol-$(Rha)_2$, Kaempferol-$(Rha)_2$-Glc, and Kaempferol-RhaGlc (Rha=rhamnose, Glc=glucose). Although the position of the sugars could not be resolved, they were likely to be kaempferol 3-*O*-rhamnoside-7-*O*-rhamnoside, kaempferol-3-*O*-[rhamnosyl (1→2 glucoside)]-7-*O*-rhamnoside and kaempferol 3-*O*-glucoside-7-*O*-rhamnoside, which are the three major flavonols in Arabidopsis leaves (Yonekura-Sakakibara et al., 2008). The analysis showed that the three flavonols decreased in response to flg22 at five hours post-treatment, when compared with mock. The decrease was still detected after 10 hours but to a lesser extent. Hypothesizing that flavonoids are released from their storage sites in response to a pathogen attack and considering that glycosylated flavonols are the storage form of flavonols, it would be tempting to speculate that the decrease observed is due to release. However, it is also not known whether flavonoids are transported to the apoplast. It would be therefore interesting to analyse the flavonoid profile in the apoplastic fluid after flg22 treatment. In addition, a pharmacological approach could be used as different transporter inhibitors, like glybenclamide or ortho-vanadate, have been shown to block flavonoid transport (Buer et al., 2007; Sugiyama et al., 2007).

Previous studies aimed at identifying metabolomic differences after *Pto* DC3000 infection or flg22 treatment did not identify changes in flavonoids (Hagemeier et al., 2001; Simon et al., 2010; Schenke et al., 2011). However, these works based their analysis at 24 hours post infection/treatment. In agreement with this, at the same time point no major differences between mock and flg22 treatment were found.

Although genetic and metabolomic analysis helped in making a hypothesis on the role of flavonoids in plant immunity, no definitive proof was gathered and a chemical approach was employed. In fact, it was previously reported that exogenous application of quercetin protects Arabidopsis for subsequent bacterial infection (Jia et al., 2010). It was therefore decided to use quercetin

to evaluate its effect on the bacteria and on the plant responses to perception of bacteria. The first aspect to assess was the direct effect of quercetin on bacteria. In fact, conflicting evidence exists in the literature. Jia and co-workers (2010) did not find quercetin to have a direct effect on bacteria by measuring the bacterial density after 24 hours of incubation with the chemical. However, different reports indicated that quercetin had an antimicrobial effect, using an antibiosis plate assay and a different *in vitro* measurement of bacterial density (Vandeputte et al., 2011; Vargas et al., 2011). In order to clarify this discrepancy, these assays were repeated. Quercetin did have a transient inhibitory dose-dependent effect on *Pto* DC3000 when grown *in vitro*, but an antibiosis assay only showed a minimal inhibition with a high concentration of quercetin (1 mM) and low bacterial density ($OD_{600}=0.002$). It is worth noting that quercetin is not water-soluble and is light sensitive. When diluted in water, it partially precipitates and the actual concentration would be lower. In addition, although the antibiosis assay was done both with quercetin diluted in DMSO and in water, the diffusion may not be optimal, leading to differences. Because no strong effect could be observed, it was concluded that if quercetin has an effect, it may be transiently bactericidal. This could be explained by the presence of a specific efflux pump in *Pto* DC3000 that would help bacteria in detoxify quercetin after initial exposure. In fact *Pto*DC3000 carries a *MexAB-OprM* operon encoding a multidrug efflux pump that is responsible for detoxification of naringenin and phloretin, although quercetin was found not to be a substrate (Vargas et al., 2011).

Addition of phloretin to *Pto* DC3000 culture reduces the number of flagella and can decrease the expression and protein accumulation of *fliC* (Vargas et al., 2013). Expression of *hrpL*, responsible for the regulation of the induction of type III secretion system (T3SS) genes, was also reduced, although the effect was independent of *HrpR* and *HrpS* (Vargas et al., 2013). Citrus flavonoids can also reduce expression of T3SS genes in *Vibrio haveyi*, although without inhibition of bacterial growth *in vitro* (Vikram et al., 2010).

Because establishment of PTI interferes with the T3SS of bacteria (Crabill et al., 2010; Oh et al., 2010; Anderson et al., 2014), the hypothesis that flavonoids may affect the T3SS is quite fascinating. However, no test was carried out in order to determine whether this was true and this interesting idea should be experimentally tested in future work.

Quercetin was found to have a dual activity towards apoplastic ROS production: it could scavenge flg22-dependent ROS production and induce accumulation of ROS when tested alone. Although surprising, there are several indications in the literature of a dual role of quercetin as antioxidant and prooxidant (Laughton et al., 1989; Bors et al., 1995; Cao et al., 1997; Metodiewa et al., 1999; Sakihama et al., 2002). The prooxidant activity was shown to be due to the presence of metal ions or a consequence of its degradation to quinone. Although Jia and co-workers (2010) showed that quercetin induced accumulation of ROS following bacterial inoculation, that observation was based on 3,3'-diaminobenzidine (DAB) staining, which measures accumulation of ROS, both cytoplasmic and apoplastic, and therefore does not contradict the finding. ROS is induced by different stresses and intracellular ROS can, in turn, activate MAPKs cascades (Mittler et al., 2011).

Although preliminary, it was observed that co-treatment of Arabidopsis seedlings with flg22 and quercetin led to initial decrease in flg22-dependent MAPK activation. Although it may suggest that quercetin is a negative regulator, the actual biological significance could be ascribed to the the scavenging activity of quercetin. In fact, flavonoids can mediate oxidative stress-induced activation of signaling cascades and can inhibit MAPK activation in animals (Lamoral-Theys et al., 2010; Agati et al., 2013). This would also be in agreement with the reduction on flg22-dependent *FRK1* activation caused by quercetin, as *FRK1* induction is dependent on MAPK activation (Asai et al., 2002). In addition, quercetin induced expression of the PTI marker genes *NHL10*, *PR1* and *CYP81F2* six hours after treatment and had a synergistic effect with flg22 on the activation of *NHL10* at one and six

hours after treatment. The effect on gene expression, however, could be due to different mechanisms. Flavonoids and their biosynthetic enzymes have been found in the nucleus and it has been suggested they may have a direct effect on gene expression (Hrazdina and Wagner, 1985; Grandmaison and Ibrahim, 1995; Saslowsky and Winkel-Shirley, 2001; Feucht et al., 2004; Saslowsky et al., 2005; Kuhn et al., 2011). However, it cannot be excluded that the gene induction could be caused by the positive effect that quercetin has on a different signalling pathways. For example, quercetin protection towards *Pto* infection was also dependent on SA (Jia et al., 2010).

Taken together, the evidence would suggest that flavonoids may be released from their storage sites to both target bacteria and act as buffers to protect the plant cell from the excessive oxidative stress that bacterial perception triggers. This would be in agreement with the transient bactericidal effect of quercetin, the decrease in glycosylated flavonols after flg22 perception, and the ability of quercetin to quench ROS burst and to reduce SGI. However, further tests will need to include glycosylated flavonols, as these are the predominant flavonol form in Arabidopsis leaves. In conclusion, flavonols may be considered phytoanticipins that were defined as "low molecular weight, antimicrobial compounds that are present in plants before challenge by microorganisms or are produced after infection solely from pre-existing constituents" (VanEtten et al., 1994).

Chapter 5. Phenotypic analysis of additional *pir* mutants

5.1 Introduction

In addition to *PIR38*, the *pir* screen identified additional loci whose mutation led to impairment in resistance towards bacteria following flg22 pretreatment. These are: *PIR20* encoding ABC2 HOMOLOG 5 (*ABCA6*), *PIR32* encoding cation/H+ exchanger 6B (*CHX6B*) and *PIR60* encoding mevalonate diphosphate decarboxylase 1 (*MVD1*). A brief introduction on each *pir* is then followed by results on their phenotypic characterization.

5.1.1 ATP-binding cassette (ABC) proteins

The ABC superfamily includes proteins characterized by the presence of the ATP-binding cassette which is a cytoplasmic nucleotide-binding domain (NBD). In the case of ABC transporters, a transmembrane domain (TMD) is present in addition to the NBD. All the ABC transporters are characterized by the presence of one or two NBDs and TMDs (Walker et al., 1982; Higgins, 1992; Hyde et al., 1990).

The NBD domain hydrolyses ATP, producing the driving force to translocate solutes through the channel made by the TMDs (Martinoia et al., 1993; Li et al., 1995). It has been suggested that due to the diversity observed within different TMD sequences, they could have an additional role in substrate recognition (Higgins and Linton, 2004). ABC transporters can be either importer or exporter (Saurin et al., 1999; Shitan et al., 2003). In addition some ABC proteins lack a TMD and are soluble proteins in the cytoplasm (Sánchez-Fernández et al., 2001).

ABC proteins are divided into eight major groups (A-H) based on the alignment of NBD amino acid sequences. In addition, group I has been added and includes ABC proteins with additional subunits that do not fit in any of the groups (Verrier et al., 2008) (Figure 5.1). *pir20* carries a T-DNA insertion in *ABCA6*, which belongs to group A, and has not been

characterized yet (Verrier et al., 2008). Among members of this group, only ABCA9 has been characterised. It was suggested that ABCA9 mediates the transport of fatty acids to the ER for the synthesis of triacylglycerol in maturing seeds (Kim et al., 2013).

Figure 5.1. *Arabidopsis thaliana* **ATP-binding cassette (ABC) protein subfamilies.**

Phylogeny of each ABC subfamily and of all Arabidopsis ABC proteins is based on their NBD sequence. For the ABCI subfamily, only the encoded domain is indicated. Domain organizations are indicated by colored symbols: blue square, TMD; red circle, NBD; green star, other domains. ABCA6/PIR20 is indicated by the red arrow (from Kang et al., 2011).

ABC transporters have been associated with many different physiological processes, including transport of hormones and secondary metabolites and xenobiotic detoxification (Kang et al., 2011).

A significant number of ABC transporters belonging to subfamily G are upregulated by JA and/or SA, and pathogens, which would point to their possible involvement in immunity (Kang et al., 2011). Of these, only two have been characterized in Arabidopsis. Mutation in *AtABCG36/AtPDR8/PEN3* leads to enhanced susceptibility to different pathogens, both biotroph and necrotroph, but enhanced resistance to *Pto* DC3000; glucosinolates were later indicated as substrates (Kobae et al., 2006; Stein et al., 2006; Bednarek et al., 2009; Clay et al., 2009). Flg22 or chitin treatment induce re-localization of PEN3 in focal points, suggesting that PEN3 is recruited at the site where pathogen invasion is perceived (Underwood and Somerville, 2013).In addition, the same transporter is involved in cadmium resistance (Kim et al., 2007). The second characterized ABC protein is AtABCG40/AtPDR12 and its expression is induced both by pathogens and SA, ET, and methyl jasmonate (Campbell et al., 2003). A tobacco orthologue, *NtPDR1* is also induced in response to different elicitors and pathogens (Sasabe et al., 2002; Stukkens et al., 2005). Mutation in *AtABCG40/AtPDR12* also increases the sensitivity to sclareol, an antimicrobial diterpenoid which is the substrate of two close orthologues, SpTUR2 in *Spirodela polyrrhiza* and NpABC1 in *Nicotiana plumbaginifolia* (Jasiński et al., 2001; Brûle and Smart, 2002; Brûle et al., 2002; Campbell et al., 2003). AtABCG40/AtPDR12 was later found to be additionally involved in lead detoxification and ABA transport (Lee et al., 2005; Kang et al., 2010). Another transporter belonging to the same subfamily, LEAF RUST 34 (LR34) confers broad spectrum resistance in wheat (Krattinger et al., 2009). Other than having a role in immunity, biochemical data supports the involvement of ABC transporter-dependent export of isoflavonoids from soybean roots which are signal inducers for *nod* genes of *Bradyrhizobium japonicum* (Kosslak et al., 1987; Sugiyama et al., 2007).

ABC transporters are also considered prime candidates for transport of secondary metabolites, although to date only ZmMRP3 in maize, involved in transport of anthocyanins in the vacuole, CjMDR1 from *Coptis japonica*, which mediates the import of the alkaloid berberin, and the above mentioned SpTUR2 and NpABC1 have been characterized (Yazaki et al., 2001; Shitan et al., 2003; Goodman et al., 2004).

5.1.2 Cation/H$^+$ exchanger

Cation/H$^+$ exchangers are a class of secondary transporters that can move ions across membranes thanks to the gradient and membrane potential created by the simultaneous counter flux of protons (Mäser et al., 2001). In Arabidopsis monovalent cation:proton transporters have been divided in three families: CATION PROTON ANTIPORTER 1 (CPA1), CATION PROTON ANTIPORTER 2 (CPA2) and Na$^+$-transporting carboxylic acid decarboxylase (NaT-DC) (Brett et al., 2005). The cation/H$^+$ exchanger (CHX) protein subfamily is part of the CPA2 family with 28 members in Arabidopsis, including *PIR32*/*CHX6B* (Sze et al., 2004) (Figure 5.2). CHX proteins share homology with *Saccharomyces cerevisiae* KHA1, a K$^+$/H$^+$ antiporter with a role in intracellular cation homeostasis and pH control (Ramírez et al., 1998; Maresova and Sychrova, 2005).
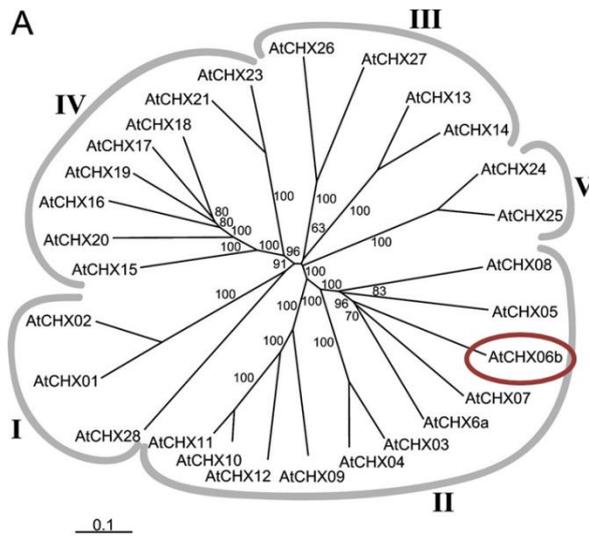
Figure 5.2. Phylogenetic tree of Arabidopsis CHX proteins.

The phylogenetic tree of Arabidopsis ABC protein subfamily A was constructed according to the full lenght protein sequence. Five major branches were identified and are indicated as I to V. PIR32/CHX6B is highlighted. Adapted from Sze et al., 2004.

Phylogenetic analysis showed that *CHX* genes are found in pairs and several have paralogues (Sze et al., 2004). Surprisingly, of the 28 *CHX* genes, 11 were either pollen specific or expressed at higher levels in pollen when compared to WT, seven were preferentially expressed in the male gamethophyte (including *PIR32*/*CHX6B*), and only six showed expression in vegetative tissues (Sze et al., 2004). Only a few members have been characterized to date, namely CHX13, CHX17, CHX20, CHX21, and CHX23. They appear to have a predominant role in K^+ uptake and homeostasis with, in some cases, additional regulation of Na^+ concentration, although no role in immunity has been described yet (Pardo et al., 2006; Pittman, 2012). Furthermore, it has been suggested that CHX proteins may have a role in modulating the sorting and trafficking of proteins in the endomembrane system through regulation of cations and pH (Pittman, 2012).

5.1.3 Mevalonic acid (MVA) biosynthetic pathway

Isoprenoids are a large class of phytochemicals with many different functions, including components of the photosynthetic machinery, hormones for growth and development and secondary metabolites necessary for the interaction with the surrounding environment (Hemmerlin et al., 2012).

All isoprenoids derive from condensation of two basic units, isopentenyl diphosphate (IPP) and dimethylallyl diphosphate (DMAPP). IPP and DMAPP can be synthesized by two independent pathways, the mevalonic acid pathway (MVA) and the plastid-localized methylerythritol (MEP) pathway (Chappell, 1995; Lichtenthaler et al., 1997; Sapir-Mir et al., 2008) (Figure 5.3). The MVA branch starts with the condensation of three molecules of acetyl-CoA to form 3-HYDROXY-3-METHYLGLUTARYL-COA (HMG-CoA) and it is catalysed by two consecutive enzymes, ACETOACETYL-COA THIOLASE (AACT) and HMG-COA SYNTHASE (HMGS) (Montamat et al., 1995; Lange and Ghassemian, 2003; Jin et al., 2012). HMG-CoA is then converted to MVA by HMG-COA REDUCTASE (HMGR) in two consecutive reduction steps (Caelles et al., 1989). In Arabidopsis there are two *HMGR* genes, encoding three isoforms, HMGR1S, HMGR1L, and HMGR2, although HMGR1 seems to prevail in function (Enjuto et al., 1994; Suzuki et al., 2004). HMGR1S is present ubiquitously within the plant, whereas HMGR1L is mostly found in seedlings, roots and inflorescences (Lumbreras et al., 1995). Both *hmgr1* and *hmgr2* have reduced levels of sterols, although less severe in *hmgr2*. In addition, *hmgr1* shows dwarfism, early senescence, and sterility, whereas *hmgr2* does not seem to have major visible phenotypes; *hmg1 hmg2* double mutant is sterile (Suzuki et al., 2004; Ohyama et al., 2007; Suzuki et al., 2009). HMGR activity is regulated at different levels through phosphorylation, proteolytic degradation, redox changes and metabolic feedbacks (Hemmerlin, 2013).

In the final steps of the pathway leading to the formation of IPP, MVA is phosphorylated by MEVALONATE KINASE (MK) and

PHOSPHOMEVALONATE KINASE (PMK) to produce MVA 5-diphosphate, followed by ATP-dependent decarboxylation controlled by MVA DIPHOSPHATE DECARBOXYLASE (PMD/MVD1/PIR60) (Riou et al., 1994; Cordier et al., 1999; Simkin et al., 2011). In Arabidopsis there are two MVA diphosphate decarboxylase paralogues, MVD1 and MVD2 (Simkin et al., 2011). *MVD1* is expressed at similar levels throughout plant development, with a peak in expression in roots, whereas *MVD2* expression is lower and mostly restricted in the reproductive organs and roots (Vranová et al., 2013). In addition, MVD1 was experimentally localized in peroxisomes and cytoplasm, but no data are available for MVD2 (Vranová et al., 2013). It has been suggested that MK, PMK and PMD/MVD may be less important in the control of the biosynthetic pathway when compared to HMGR (Bianchini et al., 1996; Tholl and Lee, 2011).
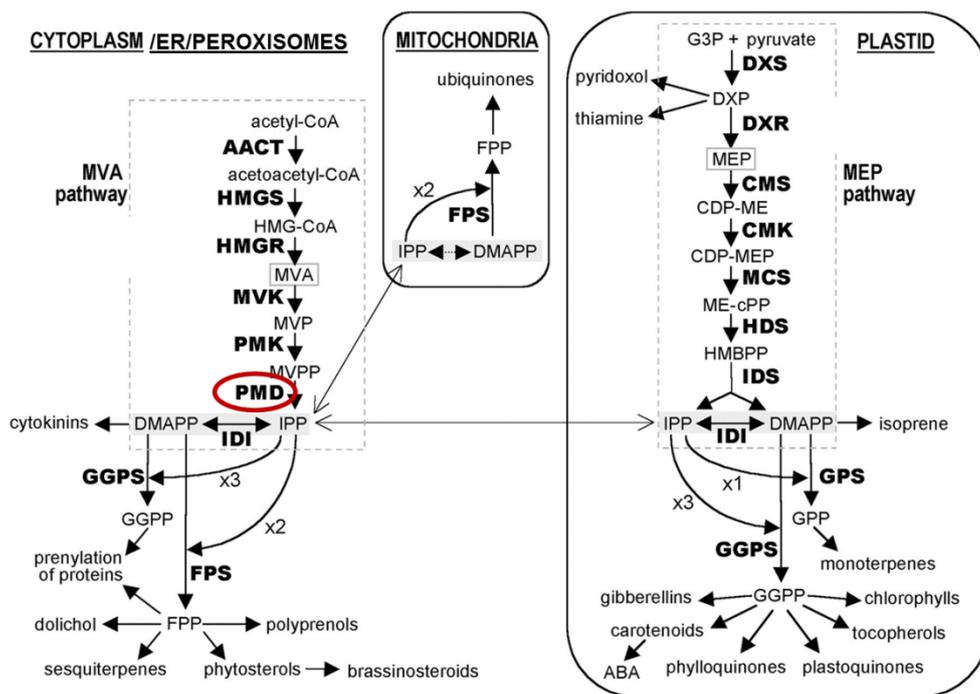
Figure 5.3. Scheme of plant isoprenoid biosynthetic pathways

Subcellular compartmentalization of the MVA and MEP pathways in plant cells. Biosynthetic enzymes are: AACT, acetoacetyl CoA thiolase; HMGS, HMG-CoA synthase; HMGR, HMG-CoA reductase; MVK, MVA kinase; PMK, MVP kinase; PMD, MVPP decarboxylase; IDI, IPP isomerase; GPS, GPP synthase; FPS, FPP synthase; GGPS, GGPP synthase; DXS; DXR, DXP reductoisomerase;CMS; CMK;MCS; HDS. PIR60/MVD1/PMD is highlighted in red. From (Rodríguez-Concepción and Boronat, 2002).

Terpenes have been shown to have a role in plant defense. Examples include the production of diterpenoids against rice blast in rice and against different fungi in maize, and the emission of volatile terpenes against herbivores (Unsicker et al., 2009; Hasegawa et al., 2010; Schmelz et al., 2011). In tobacco, *HMGR* expression is induced by different elicitors, including *Phytophtora* cell wall fragments, also leading to the production of capsidiol, a sesquiterpenoid phytoalexin (Chappell and Nable, 1987; Chappell et al., 1991). HMGR activity is also increased in potato following interaction with incompatible race of *P. infestans* or elicitors (Stermer et al., 1991; Yang et al., 1991; Choi et al., 1992). Additionally, HMGR1 interacts with the receptor kinases SYMRK, DMI2 and NORK receptors during symbiosis and HMGR1 activity is required for nodulation in *Medicago truncatula*, making the study of the role of MVA pathway in plant immunity even more intriguing (Kevei et al., 2007; Oldroyd, 2013).

5.2 Results

5.2.1 PIR20/ABCA6

The *pir20* mutant carries a T-DNA insertion in *ABCA6*, an ABC transporter belonging to subfamily A of the ABC family, which includes one full-length and 11 half-size genes (Figure 5.1) (Verrier et al., 2008). *ABCA6* is part of a cluster of seven homologous genes on chromosome 3 (Verrier et al., 2008). In *pir20-1*, the T-DNA is inserted in the last intron (Figure 5.4A). The T-DNA lies in between the ABC signature motif and the Walker B consensus sequence ((R/K)XXXXGXXXXLhhhhD), which, with the Walker A consensus sequence (GXXXXGK(T/S)), the H and the Q loop are conserved motifs of the NBD domain of ABC transporters (Higgins and Linton, 2004). Gene expression analysis by qRT-PCR showed that the T-DNA insertion caused

reduction in expression of the gene (Figure 5.4B). Additional insertion lines were obtained but no homozygous were available for tests.
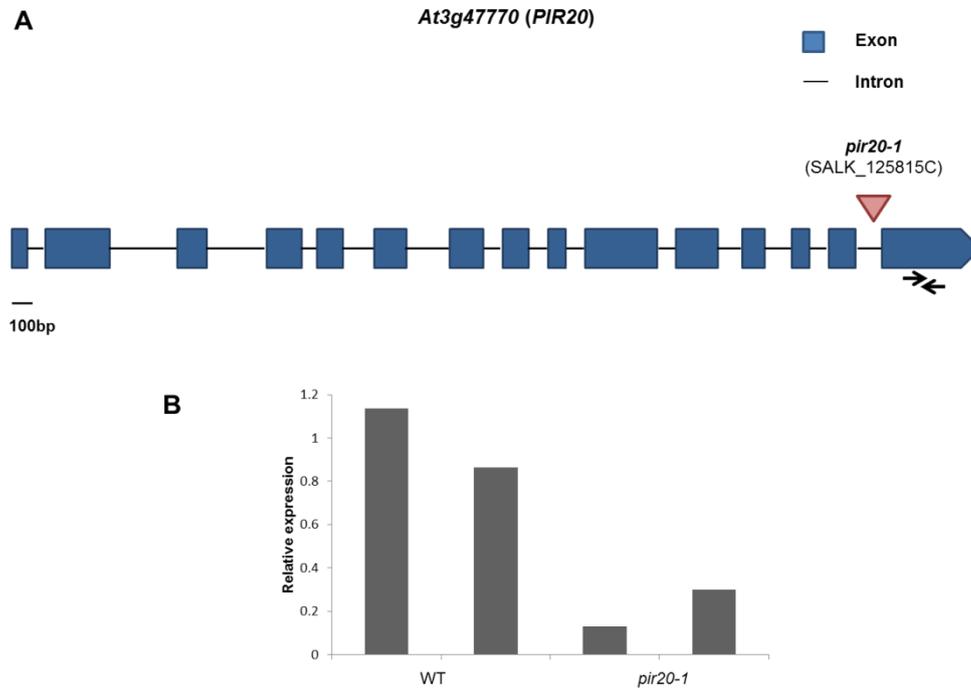
Figure 5.4. T-DNA insertion in *pir20-1* is located in the last intron and it causes reduction of *PIR20* expression.

(A) *pi20-1* carries a T-DNA insertion in the last intron. Arrows indicate the position of the primers for expression analysis. (B) Gene expression was determined by qRT-PCR using gene-specific primers. cDNA was generated from 14-days-old Arabidopsis seedlings. Expression values were normalized to the expression of the *UBOX* and relative expression was determined in comparison to WT. Bars represent two technical replicates per genotype.

Since *pir20-1* was initially isolated as a mutant impaired in induced resistance to *Pto* DC3000 triggered by flg22 perception (Figure 3.18), it was additionally tested in a spray-infection assay to evaluate the effect of this mutation on the basal level of resistance. In the only repetition carried out, *pir20-1* was found more susceptible to bacterial infection than WT (Figure 5.5). Although preliminary, this suggests that the *pir20-1* mutation affects basal levels of resistance to bacteria, other than flg22-induced resistance.
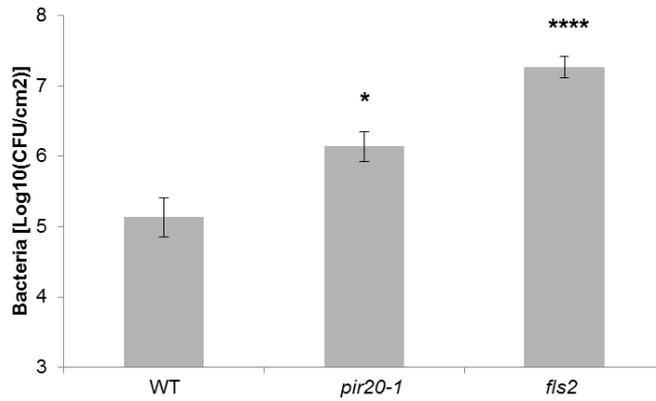
Figure 5.5. Evaluation of enhanced susceptibility to *Pto* DC3000 in *pir20-1*.

Five-weeks-old WT and mutant plants were sprayed with *Pto* DC3000 (OD_{600}=0.2). Bacterial growth was measured at 3 DPI by plating serial dilutions of homogenized leaf disks. Bars are means ± SE, n=6. Asterisks indicate significant difference (*$p < 0.05$, **** $p < 0.0001$) using two-tailed unpaired t-test.

To evaluate the role of PIR20/ABCA6 in other PTI responses, ROS and SGI were tested in *pir20-1*. For both experiments, a range of flg22 concentrations was used to evaluate a dose-response to the peptide. Results showed that flg22-triggered ROS was higher in *pir20-1* when compared to WT at the highest concentration tested (100 nM) (Figure 5.6A and D). A smaller but not significant difference was observed with an intermediate concentration (10 nM) (Figure 5.6B and D). In addition, the flg22-dependent ROS production seemed to start earlier in *pir20-1* when compared to WT at both concentrations (Figure 5.6A and B). No difference was detected at the lowest concentration (1 nM) (Figure 5.6C and D). The result obtained with 100 nM of flg22 was confirmed in two independent experiments, whereas the lower concentrations were not tested further.
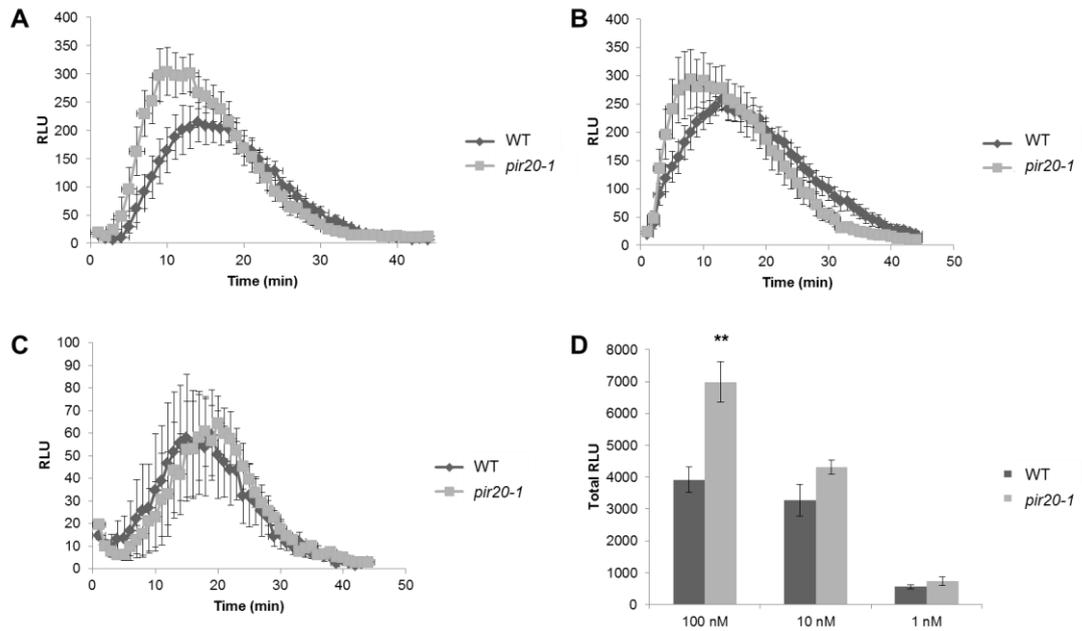
Figure 5.6. flg22-dependent ROS production in *pir20-1*.

Arabidopsis WT leaf disks were treated with flg22 100 nM (A), 10nM (B) and 1nM (C) and ROS production was quantified with a luminol-based assay and expressed as relative light units (RLU). (D) Total amount of RLU per treatment. Results are average ± SE, n=8. Asterisks indicate a statistically significant difference between WT and mutants per treatment (**p<0.01) using two-tailed unpaired t-test. The experiment was repeated twice (100 nM) with similar results.

When *pir20-1* was tested to evaluate defects in SGI, no differences were observed on the growth inhibition triggered by flg22 at any of the concentrations tested (Figure 5.7); this was consistent in two independent experiments.
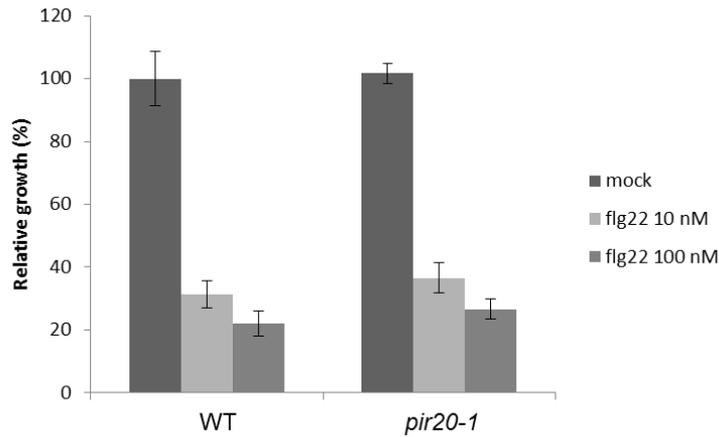
Figure 5.7. flg22-dependent SGI in *pir20-1*.

Five day-old Arabidopsis WT seedlings were transferred to a liquid media containing 0, 10 or 100 nM flg22. Weight of individual seedlings was recorded after 10 days. Results are represented as percentage of fresh weight compared to mock treatment. Bars are means ± SE, n=6. The experiment was repeated twice with similar results.

5.2.2 PIR32/CHX6B

The *pir32* mutant carries a T-DNA insertion in *CHX6B*, a cation/H$^+$ exchanger (Sze et al., 2004). Although several Arabidopsis *CHX* genes have paralogues, it does not seem the case for *CHX6B* (Figure 5.2). In *pir32-1*, the T-DNA is inserted in the last exon, close to the stop codon (Figure 5.8A). In agreement with previously published data, *PIR32*/*CHX6B* could not be amplified from cDNA from vegetative tissues, as it is mainly expressed in the male gametophyte (Sze et al., 2004). Instead, RNA was extracted from Arabidopsis inflorescences and gene expression analysis by qRT-PCR showed that the T-DNA insertion caused reduction in expression of the gene (Figure 5.8B). However, publicly available microarray data (http://bar.utoronto.ca/efp/cgi-bin/efpWeb.cgi) indicate that *PIR32*/*CHX6B* is weakly induced in leaves after four hours of flg22 treatment (Winter et al., 2007). One additional mutant allele was obtained, but no homozygous seeds were available for further tests. Furthermore, because the T-DNA insertion is at the end of the coding sequence, lines in the neighbouring gene

194

(At1g08130 - DNA ligase 1) were also obtained to rule out an effect on this gene. However, due to time constrain, these lines were not tested.
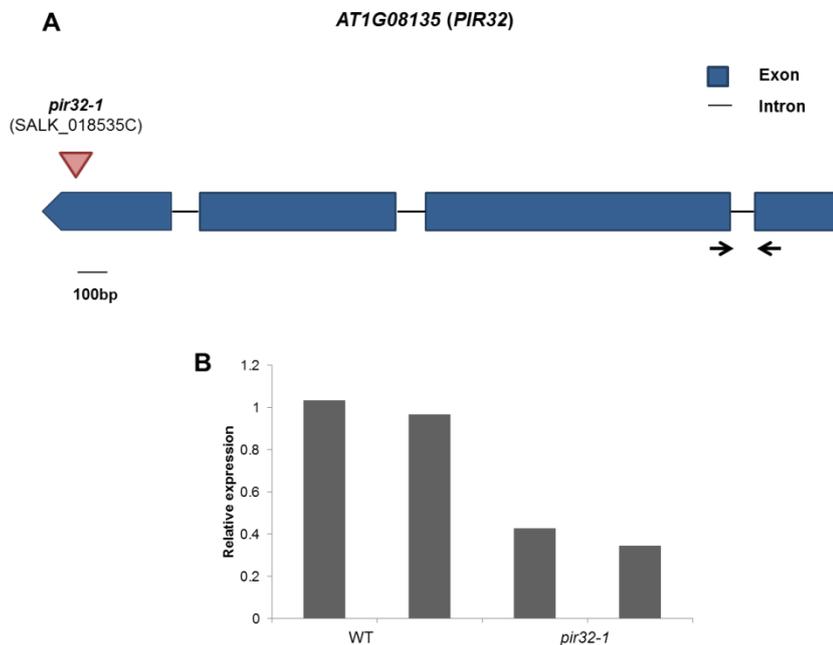
Figure 5.8. T-DNA insertion in *pir32-1* is located in the last exon and it causes reduction of *PIR32* expression.

(A) *pir32-1* carries a T-DNA insertion in the last exon. Arrows indicate the position of the primers for expression analysis. (B) Gene expression was determined by qRT-PCR using gene-specific primers. cDNA was generated from inflorescence of Arabidopsis plants. Expression values were normalized to the expression of the *UBOX* and relative expression was determined in comparison to WT. Bars represent two technical replicates per genotype.

pir32-1 was found partially impaired in flg22-induced resistance (Figure 3.17). In addition, to evaluate the impact of the mutation on the basal immunity, *pir32-1* was spray-infected with *Pto* DC3000. Results showed that *pir32-1* was more susceptible to bacteria when compared to WT in two independent experiments (Figure 5.9). This would suggest that *pir32-1* affects both basal levels of resistance and flg22-induced resistance.
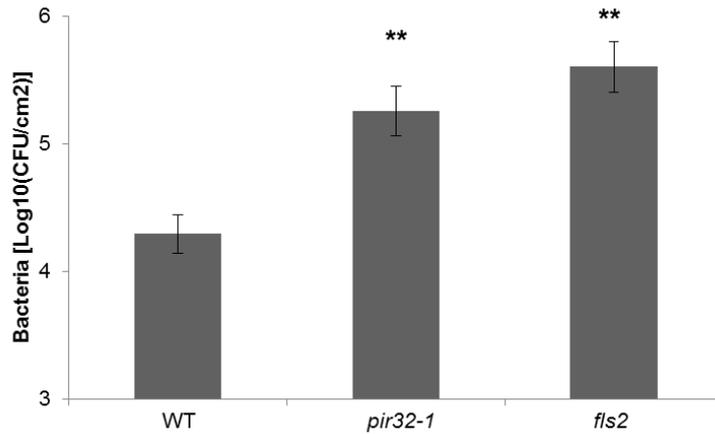
Figure 5.9. Evaluation of enhanced susceptibility to *Pto* DC3000 in *pir32-1*.

Five-weeks-old WT and mutant plants were sprayed with *Pto* DC3000 (OD_{600}=0.2). Bacterial growth was measured at 3 DPI by plating serial dilutions of homogenized leaf disks. Bars are means ± SE, n=4. Asterisks indicate significant difference (**$p < 0.01$, *** $p < 0.001$) using two-tailed unpaired t-test. The experiment was repeated twice with similar results.

To evaluate the role of PIR32/CHX6B in PTI, ROS and SGI were tested in *pir32-1*. As for *pir20-1*, a range of flg22 concentrations was used to evaluate a dose-response to the peptide. Results showed that the flg22-dependent ROS was unaffected in *pir32-1* with either concentration (Figure 5.10A to C). The only significant reduction observed, was a decrease in total ROS production when the lowest concentration (1 nM) of flg22 was used (Figure 5.10D), although the experiment has not been repeated. Moreover, at the same concentration the dynamic of ROS production seemed similar to WT (Figure 5.10C).
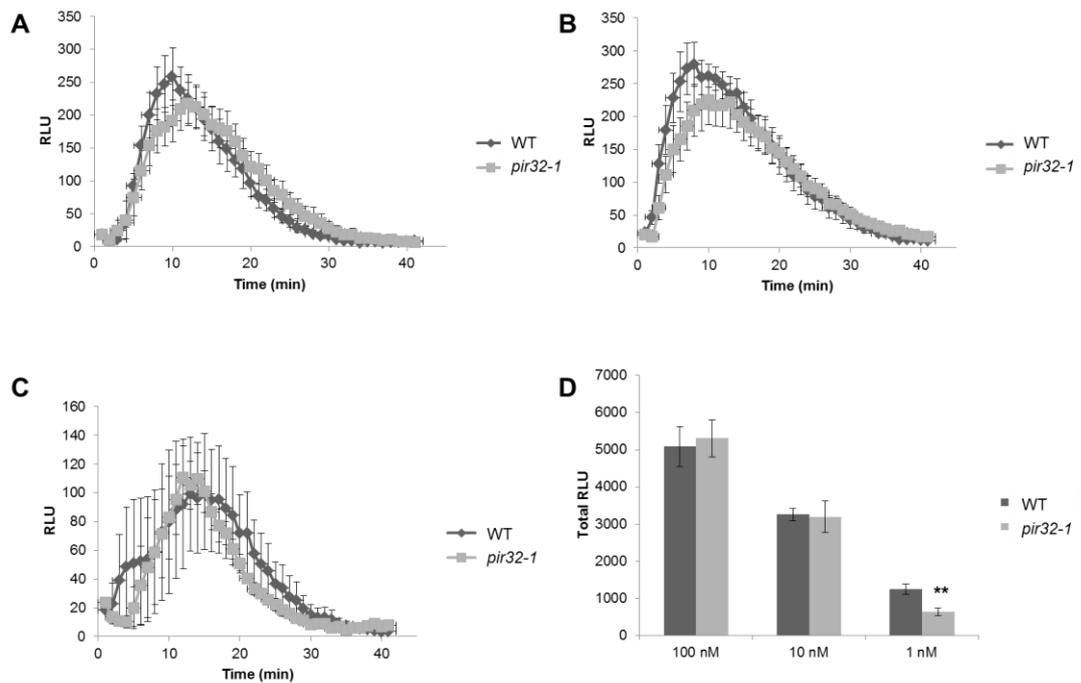
Figure 5.10. flg22-dependent ROS in *pir32-1*.

Arabidopsis WT leaf disks were treated with flg22 100 nM (A), 10 nM (B) and 1 nM (C) and ROS production was quantified with a luminol-based assay and expressed as relative light units (RLU). (D) Total amount of RLU per treatment. Results are average ± SE, n=8. Asterisks indicate a statistically significant difference between WT and mutants per treatment (**p<0.01) using two-tailed unpaired t-test. The experiment was repeated twice (100nM) with similar results.

Similarly, when *pir32-1* was tested to evaluate if the mutation leads to defects in SGI, no differences were observed with any of the concentrations of flg22 tested (Figure 5.11); this was consistent in two independent experiments.
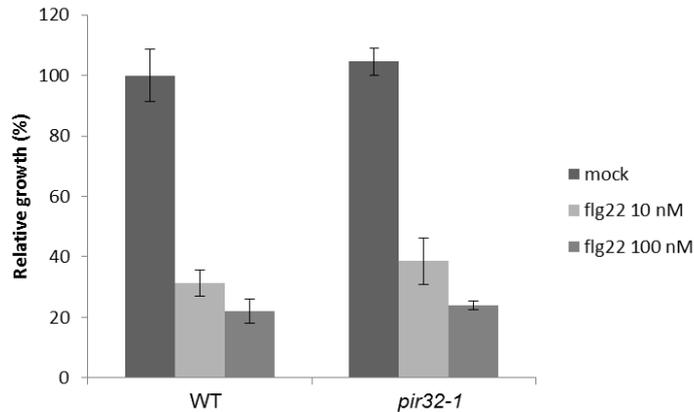
Figure 5.11. flg22-dependent SGI in *pir32-1*.

Five day-old Arabidopsis WT seedlings were transferred to a liquid media containing 0, 10 or 100nM flg22. Weight of individual seedlings was recorded after 10 days. Results are represented as percentage of fresh weight compared to mock treatment. Bars are means ± SE, n=6. The experiment was repeated twice with similar results.

5.2.3 PIR60/MVD1

The *pir60* mutant carries a T-DNA insertion in MVA diphosphate decarboxylase (*MPDC*/*MVD1*) that catalyses the last step of the MVA pathway leading to the production of IPP (Figure 5.3) (Cordier et al., 1999). MVD1 has a close homologue in Arabidopsis, MVD2 (At3g54250). Since the phenotype of the three *pir60* alleles was not very strong in adult plants (Figure 3.18), a T-DNA insertion line in *MVD2* was obtained, but no tests were carried-out due to time constraints. In addition, crosses between *mvd2* and the three *pir60* mutants were performed. Unfortunately, due to time constraint no double homozygous mutants were isolated and no tests could be performed.

Since HMGR is the key, rate-limiting enzyme in the MVA biosynthetic pathway, it was reasoned that if *pir60*/*mvd1* is defective in PTI, the same should apply for *hmgr*. Different tools were available to assess whether manipulation of HMGR activity could lead to defects in immunity.

Firstly, two transgenic lines overexpressing the short isoform of HMGR1 (HMGR1S) and its catalytic domain (HMGR1-CD) (Manzano et al., 2004) were tested for defects in flg22-induced resistance. Initial results would suggest that overexpression of *HMGR1* did not lead to any defect in this response, as bacterial levels following flg22 pre-treatment were comparable to WT (Figure 5.12). However, these two transgenic lines were in Col-glabra background and these tests were performed with Col-0 as control. Thus, further tests with the proper WT control, including spray-infection, would be needed to get a definitive result.
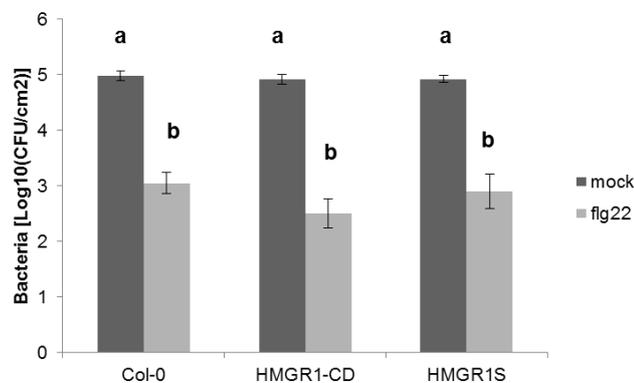
Figure 5.12. Overexpression of HMGR does not affect flg22-induced resistance.

Five-weeks-old WT and HMGR1S and HMGR-CD transgenic plants were elicited with 1 µM flg22 for 24 hours and then inoculated with *Pto* DC3000 (OD_{600}=0.0002). Bacterial growth was measured at 2 DPI by plating serial dilutions of homogenized leaf disks. Bars are means ± SE, n=6. Significantly different groups ($p < 0.0001$) are indicated with lower-case letters based on one-way ANOVA analysis and Tukey's multiple comparison post-test. The experiment was repeated twice with similar results.

Secondly, *sud1-2* was tested. This mutant harbours a mutation in *SUD1* (*SUPPRESSOR OF DRY2 DEFECTS 1*), a positive regulator of HMGR activity, which is reduced in *sud1-2* compared to WT (Doblas et al., 2013). *sud1-2* was tested to evaluate whether this mutation leads to defects in resistance to bacteria, both by flg22-induced resistance and spray-infection. Initial results indicated that amplitude of the induced resistance in *sud1-2* was comparable to that of WT (Figure 5.13A). In contrast, when *sud1-2* was

spray-infected with *Pto* DC3000, it was found more susceptible to bacteria than WT (Figure 5.13B). This result, however, needs additional replications, but, if confirmed, it would suggest that reduction of HMGR activity could lead to enhanced susceptibility to bacteria.
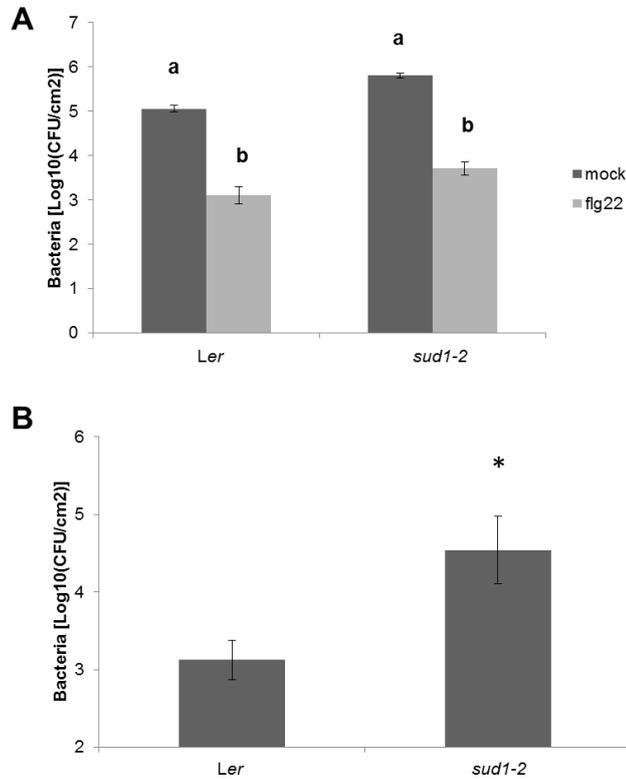
Figure 5.13. *sud1-2* is not affected in flg22-induced resistance but it is more susceptible to bacteria.

Five-weeks-old WT and *sud1-2* plants were (A) elicited with 1 µM flg22 for 24 hours and then inoculated with *Pto* DC3000 ($OD_{600}=0.0002$) or (B) spray-infected with *Pto* DC3000 ($OD_{600}=0.2$). Bacterial growth was measured at 2 (A) and 3 (B) DPI by plating serial dilutions of homogenized leaf disks. Bars are means ± SE, n=4. (A) Significantly different groups ($p < 0.0001$) are indicated with lower-case letters based on one-way ANOVA analysis and Tukey's multiple comparison post-test. Flg22-induced resistance was repeated twice with similar results. (B) Asterisk indicates significant difference (*$p < 0.05$) using two-tailed unpaired t-test.

Thirdly, a pharmacological approach was employed. Atorvastatin, a specific inhibitor of HMGR activity (Doblas et al., 2013), was used to assess whether alteration of HMGR could lead to defects in immunity. Atorvastatin was either

infiltrated in Arabidopsis leaves one day prior flg22 treatment or the mixture of atorvastatin and flg22 were co-infiltrated together. DMSO (1%) was used as control. One day after flg22/mock treatment or co-treatment with atorvastatin, plants were syringe-infiltrated with bacteria and bacterial levels were quantified two days post-inoculation. Different concentrations of atorvastatin were tested and 100 μM was found effective, opposite to 1 μM and 10 nM (data not shown). Results indicated that co-treatment with flg22 100 nM and atorvastatin 100 μM led to reduction in the induced resistance triggered by flg22 (Figure 5.14A). DMSO control and atorvastatin alone did not cause any alteration in the plant response (Figure 5.14A). When atorvastatin or DMSO were infiltrated one day prior to treatment with flg22 or mock, a minor effect of atorvastatin on the flg22-induced resistance was observed, when compared to the DMSO control (Figure 5.14B). However, this difference was not found to be significant. This result would support the hypothesis that the MVA pathway might have a role in PTI.
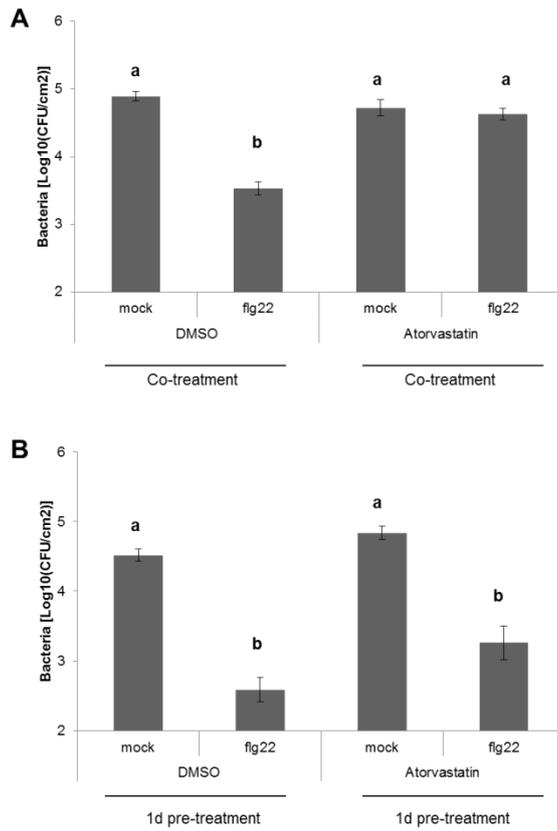
Figure 5.14. Co-treatment with flg22 and atorvastatin reduces flg22-depedent induced-resistance to *Pto* DC3000.

Five week-old plants were either co-treated with flg22 (100 nM) and atorvastatin (100 µM) or DMSO (1%) for 24 hours (A) or pre-treated with atorvastatin or DMSO one day prior elicitation with flg22 or mock (B). Plants were then inoculated with *Pto* DC3000 (OD_{600}=0.0002). Bacterial growth was measured at 2 DPI by plating serial dilutions of homogenized leaf disks. Bars are means ± SE, n=5. Significantly different groups ($p < 0.01$) are indicated with lower-case letters based on one-way ANOVA analysis and Tukey's multiple comparison post-test. The experiment was repeated twice with similar results.

5.3 Summary and discussion

The *pir* screen aimed at identifying genes with affected levels of flg22-induced resistance to bacteria. In addition to *pir38*, *pir20*, *pir32* and *pir60* were also confirmed to be impaired in this response. Interestingly, none of the genes has been previously linked to plant immunity, opening up the possibility of having discovered novel molecular components of PTI.

pir20-1 carries a T-DNA insertion in *ABCA6*, an ABC transporter that has not been characterized to date (Verrier et al., 2008). The T-DNA insertion in *pir20-1* is found in between the ABC signature motif and the Walker B sequence and, although it did not cause complete loss of gene transcript, this is likely to disrupt the functionality of the protein. Preliminary data on its phenotypic characterization showed that mutation of *PIR20*/*ABCA6* led to enhanced susceptibility to bacterial infection and higher ROS levels in response to flg22. Enhanced ROS production could be caused by altered levels of Ca^{2+}, which flg22-dependent ROS partially depends on (Nühse et al., 2007; Ogasawara et al., 2008). In fact, members of a different subfamily can regulate ion channel activity in guard cells, including Ca^{2+} channels (Suh et al., 2007). Since ABC transporters are known to transport phytochemicals (Yazaki, 2006), it would be tempting to speculate that PIR20/ABCA6 may have a role in translocation of antimicrobial compounds to the apoplast where bacteria reside. Although the localization of PIR20/ABCA6 should be first determined, tests to assess differences in metabolite content in the apoplast of *pir20*/*abca6* compared to WT following elicitor treatment should be carried out. As an additional method, a pharmacological approach could be also employed. Different inhibitors are known to block ABC transporters and these could be used to evaluate whether their application could affect PTI responses (Urbatsch et al., 1995; Sakai et al., 2002; Terasaka et al., 2003). Intriguingly, the use of one of these inhibitors, led to suppression of flavonoid movement (Buer et al., 2007). It has also been suggested that members of this subfamily may have a role in the transport of cholesterol and lipids, as observed for the human homologue ABC1 (Hamon et al., 2000; Verrier et al.,

2008), it would be interesting to assess whether the defect in immunity is linked to a defect in membrane lipid composition.

pir32-1 carries a T-DNA insertion in *CHX6B* which has been suggested to have a role in pollen development (Sze et al., 2004). Although publicly available microarray data indicate that *PIR32/CHX6B* is inducible in leaves following flg22 treatment, it would be necessary to investigate further its expression in vegetative tissues. The additional mutant available should also be tested to confirm the link between PIR32/CHX6B and PTI. In addition, since T-DNA insertion is at the very end of the gene, it should be investigated whether the T-DNA in *pir32-1* may affect the neighbouring gene (DNA ligase 1). Because mutation in *PIR32/CHX6B* led to impairment in flg22-induced resistance and enhanced susceptibility to *Pto* DC3000, PIR32/CHX6B might have a role in plant immunity. When *pir32/chx6b* was tested for defects in flg22-dependent ROS production and SGI, the results showed no differences when compared to WT. Although a more extensive characterization is needed, and its subcellular localization needs to be determined, it would be interesting to test whether this mutation could lead to altered extracellular pH following elicitor treatment. In fact PIR32/CHX6B is a cation/H^+ exchanger and elicitor treatment commonly induces K^+ efflux (Felix et al., 1999; Sze et al., 2004). Although there are no indications that PIR32/CHX6B is a K^+ exchanger, other members of the CHX family are involved in K^+ homeostasis (Pardo et al., 2006; Pittman, 2012). In addition, since several CHX proteins have been linked to endomembranes, it should be evaluated whether *pir32/chx6b* has any defect in endocytosis following elicitor perception.

The last candidate identified by the *pir* screen was *pir60-1*, which carries a T-DNA insertion in *MVD1*, a biosynthetic enzyme of the MVA pathway. Tests on its impairment in flg22-induced resistance showed only a weak effect of this mutation on the response, if compared to other *pir*s. The reason could be ascribed to the presence of a MVD1 paralogue, MVD2 (Cordier et al., 1999). Although expression of *MVD2* is lower if compared to *MVD1* (Vranová et al., 2013), it cannot be excluded that it could partially complement *mvd1*

mutation. In addition, the subcellular localization of MVD2 should also be determined and isolation and characterization of a double homozygous *mvd1 mvd2* would be required to better determine the involvement of PIR60/MVD1 in PTI. An alternative explanation for the weak phenotype in adult plants could be due to the higher expression of *MVD1* in roots compared to aerial tissues (Vranová et al., 2013). Since no further work could be done on MVD1 and MVD2 due to lack of time, it was decided to investigate the role of the MVA biosynthetic pathway in immunity by targeting HMGR both by genetics and using a HMGR inhibitor. In fact, HMGR is the key, rate-limiting enzyme of the MVA biosynthetic pathway and it is likely that its manipulation may have a stronger effect on the pathway compared to MVD1 (Hemmerlin et al., 2012; Hemmerlin, 2013). The enhanced disease susceptibility of *sud1-2* and the reduction of flg22-induced resistance by co-treatment with atorvastatin suggested that the MVA pathway has a role in plant immunity. Although one may argue that the concentration of atorvastatin used in the inhibition study (100 µM) was rather high and could have additional and unexpected effects, lovastatin, a different HMGR inhibitor, is also sometimes used at the same concentration (Alberts et al., 1980; Laule et al., 2003). Furthermore, atorvastatin alone did not cause any major effect in regard of resistance to bacteria. This should also indicate that it did not have any direct effect on the bacteria, although this was not directly tested. In addition, no intermediate concentration between 100 µM (effective) and 1 µM (ineffective) was tested. It would be also interesting to assess whether atorvastatin affects other PTI responses.

Since the characterization of these three *pir* mutants was only partial, additional elicitors and additional outputs should be measured to have a better picture of the potential role of these three proteins in PTI.

Chapter 6. General discussion and conclusions

Plants have to adapt to a constantly changing environment and are exposed to many threats, one of which is pathogen/pest attack. Despite the existence of many potential pathogens in the environment, disease is rather the exception. Although plants do not possess an adaptive immune system, they have developed a two-tier innate immune system to detect and fight invaders (Dodds and Rathjen, 2010). The first layer of defences recognizes potential pathogens at the cell surface, mostly via recognition of conserved microbial features termed PAMPs (Zipfel, 2014). This recognition triggers a downstream signalling cascade that eventually allows the plant to mount effective defences, what is known as PTI (Macho and Zipfel, 2014; Wu et al., 2014). PTI is a broad spectrum form of resistance against pathogens. Although early signalling events start to be uncovered, the knowledge on the molecular events downstream of PAMP perception at receptor complexes is still rather limited. Moreover, the exact mechanism that restricts pathogen growth after PAMP perception is still unknown.

To broaden the understanding of the mechanisms by which PTI confers induced resistance to bacteria, two different approaches were employed. A biased approach used reverse genetics to evaluate the involvement of three secondary metabolites, camalexin, glucosinolates and callose, in PTI. In fact, these are well known active defences Arabidopsis employs against fungi and oomycetes (Bednarek, 2012b), making them good candidates as antibacterial defences. However, mutants affected in the biosynthesis of these compounds were not affected in flg22-induced resistance against *Pto* DC3000, suggesting that camalexin, glucosinoates and callose are dispensable for induced antibacterial immunity to this bacterium. This would also indicate that active antibacterial defences in Arabidopsis are different from those employed against filamentous pathogens. In order to identify components required for the PAMP-triggered induced resistance to bacterial growth, a second unbiased approach was employed. For this purpose, a novel genetic screen was designed and performed with the aim of identifying Arabidopsis mutants impaired in the resistance induced by the flg22 epitope

of flagellin to *Pto* DC3000. In fact, mutations of known molecular components of PTI also cause impairment of anti-bacterial resistance, in addition to signalling defects. Therefore this approach would help in identifying signalling components and/or "executors" of PAMP-triggered-induced resistance. The screen was carried out on the T-DNA uni-mutant collection (Alonso et al., 2003; O'Malley and Ecker, 2010). After a qualitative primary screen and a quantitative secondary screen, 108 *pir* mutants were identified, including a novel allele of *fls2*, which supported the validity of the screen. Additional mutant alleles were obtained for each *pir*, in order to confirm that the impairment in induced resistance was linked to the disruption of a given gene. However, further confirmation was proven challenging. In fact, genotyping and testing alleles for each of the 108 *pir*s was laborious and time-consuming, and delayed this confirmation step. Moreover, the variability of the results also affected the validation of the phenotypes. In fact, pathogenicity assays are prone to variability, and in a genetic screen like the *pir* screen, where the differences sought are intermediate between resistance and susceptibility, the resolution provided by the experimental settings was not enough to identify candidates in an unequivocal manner. However, despite the difficulties, four mutants with reproducible compromised immunity were identified. Because the genes affected by the mutations have not been linked to immunity so far, this opens the possibility of having identified novel components of PAMP-triggered-induced resistance.

pir38 carries a T-DNA insertion in UGT78D1, a rhanmosyltransferase involved in glycosylation of flavonols (Jones et al., 2003). The T-DNA insertion induced overexpression of *UGT78D1*. However, the compromised resistance phenotype of *pir38-1* was not stable, likely due to the presence of a second insertion. Therefore, the use of transgenic lines overexpressing *UGT78D1* was employed to confirm the loss of flg22-induced resistance. Unfortunately, despite several attempts, no transgenics yielded an overexpression of the gene higher than 3 fold. This possibly indicates that *UGT78D1* expression is under tight regulation and therefore not prone to be

manipulated. However, the literature presents various reports that link flavonoids to plant immunity (Dixon, 2001; Treutter, 2006). Therefore, a comprehensive set of flavonoid biosynthetic mutants was tested for impairment of resistance to *Pto* DC3000. In fact, if any of the flavonoids contributes to antibacterial immunity, mutations upstream the key component should lead to enhanced susceptibility, or enhanced resistance, if placed downstream. This is, however, a simplistic view of the pathway that does not take into consideration feedback regulations or bi-functional enzymes. Although flg22-induced resistance was not informative, surface-inoculation with *Pto* DC3000 showed that mutants downstream of flavonol aglycones, i.e. *ugt78d2-2* and *ugt78d3*, were significantly more resistant than WT to bacterial infection. In addition, mutants upstream of flavonol aglycones (*tt4*, *tt6* and *tt7*) showed consistent enhanced susceptibility, although with no statistical significance, due to the high variability of the results. This highlights once more the difficulty of using pathogenicity assays to determine the role of candidate genes in immunity when the phenotype is subtle. To corroborate these results, exogenous application of quercetin was used. In fact, it was previously shown that exogenous application of quercetin induces resistance to *Pto* DC3000 (Jia et al., 2010). Because there are conflicting results on the direct activity of quercetin on bacteria (Jia et al., 2010; Vandeputte et al., 2011; Vargas et al., 2011), this effect was tested. It was observed that quercetin may exert a bacteriostatic effect, as bacterial growth in presence of quercetin was only reduced at early time points. However, using an antibiosis assay, only application of high concentrations of quercetin to low bacterial density induced a very subtle growth inhibition. This, however, may be due to the non-optimal diffusion of quercetin in the media. Although this would suggest that quercetin may have a direct effect on bacteria, it cannot be excluded that it could have a role inside the plant cells in inducing immunity. Therefore it was investigated whether quercetin can induce classical PAMP responses and what effect, if any, may have towards flg22-triggered responses. Quercetin induced accumulation of ROS and, at the same time, is also able to quench the flg22-dependent ROS. Although surprising, as other

antioxidant compounds, quercetin can act both as anti-oxidant and pro-oxidant (Laughton et al., 1989; Bors et al., 1995; Cao et al., 1997; Metodiewa et al., 1999; Sakihama et al., 2002). Interestingly, quercetin reduced PAMP-triggered SGI. Although the exact mechanism that leads to SGI is not known, it would be possible to speculate that part of it could be due to ROS. In fact, preliminary data also showed that the *rbohd* mutant, which is impaired in PAMP-dependent apoplastic ROS production (Nühse et al., 2007; Zhang et al., 2007), is less inhibited in growth upon PAMP treatment. However, it must be considered that *rbohd* shows higher *PR-1* expression upon bacterial challenge (Kadota et al., 2014), which could also be responsible for the reduced PAMP-triggered SGI. Moreover, it was observed that upon flg22 elicitation, glycosylated flavonol levels are reduced in the leaf tissue. Glycosylated flavonols are the storage form of flavonoids, as their aglycones are toxic for the plant cells (Dixon and Pasinetti, 2010; Petrussa et al., 2013). Although preliminary, this could indicate that perception of PAMPs induces release of glycosylated flavonols from their storage site. Because of the effect of quercetin on flg22-dependent ROS and SGI, it could be speculated that reduction in flavonoids is the consequence of their activity in buffering the oxidative stress triggered by PAMP perception. In addition, or alternatively, quercetin may be released in the extracellular space to inhibit bacteria, consistent with its bacteriostatic activity. In fact, quercetin-dependent inhibition of *Pto* DC3000 growth is visible up to 6 hours, which is the same time-frame where flavonol levels are reduced in the leaves. However, assessing whether quercetin and/or other flavonols are released in the extracellular space is a requisite to test the validity of a direct bacteriostatic effect of quercetin/flavonols towards *Pto* DC3000. Preliminary results indicated that quercetin induced expression of the PTI marker genes *NHL10*, *PR1* and *CYP81F2* within the same time-frame (6 hours post-elicitation), although additional tests need to be carried out in order to substantiate this observation. It must be considered that all these observations have been made through exogenous application of quercetin, and a genetic proof would be needed to understand the biological

significance of flavonoids in plant immunity. However, it must be always considered that manipulation of this biosynthetic pathway may lead to unexpected outcomes, as regulatory mechanisms may compensate for the lack of one enzyme.

Additional genes isolated during the *pir* screen were *ABCA6*/*PIR20*, *CHX6B* /*PIR32*, and *MVD1*/*PIR60*. Preliminary characterization indicated that *pir32* and *pir20* mutants were more susceptible to bacterial infection and that *pir20* showed higher flg22-triggered ROS. Although promising, a deeper phenotypic characterization would be required to assess the role of these genes in immunity. *pir60* was the only mutant tested with two additional alleles, and the three mutants showed weak loss of induced resistance to bacteria. A double mutant with its close homolog was generated but has not been tested yet. Therefore, to determine the involvement of *PIR60* in immunity, it was decided to target a different component of the pathway, HMGR1, since it is the key, rate-limiting enzyme of the MVA biosynthetic pathway (Hemmerlin et al., 2012; Hemmerlin, 2013). In fact, if the phenotype of *pir60* is true, manipulation of HMGR1 should have a similar and possibly stronger effect on PTI. In fact, mutation in *SUD1*, a positive regulator of HMGR1 activity (Doblas et al., 2013), showed enhanced susceptibility to bacteria. In addition, chemical inhibition of HMGR1 by application of atorvastatin affected flg22-induced resistance. Taken together, these would indicate that the MVA pathway could play a role in PTI. However it still needs to be assessed whether atorvastatin alone could affect, for example, FLS2 levels or interfere with other PTI outputs. Notably, it has been previously shown that HMGR1 interacts with SYMRK, DMI2 and NORK, which are receptor kinases involved in legume symbiosis (Kevei et al., 2007; Oldroyd, 2013). It would therefore be interesting to test whether it can also interact with PRRs.

The focus of this PhD project was to gain insights into the mechanism through which PAMP-induced resistance leads to restriction of bacterial pathogens. When a plant cell perceives PAMPs via plasma membrane

localized receptors, a series of physiological and biochemical changes happen within seconds from perception (Boller and Felix, 2009; Nicaise et al., 2009; Wu et al., 2014). These responses include production of ROS, activation of MAPKs, changes in protein phosphorylation status, altered ion fluxes, hormones biosynthesis, deposition of callose, induction of defence-related genes, production of phytoalexins and stomatal closure. Although some of these changes are rapidly triggered and return to basal levels within few hours (i.e. ion fluxes, production of ROS, activation of MAPKs), some other responses develop at later times (i.e. callose deposits, biosynthesis, of hormones and phytolexins) (Boller and Felix, 2009). However, to date, there is no data available regarding the physiological and biochemical status of Arabidopsis plants at 24 hours after flg22 treatment. Nonetheless, it would not be trivial to assume that all the changes happening following PAMP perception would ultimately contribute towards making the plant "ready to fight", with the arsenal of defences already set for a potential pathogen attack. For example, extracellular alkalinisation and generation of ROS could make the apoplastic environment unhospitable for pathogens (Nürnberger et al., 1994; Jabs et al., 1997; Felix et al., 1999; O'Brien et al., 2012). In addition, the cell wall reinforcements in the form of papillae and the deposition of lignin could make the plant cell less accessible (Xin and He, 2013; Delaunois et al., 2014; Malinovsky et al., 2014b). Interestingly, apoplastic ROS is also involved in cross-linking of proteins and phenolics in papillae, which are also the sites where antimicrobials accumulate (Lamb and Dixon, 1997; Mitchell et al., 2014; Voigt, 2014). Therefore even a short-term event like ROS production could still contribute to more long-term responses. In addition, PAMP-induced resistance also triggers hormone biosynthesis, which would contribute to late defence responses (Tsuda et al., 2009; Robert-Seilaniantz et al., 2011). Therefore it seems clear that the mechanism through which PAMP perception leads to robust immunity is a complex situation, which involves several lines of defence, which, all together, contribute to the induced resistance.

In conclusion, two of the genes isolated during the *pir* screen are enzymes of the secondary metabolism, suggesting that secondary metabolites could have a role in PTI. Secondary metabolites are widely known for their antimicrobial properties against animal pathogens (Savoia, 2012; Radulovic et al., 2013; Taylor, 2013), and therefore one could speculate they may exert similar roles in plants. Plant secondary metabolites exert multiple functions within a plant, including contributing to plant defence (Dixon, 2001; Field et al., 2006; Piasecka et al., 2015). However, the chemical diversity that arises from evolutions of secondary metabolite biosynthetic pathways warns from making generalizations (Kliebenstein and Osbourn, 2012). In fact, compounds like avenacin, 3-deoxyanthocyanidins, and glucosinolates can be found in a very limited number of species, namely oat, sorghum, and Cruciferae, respectively, and contribute to specialized defence responses in those species only (Bednarek and Osbourn, 2009; Piasecka et al., 2015). For example, 3-deoxyanthocyanidins are only found in sorghum, where they provide resistance to *Colletotrichum sublineolum* (Ibraheem et al., 2010). Therefore such compounds are likely to have evolved in response to a specific threat and are not likely to play a more widespread role in plant immunity. However, other secondary metabolites with wider distribution among plant species, like flavonoids and other phenylproanoids, have the potential of being players in plant innate immunity (Ferrer et al., 2008; Fraser and Chapple, 2011). In fact, flavonoids have appeared very early in the evolution of land plants, where they played a key role in the adaptation of plants from aquatic to terrestrial environment, and possibly also contributed to plant defence (Mouradov and Spangenberg, 2014). Lignin, which also evolved during the emergence of land plants to provide structural support, is deposited at the cell wall in response to many different biotic stresses (Vanholme et al., 2010; Sattler and Funnell-Harris, 2013; Malinovsky et al., 2014b). This would support the idea that secondary metabolites with widespread distribution among plant species can have a role in plant innate immunity. Moreover, because transporters are often associated with translocation of secondary metabolites, the identification of *PIR20/ABCA6*

213

and *PIR32/CHX6B* could be in line with this idea. Future work on assessing the role of these transporters in PTI, and better understanding on the role of flavonoids and MVA biosynthetic pathway in plant immunity, will help shed light on the role of these secondary metabolites in PTI. Although the time did not allow a thorough investigation, I hope this initial data will help develop further work to unravel the long-lasting quest for the mechanism of PAMP-induced resistance.

Appendix 1. Arabidopsis mutant and transgenic lines.

Line	SALK #	AGI	Description	Reference
Col-0			Columbia 0, WT	
L*er*			Landsberg *erecta*, WT	
No			Nossen, WT	
fls2c	SAIL_691_C4	At5g20480	T-DNA insertion	Zipfel et al., 2004
fls2-17		At5g20480	EMS	Gómez-Gómez and Boller, 2000
efr-1	SALK_044334	At5g46330	T-DNA insertion	Zipfel et al., 2006
fls2 efr	SAIL_691_C4 SALK_044334	At5g20480 At5g46330	Double T-DNA insertion mutant	Nekrasov et al., 2009
fls2 efr cerk1	SAIL_691_C4 SALK_044334 GABI_096F09	At5g20480 At5g46330 At3g21630	Triple T-DNA insertion mutant	Gimenez-Ibanez et al., 2009b
bak1-4	SALK_116202	At4g33430	T-DNA insertion	Chinchilla et al., 2007
bik1 pbl1	SALK_107225 SAIL_1236_D07	At2g39660 At3g55450	Double T-DNA insertion mutant	Zhang et al., 2010
cyp79b2 cyp89b3	SALK_130570 SAIL_56_E07	At4g39950 At2g22330	Double T-DNA insertion mutant	Zhao et al., 2002
myb28/29	SALK_136312 GABI_868E02	At5g61420 At5g07690	Double T-DNA insertion mutant	Sønderby et al., 2007
cyp79b2/b3 myb28/29	SALK_130570 SAIL_56_E07 SALK_136312 GABI_868E02	At4g39950 At2g22330 At5g61420 At5g07690	Quadruple T-DNA insertion mutant	(Sun et al., 2009)
pad3-1		At3g26830	EMS	Glazebrook and Ausubel, 1994
pmr4-1		At4g03550	EMS	Vogel and Somerville, 2000
pmr4-1 sid2-1		At4g03550 At1g74710	EMS Double mutant	Nishimura et al., 2003
sid2-1		At1g74710	EMS	Wildermuth et al., 2001
rbohD		At5g47910	*dSpm* transposon insertion	Torres et al., 2002
ugt73c6	SAIL_525_H07	At2g36790	T-DNA insertion	Yonekura-Sakakibara et al., 2007

ugt89c1-2	SALK_071113C	At1g06000	T-DNA insertion	Jones et al., 2003
ugt78d1	SAIL_568_F08	At1g30530	T-DNA insertion	Jones et al., 2003
ugt78d2-1	SALK_049338	At5g17050	T-DNA insertion	Tohge et al., 2005
ugt78d2-2	SALK_205599C	At5g17050	T-DNA insertion	This study
ugt78d3	SALK_114099C	At5g17030	T-DNA insertion	Yonekura-Sakakibara et al., 2008
tt6-3	SALK_113904C	At3g51240	T-DNA insertion	Owens et al., 2008
tt6-5	SALK_113321C	At3g51240	T-DNA insertion	This study
tt7-6	SALK_124157C	At5g07990	T-DNA insertion	This study
mvd2-1	GABI_382H01	At3g54250	T-DNA insertion	This study
tt10-7	SALK_128292C	At5g48100	T-DNA insertion	Liang et al., 2006
tt5		At3g55120	EMS	Koornneef, 1990
tt3		At5g42800	x-irradiation	Shirley et al., 1992
tt4-13	SALK_020583	At5g13930	T-DNA insertion	Buer et al., 2006
fls1-2	RIKEN_PST16145	At5g08640	T-DNA insertion	Stracke et al., 2009
omt1	SALK_135290	At5g54160	T-DNA insertion	Yonekura-Sakakibara et al., 2008
ugt78d1 ugt78d2-1	SAIL_568_F08 SALK_205599C	At1g30530/ At5g17050	Double T-DNA insertion mutant	Yin et al., 2012
sud1		At4g34100	EMS	Doblas et al., 2013
60-2	SAIL_387_F03	At2g38700	T-DNA insertion	This study
60-3	SALK_083793C	At2g38700	T-DNA insertion	This study
pBIB35S: HMGR1S		At1g76490	HMGR1 catalitic domain overexpression line	Manzano et al., 2004
pBIB35S: HMGR1-CD		At1g76490	HMGR1 overexpression line	Manzano et al., 2004
pAlligator2: UGT78D1		At1g30530	UGT78D1 overexpression line, no tag	Yin et al., 2012
pK2GW7: UGT78D2		At5g17050	UGT78D2 overexpression line, no tag	Yin et al., 2012
pGWB2: UGT78D1		At1g30530	UGT78D1 overexpression line, no tag	This study (M. Smoker, TSL)
pGWB2: UGT78D2		At5g17050	UGT78D2 overexpression line, no tag	This study (M. Smoker, TSL)
pLIC: UGT78D1		At1g30530	UGT78D1 overexpression line, TAP tag	This study (J. Monaghan, M. Smoker, TSL)

Appendix 2. Primers used in this study.

Primer name	Sequence	AGI	Mutant
LM_009-SALK_136312-LP	TTTTTCATTATGCGTTTGCAG	At5g61420	*myb28*
LM_010-SALK_136312-RP	CTCTTTCCACACCGTTTCAAC	At5g61420	*myb28*
LM_017-pmr4-1_N3858-NheI-F	TTACCAGCCCAACCAATTTC	At4g03550	*pmr4*
LM_018-pmr4-1_N3858-NheI-R	AGATCAGGGACATGGGACAG	At4g03550	*pmr4*
LM_025-cyp79B2-R	TGGACAAGTATCATGACCCAATCATCCACG	At4g39950	*cyp79b2*
LM_026-cyp79B3-R	TGTTCTATGCATGGACTGGTGGTCAACATG	At2g22330	*cyp79b3*
LM_038-SALK_020583C-LP	TCGAATAGACCTGTCCAGCAC	At5g13930	*tt4-13*
LM_039-SALK_020583C-RP	CTTCTCTGGACACCAGACAGG	At5g13930	*tt4-13*
LM_234-SALK_070074C-LP	CGCAACTATTTTTGATGCATG	At4g13965	*pir1*
LM_235-SALK_070074C-RP	AAGAATTTTGTGCGTTGATGG	At4g13965	
LM_321-SALK_128309C-LP	AAACCGTCGTTTGCTTGTATG	At5g65970	*pir6*
LM_322-SALK_128309C-RP	AACACCAAAAGCATCTTGTGG	At5g65970	
LM_347-SALK_089110C-LP	GACGATCGAAGAGAGTTCACG	At3g05545	*pir25*
LM_348-SALK_089110C-RP	ACGACAACCGTTTGCATAAAG	At3g05545	
LM_351-SALK_107900C-LP	TACGTGCTAATTAACACGGGG	At1g69560	*pir8*
LM_352-SALK_107900C-RP	ATGGATCAGACCACTTCATCG	At1g69560	
LM_355-SALK_037779C-LP	CCTTTTTCCCTTTTTAATGCG	At3g18650	*pir12*
LM_356-SALK_037779C-RP	GGGCAGAGGAGGGTACAGTAC	At3g18650	
LM_359-SALK_061729C-LP	TGAATCGGAACTTGAAAATGG	At1g31140/ At1g31150	*pir14*
LM_360-SALK_061729C-RP	AGGATCAGTGTTCAGATTGCG	At1g31140/ At1g31150	
LM_361-SALK_063824C-LP	TCCCATAAAAAGAAAAAGAAAAATG	At3g21230	*pir15*
LM_362-SALK_063824C-RP	TTTGATCAGTTCCTTCAACCG	At3g21230	
LM_363-SALK_009815C-LP	CAAAACGTGAACCTTGATTGG	At1g16980	*pir16*
LM_364-SALK_009815C-RP	TGGTTGAAAATTCTTGTTCCAG	At1g16980	
LM_397-SALK_087652C-LP	TGGCATTACTGAATCCAGGAG	At1g55930	*pir46*
LM_398-SALK_087652C-RP	AGAGCCACTTACCAACACTGC	At1g55930	
LM_403-SALK_086181C-LP	TTCTTCCATCCCTTGTGACAC	At3g45755	*pir10*
LM_404-SALK_086181C-RP	GGATATTTGATAAGGCTCCGC	At3g45755	
LM_411-SALK_049092Ca-LP	AGTCCCCCAATAGGTGCTATG	At3g01760	*pir24a*
LM_412-SALK_049092Ca-	TGGTAGCTGCTGTCATGTCTG	At3g01760	

RP			
LM_413-SALK_049092Cb-LP	AGAAAGATTTAGAGCCAGGCG	At1g62090	*pir24b*
LM_414-SALK_049092Cb-RP	CATGGACGTCATCAGGATACC	At1g62090	
LM_417-SALK_062847Ca-LP	CCTCAAGCAAGCGTTTGTTAC	At4g11100	*pir27a*
LM_418-SALK_062847Ca-RP	AAGCGGATATCCGCAAATATC	At4g11100	
LM_419-SALK_062847Cb-LP	AGAGTCAAACAACACATGGGC	At3g30802	*pir27b*
LM_420-SALK_062847Cb-RP	AGTTTTTGGAGCGGTTACCAG	At3g30802	
LM_421-SALK_138650C-LP	ACTTGAAGATGGGAGCCGTAC	At2g36480	*pir36*
LM_422-SALK_138650C-RP	TTACTGATGTCCCAGAGACCG	At2g36480	
LM_427-SALK_048972C-LP	ACGTGAAAAGAATGCATGAC	At1g30530	*pir38-1*
LM_428-SALK_048972C-RP	GAAAGAAAAGATGGTGGAGGG	At1g30530	
LM_429-SAIL_89_B04-LP	CGTTGTCAAATTCCAATTCTTG	At1g30530	*pir38-2*
LM_430-SAIL_89_B04-RP	TTGGACTCTGTTTTCCCAAAG	At1g30530	
LM_431-SALK_056086C-LP	TGATGAGGATTGGCTGATACC	At5g16650	*pir39*
LM_432-SALK_056086C-RP	CAAATGCCCATTTGATTTTTG	At5g16650	
LM_443-SALK_090688C-LP	GACGTTGCTTCAACTCCTGAC	At1g72410	*pir45*
LM_444-SALK_090688C-RP	ATTGTGATTCTTGACCGATCG	At1g72410	
LM_445-SALK_061515C-LP	CTTTAGTGACCAAGGCAGTCG	At1g55930	*pir46-2*
LM_446-SALK_061515C-RP	ATTAAACCGGTCTGGTATGGC	At1g55930	
LM_447-SAIL_1164_B06-LP	AACATATGGTTCACTGGCACC	At1g55930	*pir46-3*
LM_448-SAIL_1164_B06-RP	GGCCAAAAACTTCTCAGGTTC	At1g55930	
LM_449-SALK_074806C-LP	TTCCTCACCATGAAATAACGC	At1g05830	*pir47*
LM_450-SALK_074806C-RP	TTCATGGTTTTGGGATCTTTG	At1g05830	
LM_451-SALK_054063C-LP	CGATTCACTGGAAAAATCACG	At4g16490	*pir50*
LM_452-SALK_054063C-RP	GAAACTCCGACGCATACTCTG	At4g16490	
LM_453-SALK_046567Ca-LP	CTCTTCTTCGAACGTCGTGTC	At3g25730	*pir21a*
LM_454-SALK_046567Ca-RP	TATCTTATGGTCCACTTGCCG	At3g25730	
LM_455-SALK_046567Cb-LP	GTCAGCTCTTGCCATTTGAAG	At1g78860	*pir21b*
LM_456-SALK_046567Cb-RP	CAACAATTTGTCACCCCAAAG	At1g78860	
LM_467-SALK_143098C-LP	TCCCATTCCTACAAGCACAAC	At1g04510	*pir73*
LM_468-SALK_143098C-RP	TCAAGGTCTCGTTAAAAGGCC	At1g04510	
LM_491-SALK_139843C-LP	TGACCCTGGTTAGGGTTTCTC	At3g42790	*pir44*

LM_492-SALK_139843C-RP	TGGAACCACTTCTCACAAAGG	At3g42790	
LM_495-SALK_106920C-LP	TTTTGCAAAACCTCCACATTC	At1g49860	pir33
LM_496-SALK_106920C-RP	TTCTAAGGGCTTCAGACCACC	At1g49860	
LM_503-SALK_125391C-LP	TACCATTGATCTGTCTTCGGG	At1g71080 At1g71090	pir43
LM_504-SALK_125391C-RP	CTGGAGAAACCTGACATCTCG	At1g71080/ At1g71090	
LM_507-SALK_061320C-LP	AAAGGAGCCAACCTTGAGAAG	At5g58100	pir53
LM_508-SALK_061320C-RP	AAAGAAGCCTTTCCTTGATGC	At5g58100	
LM_511-SALK_072862Ca-LP	CTAAAGATTTGTTAAACTTGCCAC	At2g27080	pir54a
LM_512-SALK_072862Ca-RP	TCAAGTGCAGCATGTTTTGTC	At2g27080	
LM_513-SALK_072862Cb-LP	AGGAGCAATTTGAACTCCCTC	Chr3 2094491	pir54b
LM_514-SALK_072862Cb-RP	TTGGAAACCTGGATTGTTGAC	Chr3 2094491	
LM_517-SALK_062938C-LP	ACAGTGTGACCAAATTCGAGG	At5g29028	pir117
LM_518-SALK_062938C-RP	GTTCTTGGAGGACGTTTAGGG	At5g29028	
LM_529-SALK_099012C-LP	TCCATTTCGAAACGCTATGTC	At5g62560	pir19
LM_530-SALK_099012C-RP	CTGGGAGGAATAAGCAAAACC	At5g62560	
LM_531-SALK_140348C-LP	AACGAGGAAGAAGAAGCAAGG	At1g73450	pir28
LM_532-SALK_140348C-RP	GATAAACCCAAAGAAGCGTCC	At1g73450	
LM_547-SALK_039347Ca-LP	GTAAGGCACGTGGAAAATTTG	At3g61690	pir18b
LM_548-SALK_039347Ca-RP	AGCGCTAAAAGCCGTTAAGTC	At3g61690	
LM_549-SALK_039347Cb-LP	GTTTCAAGGAAATCTCGAGGG	At1g06925	pir18a
LM_550-SALK_039347Cb-RP	TCCGGGTTTGCTCAACTATAC	At1g06925	
LM_563-SALK_098044C-LP	TGTAAACTGAGTGCAGCATGG	At4g18490	pir51
LM_564-SALK_098044C-RP	GCTAAATTCTGGTTGCACTGC	At4g18490	
LM_571-SALK_030145C-LP	TAGTGCAGAACACACGGTGAC	At2g16700	pir57
LM_572-SALK_030145C-RP	ATATCGAAACCCATCTCCGTC	At2g16700	
LM_575-SALK_094830C-LP	CAGAAGGCTGACTCATTTTCG	At3g18140/ At3g18145	pir59
LM_576-SALK_094830C-RP	AGCATTGTATGAGCTCCATGG	At3g18140/ At3g18145	
LM_579-SALK_013999C-LP	CGTAGGCGAATCAATCTAACG	At2g38700	pir60-1
LM_580-SALK_013999C-RP	GACTTCGAATTTCCCTCAAGC	At2g38700	
LM_581-SAIL_387_F03-LP	GCAAAGCAAAAGATGAAGCTG	At2g38700	pir60-2
LM_582-SAIL_387_F03-RP	TTCCATCATAGCCTGCAAAAG	At2g38700	
LM_583-SALK_083793C-LP	AATTGTTTTGGTTGTGCTTGC	At2g38700	pir60-3

LM_584-SALK_083793C-RP	CCCGATGCAGAAGAATTGTAC	At2g38700	
LM_585-SALK_055351C-LP	CAATCTCTCGGGAAGTCTTCC	At5g01890	*pir66*
LM_586-SALK_055351C-RP	CCTTCTCTCACCGTCTCACAC	At5g01890	
LM_591-SALK_052748C-LP	TTCAAGATGTCCAAAGGCATC	At2g41700	*pir68*
LM_592-SALK_052748C-RP	TTCAGGTATGGATCCTGTTGC	At2g41700	
LM_595-SALK_140384C-LP	TTAATGGGTAGGTCCATGCAG	At5g49630	*pir84*
LM_596-SALK_140384C-RP	TTAAGGCTGGACAACAAATGC	At5g49630	
LM_599-SALK_037715C -LP	ATTGTATCTGGTTCGCAGTGG	At5g18230	*pir94*
LM_600-SALK_037715C -RP	GAATCCAAAAACTGAGGCTCC	At5g18230	
LM_603-SALK_030374C -LP	TTCATAGAATAGTTCCGCATGG	At2g18380	*pir96*
LM_604-SALK_030374C -RP	TCTTGGTTGATGTCAGTGTGG	At2g18380	
LM_607-SALK_027726C-LP	ATGGTGTGCGAATCTATGACC	At5g64610	*pir99*
LM_608-SALK_027726C-RP	ACGGAGAGGAAAGCTCAAGAC	At5g64610	
LM_611-SALK_125815C-LP	AGACCTCGTTCATCAACATGG	At3g47770	*pir20*
LM_612-SALK_125815C-RP	AAATTCGAACCTCCTCCTTTG	At3g47770	
LM_623-SALK_009133C-LP	CTTTCACGTTCAGATTCTCGC	At1g55290	*pir91*
LM_624-SALK_009133C-RP	TTCAAACAAAACAACCCGAAG	At1g55290	
LM_633-SALK_026829C-LP	ACATCTCCGACCAAGACATTG	At2g30220	*pir80*
LM_634-SALK_026829C-RP	TTTTAATTGGGAGGAAGCAGG	At2g30220	
LM_647-SALK_035543C-LP	CGATGCTCATCTTGTACGATG	At4g13110	*pir88*
LM_648-SALK_035543C-RP	CCTACCGATTCGAGAGATTCC	At4g13110	
LM_661-SALK_026036C-LP	CTGGTCTTCGCTCTATGATGG	At5g03540	*pir86*
LM_662-SALK_026036C-RP	AGAGTTCTTACAGCAATGCGC	At5g03540	
LM_665-SALK_138456C-LP	AAGGACTAGCCCAACCTTCAC	At1g19930	*pir74*
LM_666-SALK_138456C-RP	GACTTGACCTGTGCAAAGGAG	At1g19930	
LM_681-SALK_060611C -LP	TGATTGGTGGTTTTAGTTGGG	At1g05135	*pir87*
LM_682-SALK_060611C -RP	CTATACCGCCACCACTTCCTC	At1g05135	
LM_685-SALK_057621Ca-LP	ATTTTCCTGAGCGAAGCTTTC	At4g03390	*pir118a*
LM_686-SALK_057621Ca-RP	TTCTTCAAGGCCTTCCTCTTC	At4g03390	
LM_687-SALK_057621Cb-LP	CAGATATCCGTTTGCTTTTCG	Chr2 894894	*pir118b*
LM_688-SALK_057621Cb-RP	GATAAAAAGGATTTTTCTACTC	Chr2 894894	
LM_689-SALK_057621Cc-LP	AGTCACGGACGAAGCTAACAG	Chr5 24741454	*pir118c*

LM_690-SALK_057621Cc-RP	AATTTCACAGCTTATCATCCCC	Chr5 24741454	
LM_693-SALK_116446C-LP	TGATCGGTCCAATTTGCTATC	At4g12570	pir100
LM_694-SALK_116446C-RP	ACTTGCTCCAAGATTGGTGTG	At4g12570	
LM_707-SALK_053005C-LP	GCAAAATTTGTTGAGTCCGTG	At2g03410	pir29
LM_708-SALK_053005C-RP	CAGGCTCAGCTTCACCATTAC	At2g03410	
LM_715-SALK_093949C-LP	GTTGGGATGATGATGATGGAG	At5g56250	pir49
LM_716-SALK_093949C-RP	TTAAAACAAAAGTGGGGGTCC	At5g56250	
LM_719-SALK_015817C-LP	AGAGACTTCCAAAAGCAAGGC	At5g25470	pir23
LM_720-SALK_015817C-RP	CCTCTTGAATCCTGAAAACCC	At5g25470	
LM_729-SALK_046603C-LP	CGATAAGAACCCGTAGGGAAG	At3g56600	pir71
LM_730-SALK_046603C-RP	TCTCCGAGTATCATCAATCCG	At3g56600	
LM_733-SALK_062717C-LP	CCGATGACTTTGCGACTTTAC	At4g21323	pir106
LM_734-SALK_062717C-RP	TGACGATGATGGATATGGACC	At4g21323	
LM_737-SALK_119194C-LP	TTCTCCAGCTCTTCTTCATGC	At3g45580	pir109
LM_738-SALK_119194C-RP	CATGGAGAAATCTGCTTCTGC	At3g45580	
LM_743-SALK_116115C-LP	TTTCCGCAAAAGATGAAAATG	At4g26640	pir102
LM_744-SALK_116115C-RP	ATGAAACAGACACCATCAGC	At4g26640	
LM_745-SALK_066562C-LP	CCAAAATCAGCTTAACTTTGTCC	At4g24050	pir125
LM_746-SALK_066562C-RP	TAACGACGATCTCTGTCTCCG	At4g24050	
LM_751-SALK_037019C-LP	CTTCACTACAACAAGACCCCG	At2g45570	pir128
LM_752-SALK_037019C-RP	AATCTCTCGGAACAAGCCTTC	At2g45570	
LM_761-SALK_064346C-LP	GCATCTGTAATAGCTCCTGCC	At4g39410	pir103
LM_762-SALK_064346C-RP	TTAGGGCATGGAGTTGTCAAG	At4g39410	
LM_767-SALK_035970C-LP	ATGCTCATTGCTCCAACAAAC	At1g71850/ At1g71860	pir72
LM_768-SALK_035970C-RP	ATTGAAGTTTTTGATTGGCCC	At1g71850/ At1g71860	
LM_779-SALK_104865C-LP	GAAAAAGCAACACAGACAGGC	At1g18950	pir31
LM_780-SALK_104865C-RP	TCACCAGATTTTGTTTCTGGG	At1g18950	
LM_781-SALK_027635C-LP	CGAGAAAGGTCTCATCGTGAG	At1g06020	pir17
LM_782-SALK_027635C-RP	AAGTGCACCAACAAACGAATC	At1g06020	
LM_783-SALK_109179C-LP	TACCTTCTCTTCCTCGAAGGC	At4g10720	pir30
LM_784-SALK_109179C-RP	GCCTAACACTGTTTCAGAGCG	At4g10720	
LM_793-SALK_062231C-LP	AGATTTTGCCAAACACAATGC	At3g23550	pir114
LM_794-SALK_062231C-RP	AACATTCACCTTGGCATGAAG	At3g23550	
LM_795-SALK_071004C-LP	TCAAGCCAGGTTAGAGATGTTG	At2g41140	pir63

LM_796-SALK_071004C-RP	ACAACGTTAAACCACCAAACC	At2g41140	
LM_812-SALK_019478C-LP	TGGGAAAACAGAGTCCAAATC	At1g30530	*pir38-3*
LM_813-SALK_019478C-RP	TAATCCACAGTGGTCTGGACC	At1g30530	
LM_816-SAIL_525_H07-LP	TTTTACTTGGATAAAGATCGAACC	At2g36790	*ugt73c6*
LM_817-SAIL_525_H07-RP	AGCTCCTTGAGCTGGGACTAG	At2g36790	
LM_820-SALK_071113C-LP	GGTTCTTTCGACACACTGCTC	At1g06000	*ugt89c1*
LM_821-SALK_071113C-RP	ACATGACGGAGATCGAATGAG	At1g06000	
LM_824-SAIL_568_F08-LP	GCTTCCTTTCATGGAGAAATC	At1g30530	*ugt78d1*
LM_825-SAIL_568_F08-RP	GACATGCATGCTAACAGATGC	At1g30530	
LM_826-SALK_049338-LP	CTCTTCGTTATTTTCCTCCGG	At5g17050	*ugt78d2-1*
LM_827-SALK_049338RP	TCAAACCCATCTTTCGTGAAG	At5g17050	
LM_828-SALK_205599C-LP	TCCCAAACACAACTCCTTCTG	At5g17050	*ugt78d2-2*
LM_829-SALK_205599C-RP	TCATTCAACCAATCAAATCTTATG	At5g17050	
LM_830-SALK_114099C-LP	TTCACGAAGGATGGATTTGAG	At5g17030	*ugt78d3*
LM_831-SALK_114099C-RP	TCCGTAAGGATGCACTTGAAC	At5g17030	
LM_864-SALK_113904C-LP	TGGCTATGGATAATCTGCTCG	At3g51240	*tt6-3*
LM_865-SALK_113904C-RP	TCGTTCGTCAGTCATCACAAG	At3g51240	
LM_866-SALK_113321C-LP	AAACAGAACCAACGCAACAAC	At3g51240	*tt6-5*
LM_867-SALK_113321C-RP	AAAGAGGAGAGATCTGCCGTC	At3g51240	
LM_870-SALK_124157C-LP	CTCAGGAGCTAAACACATGGC	At5g07990	*tt7-6*
LM_871-SALK_124157C-RP	ATCTTGACCGTTCATTTCGTG	At5g07990	
LM_878-SALK_128292C-LP	CAGAATCTGCTGATTTGGCTC	At5g48100	*tt10-7*
LM_879-SALK_128292C-RP	TCAGCCATTGTTTTTGGAAAC	At5g48100	
LM_984-SALK_032655C-LP	CAAGGCAAGCTGAAGAAAATG	At3g18230	*pir119*
LM_985-SALK_032655C-RP	ACAAATCGTTGACGTACTCCG	At3g18230	
LM_998-SALK_110320C-LP	TGAATCAGAGACACATGCTCG	At2g28290	*pir35*
LM_999-SALK_110320C-RP	CCATTTGATCAACCAAAATGG	At2g28290	
LM_1002-SALK_134892C-LP	CTTGTCCTTGCTTTCCTGTTG	At1g47310	*pir64*
LM_1003-SALK_134892C-RP	GGCGGATCAAGAACCTTACTC	At1g47310	
LM_1008-SALK_089787C-LP	CCTCTTCAAGTTTCATCTGCG	At3g16230	*pir69*
LM_1009-SALK_089787C-RP	TACACACGTCCATTTGACTGC	At3g16230	
LM_1012-SALK_014602C-LP	CTAGTGCTGTCAAAAGCTCGG	At5g08600	*pir110*
LM_1013-SALK_014602C-RP	TCTGACTCCACGTTTTCATCC	At5g08600	

LM_1018-SALK_055489C-LP	TAGAGCAGCAACCTCTTTTGC	At5g59150	*pir75*
LM_1019-SALK_055489C-RP	TGTTTTCTGAATGCGTCTGTG	At5g59150	
LM_1022-SALK_018535C-LP	CAAATTTGGACAAAATTGTGATG	At1g08135	*pir32*
LM_1023-SALK_018535C-RP	AGGTGTGCTTGATTTACGTGG	At1g08135	
LM_1038-SALK_142024C-LP	TTCTGATTGCCGTTACCATTC	At2g16250	*pir34*
LM_1039-SALK_142024C-RP	TCCAATACTTCCAATGCCAAC	At2g16250	
LM_1046-SALK_053802Ca-LP	CGCTGAGTTCTCCTTTGTGTC	At1g53450	*pir104*
LM_1047-SALK_053802Ca-RP	GTTTCAAGATTGCTGACGGAG	At1g53450	
LM_1056-SALK_113810C-LP	CACTTTTTGCTGGATCCTGAC	At3g55960	*pir52*
LM_1057-SALK_113810C-RP	TCACCAACCGACTTTATCGAC	At3g55960	
LM_1062-SALK_124232C-LP	CTATGTCACAAATCGCAGTGC	At1g11790	*pir26a*
LM_1063-SALK_124232C-RP	ATATCCACGCGTCATCAAAAC	At1g11790	
LM_1068-UGT78D1_GTW-Fw	caccATGACCAAATTCTCCGAGCCA	At1g30530	
LM_1070-UGT78D1_GTW_stop-Re	CTAAACTTTCACAATTTCGTCCAAC	At1g30530	
LM_1071-UGT78D2_GTW-Fw	caccATGACCAAACCCTCCGACCCAA	At5g17050	
LM_1073-UGT78D2_GTW_stop-Re	TCAAATAATGTTTACAACTGCATCC	At5g17050	
LM_1114-CHX6B_qPCR_1-Fw	AAGACTGCTCCGACAAGCAT	At1g08135	
LM_1115-CHX6B_qPCR_1-Re	GGGAATGGATTTTTGGGAGT	At1g08135	
LM_1138-GABI_382H01-LP	TCATCCTTCGGTGTTCAAGAG	At3g54250	*mvd2-1*
LM_1139-GABI_382H01-RP	ATGCTAAGCCAGCAGCAGTAG	At3g54250	
LM_1197-cyp79b2-Re	AACGGTTTAGCCAGAAACATATCGT	At4g39950	
LM_1198-cyp79b3-Re	AGGAAACCGATCACTTGACCGCTTG	At2g22330	
LM_1199-GABI_868E02-LP	GATATTTCTCTTTGGGTCGGC	*At5g07690*	*myb29-1*
LM_1200-GABI_868E02-RP	GAGTCATAGGCAAGTGGCTTG	*At5g07690*	*myb29-1*
LM_1210-fls1-LP	TTACACATATCAACACGTACTTTA	At5g08640	*fls1-2*
LM_1211-fls1-RP	CACTGAGATCTGTATGAGCCGGTACACC	At5g08640	
LM_1212-Ds3-2a	CCGGATCGTATCGGTTTTCG	RIKEN Transposon Primer	
LM_1239-f3h-tt6_qPCR-Fw	CTTACCAATGCATGCGTCGA	At3g51240	
LM_1240-f3h-tt6_qPCR-Re	TGGCTTGTAATCCACCGACT	At3g51240	

LM_1241-f3'h-tt7_qPCR-Fw	GTGACGGAGGAAGCTTAACG	At5g07990	
LM_1242-f3'h-tt7_qPCR-Re	GGTAAGGAAGCTGAGCGATG	At5g07990	
LM_1245-UGT78D1_qPCR-Fw	TGGAACTGCTGAAACACGAG	At1g30530	
LM_1246-UGT78D1_qPCR-Re	CCTTCCACACAACCTCCACT	At1g30530	
LM_1247-UGT78D2_qPCR-Fw	AAAGTGCCGTTTGTTTGGTC	At5g17050	
LM_1248-UGT78D2_qPCR-Re	AAAATGGCCTGCAAATCATC	At5g17050	
LM_1249-UGT78D3_qPCR-Fw	CACCAAATGGGTCTTGCTTT	At5g17030	
LM_1250-UGT78D3_qPCR-Re	CGTGCACTAGCGTTGATGTT	At5g17030	
LM_1321-GK382H01_qPCR-Fw	AACGGATTTTGCAAATGGAG	At3g54250	
LM_1322-GK382H01_qPCR-Re	AACCTGTGGTGTCCCTTCAG	At3g54250	
LM_1325-UGT78D3_qPCR2-Fw	CTCCTCCGATATCCCCACAAA	At5g17030	
LM_1326-UGT78D3_qPCR2-Re	TCAACACGAATCCCTCAGGAA	At5g17030	
LM_1333- SALK_135290-LP	TTGAAACTAGCTTGGTCGGTG	At5g54160	*omt1*
LM_1334- SALK_135290-RP	AATTCTTGATGGTGGGATTCC	At5g54160	
LM_1405-ABCA6_qPCR2-Fw	CTCTGTGACCGATTGGGAAT	At3g47770	
LM_1406-ABCA6_qPCR2-Re	GAACCTCCTCCTTTGGGAAC	At3g47770	
C6	aagacccttcctctatataagg	35s_Fw	
C9	GTAAAACGACGGCCAG	M13_Fw	
C10	CAGGAAACAGCTATGAC	M13_Rv	
C21	GCTTCCTATTATATCTTCCAAATTACCAATACA	Lb2_Sail	
C26	gcgtggaccgcttgctgcaact	LBb1	
C27	cccatttggacgtgaatgtagacac	Gabi_T-Dna	
C28	attttgccgatttcggaac	LBb1.3 SALK	
C69	aacgtccgcaatgtgttattaagttgtc	P745_Lb wisc	
C72	TACGAATAAGAGCGTCCATTTTAGAGTGA	Spm32	
UBOX_qPCR-Fw	TGCGCTGCCAGATAATACACTATT	At5g15400	
UBOX_qPCR-Re	TGCTGCCCAACATCAGGTT	At5g15400	
PR1_qPCR-Fw	GGCACGAGGAGCGGTAGGCG	At2g14610	
PR1_qPCR-Re	CACGGCGGAGACGCCAGACA	At2g14610	
FRK1_qPCR-Fw	ATCTTCGCTTGGAGCTTCTC	At2g19190	

FRK1_qPCR-Re	GCAGCGCAAGGACTAGAG	At2g19190	
NHL10_qPCR-Fw	CCTGTCCGTAACCCAAAC	At2g35980	
NHL10_qPCR-Re	CCCTCGTAGTAGGCATGAGC	At2g35980	
CYP81F2_qPCR-Fw	ATGGAGAGAGAGCAACACAATG	*At5g57220*	
CYP81F2_qPCR-Re	ATCGCCCATTCCAATGTTAC	*At5g57220*	

Bibliography

Abramovitch, R.B., Janjusevic, R., Stebbins, C.E., and Martin, G.B. (2006). Type III effector AvrPtoB requires intrinsic E3 ubiquitin ligase activity to suppress plant cell death and immunity. Proc. Natl. Acad. Sci. U. S. A. *103*, 2851–2856.

Agati, G., Matteini, P., Goti, A., and Tattini, M. (2007). Chloroplast-located flavonoids can scavenge singlet oxygen. New Phytol. *174*, 77–89.

Agati, G., Azzarello, E., Pollastri, S., and Tattini, M. (2012). Flavonoids as antioxidants in plants: Location and functional significance. Plant Sci. *196*, 67–76.

Agati, G., Brunetti, C., Di Ferdinando, M., Ferrini, F., Pollastri, S., and Tattini, M. (2013). Functional roles of flavonoids in photoprotection: New evidence, lessons from the past. Plant Physiol. Biochem. *72*, 35–45.

Ahuja, I., Kissen, R., and Bones, A.M. (2012). Phytoalexins in defense against pathogens. Trends Plant Sci. *17*, 73–90.

Albert, M. (2013). Peptides as triggers of plant defence. J. Exp. Bot. *64*, 5269–5279.

Albert, S., Delseny, M., and Devic, M. (1997). BANYULS, a novel negative regulator of flavonoid biosynthesis in the Arabidopsis seed coat. Plant J. *11*, 289–299.

Alberts, A.W., Chen, J., Kuron, G., Hunt, V., Huff, J., Hoffman, C., Rothrock, J., Lopez, M., Joshua, H., Harris, E., et al. (1980). Mevinolin: a highly potent competitive inhibitor of hydroxymethylglutaryl-coenzyme A reductase and a cholesterol-lowering agent. Proc. Natl. Acad. Sci. *77*, 3957–3961.

Albrecht, C., Boutrot, F., Segonzac, C., Schwessinger, B., Gimenez-Ibanez, S., Chinchilla, D., Rathjen, J.P., Vries, S.C. de, and Zipfel, C. (2012). Brassinosteroids inhibit pathogen-associated molecular pattern–triggered immune signaling independent of the receptor kinase BAK1. Proc. Natl. Acad. Sci. *109*, 303–308.

Alfano, J.R., Charkowski, A.O., Deng, W.-L., Badel, J.L., Petnicki-Ocwieja, T., Dijk, K. van, and Collmer, A. (2000). The Pseudomonas syringae Hrp pathogenicity island has a tripartite mosaic structure composed of a cluster of type III secretion genes bounded by exchangeable effector and conserved effector loci that contribute to parasitic fitness and pathogenicity in plants. Proc. Natl. Acad. Sci. *97*, 4856–4861.

Alonso, J.M., and Ecker, J.R. (2006). Moving forward in reverse: genetic technologies to enable genome-wide phenomic screens in Arabidopsis. Nat. Rev. Genet. *7*, 524–536.

Alonso, J.M., Hirayama, T., Roman, G., Nourizadeh, S., and Ecker, J.R. (1999). EIN2, a Bifunctional Transducer of Ethylene and Stress Responses in Arabidopsis. Science *284*, 2148–2152.

Alonso, J.M., Stepanova, A.N., Leisse, T.J., Kim, C.J., Chen, H., Shinn, P., Stevenson, D.K., Zimmerman, J., Barajas, P., Cheuk, R., et al. (2003). Genome-Wide Insertional Mutagenesis of Arabidopsis thaliana. Science *301*, 653–657.

Anderson, J.C., Bartels, S., Besteiro, M.A.G., Shahollari, B., Ulm, R., and Peck, S.C. (2011). Arabidopsis MAP Kinase Phosphatase 1 (AtMKP1) negatively regulates MPK6-mediated PAMP responses and resistance against bacteria. Plant J. *67*, 258–268.

Anderson, J.C., Wan, Y., Kim, Y.-M., Pasa-Tolic, L., Metz, T.O., and Peck, S.C. (2014). Decreased abundance of type III secretion system-inducing signals in Arabidopsis mkp1 enhances resistance against Pseudomonas syringae. Proc. Natl. Acad. Sci. *111*, 6846–6851.

Andreasson, E., Jenkins, T., Brodersen, P., Thorgrimsen, S., Petersen, N.H., Zhu, S., Qiu, J.-L., Micheelsen, P., Rocher, A., Petersen, M., et al. (2005). The MAP kinase substrate MKS1 is a regulator of plant defense responses. EMBO J. *24*, 2579–2589.

Ao, Y., Li, Z., Feng, D., Xiong, F., Liu, J., Li, J.-F., Wang, M., Wang, J., Liu, B., and Wang, H.-B. (2014). OsCERK1 and OsRLCK176 play important roles in peptidoglycan and chitin signaling in rice innate immunity. Plant J. *80*, 1072–1084.

Arnaud, D., and Hwang, I. (2015). A Sophisticated Network of Signaling Pathways Regulates Stomatal Defenses to Bacterial Pathogens. Mol. Plant *8*, 566–581.

Asai, T., Tena, G., Plotnikova, J., Willmann, M.R., Chiu, W.-L., Gomez-Gomez, L., Boller, T., Ausubel, F.M., and Sheen, J. (2002). MAP kinase signalling cascade in Arabidopsis innate immunity. Nature *415*, 977–983.

Avni, A., Bailey, B.A., Mattoo, A.K., and Anderson, J.D. (1994). Induction of Ethylene Biosynthesis in Nicotiana tabacum by a Trichoderma viride Xylanase Is Correlated to the Accumulation of 1-Aminocyclopropane-1-Carboxylic Acid (ACC) Synthase and ACC Oxidase Transcripts. Plant Physiol. *106*, 1049–1055.

Badel, J.L., Shimizu, R., Oh, H.-S., and Collmer, A. (2006). A Pseudomonas syringae pv. tomato avrE1/hopM1 Mutant Is Severely Reduced in Growth and Lesion Formation in Tomato. Mol. Plant. Microbe Interact. *19*, 99–111.

Bai, M.-Y., Shang, J.-X., Oh, E., Fan, M., Bai, Y., Zentella, R., Sun, T., and Wang, Z.-Y. (2012). Brassinosteroid, gibberellin and phytochrome impinge on a common transcription module in Arabidopsis. Nat. Cell Biol. *14*, 810–817.

Bailey, B.A., Dean, J.F.D., and Anderson, J.D. (1990). An Ethylene Biosynthesis-Inducing Endoxylanase Elicits Electrolyte Leakage and Necrosis in Nicotiana tabacum cv Xanthi Leaves. Plant Physiol. *94*, 1849–1854.

Ballaré, C.L., Barnes, P.W., and Kendrick, R.E. (1991). Photomorphogenic effects of UV-B radiation on hypocotyl elongation in wild type and stable-phytochrome-deficient mutant seedlings of cucumber. Physiol. Plant. *83*, 652–658.

Bar, M., Sharfman, M., Ron, M., and Avni, A. (2010). BAK1 is required for the attenuation of ethylene-inducing xylanase (Eix)-induced defense responses by the decoy receptor LeEix1. Plant J. *63*, 791–800.

Barth, C., and Jander, G. (2006). Arabidopsis myrosinases TGG1 and TGG2 have redundant function in glucosinolate breakdown and insect defense. Plant J. *46*, 549–562.

Barz, W., and Mackenbrock, U. (1994). Constitutive and elicitation induced metabolism of isoflavones and pterocarpans in chickpea (Cicer arietinum) cell suspension cultures. Plant Cell Tissue Organ Cult. *38*, 199–211.

Baudry, A., Heim, M.A., Dubreucq, B., Caboche, M., Weisshaar, B., and Lepiniec, L. (2004). TT2, TT8, and TTG1 synergistically specify the expression of BANYULS and proanthocyanidin biosynthesis in Arabidopsis thaliana. Plant J. *39*, 366–380.

Baxter, A., Mittler, R., and Suzuki, N. (2014). ROS as key players in plant stress signalling. J. Exp. Bot. *65*, 1229–1240.

Beck, M., Zhou, J., Faulkner, C., MacLean, D., and Robatzek, S. (2012). Spatio-Temporal Cellular Dynamics of the Arabidopsis Flagellin Receptor Reveal Activation Status-Dependent Endosomal Sorting. Plant Cell Online *24*, 4205–4219.

Bednarek, P. (2012a). Sulfur-Containing Secondary Metabolites from Arabidopsis thaliana and other Brassicaceae with Function in Plant Immunity. ChemBioChem *13*, 1846–1859.

Bednarek, P. (2012b). Chemical warfare or modulators of defence responses – the function of secondary metabolites in plant immunity. Curr. Opin. Plant Biol. *15*, 407–414.

Bednarek, P., and Osbourn, A. (2009). Plant-Microbe Interactions: Chemical Diversity in Plant Defense. Science *324*, 746–748.

Bednarek, P., Piślewska-Bednarek, M., Svatoš, A., Schneider, B., Doubský, J., Mansurova, M., Humphry, M., Consonni, C., Panstruga, R., Sanchez-Vallet, A., et al. (2009). A Glucosinolate Metabolism Pathway in Living Plant Cells Mediates Broad-Spectrum Antifungal Defense. Science *323*, 101–106.

Bednarek, P., Kwon, C., and Schulze-Lefert, P. (2010). Not a peripheral issue: secretion in plant–microbe interactions. Curr. Opin. Plant Biol. *13*, 378–387.

Belkhadir, Y., Jaillais, Y., Epple, P., Balsemão-Pires, E., Dangl, J.L., and Chory, J. (2012). Brassinosteroids modulate the efficiency of plant immune responses to microbe-associated molecular patterns. Proc. Natl. Acad. Sci. *109*, 297–302.

Benschop, J.J., Mohammed, S., O'Flaherty, M., Heck, A.J.R., Slijper, M., and Menke, F.L.H. (2007). Quantitative Phosphoproteomics of Early Elicitor Signaling in Arabidopsis. Mol. Cell. Proteomics *6*, 1198–1214.

Bestwick, C.S., Bennett, M.H., and Mansfield, J.W. (1995). Hrp Mutant of Pseudomonas syringae pv phaseolicola Induces Cell Wall Alterations but Not Membrane Damage Leading to the Hypersensitive Reaction in Lettuce. Plant Physiol. *108*, 503–516.

Bethke, G., Unthan, T., Uhrig, J.F., Pöschl, Y., Gust, A.A., Scheel, D., and Lee, J. (2009). Flg22 regulates the release of an ethylene response factor substrate from MAP kinase 6 in Arabidopsis thaliana via ethylene signaling. Proc. Natl. Acad. Sci. *106*, 8067–8072.

Bethke, G., Pecher, P., Eschen-Lippold, L., Tsuda, K., Katagiri, F., Glazebrook, J., Scheel, D., and Lee, J. (2011). Activation of the Arabidopsis thaliana Mitogen-Activated Protein Kinase MPK11 by the Flagellin-Derived Elicitor Peptide, flg22. Mol. Plant. Microbe Interact. *25*, 471–480.

Bianchini, G.M., Stermer, B.A., and Paiva, N.L. (1996). Induction of early mevalonate pathway enzymes and biosynthesis of end products in potato (Solanum tuberosum) tubers by wounding and elicitation. Phytochemistry *42*, 1563–1571.

Van der Biezen, E.A., and Jones, J.D.G. (1998). The NB-ARC domain: a novel signalling motif shared by plant resistance gene products and regulators of cell death in animals. Curr. Biol. *8*, R226–R228.

Bigeard, J., Colcombet, J., and Hirt, H. (2015). Signaling Mechanisms in Pattern-Triggered Immunity (PTI). Mol. Plant *8*, 521–539.

Block, A., Guo, M., Li, G., Elowsky, C., Clemente, T.E., and Alfano, J.R. (2010). The Pseudomonas syringae type III effector HopG1 targets mitochondria, alters plant development and suppresses plant innate immunity. Cell. Microbiol. *12*, 318–330.

Blume, B., Nürnberger, T., Nass, N., and Scheel, D. (2000). Receptor-Mediated Increase in Cytoplasmic Free Calcium Required for Activation of Pathogen Defense in Parsley. Plant Cell Online *12*, 1425–1440.

Boller, T., and Felix, G. (2009). A Renaissance of Elicitors: Perception of Microbe-Associated Molecular Patterns and Danger Signals by Pattern-Recognition Receptors. Annu. Rev. Plant Biol. *60*, 379–406.

Bones, A.M., and Rossiter, J.T. (1996). The myrosinase-glucosinolate system, its organisation and biochemistry. Physiol. Plant. *97*, 194–208.

Bonza, M.C., Luoni, L., and Michelis, M.I.D. (2004). Functional expression in yeast of an N-deleted form of At-ACA8, a plasma membrane Ca2+-ATPase of Arabidopsis thaliana, and characterization of a hyperactive mutant. Planta *218*, 814–823.

Borevitz, J.O., Xia, Y., Blount, J., Dixon, R.A., and Lamb, C. (2000). Activation Tagging Identifies a Conserved MYB Regulator of Phenylpropanoid Biosynthesis. Plant Cell Online *12*, 2383–2393.

Bors, W., Michel, C., and Schikora, S. (1995). Interaction of flavonoids with ascorbate and determination of their univalent redox potentials: A pulse radiolysis study. Free Radic. Biol. Med. *19*, 45–52.

Böttcher, C., Westphal, L., Schmotz, C., Prade, E., Scheel, D., and Glawischnig, E. (2009). The Multifunctional Enzyme CYP71B15 (PHYTOALEXIN DEFICIENT3) Converts Cysteine-Indole-3-Acetonitrile to Camalexin in the Indole-3-Acetonitrile Metabolic Network of Arabidopsis thaliana. Plant Cell Online *21*, 1830–1845.

Boudsocq, M., Willmann, M.R., McCormack, M., Lee, H., Shan, L., He, P., Bush, J., Cheng, S.-H., and Sheen, J. (2010). Differential innate immune signalling via Ca2+ sensor protein kinases. Nature *464*, 418–422.

Boutrot, F., Segonzac, C., Chang, K.N., Qiao, H., Ecker, J.R., Zipfel, C., and Rathjen, J.P. (2010). Direct transcriptional control of the Arabidopsis immune receptor FLS2 by the ethylene-dependent transcription factors EIN3 and EIL1. Proc. Natl. Acad. Sci. *107*, 14502–14507.

Bouwmeester, K., de Sain, M., Weide, R., Gouget, A., Klamer, S., Canut, H., and Govers, F. (2011). The Lectin Receptor Kinase LecRK-I.9 Is a Novel Phytophthora Resistance Component and a Potential Host Target for a RXLR Effector. PLoS Pathog *7*, e1001327.

Bowles, D., Isayenkova, J., Lim, E.-K., and Poppenberger, B. (2005). Glycosyltransferases: managers of small molecules. Curr. Opin. Plant Biol. *8*, 254–263.

Brader, G., Mikkelsen, M.D., Halkier, B.A., and Tapio Palva, E. (2006). Altering glucosinolate profiles modulates disease resistance in plants. Plant J. *46*, 758–767.

Brett, C.L., Donowitz, M., and Rao, R. (2005). Evolutionary origins of eukaryotic sodium/proton exchangers. Am. J. Physiol. - Cell Physiol. *288*, C223–C239.

Bretz, J.R., Mock, N.M., Charity, J.C., Zeyad, S., Baker, C.J., and Hutcheson, S.W. (2003). A translocated protein tyrosine phosphatase of Pseudomonas syringae pv. tomato DC3000 modulates plant defence response to infection. Mol. Microbiol. *49*, 389–400.

Brosché, M., Schuler, M.A., Kalbina, I., Connor, L., and Strid, A. (2002). Gene regulation by low level UV-B radiation: identification by DNA array analysis. Photochem. Photobiol. Sci. *1*, 656–664.

Brown, B.A., Cloix, C., Jiang, G.H., Kaiserli, E., Herzyk, P., Kliebenstein, D.J., and Jenkins, G.I. (2005). A UV-B-specific signaling component orchestrates plant UV protection. Proc. Natl. Acad. Sci. U. S. A. *102*, 18225–18230.

Brown, D.E., Rashotte, A.M., Murphy, A.S., Normanly, J., Tague, B.W., Peer, W.A., Taiz, L., and Muday, G.K. (2001). Flavonoids Act as Negative Regulators of Auxin Transport in Vivo in Arabidopsis. Plant Physiol. *126*, 524–535.

Brûle, S. van den, and Smart, C.C. (2002). The plant PDR family of ABC transporters. Planta *216*, 95–106.

Brûle, S. van den, Müller, A., Fleming, A.J., and Smart, C.C. (2002). The ABC transporter SpTUR2 confers resistance to the antifungal diterpene sclareol. Plant J. *30*, 649–662.

Brutus, A., Sicilia, F., Macone, A., Cervone, F., and Lorenzo, G.D. (2010). A domain swap approach reveals a role of the plant wall-associated kinase 1 (WAK1) as a receptor of oligogalacturonides. Proc. Natl. Acad. Sci. *107*, 9452–9457.

Bruyne, L.D., Höfte, M., and Vleesschauwer, D.D. (2014). Connecting Growth and Defense: The Emerging Roles of Brassinosteroids and Gibberellins in Plant Innate Immunity. Mol. Plant *7*, 943–959.

Buer, C.S., Sukumar, P., and Muday, G.K. (2006). Ethylene Modulates Flavonoid Accumulation and Gravitropic Responses in Roots of Arabidopsis. Plant Physiol. *140*, 1384–1396.

Buer, C.S., Muday, G.K., and Djordjevic, M.A. (2007). Flavonoids Are Differentially Taken Up and Transported Long Distances in Arabidopsis. Plant Physiol. *145*, 478–490.

Buer, C.S., Muday, G.K., and Djordjevic, M.A. (2008). Implications of long-distance flavonoid movement in Arabidopsis thaliana. Plant Signal. Behav. *3*, 415–417.

Buer, C.S., Imin, N., and Djordjevic, M.A. (2010). Flavonoids: New Roles for Old Molecules. J. Integr. Plant Biol. *52*, 98–111.

Buist, G., Steen, A., Kok, J., and Kuipers, O.P. (2008). LysM, a widely distributed protein motif for binding to (peptido)glycans. Mol. Microbiol. *68*, 838–847.

Burbulis, I.E., and Winkel-Shirley, B. (1999). Interactions among enzymes of the Arabidopsis flavonoid biosynthetic pathway. Proc. Natl. Acad. Sci. *96*, 12929–12934.

Burbulis, I.E., Iacobucci, M., and Shirley, B.W. (1996). A null mutation in the first enzyme of flavonoid biosynthesis does not affect male fertility in Arabidopsis. Plant Cell Online *8*, 1013–1025.

Buxdorf, K., Yaffe, H., Barda, O., and Levy, M. (2013). The Effects of Glucosinolates and Their Breakdown Products on Necrotrophic Fungi. PLoS ONE *8*, e70771.

Caelles, C., Ferrer, A., Balcells, L., Hegardt, F.G., and Boronat, A. (1989). Isolation and structural characterization of a cDNA encoding Arabidopsis thaliana 3-hydroxy-3-methylglutaryl coenzyme A reductase. Plant Mol. Biol. *13*, 627–638.

Cai, R., Lewis, J., Yan, S., Liu, H., Clarke, C.R., Campanile, F., Almeida, N.F., Studholme, D.J., Lindeberg, M., Schneider, D., et al. (2011). The Plant Pathogen Pseudomonas syringae pv. tomato Is Genetically Monomorphic and under Strong Selection to Evade Tomato Immunity. PLoS Pathog *7*, e1002130.

Campbell, E.J., Schenk, P.M., Kazan, K., Penninckx, I.A.M.A., Anderson, J.P., Maclean, D.J., Cammue, B.P.A., Ebert, P.R., and Manners, J.M. (2003).

Pathogen-Responsive Expression of a Putative ATP-Binding Cassette Transporter Gene Conferring Resistance to the Diterpenoid Sclareol Is Regulated by Multiple Defense Signaling Pathways in Arabidopsis. Plant Physiol. *133*, 1272–1284.

Cao, G., Sofic, E., and Prior, R.L. (1997). Antioxidant and Prooxidant Behavior of Flavonoids: Structure-Activity Relationships. Free Radic. Biol. Med. *22*, 749–760.

Cao, Y., Aceti, D.J., Sabat, G., Song, J., Makino, S., Fox, B.G., and Bent, A.F. (2013). Mutations in FLS2 Ser-938 Dissect Signaling Activation in FLS2-Mediated Arabidopsis Immunity. PLoS Pathog *9*, e1003313.

Cao, Y., Liang, Y., Tanaka, K., Nguyen, C.T., Jedrzejczak, R.P., Joachimiak, A., and Stacey, G. (2014a). The kinase LYK5 is a major chitin receptor in Arabidopsis and forms a chitin-induced complex with related kinase CERK1. eLife e03766.

Cao, Y., Tanaka, K., Nguyen, C.T., and Stacey, G. (2014b). Extracellular ATP is a central signaling molecule in plant stress responses. Curr. Opin. Plant Biol. *20*, 82–87.

Cervone, F., Hahn, M.G., Lorenzo, G.D., Darvill, A., and Albersheim, P. (1989). Host-Pathogen Interactions XXXIII. A Plant Protein Converts a Fungal Pathogenesis Factor into an Elicitor of Plant Defense Responses. Plant Physiol. *90*, 542–548.

Cesari, S., Bernoux, M., Moncuquet, P., Kroj, T., and Dodds, P.N. (2014). A novel conserved mechanism for plant NLR protein pairs: the "integrated decoy" hypothesis. Plant-Microbe Interact. *5*, 606.

Chandra, S., and Low, P.S. (1995). Role of phosphorylation in elicitation of the oxidative burst in cultured soybean cells. Proc. Natl. Acad. Sci. *92*, 4120–4123.

Chappell, J. (1995). Biochemistry and Molecular Biology of the Isoprenoid Biosynthetic Pathway in Plants. Annu. Rev. Plant Physiol. Plant Mol. Biol. *46*, 521–547.

Chappell, J., and Hahlbrock, K. (1984). Transcription of plant defence genes in response to UV light or fungal elicitor. Nature *311*, 76–78.

Chappell, J., and Nable, R. (1987). Induction of Sesquiterpenoid Biosynthesis in Tobacco Cell Suspension Cultures by Fungal Elicitor. Plant Physiol. *85*, 469–473.

Chappell, J., VonLanken, C., and Vögeli, U. (1991). Elicitor-Inducible 3-Hydroxy-3-Methylglutaryl Coenzyme A Reductase Activity Is Required for

Sesquiterpene Accumulation in Tobacco Cell Suspension Cultures. Plant Physiol. *97*, 693–698.

Chen, C., and Chen, Z. (2002). Potentiation of Developmentally Regulated Plant Defense Response by AtWRKY18, a Pathogen-Induced Arabidopsis Transcription Factor. Plant Physiol. *129*, 706–716.

Chen, C.-W., Panzeri, D., Yeh, Y.-H., Kadota, Y., Huang, P.-Y., Tao, C.-N., Roux, M., Chien, S.-C., Chin, T.-C., Chu, P.-W., et al. (2014a). The Arabidopsis Malectin-Like Leucine-Rich Repeat Receptor-Like Kinase IOS1 Associates with the Pattern Recognition Receptors FLS2 and EFR and Is Critical for Priming of Pattern-Triggered Immunity. Plant Cell Online *26*, 3201–3219.

Chen, X., Chern, M., Canlas, P.E., Ruan, D., Jiang, C., and Ronald, P.C. (2010). An ATPase promotes autophosphorylation of the pattern recognition receptor XA21 and inhibits XA21-mediated immunity. Proc. Natl. Acad. Sci. *107*, 8029–8034.

Chen, X., Zuo, S., Schwessinger, B., Chern, M., Canlas, P.E., Ruan, D., Zhou, X., Wang, J., Daudi, A., Petzold, C.J., et al. (2014b). An XA21-Associated Kinase (OsSERK2) regulates immunity mediated by the XA21 and XA3 immune receptors. Mol. Plant ssu003.

Chen, Z., Agnew, J.L., Cohen, J.D., He, P., Shan, L., Sheen, J., and Kunkel, B.N. (2007). Pseudomonas syringae type III effector AvrRpt2 alters Arabidopsis thaliana auxin physiology. Proc. Natl. Acad. Sci. *104*, 20131–20136.

Cheng, W., Munkvold, K.R., Gao, H., Mathieu, J., Schwizer, S., Wang, S., Yan, Y., Wang, J., Martin, G.B., and Chai, J. (2011). Structural Analysis of Pseudomonas syringae AvrPtoB Bound to Host BAK1 Reveals Two Similar Kinase-Interacting Domains in a Type III Effector. Cell Host Microbe *10*, 616–626.

Chinchilla, D., Bauer, Z., Regenass, M., Boller, T., and Felix, G. (2006). The Arabidopsis Receptor Kinase FLS2 Binds flg22 and Determines the Specificity of Flagellin Perception. Plant Cell Online *18*, 465–476.

Chinchilla, D., Zipfel, C., Robatzek, S., Kemmerling, B., Nürnberger, T., Jones, J.D.G., Felix, G., and Boller, T. (2007). A flagellin-induced complex of the receptor FLS2 and BAK1 initiates plant defence. Nature *448*, 497–500.

Choi, D., Ward, B.L., and Bostock, R.M. (1992). Differential induction and suppression of potato 3-hydroxy-3-methylglutaryl coenzyme A reductase genes in response to Phytophthora infestans and to its elicitor arachidonic acid. Plant Cell Online *4*, 1333–1344.

Choi, J., Tanaka, K., Cao, Y., Qi, Y., Qiu, J., Liang, Y., Lee, S.Y., and Stacey, G. (2014). Identification of a Plant Receptor for Extracellular ATP. Science *343*, 290–294.

Choi, S., Tamaki, T., Ebine, K., Uemura, T., Ueda, T., and Nakano, A. (2013). RABA Members Act in Distinct Steps of Subcellular Trafficking of the FLAGELLIN SENSING2 Receptor. Plant Cell Online tpc.112.108803.

Clarke, C.R., Chinchilla, D., Hind, S.R., Taguchi, F., Miki, R., Ichinose, Y., Martin, G.B., Leman, S., Felix, G., and Vinatzer, B.A. (2013). Allelic variation in two distinct Pseudomonas syringae flagellin epitopes modulates the strength of plant immune responses but not bacterial motility. New Phytol. *200*, 847–860.

Clay, N.K., Adio, A.M., Denoux, C., Jander, G., and Ausubel, F.M. (2009). Glucosinolate Metabolites Required for an Arabidopsis Innate Immune Response. Science *323*, 95–101.

Clough, S.J., and Bent, A.F. (1998). Floral dip: a simplified method forAgrobacterium-mediated transformation ofArabidopsis thaliana. Plant J. *16*, 735–743.

Coe, E.H., McCormick, S.M., and Modena, S.A. (1981). White pollen in maize. J. Hered. *72*, 318–320.

Coll, N.S., Epple, P., and Dangl, J.L. (2011). Programmed cell death in the plant immune system. Cell Death Differ. *18*, 1247–1256.

Collmer, A., Badel, J.L., Charkowski, A.O., Deng, W.-L., Fouts, D.E., Ramos, A.R., Rehm, A.H., Anderson, D.M., Schneewind, O., Dijk, K. van, et al. (2000). Pseudomonas syringae Hrp type III secretion system and effector proteins. Proc. Natl. Acad. Sci. *97*, 8770–8777.

Collmer, A., Schneider, D.J., and Lindeberg, M. (2009). Lifestyles of the Effector Rich: Genome-Enabled Characterization of Bacterial Plant Pathogens. Plant Physiol. *150*, 1623–1630.

Conn, S.J., Gilliham, M., Athman, A., Schreiber, A.W., Baumann, U., Moller, I., Cheng, N.-H., Stancombe, M.A., Hirschi, K.D., Webb, A.A.R., et al. (2011). Cell-Specific Vacuolar Calcium Storage Mediated by CAX1 Regulates Apoplastic Calcium Concentration, Gas Exchange, and Plant Productivity in Arabidopsis. Plant Cell Online *23*, 240–257.

Cordier, H., Karst, F., and Bergès, T. (1999). Heterologous expression in Saccharomyces cerevisiae of an Arabidopsis thaliana cDNA encoding mevalonate diphosphate decarboxylase. Plant Mol. Biol. *39,* 953–967.

Crabill, E., Joe, A., Block, A., Rooyen, J.M. van, and Alfano, J.R. (2010). Plant Immunity Directly or Indirectly Restricts the Injection of Type III Effectors by the Pseudomonas syringae Type III Secretion System. Plant Physiol. *154*, 233–244.

Crosby, K.C., Pietraszewska-Bogiel, A., Gadella Jr., T.W.J., and Winkel, B.S.J. (2011). Förster resonance energy transfer demonstrates a flavonoid metabolon in living plant cells that displays competitive interactions between enzymes. FEBS Lett. *585*, 2193–2198.

Cui, H., Wang, Y., Xue, L., Chu, J., Yan, C., Fu, J., Chen, M., Innes, R.W., and Zhou, J.-M. (2010). Pseudomonas syringae Effector Protein AvrB Perturbs Arabidopsis Hormone Signaling by Activating MAP Kinase 4. Cell Host Microbe *7*, 164–175.

Cunnac, S., Chakravarthy, S., Kvitko, B.H., Russell, A.B., Martin, G.B., and Collmer, A. (2011). Genetic disassembly and combinatorial reassembly identify a minimal functional repertoire of type III effectors in Pseudomonas syringae. Proc. Natl. Acad. Sci. *108*, 2975–2980.

Cushnie, T.P.T., and Lamb, A.J. (2005). Antimicrobial activity of flavonoids. Int. J. Antimicrob. Agents *26*, 343–356.

Cushnie, T.P.T., and Lamb, A.J. (2011). Recent advances in understanding the antibacterial properties of flavonoids. Int. J. Antimicrob. Agents *38*, 99–107.

Dangl, J.L., and Jones, J.D.G. (2001). Plant pathogens and integrated defence responses to infection. Nature *411*, 826–833.

Danna, C.H., Millet, Y.A., Koller, T., Han, S.-W., Bent, A.F., Ronald, P.C., and Ausubel, F.M. (2011). The Arabidopsis flagellin receptor FLS2 mediates the perception of Xanthomonas Ax21 secreted peptides. Proc. Natl. Acad. Sci. *108*, 9286–9291.

Dardick, C., and Ronald, P. (2006). Plant and Animal Pathogen Recognition Receptors Signal through Non-RD Kinases. PLoS Pathog *2*, e2.

Daudi, A., Cheng, Z., O'Brien, J.A., Mammarella, N., Khan, S., Ausubel, F.M., and Bolwell, G.P. (2012). The Apoplastic Oxidative Burst Peroxidase in Arabidopsis Is a Major Component of Pattern-Triggered Immunity. Plant Cell *24*, 275–287.

D'Auria, J.C. (2006). Acyltransferases in plants: a good time to be BAHD. Curr. Opin. Plant Biol. *9*, 331–340.

Dean, J.F., Gamble, H.R., and Anderson, J.D. (1989). The Ethylene Biosynthesis-Inducing Xylanase: Its Induction in *Trichoderma viride* and Certain Plant Pathogens. Phytopathology *79*, 1071.

Debeaujon, I., Peeters, A.J.M., Léon-Kloosterziel, K.M., and Koornneef, M. (2001). The TRANSPARENT TESTA12 Gene of Arabidopsis Encodes a Multidrug Secondary Transporter-like Protein Required for Flavonoid Sequestration in Vacuoles of the Seed Coat Endothelium. Plant Cell Online *13*, 853–871.

DebRoy, S., Thilmony, R., Kwack, Y.-B., Nomura, K., and He, S.Y. (2004). A family of conserved bacterial effectors inhibits salicylic acid-mediated basal immunity and promotes disease necrosis in plants. Proc. Natl. Acad. Sci. U. S. A. *101*, 9927–9932.

Decreux, A., Thomas, A., Spies, B., Brasseur, R., Cutsem, P.V., and Messiaen, J. (2006). In vitro characterization of the homogalacturonan-binding domain of the wall-associated kinase WAK1 using site-directed mutagenesis. Phytochemistry *67*, 1068–1079.

DeFalco, T.A., Bender, K.W., and Snedden, W.A. (2010). Breaking the code: Ca $^{2+}$ sensors in plant signalling. Biochem. J. *425*, 27–40.

Delaunois, B., Jeandet, P., Clément, C., Baillieul, F., Dorey, S., and Cordelier, S. (2014). Uncovering plant-pathogen crosstalk through apoplastic proteomic studies. Plant-Microbe Interact. *5*, 249.

Denoux, C., Galletti, R., Mammarella, N., Gopalan, S., Werck, D., Lorenzo, G.D., Ferrari, S., Ausubel, F.M., and Dewdney, J. (2008). Activation of Defense Response Pathways by OGs and Flg22 Elicitors in Arabidopsis Seedlings. Mol. Plant *1*, 423–445.

Deslandes, L., Olivier, J., Peeters, N., Feng, D.X., Khounlotham, M., Boucher, C., Somssich, I., Genin, S., and Marco, Y. (2003). Physical interaction between RRS1-R, a protein conferring resistance to bacterial wilt, and PopP2, a type III effector targeted to the plant nucleus. Proc. Natl. Acad. Sci. *100*, 8024–8029.

Devic, M., Guilleminot, J., Debeaujon, I., Bechtold, N., Bensaude, E., Koornneef, M., Pelletier, G., and Delseny, M. (1999). The BANYULS gene encodes a DFR-like protein and is a marker of early seed coat development. Plant J. *19*, 387–398.

Dixon, R.A. (2001). Natural products and plant disease resistance. Nature *411*, 843–847.

Dixon, R.A., and Pasinetti, G.M. (2010). Flavonoids and Isoflavonoids: From Plant Biology to Agriculture and Neuroscience. Plant Physiol. *154*, 453–457.

Djordjevic, M.A., Redmond, J.W., Batley, M., and Rolfe, B.G. (1987). Clovers secrete specific phenolic compounds which either stimulate or repress nod gene expression in Rhizobium trifolii. EMBO J. *6*, 1173–1179.

Doblas, V.G., Amorim-Silva, V., Posé, D., Rosado, A., Esteban, A., Arró, M., Azevedo, H., Bombarely, A., Borsani, O., Valpuesta, V., et al. (2013). The SUD1 Gene Encodes a Putative E3 Ubiquitin Ligase and Is a Positive Regulator of 3-Hydroxy-3-Methylglutaryl Coenzyme A Reductase Activity in Arabidopsis. Plant Cell Online *25*, 728–743.

Dodds, P.N., and Rathjen, J.P. (2010). Plant immunity: towards an integrated view of plant–pathogen interactions. Nat. Rev. Genet. *11*, 539–548.

Dong, J., Chen, C., and Chen, Z. (2003). Expression profiles of the Arabidopsis WRKY gene superfamily during plant defense response. Plant Mol. Biol. *51*, 21–37.

Dou, D., and Zhou, J.-M. (2012). Phytopathogen Effectors Subverting Host Immunity: Different Foes, Similar Battleground. Cell Host Microbe *12*, 484–495.

Dubiella, U., Seybold, H., Durian, G., Komander, E., Lassig, R., Witte, C.-P., Schulze, W.X., and Romeis, T. (2013). Calcium-dependent protein kinase/NADPH oxidase activation circuit is required for rapid defense signal propagation. Proc. Natl. Acad. Sci. *110*, 8744–8749.

Ellinger, D., Naumann, M., Falter, C., Zwikowics, C., Jamrow, T., Manisseri, C., Somerville, S.C., and Voigt, C.A. (2013). Elevated Early Callose Deposition Results in Complete Penetration Resistance to Powdery Mildew in Arabidopsis. Plant Physiol. *161*, 1433–1444.

Elmore, J.M., and Coaker, G. (2011). The Role of the Plasma Membrane H+-ATPase in Plant–Microbe Interactions. Mol. Plant *4*, 416–427.

Enjuto, M., Balcells, L., Campos, N., Caelles, C., Arró, M., and Boronat, A. (1994). Arabidopsis thaliana contains two differentially expressed 3-hydroxy-3-methylglutaryl-CoA reductase genes, which encode microsomal forms of the enzyme. Proc. Natl. Acad. Sci. *91*, 927–931.

Erbs, G., Silipo, A., Aslam, S., De Castro, C., Liparoti, V., Flagiello, A., Pucci, P., Lanzetta, R., Parrilli, M., Molinaro, A., et al. (2008). Peptidoglycan and Muropeptides from Pathogens Agrobacterium and Xanthomonas Elicit Plant Innate Immunity: Structure and Activity. Chem. Biol. *15*, 438–448.

Eschen-Lippold, L., Bethke, G., Palm-Forster, M.A.T., Pecher, P., Bauer, N., Glazebrook, J., Scheel, D., and Lee, J. (2012). MPK11—a fourth elicitor-responsive mitogen-activated protein kinase in Arabidopsis thaliana. Plant Signal. Behav. *7*, 1203–1205.

Espinosa, A., Guo, M., Tam, V.C., Fu, Z.Q., and Alfano, J.R. (2003). The Pseudomonas syringae type III-secreted protein HopPtoD2 possesses protein tyrosine phosphatase activity and suppresses programmed cell death in plants. Mol. Microbiol. *49*, 377–387.

Fabro, G., Steinbrenner, J., Coates, M., Ishaque, N., Baxter, L., Studholme, D.J., Körner, E., Allen, R.L., Piquerez, S.J.M., Rougon-Cardoso, A., et al. (2011). Multiple Candidate Effectors from the Oomycete Pathogen Hyaloperonospora arabidopsidis Suppress Host Plant Immunity. PLoS Pathog *7*, e1002348.

Fahey, J.W., Zalcmann, A.T., and Talalay, P. (2001). The chemical diversity and distribution of glucosinolates and isothiocyanates among plants. Phytochemistry *56*, 5–51.

Falcone Ferreyra, M.L., Rius, S., and Casati, P. (2012). Flavonoids: biosynthesis, biological functions, and biotechnological applications. Plant Physiol. *3*, 222.

Fan, J., Crooks, C., and Lamb, C. (2008). High-throughput quantitative luminescence assay of the growth in planta of Pseudomonas syringae chromosomally tagged with Photorhabdus luminescens luxCDABE. Plant J. *53*, 393–399.

Fan, J., Crooks, C., Creissen, G., Hill, L., Fairhurst, S., Doerner, P., and Lamb, C. (2011). Pseudomonas sax Genes Overcome Aliphatic Isothiocyanate–Mediated Non-Host Resistance in Arabidopsis. Science *331*, 1185–1188.

Fan, M., Bai, M.-Y., Kim, J.-G., Wang, T., Oh, E., Chen, L., Park, C.H., Son, S.-H., Kim, S.-K., Mudgett, M.B., et al. (2014). The bHLH Transcription Factor HBI1 Mediates the Trade-Off between Growth and Pathogen-Associated Molecular Pattern–Triggered Immunity in Arabidopsis. Plant Cell Online *26*, 828–841.

Farid, A., Malinovsky, F.G., Veit, C., Schoberer, J., Zipfel, C., and Strasser, R. (2013). Specialized Roles of the Conserved Subunit OST3/6 of the Oligosaccharyltransferase Complex in Innate Immunity and Tolerance to Abiotic Stresses. Plant Physiol. *162*, 24–38.

Faulkner, C., Petutschnig, E., Benitez-Alfonso, Y., Beck, M., Robatzek, S., Lipka, V., and Maule, A.J. (2013). LYM2-dependent chitin perception limits molecular flux via plasmodesmata. Proc. Natl. Acad. Sci. *110*, 9166–9170.

Feinbaum, R.L., and Ausubel, F.M. (1988). Transcriptional regulation of the Arabidopsis thaliana chalcone synthase gene. Mol. Cell. Biol. *8*, 1985–1992.

Felix, G., and Boller, T. (2003). Molecular Sensing of Bacteria in Plants THE HIGHLY CONSERVED RNA-BINDING MOTIF RNP-1 OF BACTERIAL COLD SHOCK PROTEINS IS RECOGNIZED AS AN ELICITOR SIGNAL IN TOBACCO. J. Biol. Chem. *278*, 6201–6208.

Felix, G., Regenass, M., Spanu, P., and Boller, T. (1994). The protein phosphatase inhibitor calyculin A mimics elicitor action in plant cells and induces rapid hyperphosphorylation of specific proteins as revealed by pulse labeling with [33P]phosphate. Proc. Natl. Acad. Sci. *91*, 952–956.

Felix, G., Duran, J.D., Volko, S., and Boller, T. (1999). Plants have a sensitive perception system for the most conserved domain of bacterial flagellin. Plant J. *18*, 265–276.

Feng, F., Yang, F., Rong, W., Wu, X., Zhang, J., Chen, S., He, C., and Zhou, J.-M. (2012). A Xanthomonas uridine 5′-monophosphate transferase inhibits plant immune kinases. Nature *485*, 114–118.

Ferrari, S., Plotnikova, J.M., De Lorenzo, G., and Ausubel, F.M. (2003). Arabidopsis local resistance to Botrytis cinerea involves salicylic acid and camalexin and requires EDS4 and PAD2, but not SID2, EDS5 or PAD4. Plant J. *35*, 193–205.

Ferrari, S., Galletti, R., Denoux, C., Lorenzo, G.D., Ausubel, F.M., and Dewdney, J. (2007). Resistance to Botrytis cinerea Induced in Arabidopsis by Elicitors Is Independent of Salicylic Acid, Ethylene, or Jasmonate Signaling But Requires PHYTOALEXIN DEFICIENT3. Plant Physiol. *144*, 367–379.

Ferrari, S., Savatin, D.V., Sicilia, F., Gramegna, G., Cervone, F., and De Lorenzo, G. (2013). Oligogalacturonides: plant damage-associated molecular patterns and regulators of growth and development. Plant Physiol. *4*, 49.

Ferrer, J.-L., Austin, M.B., Stewart Jr., C., and Noel, J.P. (2008). Structure and function of enzymes involved in the biosynthesis of phenylpropanoids. Plant Physiol. Biochem. *46*, 356–370.

Fett, W.F., Osman, S.F., and Dunn, M.F. (1987). Auxin production by plant-pathogenic pseudomonads and xanthomonads. Appl. Environ. Microbiol. *53*, 1839–1845.

Feucht, W., Treutter, D., and Polster, J. (2004). Flavanol binding of nuclei from tree species. Plant Cell Rep. *22*, 430–436.

Field, B., Jordán, F., and Osbourn, A. (2006). First encounters – deployment of defence-related natural products by plants. New Phytol. *172*, 193–207.

Filipe, S.R., Tomasz, A., and Ligoxygakis, P. (2005). Requirements of peptidoglycan structure that allow detection by the Drosophila Toll pathway. EMBO Rep. *6*, 327–333.

Flors, V., Ton, J., Van Doorn, R., Jakab, G., García-Agustín, P., and Mauch-Mani, B. (2008). Interplay between JA, SA and ABA signalling during basal and induced resistance against Pseudomonas syringae and Alternaria brassicicola. Plant J. *54*, 81–92.

Forcat, S., Bennett, M., Grant, M., and Mansfield, J.W. (2010). Rapid linkage of indole carboxylic acid to the plant cell wall identified as a component of basal defence in Arabidopsis against hrp mutant bacteria. Phytochemistry *71*, 870–876.

Fradin, E.F., Zhang, Z., Ayala, J.C.J., Castroverde, C.D.M., Nazar, R.N., Robb, J., Liu, C.-M., and Thomma, B.P.H.J. (2009). Genetic Dissection of Verticillium Wilt Resistance Mediated by Tomato Ve1. Plant Physiol. *150*, 320–332.

Fraser, C.M., and Chapple, C. (2011). The Phenylpropanoid Pathway in Arabidopsis. Arab. Book Am. Soc. Plant Biol. *9*.

Fu, Z.Q., Guo, M., Jeong, B., Tian, F., Elthon, T.E., Cerny, R.L., Staiger, D., and Alfano, J.R. (2007). A type III effector ADP-ribosylates RNA-binding proteins and quells plant immunity. Nature *447*, 284–288.

Furukawa, T., Inagaki, H., Takai, R., Hirai, H., and Che, F.-S. (2013). Two Distinct EF-Tu Epitopes Induce Immune Responses in Rice and Arabidopsis. Mol. Plant. Microbe Interact. *27*, 113–124.

Gachon, C.M.M., Langlois-Meurinne, M., and Saindrenan, P. (2005). Plant secondary metabolism glycosyltransferases: the emerging functional analysis. Trends Plant Sci. *10*, 542–549.

Gallego-Bartolomé, J., Minguet, E.G., Grau-Enguix, F., Abbas, M., Locascio, A., Thomas, S.G., Alabadí, D., and Blázquez, M.A. (2012). Molecular mechanism for the interaction between gibberellin and brassinosteroid signaling pathways in Arabidopsis. Proc. Natl. Acad. Sci. *109*, 13446–13451.

Galletti, R., Denoux, C., Gambetta, S., Dewdney, J., Ausubel, F.M., Lorenzo, G.D., and Ferrari, S. (2008). The AtrbohD-Mediated Oxidative Burst Elicited by Oligogalacturonides in Arabidopsis Is Dispensable for the Activation of Defense Responses Effective against Botrytis cinerea. Plant Physiol. *148*, 1695–1706.

Gampala, S.S., Kim, T.-W., He, J.-X., Tang, W., Deng, Z., Bai, M.-Y., Guan, S., Lalonde, S., Sun, Y., Gendron, J.M., et al. (2007). An Essential Role for

14-3-3 Proteins in Brassinosteroid Signal Transduction in Arabidopsis. Dev. Cell *13*, 177–189.

Gao, X., Chen, X., Lin, W., Chen, S., Lu, D., Niu, Y., Li, L., Cheng, C., McCormack, M., Sheen, J., et al. (2013). Bifurcation of Arabidopsis NLR Immune Signaling via Ca2+-Dependent Protein Kinases. PLoS Pathog *9*, e1003127.

Gifford, J.L., Walsh, M.P., and Vogel, H.J. (2007). Structures and metal-ion-binding properties of the Ca2+-binding helix–loop–helix EF-hand motifs. Biochem. J. *405*, 199.

Gimenez-Ibanez, S., Hann, D.R., Ntoukakis, V., Petutschnig, E., Lipka, V., and Rathjen, J.P. (2009a). AvrPtoB Targets the LysM Receptor Kinase CERK1 to Promote Bacterial Virulence on Plants. Curr. Biol. *19*, 423–429.

Gimenez-Ibanez, S., Ntoukakis, V., and Rathjen, J.P. (2009b). The LysM receptor kinase CERK1 mediates bacterial perception in Arabidopsis. Plant Signal. Behav. *4*, 539–541.

Giska, F., Lichocka, M., Piechocki, M., Dadlez, M., Schmelzer, E., Hennig, J., and Krzymowska, M. (2013). Phosphorylation of HopQ1, a Type III Effector from Pseudomonas syringae, Creates a Binding Site for Host 14-3-3 Proteins. Plant Physiol. *161*, 2049–2061.

Gläßgen, W.E., Rose, A., Madlung, J., Koch, W., Gleitz, J., and Seitz, H.U. (1998). Regulation of enzymes involved in anthocyanin biosynthesis in carrot cell cultures in response to treatment with ultraviolet light and fungal elicitors. Planta *204*, 490–498.

Glazebrook, J., and Ausubel, F.M. (1994). Isolation of phytoalexin-deficient mutants of Arabidopsis thaliana and characterization of their interactions with bacterial pathogens. Proc. Natl. Acad. Sci. *91*, 8955–8959.

Glazebrook, J., Zook, M., Mert, F., Kagan, I., Rogers, E.E., Crute, I.R., Holub, E.B., Hammerschmidt, R., and Ausubel, F.M. (1997). Phytoalexin-Deficient Mutants of Arabidopsis Reveal That PAD4 Encodes a Regulatory Factor and That Four PAD Genes Contribute to Downy Mildew Resistance. Genetics *146*, 381–392.

Glickmann, E., Gardan, L., Jacquet, S., Hussain, S., Elasri, M., Petit, A., and Dessaux, Y. (1998). Auxin Production Is a Common Feature of Most Pathovars of Pseudomonas syringae. Mol. Plant. Microbe Interact. *11*, 156–162.

Göhre, V., Spallek, T., Häweker, H., Mersmann, S., Mentzel, T., Boller, T., de Torres, M., Mansfield, J.W., and Robatzek, S. (2008). Plant Pattern-

Recognition Receptor FLS2 Is Directed for Degradation by the Bacterial Ubiquitin Ligase AvrPtoB. Curr. Biol. *18*, 1824–1832.

Gómez-Gómez, L., and Boller, T. (2000). FLS2: An LRR Receptor–like Kinase Involved in the Perception of the Bacterial Elicitor Flagellin in Arabidopsis. Mol. Cell *5*, 1003–1011.

Gómez-Gómez, L., Felix, G., and Boller, T. (1999). A single locus determines sensitivity to bacterial flagellin in Arabidopsis thaliana. Plant J. *18*, 277–284.

Gómez-Gómez, L., Bauer, Z., and Boller, T. (2001). Both the Extracellular Leucine-Rich Repeat Domain and the Kinase Activity of FLS2 Are Required for Flagellin Binding and Signaling in Arabidopsis. Plant Cell Online *13*, 1155–1163.

Gonzalez, A., Zhao, M., Leavitt, J.M., and Lloyd, A.M. (2008). Regulation of the anthocyanin biosynthetic pathway by the TTG1/bHLH/Myb transcriptional complex in Arabidopsis seedlings. Plant J. *53*, 814–827.

Goodman, C.D., Casati, P., and Walbot, V. (2004). A Multidrug Resistance–Associated Protein Involved in Anthocyanin Transport in Zea mays. Plant Cell Online *16*, 1812–1826.

Grandmaison, J., and Ibrahim, R.K. (1995). Evidence for Nuclear Protein Binding of Flavonol Sulfate Esters in Flaveria chloraefolia. J. Plant Physiol. *147*, 653–660.

Grunewald, W., Smet, I.D., Lewis, D.R., Löfke, C., Jansen, L., Goeminne, G., Bossche, R.V., Karimi, M., Rybel, B.D., Vanholme, B., et al. (2012). Transcription factor WRKY23 assists auxin distribution patterns during Arabidopsis root development through local control on flavonol biosynthesis. Proc. Natl. Acad. Sci. *109,* 1554–1559.

Guo, M., Tian, F., Wamboldt, Y., and Alfano, J.R. (2009). The Majority of the Type III Effector Inventory of Pseudomonas syringae pv. tomato DC3000 Can Suppress Plant Immunity. Mol. Plant. Microbe Interact. *22*, 1069–1080.

Gust, A.A., and Felix, G. (2014). Receptor like proteins associate with SOBIR1-type of adaptors to form bimolecular receptor kinases. Curr. Opin. Plant Biol. *21*, 104–111.

Gust, A.A., Biswas, R., Lenz, H.D., Rauhut, T., Ranf, S., Kemmerling, B., Götz, F., Glawischnig, E., Lee, J., Felix, G., et al. (2007). Bacteria-derived Peptidoglycans Constitute Pathogen-associated Molecular Patterns Triggering Innate Immunity in Arabidopsis. J. Biol. Chem. *282*, 32338–32348.

Gust, A.A., Willmann, R., Desaki, Y., Grabherr, H.M., and Nürnberger, T. (2012). Plant LysM proteins: modules mediating symbiosis and immunity. Trends Plant Sci. *17*, 495–502.

Hagemeier, J., Schneider, B., Oldham, N.J., and Hahlbrock, K. (2001). Accumulation of soluble and wall-bound indolic metabolites in Arabidopsis thaliana leaves infected with virulent or avirulent Pseudomonas syringae pathovar tomato strains. Proc. Natl. Acad. Sci. *98*, 753–758.

Haglund, K., Di Fiore, P.P., and Dikic, I. (2003). Distinct monoubiquitin signals in receptor endocytosis. Trends Biochem. Sci. *28*, 598–604.

Halter, T., Imkampe, J., Mazzotta, S., Wierzba, M., Postel, S., Bücherl, C., Kiefer, C., Stahl, M., Chinchilla, D., Wang, X., et al. (2014). The Leucine-Rich Repeat Receptor Kinase BIR2 Is a Negative Regulator of BAK1 in Plant Immunity. Curr. Biol. *24*, 134–143.

Hamon, Y., Broccardo, C., Chambenoit, O., Luciani, M.-F., Toti, F., Chaslin, S., Freyssinet, J.-M., Devaux, P.F., McNeish, J., Marguet, D., et al. (2000). ABC1 promotes engulfment of apoptotic cells and transbilayer redistribution of phosphatidylserine. Nat. Cell Biol. *2*, 399–406.

Hann, D.R., and Rathjen, J.P. (2007). Early events in the pathogenicity of Pseudomonas syringae on Nicotiana benthamiana. Plant J. *49*, 607–618.

Hann, D.R., Domínguez-Ferreras, A., Motyka, V., Dobrev, P.I., Schornack, S., Jehle, A., Felix, G., Chinchilla, D., Rathjen, J.P., and Boller, T. (2014). The Pseudomonas type III effector HopQ1 activates cytokinin signaling and interferes with plant innate immunity. New Phytol. *201*, 585–598.

Haruta, M., Sabat, G., Stecker, K., Minkoff, B.B., and Sussman, M.R. (2014). A Peptide Hormone and Its Receptor Protein Kinase Regulate Plant Cell Expansion. Science *343*, 408–411.

Hasegawa, M., Mitsuhara, I., Seo, S., Imai, T., Koga, J., Okada, K., Yamane, H., and Ohashi, Y. (2010). Phytoalexin Accumulation in the Interaction Between Rice and the Blast Fungus. Mol. Plant. Microbe Interact. *23*, 1000–1011.

Hauck, P., Thilmony, R., and He, S.Y. (2003). A Pseudomonas syringae type III effector suppresses cell wall-based extracellular defense in susceptible Arabidopsis plants. Proc. Natl. Acad. Sci. *100*, 8577–8582.

Häweker, H., Rips, S., Koiwa, H., Salomon, S., Saijo, Y., Chinchilla, D., Robatzek, S., and Schaewen, A. von (2010). Pattern Recognition Receptors Require N-Glycosylation to Mediate Plant Immunity. J. Biol. Chem. *285*, 4629–4636.

Hayafune, M., Berisio, R., Marchetti, R., Silipo, A., Kayama, M., Desaki, Y., Arima, S., Squeglia, F., Ruggiero, A., Tokuyasu, K., et al. (2014). Chitin-induced activation of immune signaling by the rice receptor CEBiP relies on a unique sandwich-type dimerization. Proc. Natl. Acad. Sci. *111*, E404–E413.

He, X.-Z., and Dixon, R.A. (2000). Genetic Manipulation of Isoflavone 7-O-Methyltransferase Enhances Biosynthesis of 4′-O-Methylated Isoflavonoid Phytoalexins and Disease Resistance in Alfalfa. Plant Cell Online *12*, 1689–1702.

He, J.-X., Gendron, J.M., Yang, Y., Li, J., and Wang, Z.-Y. (2002). The GSK3-like kinase BIN2 phosphorylates and destabilizes BZR1, a positive regulator of the brassinosteroid signaling pathway in Arabidopsis. Proc. Natl. Acad. Sci. *99*, 10185–10190.

He, K., Gou, X., Yuan, T., Lin, H., Asami, T., Yoshida, S., Russell, S.D., and Li, J. (2007). BAK1 and BKK1 Regulate Brassinosteroid-Dependent Growth and Brassinosteroid-Independent Cell-Death Pathways. Curr. Biol. *17*, 1109–1115.

He, P., Shan, L., Lin, N.-C., Martin, G.B., Kemmerling, B., Nürnberger, T., and Sheen, J. (2006). Specific Bacterial Suppressors of MAMP Signaling Upstream of MAPKKK in Arabidopsis Innate Immunity. Cell *125*, 563–575.

Heese, A., Hann, D.R., Gimenez-Ibanez, S., Jones, A.M.E., He, K., Li, J., Schroeder, J.I., Peck, S.C., and Rathjen, J.P. (2007). The receptor-like kinase SERK3/BAK1 is a central regulator of innate immunity in plants. Proc. Natl. Acad. Sci. *104*, 12217–12222.

Heintzen, C., Nater, M., Apel, K., and Staiger, D. (1997). AtGRP7, a nuclear RNA-binding protein as a component of a circadian-regulated negative feedback loop in Arabidopsis thaliana. Proc. Natl. Acad. Sci. *94*, 8515–8520.

Hématy, K., Cherk, C., and Somerville, S. (2009). Host–pathogen warfare at the plant cell wall. Curr. Opin. Plant Biol. *12*, 406–413.

Hemmerlin, A. (2013). Post-translational events and modifications regulating plant enzymes involved in isoprenoid precursor biosynthesis. Plant Sci. *203–204*, 41–54.

Hemmerlin, A., Harwood, J.L., and Bach, T.J. (2012). A raison d'être for two distinct pathways in the early steps of plant isoprenoid biosynthesis? Prog. Lipid Res. *51*, 95–148.

Hernández, I., Alegre, L., Van Breusegem, F., and Munné-Bosch, S. (2009). How relevant are flavonoids as antioxidants in plants? Trends Plant Sci. *14*, 125–132.

Higgins, C.F. (1992). ABC Transporters: From Microorganisms to Man. Annu. Rev. Cell Biol. *8*, 67–113.

Higgins, C.F., and Linton, K.J. (2004). The ATP switch model for ABC transporters. Nat. Struct. Mol. Biol. *11*, 918–926.

Hirai, M.Y., Sugiyama, K., Sawada, Y., Tohge, T., Obayashi, T., Suzuki, A., Araki, R., Sakurai, N., Suzuki, H., Aoki, K., et al. (2007). Omics-based identification of Arabidopsis Myb transcription factors regulating aliphatic glucosinolate biosynthesis. Proc. Natl. Acad. Sci. *104*, 6478–6483.

Holton, N., Nekrasov, V., Ronald, P.C., and Zipfel, C. (2015). The Phylogenetically-Related Pattern Recognition Receptors EFR and XA21 Recruit Similar Immune Signaling Components in Monocots and Dicots. PLoS Pathog *11*, e1004602.

Hooper, A.M., Tsanuo, M.K., Chamberlain, K., Tittcomb, K., Scholes, J., Hassanali, A., Khan, Z.R., and Pickett, J.A. (2010). Isoschaftoside, a C-glycosylflavonoid from Desmodium uncinatum root exudate, is an allelochemical against the development of Striga. Phytochemistry *71*, 904–908.

Hoorn, R.A.L. van der, and Kamoun, S. (2008). From Guard to Decoy: A New Model for Perception of Plant Pathogen Effectors. Plant Cell Online *20*, 2009–2017.

Hou, S., Wang, X., Chen, D., Yang, X., Wang, M., Turrà, D., Di Pietro, A., and Zhang, W. (2014). The Secreted Peptide PIP1 Amplifies Immunity through Receptor-Like Kinase 7. PLoS Pathog *10*, e1004331.

Hrazdina, G., and Wagner, G.J. (1985). Metabolic pathways as enzyme complexes: Evidence for the synthesis of phenylpropanoids and flavonoids on membrane associated enzyme complexes. Arch. Biochem. Biophys. *237*, 88–100.

Huffaker, A., Pearce, G., and Ryan, C.A. (2006). An endogenous peptide signal in Arabidopsis activates components of the innate immune response. Proc. Natl. Acad. Sci. *103*, 10098–10103.

Hull, A.K., Vij, R., and Celenza, J.L. (2000). Arabidopsis cytochrome P450s that catalyze the first step of tryptophan-dependent indole-3-acetic acid biosynthesis. Proc. Natl. Acad. Sci. *97*, 2379–2384.

Huot, B., Yao, J., Montgomery, B.L., and He, S.Y. (2014). Growth–Defense Tradeoffs in Plants: A Balancing Act to Optimize Fitness. Mol. Plant *7*, 1267–1287.

Hutzler, P., Fischbach, R., Heller, W., Jungblut, T.P., Reuber, S., Schmitz, R., Veit, M., Weissenböck, G., and Schnitzler, J.-P. (1998). Tissue localization of phenolic compounds in plants by confocal laser scanning microscopy. J. Exp. Bot. *49*, 953–965.

Hyde, S.C., Emsley, P., Hartshorn, M.J., Mimmack, M.M., Gileadi, U., Pearce, S.R., Gallagher, M.P., Gill, D.R., Hubbard, R.E., and Higgins, C.F. (1990). Structural model of ATP-binding proteing associated with cystic fibrosis, multidrug resistance and bacterial transport. Nature *346*, 362–365.

Ibraheem, F., Gaffoor, I., and Chopra, S. (2010). Flavonoid Phytoalexin-Dependent Resistance to Anthracnose Leaf Blight Requires a Functional yellow seed1 in Sorghum bicolor. Genetics *184*, 915–926.

Ichimura, K., Casais, C., Peck, S.C., Shinozaki, K., and Shirasu, K. (2006). MEKK1 Is Required for MPK4 Activation and Regulates Tissue-specific and Temperature-dependent Cell Death in Arabidopsis. J. Biol. Chem. *281*, 36969–36976.

Ichino, T., Fuji, K., Ueda, H., Takahashi, H., Koumoto, Y., Takagi, J., Tamura, K., Sasaki, R., Aoki, K., Shimada, T., et al. (2014). GFS9/TT9 contributes to intracellular membrane trafficking and flavonoid accumulation in Arabidopsis thaliana. Plant J. n/a – n/a.

Igarashi, D., Tsuda, K., and Katagiri, F. (2012). The peptide growth factor, phytosulfokine, attenuates pattern-triggered immunity. Plant J. *71*, 194–204.

Iizasa, E., Mitsutomi, M., and Nagano, Y. (2010). Direct Binding of a Plant LysM Receptor-like Kinase, LysM RLK1/CERK1, to Chitin in Vitro. J. Biol. Chem. *285*, 2996–3004.

Ishiga, Y., Ishiga, T., Uppalapati, S.R., and Mysore, K.S. (2011). Arabidopsis seedling flood-inoculation technique: a rapid and reliable assay for studying plant-bacterial interactions. Plant Methods *7*, 32.

Ishihama, N., and Yoshioka, H. (2012). Post-translational regulation of WRKY transcription factors in plant immunity. Curr. Opin. Plant Biol. *15*, 431–437.

Ito, Y., Kaku, H., and Shibuya, N. (1997). Identification of a high-affinity binding protein for N-acetylchitooligosaccharide elicitor in the plasma membrane of suspension-cultured rice cells by affinity labeling. Plant J. *12*, 347–356.

Iven, T., König, S., Singh, S., Braus-Stromeyer, S.A., Bischoff, M., Tietze, L.F., Braus, G.H., Lipka, V., Feussner, I., and Dröge-Laser, W. (2012). Transcriptional Activation and Production of Tryptophan-Derived Secondary Metabolites in Arabidopsis Roots Contributes to the Defense against the

Fungal Vascular Pathogen Verticillium longisporum. Mol. Plant *5*, 1389–1402.

Jabs, T., Tschöpe, M., Colling, C., Hahlbrock, K., and Scheel, D. (1997). Elicitor-stimulated ion fluxes and O2− from the oxidative burst are essential components in triggering defense gene activation and phytoalexin synthesis in parsley. Proc. Natl. Acad. Sci. *94*, 4800–4805.

Jacobs, M., and Rubery, P.H. (1988). Naturally Occurring Auxin Transport Regulators. Science *241*, 346–349.

Jacobs, A.K., Lipka, V., Burton, R.A., Panstruga, R., Strizhov, N., Schulze-Lefert, P., and Fincher, G.B. (2003). An Arabidopsis Callose Synthase, GSL5, Is Required for Wound and Papillary Callose Formation. Plant Cell Online *15*, 2503–2513.

Janjusevic, R., Abramovitch, R.B., Martin, G.B., and Stebbins, C.E. (2006). A Bacterial Inhibitor of Host Programmed Cell Death Defenses Is an E3 Ubiquitin Ligase. Science *311*, 222–226.

Jasiński, M., Stukkens, Y., Degand, H., Purnelle, B., Marchand-Brynaert, J., and Boutry, M. (2001). A Plant Plasma Membrane ATP Binding Cassette–Type Transporter Is Involved in Antifungal Terpenoid Secretion. Plant Cell Online *13*, 1095–1107.

Jehle, A.K., Fürst, U., Lipschis, M., Albert, M., and Felix, G. (2013). Perception of the novel MAMP eMax from different Xanthomonas species requires the Arabidopsis receptor-like protein ReMAX and the receptor kinase SOBIR. Plant Signal. Behav. *8*, e27408.

Jeong, B., Lin, Y., Joe, A., Guo, M., Korneli, C., Yang, H., Wang, P., Yu, M., Cerny, R.L., Staiger, D., et al. (2011). Structure Function Analysis of an ADP-ribosyltransferase Type III Effector and Its RNA-binding Target in Plant Immunity. J. Biol. Chem. *286*, 43272–43281.

Jeong, Y.J., Shang, Y., Kim, B.H., Kim, S.Y., Song, J.H., Lee, J.S., Lee, M.M., Li, J., and Nam, K.H. (2010). BAK7 displays unequal genetic redundancy with BAK1 in brassinosteroid signaling and early senescence in arabidopsis. Mol. Cells *29*, 259–266.

Jeworutzki, E., Roelfsema, M.R.G., Anschütz, U., Krol, E., Elzenga, J.T.M., Felix, G., Boller, T., Hedrich, R., and Becker, D. (2010). Early signaling through the Arabidopsis pattern recognition receptors FLS2 and EFR involves Ca2+-associated opening of plasma membrane anion channels. Plant J. *62*, 367–378.

Jia, Y., McAdams, S.A., Bryan, G.T., Hershey, H.P., and Valent, B. (2000). Direct interaction of resistance gene and avirulence gene products confers rice blast resistance. EMBO J. *19*, 4004–4014.

Jia, Z., Zou, B., Wang, X., Qiu, J., Ma, H., Gou, Z., Song, S., and Dong, H. (2010). Quercetin-induced H2O2 mediates the pathogen resistance against Pseudomonas syringae pv. Tomato DC3000 in Arabidopsis thaliana. Biochem. Biophys. Res. Commun. *396*, 522–527.

Jiang, Y., Chen, X., Ding, X., Wang, Y., Chen, Q., and Song, W.-Y. (2013). The XA21 binding protein XB25 is required for maintaining XA21-mediated disease resistance. Plant J. *73*, 814–823.

Jin, H., Song, Z., and Nikolau, B.J. (2012). Reverse genetic characterization of two paralogous acetoacetyl CoA thiolase genes in Arabidopsis reveals their importance in plant growth and development. Plant J. *70*, 1015–1032.

Jones, J.D.G., and Dangl, J.L. (2006). The plant immune system. Nature *444*, 323–329.

Jones, P., Messner, B., Nakajima, J.-I., Schäffner, A.R., and Saito, K. (2003). UGT73C6 and UGT78D1, Glycosyltransferases Involved in Flavonol Glycoside Biosynthesis in Arabidopsis thaliana. J. Biol. Chem. *278*, 43910–43918.

Jonge, R. de, Esse, H.P. van, Maruthachalam, K., Bolton, M.D., Santhanam, P., Saber, M.K., Zhang, Z., Usami, T., Lievens, B., Subbarao, K.V., et al. (2012). Tomato immune receptor Ve1 recognizes effector of multiple fungal pathogens uncovered by genome and RNA sequencing. Proc. Natl. Acad. Sci. *109*, 5110–5115.

Joshi-Saha, A., Valon, C., and Leung, J. (2011). A Brand New START: Abscisic Acid Perception and Transduction in the Guard Cell. Sci. Signal. *4*, re4–re4.

Kadota, Y., Sklenar, J., Derbyshire, P., Stransfeld, L., Asai, S., Ntoukakis, V., Jones, J.D., Shirasu, K., Menke, F., Jones, A., et al. (2014). Direct Regulation of the NADPH Oxidase RBOHD by the PRR-Associated Kinase BIK1 during Plant Immunity. Mol. Cell *54*, 43–55.

Kaku, H., Nishizawa, Y., Ishii-Minami, N., Akimoto-Tomiyama, C., Dohmae, N., Takio, K., Minami, E., and Shibuya, N. (2006). Plant cells recognize chitin fragments for defense signaling through a plasma membrane receptor. Proc. Natl. Acad. Sci. *103*, 11086–11091.

Kang, J., Hwang, J.-U., Lee, M., Kim, Y.-Y., Assmann, S.M., Martinoia, E., and Lee, Y. (2010). PDR-type ABC transporter mediates cellular uptake of the phytohormone abscisic acid. Proc. Natl. Acad. Sci. *107*, 2355–2360.

Kang, J., Park, J., Choi, H., Burla, B., Kretzschmar, T., Lee, Y., and Martinoia, E. (2011). Plant ABC Transporters. Arab. Book e0153.

Kawchuk, L.M., Hachey, J., Lynch, D.R., Kulcsar, F., Rooijen, G. van, Waterer, D.R., Robertson, A., Kokko, E., Byers, R., Howard, R.J., et al. (2001). Tomato Ve disease resistance genes encode cell surface-like receptors. Proc. Natl. Acad. Sci. *98*, 6511–6515.

Keinath, N.F., Kierszniowska, S., Lorek, J., Bourdais, G., Kessler, S.A., Shimosato-Asano, H., Grossniklaus, U., Schulze, W.X., Robatzek, S., and Panstruga, R. (2010). PAMP (Pathogen-associated Molecular Pattern)-induced Changes in Plasma Membrane Compartmentalization Reveal Novel Components of Plant Immunity. J. Biol. Chem. *285*, 39140–39149.

Kemmerling, B., Schwedt, A., Rodriguez, P., Mazzotta, S., Frank, M., Qamar, S.A., Mengiste, T., Betsuyaku, S., Parker, J.E., Müssig, C., et al. (2007). The BRI1-Associated Kinase 1, BAK1, Has a Brassinolide-Independent Role in Plant Cell-Death Control. Curr. Biol. *17*, 1116–1122.

Kevei, Z., Lougnon, G., Mergaert, P., Horváth, G.V., Kereszt, A., Jayaraman, D., Zaman, N., Marcel, F., Regulski, K., Kiss, G.B., et al. (2007). 3-Hydroxy-3-Methylglutaryl Coenzyme A Reductase1 Interacts with NORK and Is Crucial for Nodulation in Medicago truncatula. Plant Cell Online *19*, 3974–3989.

Khan, Z.R., Midega, C.A.O., Bruce, T.J.A., Hooper, A.M., and Pickett, J.A. (2010). Exploiting phytochemicals for developing a "push–pull" crop protection strategy for cereal farmers in Africa. J. Exp. Bot. *61*, 4185–4196.

Kim, D.-Y., Bovet, L., Maeshima, M., Martinoia, E., and Lee, Y. (2007). The ABC transporter AtPDR8 is a cadmium extrusion pump conferring heavy metal resistance. Plant J. *50*, 207–218.

Kim, M.G., da Cunha, L., McFall, A.J., Belkhadir, Y., DebRoy, S., Dangl, J.L., and Mackey, D. (2005). Two Pseudomonas syringae Type III Effectors Inhibit RIN4-Regulated Basal Defense in Arabidopsis. Cell *121*, 749–759.

Kim, S., Yamaoka, Y., Ono, H., Kim, H., Shim, D., Maeshima, M., Martinoia, E., Cahoon, E.B., Nishida, I., and Lee, Y. (2013). AtABCA9 transporter supplies fatty acids for lipid synthesis to the endoplasmic reticulum. Proc. Natl. Acad. Sci. *110*, 773–778.

Kirik, V., Grini, P.E., Mathur, J., Klinkhammer, I., Adler, K., Bechtold, N., Herzog, M., Bonneville, J.-M., and Hülskamp, M. (2002). The Arabidopsis TUBULIN-FOLDING COFACTOR A Gene Is Involved in the Control of the α/β-Tubulin Monomer Balance. Plant Cell Online *14*, 2265–2276.

Kliebenstein, D.J., and Osbourn, A. (2012). Making new molecules – evolution of pathways for novel metabolites in plants. Curr. Opin. Plant Biol. *15*, 415–423.

Kliebenstein, D.J., Rowe, H.C., and Denby, K.J. (2005). Secondary metabolites influence Arabidopsis/Botrytis interactions: variation in host production and pathogen sensitivity. Plant J. *44*, 25–36.

Kobae, Y., Sekino, T., Yoshioka, H., Nakagawa, T., Martinoia, E., and Maeshima, M. (2006). Loss of AtPDR8, a Plasma Membrane ABC Transporter of Arabidopsis thaliana, Causes Hypersensitive Cell Death Upon Pathogen Infection. Plant Cell Physiol. *47*, 309–318.

Komori, R., Amano, Y., Ogawa-Ohnishi, M., and Matsubayashi, Y. (2009). Identification of tyrosylprotein sulfotransferase in Arabidopsis. Proc. Natl. Acad. Sci. *106*, 15067–15072.

Kong, Q., Qu, N., Gao, M., Zhang, Z., Ding, X., Yang, F., Li, Y., Dong, O.X., Chen, S., Li, X., et al. (2012). The MEKK1-MKK1/MKK2-MPK4 Kinase Cascade Negatively Regulates Immunity Mediated by a Mitogen-Activated Protein Kinase Kinase Kinase in Arabidopsis. Plant Cell Online *24*, 2225–2236.

Kosslak, R.M., Bookland, R., Barkei, J., Paaren, H.E., and Appelbaum, E.R. (1987). Induction of Bradyrhizobium japonicum common nod genes by isoflavones isolated from Glycine max. Proc. Natl. Acad. Sci. *84*, 7428–7432.

Kouzai, Y., Mochizuki, S., Nakajima, K., Desaki, Y., Hayafune, M., Miyazaki, H., Yokotani, N., Ozawa, K., Minami, E., Kaku, H., et al. (2014). Targeted Gene Disruption of OsCERK1 Reveals Its Indispensable Role in Chitin Perception and Involvement in the Peptidoglycan Response and Immunity in Rice. Mol. Plant. Microbe Interact. *27*, 975–982.

Krattinger, S.G., Lagudah, E.S., Spielmeyer, W., Singh, R.P., Huerta-Espino, J., McFadden, H., Bossolini, E., Selter, L.L., and Keller, B. (2009). A Putative ABC Transporter Confers Durable Resistance to Multiple Fungal Pathogens in Wheat. Science *323*, 1360–1363.

Kreuzaler, F., and Hahlbrock, K. (1972). Enzymatic synthesis of aromatic compounds in higher plants: Formation of naringenin (5,7,4′-trihydroxyflavanone) from p-coumaroyl coenzyme A and malonyl coenzyme A. FEBS Lett. *28*, 69–72.

Krol, E., Mentzel, T., Chinchilla, D., Boller, T., Felix, G., Kemmerling, B., Postel, S., Arents, M., Jeworutzki, E., Al-Rasheid, K.A.S., et al. (2010). Perception of the Arabidopsis Danger Signal Peptide 1 Involves the Pattern Recognition Receptor AtPEPR1 and Its Close Homologue AtPEPR2. J. Biol. Chem. *285*, 13471–13479.

Kroymann, J. (2011). Natural diversity and adaptation in plant secondary metabolism. Curr. Opin. Plant Biol. *14*, 246–251.

Krysan, P.J., Young, J.C., and Sussman, M.R. (1999). T-DNA as an Insertional Mutagen in Arabidopsis. Plant Cell Online *11*, 2283–2290.

Kubasek, W.L., Ausubel, F.M., and Shirley, B.W. (1998). A light-independent developmental mechanism potentiates flavonoid gene expression in Arabidopsis seedlings. Plant Mol. Biol. *37*, 217–223.

Kubori, T., Matsushima, Y., Nakamura, D., Uralil, J., Lara-Tejero, M., Sukhan, A., Galán, J.E., and Aizawa, S.-I. (1998). Supramolecular Structure of the Salmonella typhimurium Type III Protein Secretion System. Science *280*, 602–605.

Kudla, J., Batistič, O., and Hashimoto, K. (2010). Calcium Signals: The Lead Currency of Plant Information Processing. Plant Cell *22*, 541–563.

Kuhn, B.M., Geisler, M., Bigler, L., and Ringli, C. (2011). Flavonols Accumulate Asymmetrically and Affect Auxin Transport in Arabidopsis. Plant Physiol. *156*, 585–595.

Kunze, G., Zipfel, C., Robatzek, S., Niehaus, K., Boller, T., and Felix, G. (2004). The N Terminus of Bacterial Elongation Factor Tu Elicits Innate Immunity in Arabidopsis Plants. Plant Cell Online *16*, 3496–3507.

Kusano, M., Tohge, T., Fukushima, A., Kobayashi, M., Hayashi, N., Otsuki, H., Kondou, Y., Goto, H., Kawashima, M., Matsuda, F., et al. (2011). Metabolomics reveals comprehensive reprogramming involving two independent metabolic responses of Arabidopsis to UV-B light. Plant J. *67*, 354–369.

Kvitko, B.H., Park, D.H., Velásquez, A.C., Wei, C.-F., Russell, A.B., Martin, G.B., Schneider, D.J., and Collmer, A. (2009). Deletions in the Repertoire of Pseudomonas syringae pv. tomato DC3000 Type III Secretion Effector Genes Reveal Functional Overlap among Effectors. PLoS Pathog *5*, e1000388.

Lacombe, S., Rougon-Cardoso, A., Sherwood, E., Peeters, N., Dahlbeck, D., van Esse, H.P., Smoker, M., Rallapalli, G., Thomma, B.P.H.J., Staskawicz, B., et al. (2010). Interfamily transfer of a plant pattern-recognition receptor confers broad-spectrum bacterial resistance. Nat. Biotechnol. *28*, 365–369.

Laemmli, U.K. (1970). Cleavage of Structural Proteins during the Assembly of the Head of Bacteriophage T4. Nature *227*, 680–685.

Laluk, K., Luo, H., Chai, M., Dhawan, R., Lai, Z., and Mengiste, T. (2011). Biochemical and Genetic Requirements for Function of the Immune

Response Regulator BOTRYTIS-INDUCED KINASE1 in Plant Growth, Ethylene Signaling, and PAMP-Triggered Immunity in Arabidopsis. Plant Cell Online *23*, 2831–2849.

Lamb, C., and Dixon, R.A. (1997). The Oxidative Burst in Plant Disease Resistance. Annu. Rev. Plant Physiol. Plant Mol. Biol. *48*, 251–275.

Lamoral-Theys, D., Pottier, L., Dufrasne, F., Neve, J., Dubois, J., Kornienko, A., Kiss, R., and Ingrassia, L. (2010). Natural Polyphenols that Display Anticancer Properties through Inhibition of Kinase Activity. Curr. Med. Chem. *17*, 812–825.

Lange, B.M., and Ghassemian, M. (2003). Genome organization in Arabidopsis thaliana: a survey for genes involved in isoprenoid and chlorophyll metabolism. Plant Mol. Biol. *51*, 925–948.

Laughton, M.J., Halliwell, B., Evans, P.J., and Hoult, J.R. (1989). Antioxidant and pro-oxidant actions of the plant phenolics quercetin, gossypol and myricetin. Effects on lipid peroxidation, hydroxyl radical generation and bleomycin-dependent damage to DNA. Biochem. Pharmacol. *38*, 2859–2865.

Laule, O., Fürholz, A., Chang, H.-S., Zhu, T., Wang, X., Heifetz, P.B., Gruissem, W., and Lange, M. (2003). Crosstalk between cytosolic and plastidial pathways of isoprenoid biosynthesis in Arabidopsis thaliana. Proc. Natl. Acad. Sci. *100*, 6866–6871.

Le, M.H., Cao, Y., Zhang, X.-C., and Stacey, G. (2014). LIK1, A CERK1-Interacting Kinase, Regulates Plant Immune Responses in Arabidopsis. PLoS ONE *9*, e102245.

Lecourieux, D., Mazars, C., Pauly, N., Ranjeva, R., and Pugin, A. (2002). Analysis and Effects of Cytosolic Free Calcium Increases in Response to Elicitors in Nicotiana plumbaginifolia Cells. Plant Cell Online *14*, 2627–2641.

Lee, M., Lee, K., Lee, J., Noh, E.W., and Lee, Y. (2005). AtPDR12 Contributes to Lead Resistance in Arabidopsis. Plant Physiol. *138*, 827–836.

Levitzki, A., and Mishani, E. (2006). Tyrphostins and Other Tyrosine Kinase Inhibitors. Annu. Rev. Biochem. *75*, 93–109.

Lewis, D.R., Ramirez, M.V., Miller, N.D., Vallabhaneni, P., Ray, W.K., Helm, R.F., Winkel, B.S.J., and Muday, G.K. (2011). Auxin and Ethylene Induce Flavonol Accumulation through Distinct Transcriptional Networks. Plant Physiol. *156*, 144–164.

Li, S., and Zachgo, S. (2013). TCP3 interacts with R2R3-MYB proteins, promotes flavonoid biosynthesis and negatively regulates the auxin response in Arabidopsis thaliana. Plant J. *76*, 901–913.

Li, B., Lu, D., and Shan, L. (2014a). Ubiquitination of pattern recognition receptors in plant innate immunity. Mol. Plant Pathol. *15*, 737–746.

Li, J., Ou-Lee, T.M., Raba, R., Amundson, R.G., and Last, R.L. (1993). Arabidopsis Flavonoid Mutants Are Hypersensitive to UV-B Irradiation. Plant Cell Online *5*, 171–179.

Li, J., Wen, J., Lease, K.A., Doke, J.T., Tax, F.E., and Walker, J.C. (2002). BAK1, an Arabidopsis LRR Receptor-like Protein Kinase, Interacts with BRI1 and Modulates Brassinosteroid Signaling. Cell *110*, 213–222.

Li, J., Zhao-Hui, C., Batoux, M., Nekrasov, V., Roux, M., Chinchilla, D., Zipfel, C., and Jones, J.D.G. (2009). Specific ER quality control components required for biogenesis of the plant innate immune receptor EFR. Proc. Natl. Acad. Sci. U. S. A. *106*, 15973–15978.

Li, L., Li, M., Yu, L., Zhou, Z., Liang, X., Liu, Z., Cai, G., Gao, L., Zhang, X., Wang, Y., et al. (2014b). The FLS2-Associated Kinase BIK1 Directly Phosphorylates the NADPH Oxidase RbohD to Control Plant Immunity. Cell Host Microbe *15*, 329–338.

Li, Q.-F., Wang, C., Jiang, L., Li, S., Sun, S.S.M., and He, J.-X. (2012). An Interaction Between BZR1 and DELLAs Mediates Direct Signaling Crosstalk Between Brassinosteroids and Gibberellins in Arabidopsis. Sci. Signal. *5*, ra72–ra72.

Li, W., Yadeta, K.A., Elmore, J.M., and Coaker, G. (2013). The Pseudomonas syringae Effector HopQ1 Promotes Bacterial Virulence and Interacts with Tomato 14-3-3 Proteins in a Phosphorylation-Dependent Manner. Plant Physiol. *161*, 2062–2074.

Li, X., Lin, H., Zhang, W., Zou, Y., Zhang, J., Tang, X., and Zhou, J.-M. (2005). Flagellin induces innate immunity in nonhost interactions that is suppressed by Pseudomonas syringae effectors. Proc. Natl. Acad. Sci. U. S. A. *102*, 12990–12995.

Li, Y., Baldauf, S., Lim, E.-K., and Bowles, D.J. (2001). Phylogenetic Analysis of the UDP-glycosyltransferase Multigene Family of Arabidopsis thaliana. J. Biol. Chem. *276*, 4338–4343.

Li, Z.S., Zhao, Y., and Rea, P.A. (1995). Magnesium Adenosine 5[prime]-Triphosphate-Energized Transport of Glutathione-S-Conjugates by Plant Vacuolar Membrane Vesicles. Plant Physiol. *107*, 1257–1268.

Lichtenthaler, H.K., Rohmer, M., and Schwender, J. (1997). Two independent biochemical pathways for isopentenyl diphosphate and isoprenoid biosynthesis in higher plants. Physiol. Plant. *101*, 643–652.

Liebrand, T.W.H., Berg, G.C.M. van den, Zhang, Z., Smit, P., Cordewener, J.H.G., America, A.H.P., Sklenar, J., Jones, A.M.E., Tameling, W.I.L., Robatzek, S., et al. (2013). Receptor-like kinase SOBIR1/EVR interacts with receptor-like proteins in plant immunity against fungal infection. Proc. Natl. Acad. Sci. *110*, 10010–10015.

Lillo, C., Lea, U.S., and Ruoff, P. (2008). Nutrient depletion as a key factor for manipulating gene expression and product formation in different branches of the flavonoid pathway. Plant Cell Environ. *31*, 587–601.

Lin, W., Lu, D., Gao, X., Jiang, S., Ma, X., Wang, Z., Mengiste, T., He, P., and Shan, L. (2013). Inverse modulation of plant immune and brassinosteroid signaling pathways by the receptor-like cytoplasmic kinase BIK1. Proc. Natl. Acad. Sci. *110*, 12114–12119.

Lin, W., Li, B., Lu, D., Chen, S., Zhu, N., He, P., and Shan, L. (2014). Tyrosine phosphorylation of protein kinase complex BAK1/BIK1 mediates Arabidopsis innate immunity. Proc. Natl. Acad. Sci. *111*, 3632–3637.

Lindeberg, M., Cunnac, S., and Collmer, A. (2012). Pseudomonas syringae type III effector repertoires: last words in endless arguments. Trends Microbiol. *20*, 199–208.

Lipka, V., Dittgen, J., Bednarek, P., Bhat, R., Wiermer, M., Stein, M., Landtag, J., Brandt, W., Rosahl, S., Scheel, D., et al. (2005). Pre- and Postinvasion Defenses Both Contribute to Nonhost Resistance in Arabidopsis. Science *310*, 1180–1183.

Liu, Y., and Zhang, S. (2004). Phosphorylation of 1-Aminocyclopropane-1-Carboxylic Acid Synthase by MPK6, a Stress-Responsive Mitogen-Activated Protein Kinase, Induces Ethylene Biosynthesis in Arabidopsis. Plant Cell Online *16*, 3386–3399.

Liu, B., Li, J.-F., Ao, Y., Qu, J., Li, Z., Su, J., Zhang, Y., Liu, J., Feng, D., Qi, K., et al. (2012a). Lysin Motif–Containing Proteins LYP4 and LYP6 Play Dual Roles in Peptidoglycan and Chitin Perception in Rice Innate Immunity. Plant Cell Online *24*, 3406–3419.

Liu, H., Du, Y., Chu, H., Shih, C.H., Wong, Y.W., Wang, M., Chu, I.K., Tao, Y., and Lo, C. (2010). Molecular Dissection of the Pathogen-Inducible 3-Deoxyanthocyanidin Biosynthesis Pathway in Sorghum. Plant Cell Physiol. *51*, 1173–1185.

Liu, J., Elmore, J.M., Fuglsang, A.T., Palmgren, M.G., Staskawicz, B.J., and Coaker, G. (2009). RIN4 Functions with Plasma Membrane H+-ATPases to Regulate Stomatal Apertures during Pathogen Attack. PLoS Biol *7*, e1000139.

Liu, J., Ding, P., Sun, T., Nitta, Y., Dong, O., Huang, X., Yang, W., Li, X., Botella, J.R., and Zhang, Y. (2013a). Heterotrimeric G Proteins Serve as a Converging Point in Plant Defense Signaling Activated by Multiple Receptor-Like Kinases. Plant Physiol. *161*, 2146–2158.

Liu, T., Liu, Z., Song, C., Hu, Y., Han, Z., She, J., Fan, F., Wang, J., Jin, C., Chang, J., et al. (2012b). Chitin-Induced Dimerization Activates a Plant Immune Receptor. Science *336*, 1160–1164.

Liu, Z., Wu, Y., Yang, F., Zhang, Y., Chen, S., Xie, Q., Tian, X., and Zhou, J.-M. (2013b). BIK1 interacts with PEPRs to mediate ethylene-induced immunity. Proc. Natl. Acad. Sci. *110*, 6205–6210.

Lois M. Browne, K.L.C. (1991). The camalexins: New phytoalexins produced in the leaves of camelinasativa (cruciferae). Tetrahedron *47*, 3909–3914.

López-Gresa, M.P., Torres, C., Campos, L., Lisón, P., Rodrigo, I., Bellés, J.M., and Conejero, V. (2011). Identification of defence metabolites in tomato plants infected by the bacterial pathogen Pseudomonas syringae. Environ. Exp. Bot. *74*, 216–228.

Lorenzen, M., Racicot, V., Strack, D., and Chapple, C. (1996). Sinapic Acid Ester Metabolism in Wild Type and a Sinapoylglucose-Accumulating Mutant of Arabidopsis. Plant Physiol. *112*, 1625–1630.

Lozano-Durán, R., Macho, A.P., Boutrot, F., Segonzac, C., Somssich, I.E., and Zipfel, C. (2013). The transcriptional regulator BZR1 mediates trade-off between plant innate immunity and growth. eLife *2*, e00983.

Lozano-Durán, R., Bourdais, G., He, S.Y., and Robatzek, S. (2014). The bacterial effector HopM1 suppresses PAMP-triggered oxidative burst and stomatal immunity. New Phytol. *202*, 259–269.

Lozoya, E., Block, A., Lois, R., Hahlbrock, K., and Scheel, D. (1991). Transcriptional repression of light-induced flavonoid synthesis by elicitor treatment of cultured parsley cells. Plant J. *1*, 227–234.

Lu, D., Wu, S., Gao, X., Zhang, Y., Shan, L., and He, P. (2010). A receptor-like cytoplasmic kinase, BIK1, associates with a flagellin receptor complex to initiate plant innate immunity. Proc. Natl. Acad. Sci. *107*, 496–501.

Lu, D., Lin, W., Gao, X., Wu, S., Cheng, C., Avila, J., Heese, A., Devarenne, T.P., He, P., and Shan, L. (2011). Direct Ubiquitination of Pattern Recognition Receptor FLS2 Attenuates Plant Innate Immunity. Science *332*, 1439–1442.

Lu, X., Tintor, N., Mentzel, T., Kombrink, E., Boller, T., Robatzek, S., Schulze-Lefert, P., and Saijo, Y. (2009). Uncoupling of sustained MAMP

receptor signaling from early outputs in an Arabidopsis endoplasmic reticulum glucosidase II allele. Proc. Natl. Acad. Sci. *106*, 22522–22527.

Lumbreras, V., Campos, N., and Boronat, A. (1995). The use of an alternative promoter in the Arabidopsis thaliana HMG1 gene generates an mRNA that encodes a novel 3-hydroxy-3-methylglutaryl coenzyme A reductase isoform with an extended N-terminal region. Plant J. *8*, 541–549.

Macho, A.P., and Zipfel, C. (2014). Plant PRRs and the Activation of Innate Immune Signaling. Mol. Cell *54*, 263–272.

Macho, A.P., Boutrot, F., Rathjen, J.P., and Zipfel, C. (2012). ASPARTATE OXIDASE Plays an Important Role in Arabidopsis Stomatal Immunity. Plant Physiol. *159*, 1845–1856.

Macho, A.P., Schwessinger, B., Ntoukakis, V., Brutus, A., Segonzac, C., Roy, S., Kadota, Y., Oh, M.-H., Sklenar, J., Derbyshire, P., et al. (2014). A Bacterial Tyrosine Phosphatase Inhibits Plant Pattern Recognition Receptor Activation. Science *343*, 1509–1512.

MacKintosh, C., Lyon, G.D., and MacKintosh, R.W. (1994). Protein phosphatase inhibitors activate anti-fungal defence responses of soybean cotyledons and cell cultures. Plant J. *5*, 137–147.

Malinovsky, F.G., Batoux, M., Schwessinger, B., Youn, J.H., Stransfeld, L., Win, J., Kim, S.-K., and Zipfel, C. (2014a). Antagonistic Regulation of Growth and Immunity by the Arabidopsis Basic Helix-Loop-Helix Transcription Factor HOMOLOG OF BRASSINOSTEROID ENHANCED EXPRESSION2 INTERACTING WITH INCREASED LEAF INCLINATION1 BINDING bHLH1. Plant Physiol. *164*, 1443–1455.

Malinovsky, F.G., Fangel, J.U., and Willats, W.G.T. (2014b). The role of the cell wall in plant immunity. Plant-Microbe Interact. *5*, 178.

Manzano, D., Fernández-Busquets, X., Schaller, H., González, V., Boronat, A., Arró, M., and Ferrer, A. (2004). The metabolic imbalance underlying lesion formation in Arabidopsis thaliana overexpressing farnesyl diphosphate synthase (isoform 1S) leads to oxidative stress and is triggered by the developmental decline of endogenous HMGR activity. Planta *219*, 982–992.

Mao, G., Meng, X., Liu, Y., Zheng, Z., Chen, Z., and Zhang, S. (2011). Phosphorylation of a WRKY Transcription Factor by Two Pathogen-Responsive MAPKs Drives Phytoalexin Biosynthesis in Arabidopsis. Plant Cell Online *23*, 1639–1653.

Maresova, L., and Sychrova, H. (2005). Physiological characterization of Saccharomyces cerevisiae kha1 deletion mutants. Mol. Microbiol. *55*, 588–600.

Marino, D., Dunand, C., Puppo, A., and Pauly, N. (2012). A burst of plant NADPH oxidases. Trends Plant Sci. *17*, 9–15.

Marinova, K., Pourcel, L., Weder, B., Schwarz, M., Barron, D., Routaboul, J.-M., Debeaujon, I., and Klein, M. (2007). The Arabidopsis MATE Transporter TT12 Acts as a Vacuolar Flavonoid/H+-Antiporter Active in Proanthocyanidin-Accumulating Cells of the Seed Coat. Plant Cell Online *19*, 2023–2038.

Martens, S., Preuß, A., and Matern, U. (2010). Multifunctional flavonoid dioxygenases: Flavonol and anthocyanin biosynthesis in Arabidopsis thaliana L. Phytochemistry *71*, 1040–1049.

Martinoia, E., Grill, E., Tommasini, R., Kreuz, K., and Amrhein, N. (1993). ATP-dependent glutathione S-conjugate "export" pump in the vacuolar membrane of plants. Nature *364*, 247–249.

Mäser, P., Thomine, S., Schroeder, J.I., Ward, J.M., Hirschi, K., Sze, H., Talke, I.N., Amtmann, A., Maathuis, F.J.M., Sanders, D., et al. (2001). Phylogenetic Relationships within Cation Transporter Families of Arabidopsis. Plant Physiol. *126*, 1646–1667.

Matsubayashi, Y., and Sakagami, Y. (1996). Phytosulfokine, sulfated peptides that induce the proliferation of single mesophyll cells of Asparagus officinalis L. Proc. Natl. Acad. Sci. *93*, 7623–7627.

Matsubayashi, Y., and Sakagami, Y. (2006). Peptide Hormones in Plants. Annu. Rev. Plant Biol. *57*, 649–674.

Matsubayashi, Y., Ogawa, M., Morita, A., and Sakagami, Y. (2002). An LRR Receptor Kinase Involved in Perception of a Peptide Plant Hormone, Phytosulfokine. Science *296*, 1470–1472.

Matsubayashi, Y., Ogawa, M., Kihara, H., Niwa, M., and Sakagami, Y. (2006). Disruption and Overexpression of Arabidopsis Phytosulfokine Receptor Gene Affects Cellular Longevity and Potential for Growth. Plant Physiol. *142*, 45–53.

McDonald, C., Inohara, N., and Nuñez, G. (2005). Peptidoglycan Signaling in Innate Immunity and Inflammatory Disease. J. Biol. Chem. *280*, 20177–20180.

Mehrtens, F., Kranz, H., Bednarek, P., and Weisshaar, B. (2005). The Arabidopsis Transcription Factor MYB12 Is a Flavonol-Specific Regulator of Phenylpropanoid Biosynthesis. Plant Physiol. *138*, 1083–1096.

Melotto, M., Underwood, W., Koczan, J., Nomura, K., and He, S.Y. (2006). Plant Stomata Function in Innate Immunity against Bacterial Invasion. Cell *126*, 969–980.

Melotto, M., Underwood, W., and He, S.Y. (2008). Role of Stomata in Plant Innate Immunity and Foliar Bacterial Diseases. Annu. Rev. Phytopathol. *46*, 101–122.

Meng, X., and Zhang, S. (2013). MAPK Cascades in Plant Disease Resistance Signaling. Annu. Rev. Phytopathol. *51*, 245–266.

Merlot, S., Leonhardt, N., Fenzi, F., Valon, C., Costa, M., Piette, L., Vavasseur, A., Genty, B., Boivin, K., Müller, A., et al. (2007). Constitutive activation of a plasma membrane H+-ATPase prevents abscisic acid-mediated stomatal closure. EMBO J. *26*, 3216–3226.

Mersmann, S., Bourdais, G., Rietz, S., and Robatzek, S. (2010). Ethylene Signaling Regulates Accumulation of the FLS2 Receptor and Is Required for the Oxidative Burst Contributing to Plant Immunity. Plant Physiol. *154*, 391–400.

Metodiewa, D., Jaiswal, A.K., Cenas, N., Dickancaité, E., and Segura-Aguilar, J. (1999). Quercetin may act as a cytotoxic prooxidant after its metabolic activation to semiquinone and quinoidal product. Free Radic. Biol. Med. *26*, 107–116.

Mikkelsen, M.D., Hansen, C.H., Wittstock, U., and Halkier, B.A. (2000). Cytochrome P450 CYP79B2 from Arabidopsis Catalyzes the Conversion of Tryptophan to Indole-3-acetaldoxime, a Precursor of Indole Glucosinolates and Indole-3-acetic Acid. J. Biol. Chem. *275*, 33712–33717.

Millet, Y.A., Danna, C.H., Clay, N.K., Songnuan, W., Simon, M.D., Werck-Reichhart, D., and Ausubel, F.M. (2010). Innate Immune Responses Activated in Arabidopsis Roots by Microbe-Associated Molecular Patterns. Plant Cell Online *22*, 973–990.

Mitchell, K., Brown, I., Knox, P., and Mansfield, J. (2014). The role of cell wall-based defences in the early restriction of non-pathogenic hrp mutant bacteria in Arabidopsis. Phytochemistry.

Mittler, R., Vanderauwera, S., Suzuki, N., Miller, G., Tognetti, V.B., Vandepoele, K., Gollery, M., Shulaev, V., and Van Breusegem, F. (2011). ROS signaling: the new wave? Trends Plant Sci. *16*, 300–309.

Miya, A., Albert, P., Shinya, T., Desaki, Y., Ichimura, K., Shirasu, K., Narusaka, Y., Kawakami, N., Kaku, H., and Shibuya, N. (2007). CERK1, a LysM receptor kinase, is essential for chitin elicitor signaling in Arabidopsis. Proc. Natl. Acad. Sci. *104*, 19613–19618.

Mo, Y., Nagel, C., and Taylor, L.P. (1992). Biochemical complementation of chalcone synthase mutants defines a role for flavonols in functional pollen. Proc. Natl. Acad. Sci. *89*, 7213–7217.

Monaghan, J., Matschi, S., Shorinola, O., Rovenich, H., Matei, A., Segonzac, C., Malinovsky, F.G., Rathjen, J.P., MacLean, D., Romeis, T., et al. (2014). The Calcium-Dependent Protein Kinase CPK28 Buffers Plant Immunity and Regulates BIK1 Turnover. Cell Host Microbe *16*, 605–615.

Montamat, F., Guilloton, M., Karst, F., and Delrot, S. (1995). Isolation and characterization of a cDNA encoding Arabidopsis thaliana 3-hydroxy-3-methylglutaryl-coenzyme A synthase. Gene *167*, 197–201.

Montillet, J.-L., Leonhardt, N., Mondy, S., Tranchimand, S., Rumeau, D., Boudsocq, M., Garcia, A.V., Douki, T., Bigeard, J., Laurière, C., et al. (2013). An Abscisic Acid-Independent Oxylipin Pathway Controls Stomatal Closure and Immune Defense in Arabidopsis. PLoS Biol *11*, e1001513.

Mott, G.A., Middleton, M.A., Desveaux, D., and Guttman, D.S. (2014). Peptides and small molecules of the plant-pathogen apoplastic arena. Plant Physiol. *5*, 677.

Mouradov, A., and Spangenberg, G. (2014). Flavonoids: a metabolic network mediating plants adaptation to their real estate. Plant Metab. Chemodiversity *5*, 620.

Mueller, L.A., Goodman, C.D., Silady, R.A., and Walbot, V. (2000). AN9, a Petunia Glutathione S-Transferase Required for Anthocyanin Sequestration, Is a Flavonoid-Binding Protein. Plant Physiol. *123*, 1561–1570.

Mur, L.A.J., Kenton, P., Lloyd, A.J., Ougham, H., and Prats, E. (2008). The hypersensitive response; the centenary is upon us but how much do we know? J. Exp. Bot. *59*, 501–520.

Murphy, A., Peer, W.A., and Taiz, L. (2000). Regulation of auxin transport by aminopeptidases and endogenous flavonoids. Planta *211*, 315–324.

Murphy, A.S., Bandyopadhyay, A., Holstein, S.E., and Peer, W.A. (2005). Endocytotic Cycling of Pm Proteins. Annu. Rev. Plant Biol. *56*, 221–251.

Nafisi, M., Goregaoker, S., Botanga, C.J., Glawischnig, E., Olsen, C.E., Halkier, B.A., and Glazebrook, J. (2007). Arabidopsis Cytochrome P450 Monooxygenase 71A13 Catalyzes the Conversion of Indole-3-Acetaldoxime in Camalexin Synthesis. Plant Cell Online *19*, 2039–2052.

Naito, K., Taguchi, F., Suzuki, T., Inagaki, Y., Toyoda, K., Shiraishi, T., and Ichinose, Y. (2008). Amino Acid Sequence of Bacterial Microbe-Associated Molecular Pattern flg22 Is Required for Virulence. Mol. Plant. Microbe Interact. *21*, 1165–1174.

Nakagami, H., Soukupová, H., Schikora, A., Zárský, V., and Hirt, H. (2006). A Mitogen-activated Protein Kinase Kinase Kinase Mediates Reactive Oxygen Species Homeostasis in Arabidopsis. J. Biol. Chem. *281*, 38697–38704.

Nakagawa, T., Kurose, T., Hino, T., Tanaka, K., Kawamukai, M., Niwa, Y., Toyooka, K., Matsuoka, K., Jinbo, T., and Kimura, T. (2007). Development of series of gateway binary vectors, pGWBs, for realizing efficient construction of fusion genes for plant transformation. J. Biosci. Bioeng. *104*, 34–41.

Nam, K.H., and Li, J. (2002). BRI1/BAK1, a Receptor Kinase Pair Mediating Brassinosteroid Signaling. Cell *110*, 203–212.

Naoumkina, M.A., Zhao, Q., Gallego-Giraldo, L., Dai, X., Zhao, P.X., and Dixon, R.A. (2010). Genome-wide analysis of phenylpropanoid defence pathways. Mol. Plant Pathol. *11*, 829–846.

Navarro, L., Dunoyer, P., Jay, F., Arnold, B., Dharmasiri, N., Estelle, M., Voinnet, O., and Jones, J.D.G. (2006). A Plant miRNA Contributes to Antibacterial Resistance by Repressing Auxin Signaling. Science *312*, 436–439.

Navarro, L., Bari, R., Achard, P., Lisón, P., Nemri, A., Harberd, N.P., and Jones, J.D.G. (2008). DELLAs Control Plant Immune Responses by Modulating the Balance of Jasmonic Acid and Salicylic Acid Signaling. Curr. Biol. *18*, 650–655.

Nawrath, C., and Métraux, J.-P. (1999). Salicylic Acid Induction–Deficient Mutants of Arabidopsis Express PR-2 and PR-5 and Accumulate High Levels of Camalexin after Pathogen Inoculation. Plant Cell Online *11*, 1393–1404.

Nekrasov, V., Li, J., Batoux, M., Roux, M., Chu, Z.-H., Lacombe, S., Rougon, A., Bittel, P., Kiss-Papp, M., Chinchilla, D., et al. (2009). Control of the pattern-recognition receptor EFR by an ER protein complex in plant immunity. EMBO J. *28*, 3428–3438.

Nguyen, H.P., Chakravarthy, S., Velásquez, A.C., McLane, H.L., Zeng, L., Nakayashiki, H., Park, D.-H., Collmer, A., and Martin, G.B. (2010). Methods to Study PAMP-Triggered Immunity Using Tomato and Nicotiana benthamiana. Mol. Plant. Microbe Interact. *23*, 991–999.

Nicaise, V., Roux, M., and Zipfel, C. (2009). Recent Advances in PAMP-Triggered Immunity against Bacteria: Pattern Recognition Receptors Watch over and Raise the Alarm. Plant Physiol. *150*, 1638–1647.

Nicaise, V., Joe, A., Jeong, B., Korneli, C., Boutrot, F., Westedt, I., Staiger, D., Alfano, J.R., and Zipfel, C. (2013). Pseudomonas HopU1 modulates plant immune receptor levels by blocking the interaction of their mRNAs with GRP7. EMBO J. *32*, 701–712.

Nishimura, M.T., Stein, M., Hou, B.-H., Vogel, J.P., Edwards, H., and Somerville, S.C. (2003). Loss of a Callose Synthase Results in Salicylic Acid-Dependent Disease Resistance. Science *301*, 969–972.

Nomura, K., DebRoy, S., Lee, Y.H., Pumplin, N., Jones, J., and He, S.Y. (2006). A Bacterial Virulence Protein Suppresses Host Innate Immunity to Cause Plant Disease. Science *313*, 220–223.

Nomura, K., Mecey, C., Lee, Y.-N., Imboden, L.A., Chang, J.H., and He, S.Y. (2011). Effector-triggered immunity blocks pathogen degradation of an immunity-associated vesicle traffic regulator in Arabidopsis. Proc. Natl. Acad. Sci. *108*, 10774–10779.

Nühse, T.S., Peck, S.C., Hirt, H., and Boller, T. (2000). Microbial Elicitors Induce Activation and Dual Phosphorylation of the Arabidopsis thaliana MAPK 6. J. Biol. Chem. *275*, 7521–7526.

Nühse, T.S., Bottrill, A.R., Jones, A.M.E., and Peck, S.C. (2007). Quantitative phosphoproteomic analysis of plasma membrane proteins reveals regulatory mechanisms of plant innate immune responses. Plant J. *51*, 931–940.

Nürnberger, T., Nennstiel, D., Jabs, T., Sacks, W.R., Hahlbrock, K., and Scheel, D. (1994). High affinity binding of a fungal oligopeptide elicitor to parsley plasma membranes triggers multiple defense responses. Cell *78*, 449–460.

Nürnberger, T., Brunner, F., Kemmerling, B., and Piater, L. (2004). Innate immunity in plants and animals: striking similarities and obvious differences. Immunol. Rev. *198*, 249–266.

O'Brien, J.A., Daudi, A., Butt, V.S., and Bolwell, G.P. (2012). Reactive oxygen species and their role in plant defence and cell wall metabolism. Planta *236*, 765–779.

Ogasawara, Y., Kaya, H., Hiraoka, G., Yumoto, F., Kimura, S., Kadota, Y., Hishinuma, H., Senzaki, E., Yamagoe, S., Nagata, K., et al. (2008). Synergistic Activation of the Arabidopsis NADPH Oxidase AtrbohD by Ca2+ and Phosphorylation. J. Biol. Chem. *283*, 8885–8892.

Oh, H.-S., and Collmer, A. (2005). Basal resistance against bacteria in Nicotiana benthamiana leaves is accompanied by reduced vascular staining and suppressed by multiple Pseudomonas syringae type III secretion system effector proteins. Plant J. *44*, 348–359.

Oh, E., Zhu, J.-Y., and Wang, Z.-Y. (2012). Interaction between BZR1 and PIF4 integrates brassinosteroid and environmental responses. Nat. Cell Biol. *14*, 802–809.

Oh, H.-S., Park, D.H., and Collmer, A. (2010). Components of the Pseudomonas syringae Type III Secretion System Can Suppress and May Elicit Plant Innate Immunity. Mol. Plant. Microbe Interact. *23*, 727–739.

Ohyama, K., Suzuki, M., Masuda, K., Yoshida, S., and Muranaka, T. (2007). Chemical Phenotypes of the hmg1 and hmg2 Mutants of Arabidopsis Demonstrate the In-planta Role of HMG-CoA Reductase in Triterpene Biosynthesis. Chem. Pharm. Bull. (Tokyo) *55*, 1518–1521.

Oldroyd, G.E.D. (2013). Speak, friend, and enter: signalling systems that promote beneficial symbiotic associations in plants. Nat. Rev. Microbiol. *11*, 252–263.

Olsen, K.M., Slimestad, R., Lea, U.S., Brede, C., Løvdal, T., Ruoff, P., Verheul, M., and Lillo, C. (2009). Temperature and nitrogen effects on regulators and products of the flavonoid pathway: experimental and kinetic model studies. Plant Cell Environ. *32*, 286–299.

O'Malley, R.C., and Ecker, J.R. (2010). Linking genotype to phenotype using the Arabidopsis unimutant collection. Plant J. *61*, 928–940.

Østergaard, L., Petersen, M., Mattsson, O., and Mundy, J. (2002). An Arabidopsis callose synthase. Plant Mol. Biol. *49*, 559–566.

Owens, D.K., Crosby, K.C., Runac, J., Howard, B.A., and Winkel, B.S.J. (2008a). Biochemical and genetic characterization of Arabidopsis flavanone 3β-hydroxylase. Plant Physiol. Biochem. *46*, 833–843.

Owens, D.K., Alerding, A.B., Crosby, K.C., Bandara, A.B., Westwood, J.H., and Winkel, B.S.J. (2008b). Functional Analysis of a Predicted Flavonol Synthase Gene Family in Arabidopsis. Plant Physiol. *147*, 1046–1061.

Palme, K., and Gälweiler, L. (1999). PIN-pointing the molecular basis of auxin transport. Curr. Opin. Plant Biol. *2*, 375–381.

Pardo, J.M., Cubero, B., Leidi, E.O., and Quintero, F.J. (2006). Alkali cation exchangers: roles in cellular homeostasis and stress tolerance. J. Exp. Bot. *57*, 1181–1199.

Park, C.-J., Peng, Y., Chen, X., Dardick, C., Ruan, D., Bart, R., Canlas, P.E., and Ronald, P.C. (2008). Rice XB15, a Protein Phosphatase 2C, Negatively Regulates Cell Death and XA21-Mediated Innate Immunity. PLoS Biol *6*, e231.

Pearce, G., Moura, D.S., Stratmann, J., and Ryan, C.A. (2001a). RALF, a 5-kDa ubiquitous polypeptide in plants, arrests root growth and development. Proc. Natl. Acad. Sci. *98*, 12843–12847.

Pearce, G., Moura, D.S., Stratmann, J., and Ryan, C.A. (2001b). Production of multiple plant hormones from a single polyprotein precursor. Nature *411*, 817–820.

Peer, W.A., and Murphy, A.S. (2007). Flavonoids and auxin transport: modulators or regulators? Trends Plant Sci. *12*, 556–563.

Peer, W.A., Brown, D.E., Tague, B.W., Muday, G.K., Taiz, L., and Murphy, A.S. (2001). Flavonoid Accumulation Patterns of Transparent Testa Mutants of Arabidopsis. Plant Physiol. *126*, 536–548.

Peer, W.A., Bandyopadhyay, A., Blakeslee, J.J., Makam, S.N., Chen, R.J., Masson, P.H., and Murphy, A.S. (2004). Variation in Expression and Protein Localization of the PIN Family of Auxin Efflux Facilitator Proteins in Flavonoid Mutants with Altered Auxin Transport in Arabidopsis thaliana. Plant Cell Online *16*, 1898–1911.

Pel, M.J.C., and Pieterse, C.M.J. (2012). Microbial recognition and evasion of host immunity. J. Exp. Bot. ers262.

Pelletier, M.K., and Shirley, B.W. (1996). Analysis of Flavanone 3-Hydroxylase in Arabidopsis Seedlings (Coordinate Regulation with Chalcone Synthase and Chalcone Isomerase). Plant Physiol. *111*, 339–345.

Pelletier, M.K., Murrell, J.R., and Shirley, B.W. (1997). Characterization of Flavonol Synthase and Leucoanthocyanidin Dioxygenase Genes in Arabidopsis (Further Evidence for Differential Regulation of "Early" and "Late" Genes). Plant Physiol. *113*, 1437–1445.

Pelletier, M.K., Burbulis, I.E., and Winkel-Shirley, B. (1999). Disruption of specific flavonoid genes enhances the accumulation of flavonoid enzymes and end-products in Arabidopsis seedlings. Plant Mol. Biol. *40*, 45–54.

Peng, J., Carol, P., Richards, D.E., King, K.E., Cowling, R.J., Murphy, G.P., and Harberd, N.P. (1997). The Arabidopsis GAI gene defines a signaling pathway that negatively regulates gibberellin responses. Genes Dev. *11*, 3194–3205.

Peng, Y., Bartley, L.E., Chen, X., Dardick, C., Chern, M., Ruan, R., Canlas, P.E., and Ronald, P.C. (2008). OsWRKY62 is a Negative Regulator of Basal and Xa21-Mediated Defense against Xanthomonas oryzae pv. oryzae in Rice. Mol. Plant *1*, 446–458.

Peters, N.K., and Long, S.R. (1988). Alfalfa Root Exudates and Compounds which Promote or Inhibit Induction of Rhizobium meliloti Nodulation Genes. Plant Physiol. *88*, 396–400.

Peters, N.K., Frost, J.W., and Long, S.R. (1986). A plant flavone, luteolin, induces expression of Rhizobium meliloti nodulation genes. Science *233*, 977–980.

Petrussa, E., Braidot, E., Zancani, M., Peresson, C., Bertolini, A., Patui, S., and Vianello, A. (2013). Plant Flavonoids—Biosynthesis, Transport and Involvement in Stress Responses. Int. J. Mol. Sci. *14*, 14950–14973.

Petutschnig, E.K., Jones, A.M.E., Serazetdinova, L., Lipka, U., and Lipka, V. (2010). The Lysin Motif Receptor-like Kinase (LysM-RLK) CERK1 Is a Major Chitin-binding Protein in Arabidopsis thaliana and Subject to Chitin-induced Phosphorylation. J. Biol. Chem. *285*, 28902–28911.

Pfund, C., Tans-Kersten, J., Dunning, F.M., Alonso, J.M., Ecker, J.R., Allen, C., and Bent, A.F. (2004). Flagellin Is Not a Major Defense Elicitor in Ralstonia solanacearum Cells or Extracts Applied to Arabidopsis thaliana. Mol. Plant. Microbe Interact. *17*, 696–706.

Piasecka, A., Jedrzejczak-Rey, N., and Bednarek, P. (2015). Secondary metabolites in plant innate immunity: conserved function of divergent chemicals. New Phytol. n/a – n/a.

Pieterse, C.M.J., Van der Does, D., Zamioudis, C., Leon-Reyes, A., and Van Wees, S.C.M. (2012). Hormonal Modulation of Plant Immunity. Annu. Rev. Cell Dev. Biol. *28*, 489–521.

Pittman, J. (2012). Multiple transport pathways for mediating intracellular pH homeostasis: the contribution of H+/ion exchangers. Plant Traffic Transp. *3*, 11.

Popescu, S.C., Popescu, G.V., Bachan, S., Zhang, Z., Seay, M., Gerstein, M., Snyder, M., and Dinesh-Kumar, S.P. (2007). Differential binding of calmodulin-related proteins to their targets revealed through high-density Arabidopsis protein microarrays. Proc. Natl. Acad. Sci. *104*, 4730–4735.

Postel, S., Küfner, I., Beuter, C., Mazzotta, S., Schwedt, A., Borlotti, A., Halter, T., Kemmerling, B., and Nürnberger, T. (2010). The multifunctional leucine-rich repeat receptor kinase BAK1 is implicated in Arabidopsis development and immunity. Eur. J. Cell Biol. *89*, 169–174.

Pourcel, L., Routaboul, J.-M., Kerhoas, L., Caboche, M., Lepiniec, L., and Debeaujon, I. (2005). TRANSPARENT TESTA10 Encodes a Laccase-Like Enzyme Involved in Oxidative Polymerization of Flavonoids in Arabidopsis Seed Coat. Plant Cell Online *17*, 2966–2980.

Pourcel, L., Irani, N.G., Lu, Y., Riedl, K., Schwartz, S., and Grotewold, E. (2010). The Formation of Anthocyanic Vacuolar Inclusions in Arabidopsis

thaliana and Implications for the Sequestration of Anthocyanin Pigments. Mol. Plant *3*, 78–90.

Pourcel, L., Irani, N.G., Koo, A.J.K., Bohorquez-Restrepo, A., Howe, G.A., and Grotewold, E. (2013). A chemical complementation approach reveals genes and interactions of flavonoids with other pathways. Plant J. *74*, 383–397.

Poustka, F., Irani, N.G., Feller, A., Lu, Y., Pourcel, L., Frame, K., and Grotewold, E. (2007). A Trafficking Pathway for Anthocyanins Overlaps with the Endoplasmic Reticulum-to-Vacuole Protein-Sorting Route in Arabidopsis and Contributes to the Formation of Vacuolar Inclusions. Plant Physiol. *145*, 1323–1335.

Prince, D.C., Drurey, C., Zipfel, C., and Hogenhout, S.A. (2014). The Leucine-Rich Repeat Receptor-Like Kinase BRASSINOSTEROID INSENSITIVE1-ASSOCIATED KINASE1 and the Cytochrome P450 PHYTOALEXIN DEFICIENT3 Contribute to Innate Immunity to Aphids in Arabidopsis. Plant Physiol. *164*, 2207–2219.

Qiu, J.-L., Zhou, L., Yun, B.-W., Nielsen, H.B., Fiil, B.K., Petersen, K., MacKinlay, J., Loake, G.J., Mundy, J., and Morris, P.C. (2008a). Arabidopsis Mitogen-Activated Protein Kinase Kinases MKK1 and MKK2 Have Overlapping Functions in Defense Signaling Mediated by MEKK1, MPK4, and MKS1. Plant Physiol. *148*, 212–222.

Qiu, J.-L., Fiil, B.K., Petersen, K., Nielsen, H.B., Botanga, C.J., Thorgrimsen, S., Palma, K., Suarez-Rodriguez, M.C., Sandbech-Clausen, S., Lichota, J., et al. (2008b). Arabidopsis MAP kinase 4 regulates gene expression through transcription factor release in the nucleus. EMBO J. *27*, 2214–2221.

Radulovic, N.S., Blagojevic, P.D., Stojanovic-Radic, Z.Z., and Stojanovic, N.M. (2013). Antimicrobial Plant Metabolites: Structural Diversity and Mechanism of Action. Curr. Med. Chem. *20*, 932–952.

Ramírez, J., Ramírez, O., Saldaña, C., Coria, R., and Peña, A. (1998). A Saccharomyces cerevisiae Mutant Lacking a K+/H+ Exchanger. J. Bacteriol. *180*, 5860–5865.

Ranf, S., Eschen-Lippold, L., Pecher, P., Lee, J., and Scheel, D. (2011). Interplay between calcium signalling and early signalling elements during defence responses to microbe- or damage-associated molecular patterns. Plant J. *68*, 100–113.

Rayapuram, N., Bonhomme, L., Bigeard, J., Haddadou, K., Przybylski, C., Hirt, H., and Pflieger, D. (2014). Identification of Novel PAMP-Triggered Phosphorylation and Dephosphorylation Events in Arabidopsis thaliana by Quantitative Phosphoproteomic Analysis. J. Proteome Res. *13*, 2137–2151.

Redmond, J.W., Batley, M., Djordjevic, M.A., Innes, R.W., Kuempel, P.L., and Rolfe, B.G. (1986). Flavones induce expression of nodulation genes in Rhizobium. Nature *323*, 632–635.

Ren, D., Yang, H., and Zhang, S. (2002). Cell Death Mediated by MAPK Is Associated with Hydrogen Peroxide Production in Arabidopsis. J. Biol. Chem. *277*, 559–565.

Ren, D., Liu, Y., Yang, K.-Y., Han, L., Mao, G., Glazebrook, J., and Zhang, S. (2008). A fungal-responsive MAPK cascade regulates phytoalexin biosynthesis in Arabidopsis. Proc. Natl. Acad. Sci. *105*, 5638–5643.

Reyes, F.C., Buono, R., and Otegui, M.S. (2011). Plant endosomal trafficking pathways. Curr. Opin. Plant Biol. *14*, 666–673.

Rice-Evans, C.A., Miller, N.J., Bolwell, P.G., Bramley, P.M., and Pridham, J.B. (1995). The Relative Antioxidant Activities of Plant-Derived Polyphenolic Flavonoids. Free Radic. Res. *22*, 375–383.

Riou, C., Tourte, Y., Lacroute, F., and Karst, F. (1994). Isolation and characterization of a cDNA encoding Arabidopsis thaliana mevalonate kinase by genetic complementation in yeast. Gene *148*, 293–297.

Robatzek, S., Chinchilla, D., and Boller, T. (2006). Ligand-induced endocytosis of the pattern recognition receptor FLS2 in Arabidopsis. Genes Dev. *20*, 537–542.

Robatzek, S., Bittel, P., Chinchilla, D., Köchner, P., Felix, G., Shiu, S.-H., and Boller, T. (2007). Molecular identification and characterization of the tomato flagellin receptor LeFLS2, an orthologue of Arabidopsis FLS2 exhibiting characteristically different perception specificities. Plant Mol. Biol. *64*, 539–547.

Robert-Seilaniantz, A., Shan, L., Zhou, J.-M., and Tang, X. (2006). The Pseudomonas syringae pv. tomatoDC3000 Type III Effector HopF2 Has a Putative Myristoylation Site Required for Its Avirulence and Virulence Functions. Mol. Plant. Microbe Interact. *19*, 130–138.

Robert-Seilaniantz, A., Grant, M., and Jones, J.D.G. (2011). Hormone Crosstalk in Plant Disease and Defense: More Than Just JASMONATE-SALICYLATE Antagonism. Annu. Rev. Phytopathol. *49*, 317–343.

Rodríguez-Concepción, M., and Boronat, A. (2002). Elucidation of the Methylerythritol Phosphate Pathway for Isoprenoid Biosynthesis in Bacteria and Plastids. A Metabolic Milestone Achieved through Genomics. Plant Physiol. *130*, 1079–1089.

Rogers, E.E. (1996). Mode of Action of the Arabidopsis thaliana Phytoalexin Camalexin and Its Role in Arabidopsis-Pathogen Interactions. Mol. Plant. Microbe Interact. *9*, 748.

Roine, E., Wei, W., Yuan, J., Nurmiaho-Lassila, E.-L., Kalkkinen, N., Romantschuk, M., and He, S.Y. (1997). Hrp pilus: An hrp-dependent bacterial surface appendage produced by Pseudomonas syringae pv. tomato DC3000. Proc. Natl. Acad. Sci. *94*, 3459–3464.

Ron, M., and Avni, A. (2004). The Receptor for the Fungal Elicitor Ethylene-Inducing Xylanase Is a Member of a Resistance-Like Gene Family in Tomato. Plant Cell Online *16*, 1604–1615.

Roux, M., Schwessinger, B., Albrecht, C., Chinchilla, D., Jones, A., Holton, N., Malinovsky, F.G., Tör, M., Vries, S. de, and Zipfel, C. (2011). The Arabidopsis Leucine-Rich Repeat Receptor–Like Kinases BAK1/SERK3 and BKK1/SERK4 Are Required for Innate Immunity to Hemibiotrophic and Biotrophic Pathogens. Plant Cell Online *23*, 2440–2455.

Ryan, K., Swinny, E., Winefield, C., and Markham, K. (2001). Flavonoids and UV photoprotection in Arabidopsis mutants. Z Naturforsch C *56*, 745–754.

Ryu, H., Kim, K., Cho, H., Park, J., Choe, S., and Hwang, I. (2007). Nucleocytoplasmic Shuttling of BZR1 Mediated by Phosphorylation Is Essential in Arabidopsis Brassinosteroid Signaling. Plant Cell Online *19*, 2749–2762.

Saijo, Y., Tintor, N., Lu, X., Rauf, P., Pajerowska-Mukhtar, K., Haweker, H., Dong, X., Robatzek, S., and Schulze-Lefert, P. (2009). Receptor quality control in the endoplasmic reticulum for plant innate immunity. EMBO J. *28*, 3439–3449.

Saito, K., Yonekura-Sakakibara, K., Nakabayashi, R., Higashi, Y., Yamazaki, M., Tohge, T., and Fernie, A.R. (2013). The flavonoid biosynthetic pathway in Arabidopsis: Structural and genetic diversity. Plant Physiol. Biochem. *72*, 21–34.

Sakai, K., Shitan, N., Sato, F., Ueda, K., and Yazaki, K. (2002). Characterization of berberine transport into Coptis japonica cells and the involvement of ABC protein. J. Exp. Bot. *53*, 1879–1886.

Sakihama, Y., Cohen, M.F., Grace, S.C., and Yamasaki, H. (2002). Plant phenolic antioxidant and prooxidant activities: phenolics-induced oxidative damage mediated by metals in plants. Toxicology *177*, 67–80.

Salomon, S., and Robatzek, S. (2006). Induced Endocytosis of the Receptor Kinase FLS2. Plant Signal. Behav. *1*, 293–295.

Sánchez-Fernández, R., Davies, T.G.E., Coleman, J.O.D., and Rea, P.A. (2001). The Arabidopsis thaliana ABC Protein Superfamily, a Complete Inventory. J. Biol. Chem. *276*, 30231–30244.

Sanchez-Vallet, A., Ramos, B., Bednarek, P., López, G., Piślewska-Bednarek, M., Schulze-Lefert, P., and Molina, A. (2010). Tryptophan-derived secondary metabolites in Arabidopsis thaliana confer non-host resistance to necrotrophic Plectosphaerella cucumerina fungi. Plant J. *63*, 115–127.

Santiago, J., Henzler, C., and Hothorn, M. (2013). Molecular Mechanism for Plant Steroid Receptor Activation by Somatic Embryogenesis Co-Receptor Kinases. Science *341*, 889–892.

Sapir-Mir, M., Mett, A., Belausov, E., Tal-Meshulam, S., Frydman, A., Gidoni, D., and Eyal, Y. (2008). Peroxisomal Localization of Arabidopsis Isopentenyl Diphosphate Isomerases Suggests That Part of the Plant Isoprenoid Mevalonic Acid Pathway Is Compartmentalized to Peroxisomes. Plant Physiol. *148*, 1219–1228.

Sasabe, M., Toyoda, K., Shiraishi, T., Inagaki, Y., and Ichinose, Y. (2002). cDNA cloning and characterization of tobacco ABC transporter: NtPDR1 is a novel elicitor-responsive gene1. FEBS Lett. *518*, 164–168.

Saslowsky, D., and Winkel-Shirley, B. (2001). Localization of flavonoid enzymes in Arabidopsis roots. Plant J. *27*, 37–48.

Saslowsky, D.E., Warek, U., and Winkel, B.S.J. (2005). Nuclear Localization of Flavonoid Enzymes in Arabidopsis. J. Biol. Chem. *280*, 23735–23740.

Sattler, S., and Funnell-Harris, D. (2013). Modifying lignin to improve bioenergy feedstocks: strengthening the barrier against pathogens?†. Plant Biotechnol. *4*, 70.

Saunders, J., and O'Neill, N. (2004). The characterization of defense responses to fungal infection in alfalfa. BioControl *49*, 715–728.

Saurin, W., Hofnung, M., and Dassa, E. (1999). Getting In or Out: Early Segregation Between Importers and Exporters in the Evolution of ATP-Binding Cassette (ABC) Transporters. J. Mol. Evol. *48*, 22–41.

Savoia, D. (2012). Plant-derived antimicrobial compounds: alternatives to antibiotics. Future Microbiol. *7*, 979–990.

Savouré, A., Sallaud, C., El-Turk, J., Zuanazzi, J., Ratet, P., Schultze, M., Kondorosi, A., Esnault, R., and Kondorosi, E. (1997). Distinct response of Medicago suspension cultures and roots to Nod factors and chitin oligomers in the elicitation of defense-related responses. Plant J. *11*, 277–287.

Schenke, D., Böttcher, C., and Scheel, D. (2011). Crosstalk between abiotic ultraviolet-B stress and biotic (flg22) stress signalling in Arabidopsis prevents flavonol accumulation in favor of pathogen defence compound production. Plant Cell Environ. *34*, 1849–1864.

Scheuring, D., Künzl, F., Viotti, C., Yan, M.S.W., Jiang, L., Schellmann, S., Robinson, D.G., and Pimpl, P. (2012). Ubiquitin initiates sorting of Golgi and plasma membrane proteins into the vacuolar degradation pathway. BMC Plant Biol. *12*, 164.

Schlaeppi, K., Abou-Mansour, E., Buchala, A., and Mauch, F. (2010). Disease resistance of Arabidopsis to Phytophthora brassicae is established by the sequential action of indole glucosinolates and camalexin. Plant J. *62*, 840–851.

Schmelz, E.A., Kaplan, F., Huffaker, A., Dafoe, N.J., Vaughan, M.M., Ni, X., Rocca, J.R., Alborn, H.T., and Teal, P.E. (2011). Identity, regulation, and activity of inducible diterpenoid phytoalexins in maize. Proc. Natl. Acad. Sci. *108*, 5455–5460.

Schoenbohm, C., Martens, S., Eder, C., Forkmann, G., and Weisshaar, B. (2005). Identification of the Arabidopsis thaliana Flavonoid 3'-Hydroxylase Gene and Functional Expression of the Encoded P450 Enzyme. Biol. Chem. *381*, 749–753.

Schreiber, K., Ckurshumova, W., Peek, J., and Desveaux, D. (2008). A high-throughput chemical screen for resistance to Pseudomonas syringae in Arabidopsis. Plant J. *54*, 522–531.

Schuhegger, R., Nafisi, M., Mansourova, M., Petersen, B.L., Olsen, C.E., Svatoš, A., Halkier, B.A., and Glawischnig, E. (2006). CYP71B15 (PAD3) Catalyzes the Final Step in Camalexin Biosynthesis. Plant Physiol. *141*, 1248–1254.

Schulze, B., Mentzel, T., Jehle, A.K., Mueller, K., Beeler, S., Boller, T., Felix, G., and Chinchilla, D. (2010). Rapid Heteromerization and Phosphorylation of Ligand-activated Plant Transmembrane Receptors and Their Associated Kinase BAK1. J. Biol. Chem. *285*, 9444–9451.

Schweighofer, A., Hirt, H., and Meskiene, I. (2004). Plant PP2C phosphatases: emerging functions in stress signaling. Trends Plant Sci. *9*, 236–243.

Schwessinger, B., Roux, M., Kadota, Y., Ntoukakis, V., Sklenar, J., Jones, A., and Zipfel, C. (2011). Phosphorylation-Dependent Differential Regulation of Plant Growth, Cell Death, and Innate Immunity by the Regulatory Receptor-Like Kinase BAK1. PLoS Genet *7*, e1002046.

Schwessinger, B., Bahar, O., Thomas, N., Holton, N., Nekrasov, V., Ruan, D., Canlas, P.E., Daudi, A., Petzold, C.J., Singan, V.R., et al. (2015). Transgenic Expression of the Dicotyledonous Pattern Recognition Receptor EFR in Rice Leads to Ligand-Dependent Activation of Defense Responses. PLoS Pathog *11*, e1004809.

Segonzac, C., Macho, A.P., Sanmartín, M., Ntoukakis, V., Sánchez-Serrano, J.J., and Zipfel, C. (2014). Negative control of BAK1 by protein phosphatase 2A during plant innate immunity. EMBO J.

Shan, L., He, P., Li, J., Heese, A., Peck, S.C., Nürnberger, T., Martin, G.B., and Sheen, J. (2008). Bacterial Effectors Target the Common Signaling Partner BAK1 to Disrupt Multiple MAMP Receptor-Signaling Complexes and Impede Plant Immunity. Cell Host Microbe *4*, 17–27.

Shao, F., Golstein, C., Ade, J., Stoutemyer, M., Dixon, J.E., and Innes, R.W. (2003). Cleavage of Arabidopsis PBS1 by a Bacterial Type III Effector. Science *301*, 1230–1233.

Sharfman, M., Bar, M., Ehrlich, M., Schuster, S., Melech-Bonfil, S., Ezer, R., Sessa, G., and Avni, A. (2011). Endosomal signaling of the tomato leucine-rich repeat receptor-like protein LeEix2. Plant J. *68*, 413–423.

Shi, H., Shen, Q., Qi, Y., Yan, H., Nie, H., Chen, Y., Zhao, T., Katagiri, F., and Tang, D. (2013). BR-SIGNALING KINASE1 Physically Associates with FLAGELLIN SENSING2 and Regulates Plant Innate Immunity in Arabidopsis. Plant Cell Online *25*, 1143–1157.

Shibuya, N., and Minami, E. (2001). Oligosaccharide signalling for defence responses in plant. Physiol. Mol. Plant Pathol. *59*, 223–233.

Shimizu, T., Nakano, T., Takamizawa, D., Desaki, Y., Ishii-Minami, N., Nishizawa, Y., Minami, E., Okada, K., Yamane, H., Kaku, H., et al. (2010). Two LysM receptor molecules, CEBiP and OsCERK1, cooperatively regulate chitin elicitor signaling in rice. Plant J. *64*, 204–214.

Shinya, T., Motoyama, N., Ikeda, A., Wada, M., Kamiya, K., Hayafune, M., Kaku, H., and Shibuya, N. (2012). Functional Characterization of CEBiP and CERK1 Homologs in Arabidopsis and Rice Reveals the Presence of Different Chitin Receptor Systems in Plants. Plant Cell Physiol. *53*, 1696–1706.

Shirley, B.W., Hanley, S., and Goodman, H.M. (1992). Effects of ionizing radiation on a plant genome: analysis of two Arabidopsis transparent testa mutations. Plant Cell Online *4*, 333–347.

Shirley, B.W., Kubasek, W.L., Storz, G., Bruggemann, E., Koornneef, M., Ausubel, F.M., and Goodman, H.M. (1995). Analysis of Arabidopsis mutants deficient in flavonoid biosynthesis. Plant J. *8*, 659–671.

Shitan, N., Bazin, I., Dan, K., Obata, K., Kigawa, K., Ueda, K., Sato, F., Forestier, C., and Yazaki, K. (2003). Involvement of CjMDR1, a plant multidrug-resistance-type ATP-binding cassette protein, in alkaloid transport in Coptis japonica. Proc. Natl. Acad. Sci. *100*, 751–756.

Shiu, S.-H., and Bleecker, A.B. (2001). Receptor-like kinases from Arabidopsis form a monophyletic gene family related to animal receptor kinases. Proc. Natl. Acad. Sci. *98*, 10763–10768.

Shiu, S.-H., Karlowski, W.M., Pan, R., Tzeng, Y.-H., Mayer, K.F.X., and Li, W.-H. (2004). Comparative Analysis of the Receptor-Like Kinase Family in Arabidopsis and Rice. Plant Cell Online *16*, 1220–1234.

Silverstone, A.L., Ciampaglio, C.N., and Sun, T. (1998). The Arabidopsis RGA Gene Encodes a Transcriptional Regulator Repressing the Gibberellin Signal Transduction Pathway. Plant Cell Online *10*, 155–169.

Silverstone, A.L., Jung, H.-S., Dill, A., Kawaide, H., Kamiya, Y., and Sun, T. (2001). Repressing a Repressor Gibberellin-Induced Rapid Reduction of the RGA Protein in Arabidopsis. Plant Cell Online *13*, 1555–1566.

Simkin, A.J., Guirimand, G., Papon, N., Courdavault, V., Thabet, I., Ginis, O., Bouzid, S., Giglioli-Guivarc'h, N., and Clastre, M. (2011). Peroxisomal localisation of the final steps of the mevalonic acid pathway in. Planta *234*, 903–914.

Simon, C., Langlois-Meurinne, M., Bellvert, F., Garmier, M., Didierlaurent, L., Massoud, K., Chaouch, S., Marie, A., Bodo, B., Kauffmann, S., et al. (2010). The differential spatial distribution of secondary metabolites in Arabidopsis leaves reacting hypersensitively to Pseudomonas syringae pv. tomato is dependent on the oxidative burst. J. Exp. Bot. *61*, 3355–3370.

Singer, A.U., Desveaux, D., Betts, L., Chang, J.H., Nimchuk, Z., Grant, S.R., Dangl, J.L., and Sondek, J. (2004). Crystal Structures of the Type III Effector Protein AvrPphF and Its Chaperone Reveal Residues Required for Plant Pathogenesis. Structure *12*, 1669–1681.

Singh, P., Kuo, Y.-C., Mishra, S., Tsai, C.-H., Chien, C.-C., Chen, C.-W., Desclos-Theveniau, M., Chu, P.-W., Schulze, B., Chinchilla, D., et al. (2012). The Lectin Receptor Kinase-VI.2 Is Required for Priming and Positively Regulates Arabidopsis Pattern-Triggered Immunity. Plant Cell Online *24*, 1256–1270.

Smith, J.M., Salamango, D.J., Leslie, M.E., Collins, C.A., and Heese, A. (2014). Sensitivity to Flg22 Is Modulated by Ligand-Induced Degradation and de Novo Synthesis of the Endogenous Flagellin-Receptor FLAGELLIN-SENSING2. Plant Physiol. *164*, 440–454.

Snyder, B.A., and Nicholson, R.L. (1990). Synthesis of Phytoalexins in Sorghum as a Site-Specific Response to Fungal Ingress. Science *248*, 1637–1639.

Sønderby, I.E., Hansen, B.G., Bjarnholt, N., Ticconi, C., Halkier, B.A., and Kliebenstein, D.J. (2007). A Systems Biology Approach Identifies a R2R3 MYB Gene Subfamily with Distinct and Overlapping Functions in Regulation of Aliphatic Glucosinolates. PLoS ONE *2*, e1322.

Sønderby, I.E., Geu-Flores, F., and Halkier, B.A. (2010). Biosynthesis of glucosinolates – gene discovery and beyond. Trends Plant Sci. *15*, 283–290.

Song, W.-Y., Wang, G.-L., Chen, L.-L., Kim, H.-S., Pi, L.-Y., Holsten, T., Gardner, J., Wang, B., Zhai, W.-X., Zhu, L.-H., et al. (1995). A Receptor Kinase-Like Protein Encoded by the Rice Disease Resistance Gene, Xa21. Science *270*, 1804–1806.

Sorin, C., Bussell, J.D., Camus, I., Ljung, K., Kowalczyk, M., Geiss, G., McKhann, H., Garcion, C., Vaucheret, H., Sandberg, G., et al. (2005). Auxin and Light Control of Adventitious Rooting in Arabidopsis Require ARGONAUTE1. Plant Cell Online *17*, 1343–1359.

Soylu, S., Brown, I., and Mansfield, J.W. (2005). Cellular reactions in Arabidopsis following challenge by strains of Pseudomonas syringae: From basal resistance to compatibility. Physiol. Mol. Plant Pathol. *66*, 232–243.

Spallek, T., Beck, M., Ben Khaled, S., Salomon, S., Bourdais, G., Schellmann, S., and Robatzek, S. (2013). ESCRT-I Mediates FLS2 Endosomal Sorting and Plant Immunity. PLoS Genet *9*, e1004035.

Srivastava, R., Liu, J.-X., and Howell, S.H. (2008). Proteolytic processing of a precursor protein for a growth-promoting peptide by a subtilisin serine protease in Arabidopsis. Plant J. *56*, 219–227.

Staiger, D., Zecca, L., Kirk, D.A.W., Apel, K., and Eckstein, L. (2003). The circadian clock regulated RNA-binding protein AtGRP7 autoregulates its expression by influencing alternative splicing of its own pre-mRNA. Plant J. *33*, 361–371.

Stegmann, M., Anderson, R.G., Ichimura, K., Pecenkova, T., Reuter, P., Žárský, V., McDowell, J.M., Shirasu, K., and Trujillo, M. (2012). The Ubiquitin Ligase PUB22 Targets a Subunit of the Exocyst Complex Required for PAMP-Triggered Responses in Arabidopsis. Plant Cell Online *24*, 4703–4716.

Stein, M., Dittgen, J., Sánchez-Rodríguez, C., Hou, B.-H., Molina, A., Schulze-Lefert, P., Lipka, V., and Somerville, S. (2006). Arabidopsis PEN3/PDR8, an ATP Binding Cassette Transporter, Contributes to Nonhost

Resistance to Inappropriate Pathogens That Enter by Direct Penetration. Plant Cell Online *18*, 731–746.

Stermer, B.A., Edwards, L.A., Edington, B.V., and Dixon, R.A. (1991). Analysis of elicitor-inducible transcripts encoding 3-hydroxy-3-methylglutaryl coenzyme A reductase in potato. Physiol. Mol. Plant Pathol. *39*, 135–145.

Stewart, A.J., Chapman, W., Jenkins, G.I., Graham, I., Martin, T., and Crozier, A. (2001). The effect of nitrogen and phosphorus deficiency on flavonol accumulation in plant tissues. Plant Cell Environ. *24*, 1189–1197.

Stotz, H.U., Sawada, Y., Shimada, Y., Hirai, M.Y., Sasaki, E., Krischke, M., Brown, P.D., Saito, K., and Kamiya, Y. (2011). Role of camalexin, indole glucosinolates, and side chain modification of glucosinolate-derived isothiocyanates in defense of Arabidopsis against Sclerotinia sclerotiorum. Plant J. *67*, 81–93.

Stracke, R., Ishihara, H., Huep, G., Barsch, A., Mehrtens, F., Niehaus, K., and Weisshaar, B. (2007). Differential regulation of closely related R2R3-MYB transcription factors controls flavonol accumulation in different parts of the Arabidopsis thaliana seedling. Plant J. *50*, 660–677.

Stracke, R., Vos, R.C.H.D., Bartelniewoehner, L., Ishihara, H., Sagasser, M., Martens, S., and Weisshaar, B. (2009). Metabolomic and genetic analyses of flavonol synthesis in Arabidopsis thaliana support the in vivo involvement of leucoanthocyanidin dioxygenase. Planta *229*, 427–445.

Stracke, R., Jahns, O., Keck, M., Tohge, T., Niehaus, K., Fernie, A.R., and Weisshaar, B. (2010). Analysis of PRODUCTION OF FLAVONOL GLYCOSIDES-dependent flavonol glycoside accumulation in Arabidopsis thaliana plants reveals MYB11-, MYB12- and MYB111-independent flavonol glycoside accumulation. New Phytol. *188*, 985–1000.

Strange, R.N., and Scott, P.R. (2005). Plant Disease: A Threat to Global Food Security. Annu. Rev. Phytopathol. *43*, 83–116.

Stukkens, Y., Bultreys, A., Grec, S., Trombik, T., Vanham, D., and Boutry, M. (2005). NpPDR1, a Pleiotropic Drug Resistance-Type ATP-Binding Cassette Transporter from Nicotiana plumbaginifolia, Plays a Major Role in Plant Pathogen Defense. Plant Physiol. *139*, 341–352.

Suarez-Rodriguez, M.C., Adams-Phillips, L., Liu, Y., Wang, H., Su, S.-H., Jester, P.J., Zhang, S., Bent, A.F., and Krysan, P.J. (2007). MEKK1 Is Required for flg22-Induced MPK4 Activation in Arabidopsis Plants. Plant Physiol. *143*, 661–669.

Subramanian, S., Stacey, G., and Yu, O. (2006). Endogenous isoflavones are essential for the establishment of symbiosis between soybean and Bradyrhizobium japonicum. Plant J. *48*, 261–273.

Sugiyama, A., Shitan, N., and Yazaki, K. (2007). Involvement of a Soybean ATP-Binding Cassette-Type Transporter in the Secretion of Genistein, a Signal Flavonoid in Legume-Rhizobium Symbiosis. Plant Physiol. *144*, 2000–2008.

Suh, S.J., Wang, Y.-F., Frelet, A., Leonhardt, N., Klein, M., Forestier, C., Mueller-Roeber, B., Cho, M.H., Martinoia, E., and Schroeder, J.I. (2007). The ATP Binding Cassette Transporter AtMRP5 Modulates Anion and Calcium Channel Activities in Arabidopsis Guard Cells. J. Biol. Chem. *282*, 1916–1924.

Sun, J.Y., Sønderby, I.E., Halkier, B.A., Jander, G., and Vos, M. de (2009). Non-Volatile Intact Indole Glucosinolates are Host Recognition Cues for Ovipositing Plutella xylostella. J. Chem. Ecol. *35*, 1427–1436.

Sun, W., Dunning, F.M., Pfund, C., Weingarten, R., and Bent, A.F. (2006). Within-Species Flagellin Polymorphism in Xanthomonas campestris pv campestris and Its Impact on Elicitation of Arabidopsis FLAGELLIN SENSING2–Dependent Defenses. Plant Cell Online *18*, 764–779.

Sun, Y., Fan, X.-Y., Cao, D.-M., Tang, W., He, K., Zhu, J.-Y., He, J.-X., Bai, M.-Y., Zhu, S., Oh, E., et al. (2010). Integration of Brassinosteroid Signal Transduction with the Transcription Network for Plant Growth Regulation in Arabidopsis. Dev. Cell *19*, 765–777.

Sun, Y., Li, H., and Huang, J.-R. (2011). Arabidopsis TT19 Functions as a Carrier to Transport Anthocyanin from the Cytosol to Tonoplasts. Mol. Plant 387–400.

Sun, Y., Li, L., Macho, A.P., Han, Z., Hu, Z., Zipfel, C., Zhou, J.-M., and Chai, J. (2013a). Structural Basis for flg22-Induced Activation of the Arabidopsis FLS2-BAK1 Immune Complex. Science *342*, 624–628.

Sun, Y., Han, Z., Tang, J., Hu, Z., Chai, C., Zhou, B., and Chai, J. (2013b). Structure reveals that BAK1 as a co-receptor recognizes the BRI1-bound brassinolide. Cell Res. *23*, 1326–1329.

Suzuki, M., Kamide, Y., Nagata, N., Seki, H., Ohyama, K., Kato, H., Masuda, K., Sato, S., Kato, T., Tabata, S., et al. (2004). Loss of function of 3-hydroxy-3-methylglutaryl coenzyme A reductase 1 (HMG1) in Arabidopsis leads to dwarfing, early senescence and male sterility, and reduced sterol levels. Plant J. *37*, 750–761.

Suzuki, M., Nakagawa, S., Kamide, Y., Kobayashi, K., Ohyama, K., Hashinokuchi, H., Kiuchi, R., Saito, K., Muranaka, T., and Nagata, N. (2009). Complete blockage of the mevalonate pathway results in male gametophyte lethality. J. Exp. Bot. *60*, 2055–2064.

Sze, H., Padmanaban, S., Cellier, F., Honys, D., Cheng, N.-H., Bock, K.W., Conéjéro, G., Li, X., Twell, D., Ward, J.M., et al. (2004). Expression Patterns of a Novel AtCHX Gene Family Highlight Potential Roles in Osmotic Adjustment and K+ Homeostasis in Pollen Development. Plant Physiol. *136*, 2532–2547.

Taguchi, F., Shimizu, R., Inagaki, Y., Toyoda, K., Shiraishi, T., and Ichinose, Y. (2003). Post-Translational Modification of Flagellin Determines the Specificity of HR Induction. Plant Cell Physiol. *44*, 342–349.

Takai, R., Isogai, A., Takayama, S., and Che, F.-S. (2008). Analysis of Flagellin Perception Mediated by flg22 Receptor OsFLS2 in Rice. Mol. Plant. Microbe Interact. *21*, 1635–1642.

Takken, F.L., and Goverse, A. (2012). How to build a pathogen detector: structural basis of NB-LRR function. Curr. Opin. Plant Biol. *15*, 375–384.

Tanabe, S., OKADA, M., JIKUMARU, Y., YAMANE, H., KAKU, H., SHIBUYA, N., and MINAMI, E. (2006). Induction of Resistance against Rice Blast Fungus in Rice Plants Treated with a Potent Elicitor, N-Acetylchitooligosaccharide. Biosci. Biotechnol. Biochem. *70*, 1599–1605.

Tang, W., Kim, T.-W., Oses-Prieto, J.A., Sun, Y., Deng, Z., Zhu, S., Wang, R., Burlingame, A.L., and Wang, Z.-Y. (2008). BSKs Mediate Signal Transduction from the Receptor Kinase BRI1 in Arabidopsis. Science *321*, 557–560.

Taylor, P.W. (2013). Alternative natural sources for a new generation of antibacterial agents. Int. J. Antimicrob. Agents *42*, 195–201.

Taylor, L.P., and Grotewold, E. (2005). Flavonoids as developmental regulators. Curr. Opin. Plant Biol. *8*, 317–323.

Taylor, L.P., and Jorgensen, R. (1992). Conditional Male Fertility in Chalcone Synthase-Deficient Petunia. J. Hered. *83*, 11–17.

Tena, G., Asai, T., Chiu, W.-L., and Sheen, J. (2001). Plant mitogen-activated protein kinase signaling cascades. Curr. Opin. Plant Biol. *4*, 392–400.

Terasaka, K., Sakai, K., Sato, F., Yamamoto, H., and Yazaki, K. (2003). Thalictrum minus cell cultures and ABC-like transporter. Phytochemistry *62*, 483–489.

276

Thilmony, R., Underwood, W., and He, S.Y. (2006). Genome-wide transcriptional analysis of the Arabidopsis thaliana interaction with the plant pathogen Pseudomonas syringae pv. tomato DC3000 and the human pathogen Escherichia coli O157:H7. Plant J. *46*, 34–53.

Tholl, D., and Lee, S. (2011). Terpene Specialized Metabolism in Arabidopsis thaliana. Arab. Book e0143.

Thomma, B.P.H.J., Nelissen, I., Eggermont, K., and Broekaert, W.F. (1999). Deficiency in phytoalexin production causes enhanced susceptibility of Arabidopsis thaliana to the fungus Alternaria brassicicola. Plant J. *19*, 163–171.

Tierens, K.F.M.-J., Thomma, B.P.H.J., Brouwer, M., Schmidt, J., Kistner, K., Porzel, A., Mauch-Mani, B., Cammue, B.P.A., and Broekaert, W.F. (2001). Study of the Role of Antimicrobial Glucosinolate-Derived Isothiocyanates in Resistance of Arabidopsis to Microbial Pathogens. Plant Physiol. *125*, 1688–1699.

Tintor, N., Ross, A., Kanehara, K., Yamada, K., Fan, L., Kemmerling, B., Nürnberger, T., Tsuda, K., and Saijo, Y. (2013). Layered pattern receptor signaling via ethylene and endogenous elicitor peptides during Arabidopsis immunity to bacterial infection. Proc. Natl. Acad. Sci. *110*, 6211–6216.

Tohge, T., Nishiyama, Y., Hirai, M.Y., Yano, M., Nakajima, J., Awazuhara, M., Inoue, E., Takahashi, H., Goodenowe, D.B., Kitayama, M., et al. (2005). Functional genomics by integrated analysis of metabolome and transcriptome of Arabidopsis plants over-expressing an MYB transcription factor. Plant J. *42*, 218–235.

Tohge, T., Yonekura-Sakakibara, K., Niida, R., Watanabe-Takahashi, A., and Saito, K. (2009). Phytochemical genomics in Arabidopsis thaliana: A case study for functional identification of flavonoid biosynthesis genes. Pure Appl. Chem. *79*, 811–823.

Torres, M.A. (2010). ROS in biotic interactions. Physiol. Plant. *138*, 414–429.

Torres, M.A., Dangl, J.L., and Jones, J.D.G. (2002). Arabidopsis gp91phox homologues AtrbohD and AtrbohF are required for accumulation of reactive oxygen intermediates in the plant defense response. Proc. Natl. Acad. Sci. *99*, 517–522.

Torres, M.A., Jones, J.D.G., and Dangl, J.L. (2006). Reactive Oxygen Species Signaling in Response to Pathogens. Plant Physiol. *141*, 373–378.

Trabelsi, N., Petit, P., Manigand, C., Langlois d'Estaintot, B., Granier, T., Chaudière, J., and Gallois, B. (2008). Structural evidence for the inhibition of

grape dihydroflavonol 4-reductase by flavonols. Acta Crystallogr. Sect. D *64*, 883–891.

Trethewey, R.N. (2004). Metabolite profiling as an aid to metabolic engineering in plants. Curr. Opin. Plant Biol. *7*, 196–201.

Treutter, D. (2006). Significance of flavonoids in plant resistance: a review. Environ. Chem. Lett. *4*, 147–157.

Trujillo, M., Ichimura, K., Casais, C., and Shirasu, K. (2008). Negative Regulation of PAMP-Triggered Immunity by an E3 Ubiquitin Ligase Triplet in Arabidopsis. Curr. Biol. *18*, 1396–1401.

Tsuda, K., Sato, M., Stoddard, T., Glazebrook, J., and Katagiri, F. (2009). Network Properties of Robust Immunity in Plants. PLoS Genet *5*, e1000772.

Tsuji, J., Jackson, E.P., Gage, D.A., Hammerschmidt, R., and Somerville, S.C. (1992). Phytoalexin Accumulation in Arabidopsis thaliana during the Hypersensitive Reaction to Pseudomonas syringae pv syringae. Plant Physiol. *98*, 1304–1309.

Turnbull, J.J., Sobey, W.J., Aplin, R.T., Hassan, A., Firmin, J.L., Schofield, C.J., and Prescott, A.G. (2000). Are anthocyanidins the immediate products of anthocyanidin synthase? Chem. Commun. 2473–2474.

Ülker, B., Peiter, E., Dixon, D.P., Moffat, C., Capper, R., Bouché, N., Edwards, R., Sanders, D., Knight, H., and Knight, M.R. (2008). Getting the most out of publicly available T-DNA insertion lines. Plant J. *56*, 665–677.

Ulm, R., and Nagy, F. (2005). Signalling and gene regulation in response to ultraviolet light. Curr. Opin. Plant Biol. *8*, 477–482.

Ulm, R., Baumann, A., Oravecz, A., Máté, Z., Ádám, É., Oakeley, E.J., Schäfer, E., and Nagy, F. (2004). Genome-wide analysis of gene expression reveals function of the bZIP transcription factor HY5 in the UV-B response of Arabidopsis. Proc. Natl. Acad. Sci. U. S. A. *101*, 1397–1402.

Underwood, W., and Somerville, S.C. (2013). Perception of conserved pathogen elicitors at the plasma membrane leads to relocalization of the Arabidopsis PEN3 transporter. Proc. Natl. Acad. Sci. *110*, 12492–12497.

Underwood, W., Zhang, S., and He, S.Y. (2007). The Pseudomonas syringae type III effector tyrosine phosphatase HopAO1 suppresses innate immunity in Arabidopsis thaliana. Plant J. *52*, 658–672.

Unsicker, S.B., Kunert, G., and Gershenzon, J. (2009). Protective perfumes: the role of vegetative volatiles in plant defense against herbivores. Curr. Opin. Plant Biol. *12*, 479–485.

Urano, D., and Jones, A.M. (2014). Heterotrimeric G Protein–Coupled Signaling in Plants. Annu. Rev. Plant Biol. *65*, 365–384.

Urbatsch, I.L., Sankaran, B., Weber, J., and Senior, A.E. (1995). P-glycoprotein Is Stably Inhibited by Vanadate-induced Trapping of Nucleotide at a Single Catalytic Site. J. Biol. Chem. *270*, 19383–19390.

Vandeputte, O.M., Kiendrebeogo, M., Rasamiravaka, T., Stévigny, C., Duez, P., Rajaonson, S., Diallo, B., Mol, A., Baucher, M., and Jaziri, M.E. (2011). The flavanone naringenin reduces the production of quorum sensing-controlled virulence factors in Pseudomonas aeruginosa PAO1. Microbiology *157*, 2120–2132.

VanEtten, H.D., Mansfield, J.W., Bailey, J.A., and Farmer, E.E. (1994). Two Classes of Plant Antibiotics: Phytoalexins versus "Phytoanticipins." Plant Cell Online *6*, 1191–1192.

Vanholme, R., Demedts, B., Morreel, K., Ralph, J., and Boerjan, W. (2010). Lignin Biosynthesis and Structure. Plant Physiol. *153*, 895–905.

Vargas, P., Felipe, A., Michán, C., and Gallegos, M.-T. (2011). Induction of Pseudomonas syringae pv. tomato DC3000 MexAB-OprM Multidrug Efflux Pump by Flavonoids Is Mediated by the Repressor PmeR. Mol. Plant. Microbe Interact. *24*, 1207–1219.

Vargas, P., Farias, G.A., Nogales, J., Prada, H., Carvajal, V., Barón, M., Rivilla, R., Martín, M., Olmedilla, A., and Gallegos, M.-T. (2013). Plant flavonoids target Pseudomonas syringae pv. tomato DC3000 flagella and type III secretion system. Environ. Microbiol. Rep. *5*, 841–850.

Verrier, P.J., Bird, D., Burla, B., Dassa, E., Forestier, C., Geisler, M., Klein, M., Kolukisaoglu, Ü., Lee, Y., Martinoia, E., et al. (2008). Plant ABC proteins – a unified nomenclature and updated inventory. Trends Plant Sci. *13*, 151–159.

Ververidis, F., Trantas, E., Douglas, C., Vollmer, G., Kretzschmar, G., and Panopoulos, N. (2007). Biotechnology of flavonoids and other phenylpropanoid-derived natural products. Part I: Chemical diversity, impacts on plant biology and human health. Biotechnol. J. *2*, 1214–1234.

Vikram, A., Jayaprakasha, G. k., Jesudhasan, P. r., Pillai, S. d., and Patil, B. s. (2010). Suppression of bacterial cell–cell signalling, biofilm formation and type III secretion system by citrus flavonoids. J. Appl. Microbiol. *109*, 515–527.

Vogel, J., and Somerville, S. (2000). Isolation and characterization of powdery mildew-resistant Arabidopsis mutants. Proc. Natl. Acad. Sci. *97*, 1897–1902.

Vogt, T., and Jones, P. (2000). Glycosyltransferases in plant natural product synthesis: characterization of a supergene family. Trends Plant Sci. *5*, 380–386.

Voigt, C.A. (2014). Callose-mediated resistance to pathogenic intruders in plant defense-related papillae. Plant-Microbe Interact. *5*, 168.

Vranová, E., Coman, D., and Gruissem, W. (2013). Network Analysis of the MVA and MEP Pathways for Isoprenoid Synthesis. Annu. Rev. Plant Biol. *64*, 665–700.

Walker, J.E., Saraste, M., Runswick, M.J., and Gay, N.J. (1982). Distantly related sequences in the alpha- and beta-subunits of ATP synthase, myosin, kinases and other ATP-requiring enzymes and a common nucleotide binding fold. EMBO J. *1*, 945–951.

Wan, J., Zhang, X.-C., Neece, D., Ramonell, K.M., Clough, S., Kim, S., Stacey, M.G., and Stacey, G. (2008). A LysM Receptor-Like Kinase Plays a Critical Role in Chitin Signaling and Fungal Resistance in Arabidopsis. Plant Cell Online *20*, 471–481.

Wan, J., Tanaka, K., Zhang, X.-C., Son, G.H., Brechenmacher, L., Nguyen, T.H.N., and Stacey, G. (2012). LYK4, a Lysin Motif Receptor-Like Kinase, Is Important for Chitin Signaling and Plant Innate Immunity in Arabidopsis. Plant Physiol. *160*, 396–406.

Wang, Y.H. (2008). How effective is T-DNA insertional mutagenesis in Arabidopsis? J. Biochem. Technol. *1*, 11–20.

Wang, J., Kucukoglu, M., Zhang, L., Chen, P., Decker, D., Nilsson, O., Jones, B., Sandberg, G., and Zheng, B. (2013). The Arabidopsis LRR-RLK, PXC1, is a regulator of secondary wall formation correlated with the TDIF-PXY/TDR-WOX4 signaling pathway. BMC Plant Biol. *13*, 94.

Wang, Y., Li, J., Hou, S., Wang, X., Li, Y., Ren, D., Chen, S., Tang, X., and Zhou, J.-M. (2010). A Pseudomonas syringae ADP-Ribosyltransferase Inhibits Arabidopsis Mitogen-Activated Protein Kinase Kinases. Plant Cell Online *22*, 2033–2044.

Wang, Y.-S., Pi, L.-Y., Chen, X., Chakrabarty, P.K., Jiang, J., Leon, A.L.D., Liu, G.-Z., Li, L., Benny, U., Oard, J., et al. (2006). Rice XA21 Binding Protein 3 Is a Ubiquitin Ligase Required for Full Xa21-Mediated Disease Resistance. Plant Cell Online *18*, 3635–3646.

Wang, Z.-Y., Nakano, T., Gendron, J., He, J., Chen, M., Vafeados, D., Yang, Y., Fujioka, S., Yoshida, S., Asami, T., et al. (2002). Nuclear-Localized BZR1 Mediates Brassinosteroid-Induced Growth and Feedback Suppression of Brassinosteroid Biosynthesis. Dev. Cell *2*, 505–513.

Wasson, A.P., Pellerone, F.I., and Mathesius, U. (2006). Silencing the Flavonoid Pathway in Medicago truncatula Inhibits Root Nodule Formation and Prevents Auxin Transport Regulation by Rhizobia. Plant Cell Online *18*, 1617–1629.

Watkins, J.M., Hechler, P.J., and Muday, G.K. (2014). Ethylene-Induced Flavonol Accumulation in Guard Cells Suppresses Reactive Oxygen Species and Moderates Stomatal Aperture. Plant Physiol. *164*, 1707–1717.

Welford, R.W.D., Turnbull, J.J., Claridge, T.D.W., Prescott, A.G., and Schofield, C.J. (2001). Evidence for oxidation at C-3 of the flavonoid C-ring during anthocyanin biosynthesis. Chem. Commun. 1828–1829.

Whalen, M.C., Innes, R.W., Bent, A.F., and Staskawicz, B.J. (1991). Identification of Pseudomonas syringae pathogens of Arabidopsis and a bacterial locus determining avirulence on both Arabidopsis and soybean. Plant Cell Online *3*, 49–59.

Wildermuth, M.C., Dewdney, J., Wu, G., and Ausubel, F.M. (2001). Isochorismate synthase is required to synthesize salicylic acid for plant defence. Nature *414*, 562–565.

Willmann, R., Lajunen, H.M., Erbs, G., Newman, M.-A., Kolb, D., Tsuda, K., Katagiri, F., Fliegmann, J., Bono, J.-J., Cullimore, J.V., et al. (2011). Arabidopsis lysin-motif proteins LYM1 LYM3 CERK1 mediate bacterial peptidoglycan sensing and immunity to bacterial infection. Proc. Natl. Acad. Sci. *108*, 19824–19829.

Wilson, M.I., and Greenberg, B.M. (1993). Specificity and Photomorphogenic Nature of Ultraviolet-B-Induced Cotyledon Curling in Brassica napus L. Plant Physiol. *102*, 671–677.

Win, J., Chaparro-Garcia, A., Belhaj, K., Saunders, D.G.O., Yoshida, K., Dong, S., Schornack, S., Zipfel, C., Robatzek, S., Hogenhout, S.A., et al. (2012). Effector Biology of Plant-Associated Organisms: Concepts and Perspectives. Cold Spring Harb. Symp. Quant. Biol. *77*, 235–247.

Winkel-Shirley, B. (2001). Flavonoid Biosynthesis. A Colorful Model for Genetics, Biochemistry, Cell Biology, and Biotechnology. Plant Physiol. *126*, 485–493.

Winter, D., Vinegar, B., Nahal, H., Ammar, R., Wilson, G.V., and Provart, N.J. (2007). An "Electronic Fluorescent Pictograph" Browser for Exploring and Analyzing Large-Scale Biological Data Sets. PLoS ONE *2*, e718.

Wittstock, U., and Halkier, B.A. (2000). Cytochrome P450 CYP79A2 from Arabidopsis thaliana L. Catalyzes the Conversion of l-Phenylalanine to

Phenylacetaldoxime in the Biosynthesis of Benzylglucosinolate. J. Biol. Chem. *275*, 14659–14666.

Wu, C.-H., Krasileva, K.V., Banfield, M.J., Terauchi, R., and Kamoun, S. (2015). The "sensor domains" of plant NLR proteins: more than decoys? Plant-Microbe Interact. *6*, 134.

Wu, S., Lu, D., Kabbage, M., Wei, H.-L., Swingle, B., Records, A.R., Dickman, M., He, P., and Shan, L. (2011). Bacterial Effector HopF2 Suppresses Arabidopsis Innate Immunity at the Plasma Membrane. Mol. Plant. Microbe Interact. *24*, 585–593.

Wu, S., Shan, L., and He, P. (2014). Microbial signature-triggered plant defense responses and early signaling mechanisms. Plant Sci.

Xiang, T., Zong, N., Zou, Y., Wu, Y., Zhang, J., Xing, W., Li, Y., Tang, X., Zhu, L., Chai, J., et al. (2008). Pseudomonas syringae Effector AvrPto Blocks Innate Immunity by Targeting Receptor Kinases. Curr. Biol. *18*, 74–80.

Xiang, T., Zong, N., Zhang, J., Chen, J., Chen, M., and Zhou, J.-M. (2011). BAK1 Is Not a Target of the Pseudomonas syringae Effector AvrPto. Mol. Plant. Microbe Interact. *24*, 100–107.

Xin, X.-F., and He, S.Y. (2013). Pseudomonas syringae pv. tomato DC3000: A Model Pathogen for Probing Disease Susceptibility and Hormone Signaling in Plants. Annu. Rev. Phytopathol. *51*, 473–498.

Xu, J., Li, Y., Wang, Y., Liu, H., Lei, L., Yang, H., Liu, G., and Ren, D. (2008). Activation of MAPK Kinase 9 Induces Ethylene and Camalexin Biosynthesis and Enhances Sensitivity to Salt Stress in Arabidopsis. J. Biol. Chem. *283*, 26996–27006.

Xu, W.-H., Wang, Y.-S., Liu, G.-Z., Chen, X., Tinjuangjun, P., Pi, L.-Y., and Song, W.-Y. (2006a). The autophosphorylated Ser686, Thr688, and Ser689 residues in the intracellular juxtamembrane domain of XA21 are implicated in stability control of rice receptor-like kinase. Plant J. *45*, 740–751.

Xu, X., Chen, C., Fan, B., and Chen, Z. (2006b). Physical and Functional Interactions between Pathogen-Induced Arabidopsis WRKY18, WRKY40, and WRKY60 Transcription Factors. Plant Cell Online *18*, 1310–1326.

Yamaguchi, K., Yamada, K., Ishikawa, K., Yoshimura, S., Hayashi, N., Uchihashi, K., Ishihama, N., Kishi-Kaboshi, M., Takahashi, A., Tsuge, S., et al. (2013a). A Receptor-like Cytoplasmic Kinase Targeted by a Plant Pathogen Effector Is Directly Phosphorylated by the Chitin Receptor and Mediates Rice Immunity. Cell Host Microbe *13*, 347–357.

Yamaguchi, K., Nakamura, Y., Ishikawa, K., Yoshimura, Y., Tsuge, S., and Kawasaki, T. (2013b). Suppression of rice immunity by Xanthomonas oryzae type III effector Xoo2875. Biosci. Biotechnol. Biochem. *77*, 796–801.

Yamaguchi, Y., Pearce, G., and Ryan, C.A. (2006). The cell surface leucine-rich repeat receptor for AtPep1, an endogenous peptide elicitor in Arabidopsis, is functional in transgenic tobacco cells. Proc. Natl. Acad. Sci. *103*, 10104–10109.

Yamaguchi, Y., Huffaker, A., Bryan, A.C., Tax, F.E., and Ryan, C.A. (2010). PEPR2 Is a Second Receptor for the Pep1 and Pep2 Peptides and Contributes to Defense Responses in Arabidopsis. Plant Cell Online *22*, 508–522.

Yamasaki, H., Sakihama, Y., and Ikehara, N. (1997). Flavonoid-Peroxidase Reaction as a Detoxification Mechanism of Plant Cells against H2O2. Plant Physiol. *115*, 1405–1412.

Yang, C.-Q., Fang, X., Wu, X.-M., Mao, Y.-B., Wang, L.-J., and Chen, X.-Y. (2012). Transcriptional Regulation of Plant Secondary Metabolism. J. Integr. Plant Biol. *54*, 703–712.

Yang, H., Matsubayashi, Y., Nakamura, K., and Sakagami, Y. (1999). Oryza sativa PSK gene encodes a precursor of phytosulfokine-α, a sulfated peptide growth factor found in plants. Proc. Natl. Acad. Sci. *96*, 13560–13565.

Yang, H., Matsubayashi, Y., Nakamura, K., and Sakagami, Y. (2001). Diversity of Arabidopsis Genes Encoding Precursors for Phytosulfokine, a Peptide Growth Factor. Plant Physiol. *127*, 842–851.

Yang, Z., Park, H., Lacy, G.H., and Cramer, C.L. (1991). Differential activation of potato 3-hydroxy-3-methylglutaryl coenzyme A reductase genes by wounding and pathogen challenge. Plant Cell Online *3*, 397–405.

Yazaki, K. (2006). ABC transporters involved in the transport of plant secondary metabolites. FEBS Lett. *580*, 1183–1191.

Yazaki, K., Shitan, N., Takamatsu, H., Ueda, K., and Sato, F. (2001). A novel Coptis japonica multidrug-resistant protein preferentially expressed in the alkaloid-accumulating rhizome. J. Exp. Bot. *52*, 877–879.

Yin, R., Messner, B., Faus-Kessler, T., Hoffmann, T., Schwab, W., Hajirezaei, M.-R., Paul, V. von S., Heller, W., and Schäffner, A.R. (2012). Feedback inhibition of the general phenylpropanoid and flavonol biosynthetic pathways upon a compromised flavonol-3-O-glycosylation. J. Exp. Bot. *63*, 2465–2478.

Yonekura-Sakakibara, K., and Hanada, K. (2011). An evolutionary view of functional diversity in family 1 glycosyltransferases. Plant J. *66*, 182–193.

Yonekura-Sakakibara, K., Tohge, T., Niida, R., and Saito, K. (2007). Identification of a Flavonol 7-O-Rhamnosyltransferase Gene Determining Flavonoid Pattern in Arabidopsis by Transcriptome Coexpression Analysis and Reverse Genetics. J. Biol. Chem. *282*, 14932–14941.

Yonekura-Sakakibara, K., Tohge, T., Matsuda, F., Nakabayashi, R., Takayama, H., Niida, R., Watanabe-Takahashi, A., Inoue, E., and Saito, K. (2008). Comprehensive Flavonol Profiling and Transcriptome Coexpression Analysis Leading to Decoding Gene–Metabolite Correlations in Arabidopsis. Plant Cell Online *20*, 2160–2176.

Yonekura-Sakakibara, K., Fukushima, A., Nakabayashi, R., Hanada, K., Matsuda, F., Sugawara, S., Inoue, E., Kuromori, T., Ito, T., Shinozaki, K., et al. (2012). Two glycosyltransferases involved in anthocyanin modification delineated by transcriptome independent component analysis in Arabidopsis thaliana. Plant J. *69*, 154–167.

Yoo, S.-D., Cho, Y.-H., Tena, G., Xiong, Y., and Sheen, J. (2008). Dual control of nuclear EIN3 by bifurcate MAPK cascades in C2H4 signalling. Nature *451*, 789–795.

Yuan, J., and He, S.Y. (1996). The Pseudomonas syringae Hrp regulation and secretion system controls the production and secretion of multiple extracellular proteins. J. Bacteriol. *178*, 6399–6402.

Zeng, W., and He, S.Y. (2010). A Prominent Role of the Flagellin Receptor FLAGELLIN-SENSING2 in Mediating Stomatal Response to Pseudomonas syringae pv tomato DC3000 in Arabidopsis. Plant Physiol. *153*, 1188–1198.

Zeng, L., Velásquez, A.C., Munkvold, K.R., Zhang, J., and Martin, G.B. (2012). A tomato LysM receptor-like kinase promotes immunity and its kinase activity is inhibited by AvrPtoB. Plant J. *69*, 92–103.

Zhang, F., Gonzalez, A., Zhao, M., Payne, C.T., and Lloyd, A. (2003). A network of redundant bHLH proteins functions in all TTG1-dependent pathways of Arabidopsis. Development *130*, 4859–4869.

Zhang, J., Shao, F., Li, Y., Cui, H., Chen, L., Li, H., Zou, Y., Long, C., Lan, L., Chai, J., et al. (2007). A Pseudomonas syringae Effector Inactivates MAPKs to Suppress PAMP-Induced Immunity in Plants. Cell Host Microbe *1*, 175–185.

Zhang, J., Li, W., Xiang, T., Liu, Z., Laluk, K., Ding, X., Zou, Y., Gao, M., Zhang, X., Chen, S., et al. (2010). Receptor-like Cytoplasmic Kinases

Integrate Signaling from Multiple Plant Immune Receptors and Are Targeted by a Pseudomonas syringae Effector. Cell Host Microbe *7*, 290–301.

Zhang, L., Kars, I., Essenstam, B., Liebrand, T.W.H., Wagemakers, L., Elberse, J., Tagkalaki, P., Tjoitang, D., Ackerveken, G. van den, and Kan, J.A.L. van (2014). Fungal Endopolygalacturonases Are Recognized as Microbe-Associated Molecular Patterns by the Arabidopsis Receptor-Like Protein RESPONSIVENESS TO BOTRYTIS POLYGALACTURONASES1. Plant Physiol. *164*, 352–364.

Zhang, W., He, S.Y., and Assmann, S.M. (2008). The plant innate immunity response in stomatal guard cells invokes G-protein-dependent ion channel regulation. Plant J. *56*, 984–996.

Zhang, W., Fraiture, M., Kolb, D., Löffelhardt, B., Desaki, Y., Boutrot, F.F.G., Tör, M., Zipfel, C., Gust, A.A., and Brunner, F. (2013a). Arabidopsis RECEPTOR-LIKE PROTEIN30 and Receptor-Like Kinase SUPPRESSOR OF BIR1-1/EVERSHED Mediate Innate Immunity to Necrotrophic Fungi. Plant Cell Online *25*, 4227–4241.

Zhang, Y., Butelli, E., De Stefano, R., Schoonbeek, H., Magusin, A., Pagliarani, C., Wellner, N., Hill, L., Orzaez, D., Granell, A., et al. (2013b). Anthocyanins Double the Shelf Life of Tomatoes by Delaying Overripening and Reducing Susceptibility to Gray Mold. Curr. Biol. *23*, 1094–1100.

Zhang, Z., Wu, Y., Gao, M., Zhang, J., Kong, Q., Liu, Y., Ba, H., Zhou, J., and Zhang, Y. (2012). Disruption of PAMP-Induced MAP Kinase Cascade by a Pseudomonas syringae Effector Activates Plant Immunity Mediated by the NB-LRR Protein SUMM2. Cell Host Microbe *11*, 253–263.

Zhao, J., and Dixon, R.A. (2010). The "ins" and "outs" of flavonoid transport. Trends Plant Sci. *15*, 72–80.

Zhao, J., Williams, C.C., and Last, R.L. (1998). Induction of Arabidopsis Tryptophan Pathway Enzymes and Camalexin by Amino Acid Starvation, Oxidative Stress, and an Abiotic Elicitor. Plant Cell Online *10*, 359–370.

Zhao, Y., Hull, A.K., Gupta, N.R., Goss, K.A., Alonso, J., Ecker, J.R., Normanly, J., Chory, J., and Celenza, J.L. (2002). Trp-dependent auxin biosynthesis in Arabidopsis: involvement of cytochrome P450s CYP79B2 and CYP79B3. Genes Dev. *16*, 3100–3112.

Zhao, Z., Zhang, W., Stanley, B.A., and Assmann, S.M. (2008). Functional Proteomics of Arabidopsis thaliana Guard Cells Uncovers New Stomatal Signaling Pathways. Plant Cell Online *20*, 3210–3226.

Zhou, H., Lin, J., Johnson, A., Morgan, R.L., Zhong, W., and Ma, W. (2011). Pseudomonas syringae Type III Effector HopZ1 Targets a Host Enzyme to

Suppress Isoflavone Biosynthesis and Promote Infection in Soybean. Cell Host Microbe *9*, 177–186.

Zhou, J., Wu, S., Chen, X., Liu, C., Sheen, J., Shan, L., and He, P. (2014). The Pseudomonas syringae effector HopF2 suppresses Arabidopsis immunity by targeting BAK1. Plant J. *77*, 235–245.

Zipfel, C. (2013). Combined roles of ethylene and endogenous peptides in regulating plant immunity and growth. Proc. Natl. Acad. Sci. *110*, 5748–5749.

Zipfel, C. (2014). Plant pattern-recognition receptors. Trends Immunol. *35*, 345–351.

Zipfel, C., Robatzek, S., Navarro, L., Oakeley, E.J., Jones, J.D.G., Felix, G., and Boller, T. (2004). Bacterial disease resistance in Arabidopsis through flagellin perception. Nature *428*, 764–767.

Zipfel, C., Kunze, G., Chinchilla, D., Caniard, A., Jones, J.D.G., Boller, T., and Felix, G. (2006). Perception of the Bacterial PAMP EF-Tu by the Receptor EFR Restricts Agrobacterium-Mediated Transformation. Cell *125*, 749–760.

Zong, N., Xiang, T., Zou, Y., Chai, J., and Zhou, J.-M. (2008). Blocking and triggering of plant immunity by Pseudomonas syringae effector AvrPto. Plant Signal. Behav. *3*, 583–585.

Zuanazzi, J.A.S., Clergeot, P.H., Quirion, J.-C., Husson, H.-P., Kondorosi, A., and Ratet, P. (1998). Production of Sinorhizobium meliloti nod Gene Activator and Repressor Flavonoids from Medicago sativa Roots. Mol. Plant. Microbe Interact. *11*, 784–794.